




Loma Linda University Electronic Theses, Dissertations & Projects

9-2016

Synthesis of HuaCat® Analogues as Novel Organocatalysts for the Formation of Asymmetric C-C Bonds

Kenneth Laboy

Follow this and additional works at: <https://scholarsrepository.llu.edu/etd>

 Part of the [Biochemistry, Biophysics, and Structural Biology Commons](#), and the [Medicinal and Pharmaceutical Chemistry Commons](#)

Recommended Citation

Laboy, Kenneth, "Synthesis of HuaCat® Analogues as Novel Organocatalysts for the Formation of Asymmetric C-C Bonds" (2016). *Loma Linda University Electronic Theses, Dissertations & Projects*. 382. <https://scholarsrepository.llu.edu/etd/382>

This Thesis is brought to you for free and open access by TheScholarsRepository@LLU: Digital Archive of Research, Scholarship & Creative Works. It has been accepted for inclusion in Loma Linda University Electronic Theses, Dissertations & Projects by an authorized administrator of TheScholarsRepository@LLU: Digital Archive of Research, Scholarship & Creative Works. For more information, please contact scholarsrepository@llu.edu.

LOMA LINDA UNIVERSITY
School of Medicine
in conjunction with the
Faculty of Graduate Studies

Synthesis of HuaCat® Analogues as Novel Organocatalysts for the Formation of
Asymmetric C-C Bonds

by

Kenneth Laboy

A Dissertation submitted in partial satisfaction of
the requirements for the degree
Master of Science in Biochemistry

September 2016

© 2016

Kenneth Laboy
All Rights Reserved

Each person whose signature appears below certifies that this thesis in his opinion is adequate, in scope and quality, as a thesis for the degree Master of Science.

_____, Chairperson
David Weldon, Associate Professor of Pharmaceutical and Administrative Sciences

Willie Davis, Associate Professor of Pharmaceutical and Administrative Sciences

Nathan Wall, Associate Professor of Biochemistry and Molecular Biology

ACKNOWLEDGEMENTS

I would like to express my deepest gratitude to my advisor Dr. David Weldon for giving me the opportunity to embark on this long journey with him in the field of Medicinal Chemistry. It's been a long road and I know it's been tough for him trying to teach me to keep my head down and screwed on straight. Throughout it all he had my back and became my family. Doc, I want to thank you for everything, and hope that you can be proud of the work you put in and sacrifices you made to make me a better man.

I would also like to give thanks to Dr. Marvin Payne for introducing me into the field of science in a manner that gave me a thirst for knowledge that I never had before. I feel indebted to him for all the advice and direction you've given me over the years. I still remember when you brought me into your office and told me to go to the VA for help. All the times you gave me a ride to therapy and watched out for me really made a difference in my life.

I'd also like to thank Dr. Nathan Wall for being my swim buddy, keeping me motivated when I wanted to quit. Moreover, I feel so grateful to him for kicking me in the rear when I needed it and patting me on the back when it was necessary. Thanks for being patient with me sir.

To Dr. Willie Davis, thank you for your support and guidance throughout these years in the lab. Skipper, you've always kept from becoming complacent and your leadership was key to keeping me accountable for my actions. And finally, I would like to thank the School of Pharmacy and Dr. Rashid Mosavin for providing me the opportunity to study and pursuit my goals.

CONTENT

Approval Page.....	iii
Acknowledgements.....	iv
List of Figures	viii
List of Tables	x
List of Abbreviations	xi
Abstract.....	xiii
Chapter	
1. Introduction.....	1
The importance/significance of carbon-carbon bond formation.....	1
The significance of a broad selection of catalysts and reagents	8
Various methods of carbon-carbon bond formation	13
Stereochemistry and Regiochemistry	20
The major advantages of HuaCat®.....	28
2. Materials and Methods.....	36
General.....	
3. Synthetic strategy, Results, and Discussion.....	39
Design Strategy.....	39
Examination of Results and Discussion.....	45
Conclusion	48
Experimental section.....	49
Various attempted experimental procedures.....	54
References.....	67
Appendices	
A. Flash chromatography purification reports.....	87
B. NMR Analysis reports	139

Carbon NMR.....	139
Proton NMR.....	153
C. Vita.....	194

FIGURES

Figures	Page
1. Aldol condensation reaction	4
2. Citrate synthase aldol condensation reaction of the first step of the Krebs cycle	4
3. Aldolase catalyzed reaction of GAP & DHAP	5
4. Biosynthesis of Lanosterol.....	6
5. Metal catalyst framework for C-C bonds.....	7
6. Ziegler-Natta catalysis of isoprene units.....	8
7. Catalyzed carboxylation of methane.....	9
8. Palladium catalyzed synthesis of Lactones.....	10
9. Ruthenium catalyzed synthesis of Vinyl-carbamates	10
10. Michael addition reaction	15
11. Mannich reaction	16
12. Diels-Alder reaction.....	17
13. Horner-Wadsworth-Emmons (HWE) reaction	18
14. Suzuki reaction scheme and catalytic cycle with Pd	20
15. Example of stereoisomers using 2-bromo-3-chlorobutane	21
16. Structures of Carvone	22
17. Structure of Ibuprofen.....	23
18. Structure of Thalidamide	24
19. Markovnikov addition.....	26
20. Zimmer model for chair confirmation transition state.....	30
21. Proposed mechanism for Proline aldol reaction with transition state chair confirmation.....	31

22. Tetrazoles (A); Sulfonamides (B).....	33
23. HuaCat® facilitated asymmetric reactions: (A) Aldol reaction (B) Mannich reaction (C) intramolecular Michael addition.....	35
24. Desired products	36
25. Projected transition states of desired products.....	39
26. Three building block regions of diversification.....	40
27. Phase 1 steps	41
28. Standard peptide coupling conditions.....	42
29. Acid Chloride coupling reaction.....	43
30. General scheme for the formation of the desired organocatalysts	45
31. Initial protocol for synthesis	47
32. Newly identified synthetic route to overcome the limitations of previous synthetic attempts Initial protocol for synthesis	48
33. Step one for production of compound 1	49
34. Step two for production of compound 2	50
35. Step three for production of compound 3	51
36. Step four for production of compound 4.....	53
37. Previous experimental procedures, 1-6 reactions	54
38. Previous experimental procedures, 7-12 reactions	55
39. Previous experimental procedures, 13-18 reactions	56
40. Experimental procedure for 2	57
41. Experimental procedure for 3a.....	57
42. Experimental procedure for 4a.....	58
43. Experimental procedure for 4b	59
44. Experimental procedure for 4c.....	60
45. Experimental procedure for 4d	61

46. Experimental procedure for 4b using oxalyl chloride.....	62
47. Experimental procedure for 4b using HATU.....	63
48. Experimental procedure for 4b using HOBt	64
49. Experimental procedure for 4e using PyBOP and Iodo-benzene sulfonamide.....	65
50. Experimental procedure for 4d using HBTU	65
51. Experimental procedure for 4d using TBAS and sulfonyl chloride through acid catalysis	66
52. Experimental procedure for 4b using NaH and sulfonyl chloride	67

TABLES

Tables	Page
1. Sample of attempted reactions to achieve the desired final organocatalyst.....	45
2. Details of reaction conditions A-E.....	45
3. Step one quantities	49
4. Step two quantities.....	50
5. Step three quantities.....	52

ABBREVIATIONS

Al	Aluminum
As	Arsenic
Boc	tert-butyloxycarbonyl - protecting group
Cl ⁻	Chloride Ion
Cbz	Carboxybenzyl - protecting group
CDCl ₃	Deuterated chloroform
CDK	Cyclin dependent kinase
CoA	Coenzyme A
CO ₂	Carbon Dioxide
DBU	1,8-Diazabicyclo[5.4.0]undec-7-ene
DCM	Dichloromethane
DHAP	dihydroxyacetone phosphate
DIBAL	Diisobutylaluminium hydride, (Aluminum, hydrobis(2-methylpropyl)-)
DIPEA	N,N-Diisopropylethylamine
DMAP	4-dimethylaminopyridine
DMAPP	dimethylallyl pyrophosphate
DMF	Dimethylformamide
DMSO	Dimethyl sulfoxide
EDCI	1-Ethyl-3-(3-dimethylaminopropyl) carbodiimide
EtOAc	Ethyl Acetate
Fmoc	9H-fluoren-9-ylmethyl ester (Fluorenylmethyloxycarbonyl)

Ga	Gallium
GAP	glyceraldehyde-3-phosphate
H ₂ O ₂	Hydrogen Peroxide
H ₂ SO ₄	Sulfuric Acid
HATU	O-(7-Azabenzotriazol-1-yl)-N,N,N',N'-tetramethyluronium hexafluorophosphate
HBTU	O-(Benzotriazol-1-yl)-N,N,N',N'-tetramethyluronium
HMG	3-hydroxy-3-methylglutaryl
HOBt	N-Hydroxybenzotriazole (Benzotriazol-1-ol)
HWE	Horner-Wadsworth-Emmons
Hz	Hertz
Ir	Iridium
Li	Lithium
MCPBA	m-Chloroperoxybenzoic acid
Mg	Magnesium
MTBD	7-Methyl-1,5,7-triazabicyclo[4.4.0]dec-5-ene
NaH	Sodium hydride
NMR	Nuclear Magnetic Resonance
Pb	Lead
PP or IPP	isopentenyl pyrophosphate
Pro or P	Proline – Amino acid
Pybop	benzotriazol-1-yl-oxypyrrolidinophosphonium hexafluorophosphate

ROS	Reactive Oxygen Species
SAR	structure-activity relationship
Sn	Tin
THF	Tetrahydrofuran
TMS	Tetramethylsilane
TBAHS	Tetrabutylammonium hydrogen sulfate
TLC	Thin Layer Chromatography
TiCl ₄	Titanium (IV) chloride
ZnCl ₂	Zinc chloride

ABSTRACT OF THESIS

Synthesis of HuaCat® Analogues as Novel Organocatalyst for the Formation of Asymmetric Carbon-carbon Bonds

by

Kenneth Laboy

Master of Science, Graduate Program in Biochemistry
Loma Linda University, September 2016
Dr. David J. Weldon, Chairperson

The synthesis of organic compounds with preferential stereochemistry is ubiquitous in the scientific community. A chemical reaction that asymmetrically induces one stereoisomer over another is achieved through the use of catalysts and various coupling reagents.¹ Inorganic catalysts, such as TiCl_4 and ZnCl_2 , have been documented for many decades as effective agents in the synthesis of asymmetric bonds, however, there are environmental limitations to their use. First, the asymmetric reactions involving these metal catalysts require solvents that are not environmentally-friendly, especially when used on an industrial scale and second, the metal catalysts are recycled when possible, however, there is always metal waste that is equally unfriendly to the environment. One solution is to develop organocatalysts (non-metal catalyst) that will accomplish the same asymmetric reactions in aqueous reaction conditions. HuaCat® and HuaCatII® are organocatalysts developed by Dr. Rich Carter at Oregon State University that are able to achieve a single stereochemistry in 98% yield with greater than 95% diastereomeric excess.^{2, 3} These catalyst are not metal-containing and do work in aqueous conditions, but they still require the use of some solvent. The development of analogues of HuaCat® by substituting aromatic substituents with different electron

withdrawing/donating groups will afford catalysts with increased yield and more predictable stereochemistry in aqueous conditions. One of the major challenges of the project is the formation of the key peptide bond of an amino acid and a sulfonamide containing a highly electronegative aromatic substituent in the ortho position, a feat that has minimal (and questionable) literature support to date. In this paper, we will detail the methods that have been attempted and the future plans for overcoming this unfavorable reaction to achieve what could be a new path to a unique organic structure for further synthetic manipulation.

CHAPTER ONE

INTRODUCTION

The Importance/Significance of Carbon-Carbon Bond Formation

Carbon-carbon (C-C) bond formation is the foundation to organic life here on earth.⁴ Any attempt to understand and expand upon the properties of organic life start with reactions of organic compounds and is further preceded by their chemical structure.⁵ Biomedical translational research hopes to convert what the scientist elucidates in the laboratory into practical application that can be employed in a clinical setting for organic life;⁶ therefore, it is explicit that the two fields have cohesion. The focus of this thesis will be intrinsic carbon-carbon bond forming activities in nature and the organic synthetic processes utilized to make novel structures with biological importance.

Nature affords a large number of structurally diverse compounds capable of regulating many biological processes, including cell division, differentiation and enlargement, chloroplast development and senescence. In order to access compounds with improved properties in comparison to those found naturally-occurring, it is essential to establish their structure-activity relationship (SAR). SAR research area in organic chemistry entails defining the role of the molecular features of any biologically-active chemical structure with respect to its target.⁷ SAR research involves the construction of a diverse and systematic library of derivatives that can then be compared to a pharmacophore model of the natural product to determine the role of the manipulated areas defined by the derivative library.⁸ A pharmacophore is defined by Yang as “the ensemble of steric and electronic features that is necessary to ensure the optimal supra-molecular interactions with a specific biological target and to trigger (or block) its

biological response.”⁹ In other words, the pharmacophore is the minimal molecular features of any biological compound that are absolutely necessary to appreciably interact with the target. Defining a pharmacophore for a class of therapeutics is an early and essential step of translational research and modern drug discovery has an intense demand for stereoselective transformations of potential drug candidates.¹⁰ The search for potential pharmacophores has necessitated the use of catalysts that can facilitate the synthesis of natural products and their derivatives.¹¹ Leading to the rational observation that the pioneering of effective synthetic organic catalysts that can stereo- and regioselectively manipulate favorable chemical reactions with high product yields, minimal cost, and minimal environmental implications is fundamental to the scientific and health community.

Organic synthesis can be divided into various categories with two main types of reactions: C-C bond formations and functional group transformations.¹² C-C bond formation is the core of organic synthesis¹³ and furnishes the basis for producing more intricate organic compounds from simpler ones. The ability to manipulate the carbon backbone of various organic molecules through C-C bond formation makes it one of the cornerstones to transformation in organic synthesis.¹⁴ It is fundamental in medicinal chemistry to have the capability to expound and develop the carbon framework of organic molecules via a series of C-C bond forming reactions.¹⁵ Its function in nature for biosynthesis and metabolism is critical to the survival of organic lifeforms in order to maintain homeostasis.¹⁶ Moreover, it can be applied to organometallic¹⁷, agrochemical¹⁸, and biocatalytic organic synthesis.¹⁹

In nature, organic substances found in living organisms are conceived innately. Molecules from nature are essentially blueprints for organic chemists to develop novel techniques for determining structures, analyzing mechanisms of reactions, exploring the effects conformation and stereochemistry have on reactions, and pioneering challenging new targets to synthesize.²⁰ Harnessing the powerful techniques of organic molecules in their biological hosts, such as the enzymes that synthesize endogenous molecules and the complex processes that occur in a cell, is a valuable tool.¹⁵ In this congruent perspective, bioorganic chemistry hopes to understand the chemical mechanisms of enzyme-catalyzed reactions, to develop techniques to identify and to study how structure determines function in biosynthetic enzymes²⁰ with protein substrates obtained by organic synthesis through the use of catalyzed C-C bond formation.²¹

Expanding on the importance of C-C bond formation leads to a focus on biochemical enzymatic reactions, which are often overlooked as a method for organic synthesis of C-C bond formation. Biochemical reactions are generally catalyzed by an enzyme and are classified in one of these four broad categories: (1) group-transfer reactions, (2) oxidation and reductions, (3) eliminations, isomerizations, and rearrangements, and (4) reactions that make or break carbon-carbon bonds.²⁰ It is noted that elimination reaction mechanisms using dehydration resulting in the formation of a C=C double bond (e.g. enolase, fumarase) should be considered C-C bond formation;²² The focus of this research project is primarily C-C bond formation, the fourth category of biochemical enzymatic reactions.

There are many examples of catalysis in biological processes. One example are aldolases, a class of enzymes that act as catalysts for aldol condensation reactions.²³ An

aldol condensation is an organic chemical reaction in which an enol, or an enolate ion, reacts with a carbonyl compound to form a β -hydroxyaldehyde or β -hydroxyketone, followed by a dehydration step to yield a conjugated enone (**Figure 1**).²⁴

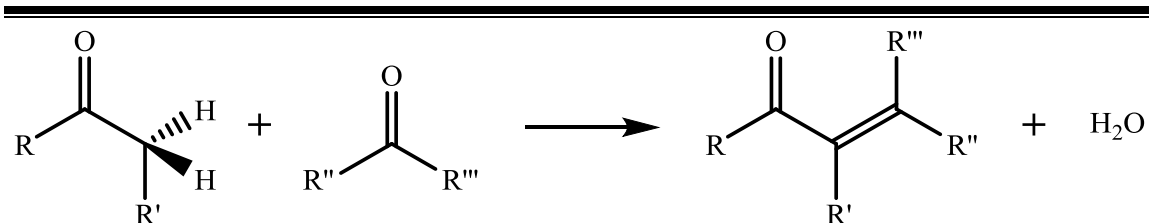


Figure 1 - General Aldol condensation reaction

In the first step of the Krebs cycle, citrate synthase catalyzes the reaction of acetyl coenzyme A (acetyl CoA) and oxaloacetate to produce citrate through an aldol mechanism (**Figure 2**). In this specific reaction, it is not an aldehyde or a ketone that acts as the nucleophile as shown in **Figure 1**, but rather thioester Acetyl-CoA.²⁵ Generally speaking Biochemists refer to this reaction as an aldol condensation reaction describing the first step of the process, the addition initiated by base deprotonation of an α -Hydrogen from acetyl CoA forming an enolate nucleophile that subsequently attacks the electrophilic carbonyl carbon of Oxaloacetate ion. Protonation eventually leads to the final product with the generation of a new C-C bond and a new stereo-center.²⁶

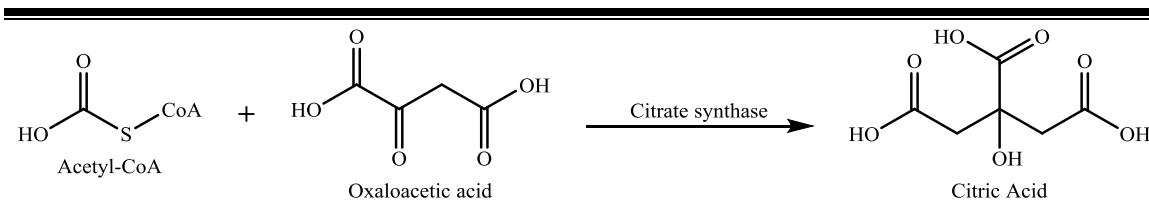


Figure 2 - Citrate synthase aldol condensation reaction of the first step of the Krebs cycle

Another example of this particular reaction takes place in gluconeogenesis. The reaction between two 3-carbon containing sugars, specifically glyceraldehyde-3-phosphate (GAP) and dihydroxyacetone phosphate (DHAP), to form the six-carbon product fructose 1, 6-bisphosphate (F1,6-BP) (**Figure 3**). This reaction is catalyzed by the enzyme fructose 1,6-bisphosphate aldolase.²⁵ It must be noted that the aldol reaction is not formally a condensation reaction because it does not involve the loss of a small molecule, however, it is an important example where a catalyzed C-C bond formation is used in biochemistry, thereby alluding to its significance in nature.

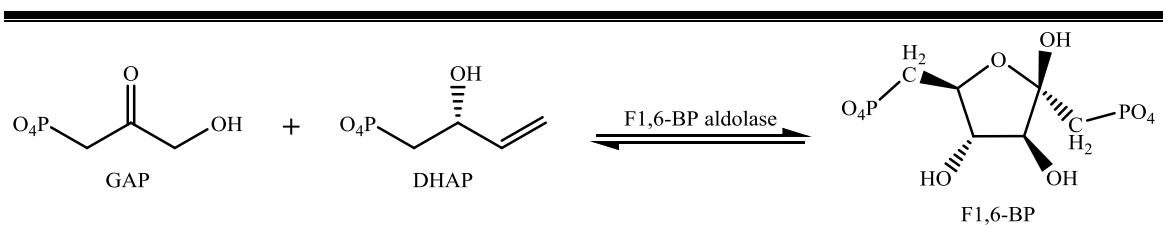


Figure 3 - Aldolase catalyzed reaction of GAP & DHAP

Steroids present another example of C-C bond formation in nature. Steroid biosynthesis is an anabolic pathway which produces steroids from simple precursors. Following the biosynthetic pathway in animals is a common method for drug development of targets for antibiotics and other anti-infection drugs.^{9, 27} Steroid metabolism in humans is also the target of cholesterol-lowering drugs.^{9, 13} The biosynthesis of steroids flows through the mevalonate pathway, which uses acetyl-CoA as building blocks to make lanosterol, a precursor to steroids found in animals, fungi, and plants.^{25, 27} In the mevalonate pathway, or the HMG-CoA reductase pathway, isoprene units donated by intermediates, isopentenyl pyrophosphate (PP or IPP) and dimethylallyl

pyrophosphate (DMAPP), that were formed by acetyl-CoA subunits are coupled into more complex compounds making squalene.²⁷ These compounds are then folded and rearranged into lanosterol for subsequent steroid biosynthesis (**Figure 4**). The coupling of these small subunits into larger more complex compounds is done through enzymatic catalysis of C-C bond formation.

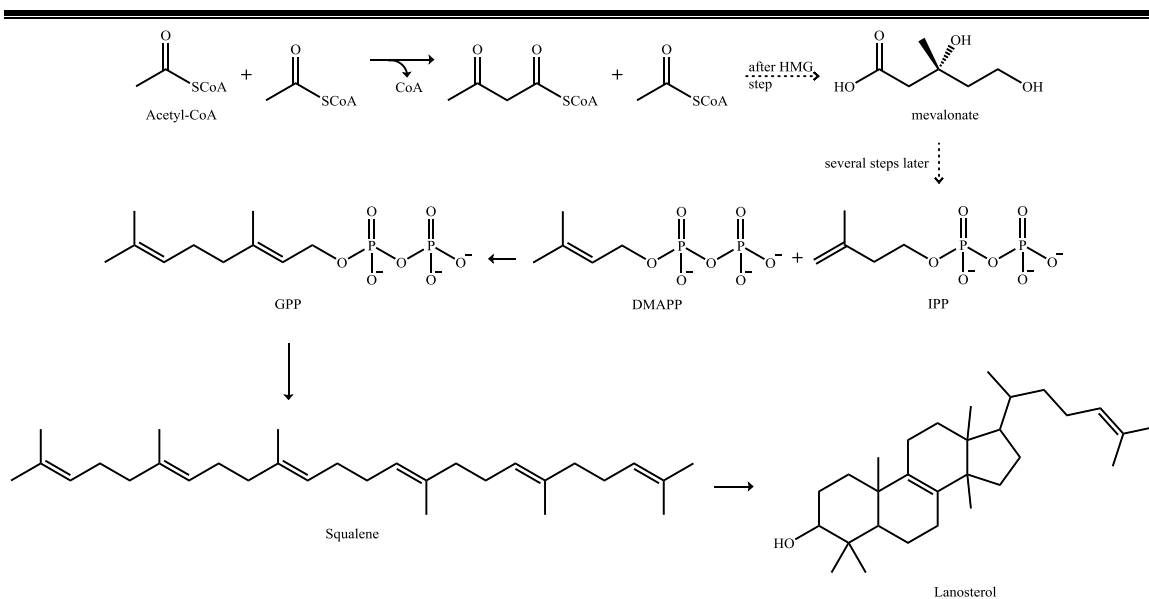


Figure 4 - Biosynthesis of lanosterol from acetyl-CoA building blocks

While many processes in nature use organic-based catalysts known as organocatalysts, organometallic reactions leading to the formation of new C-C bonds are commonly used in synthetic organic chemistry. There are two classes of note that can be distinguished.¹⁷ The first is when the metal acts as a template that mediates the incidence of a peripheral reagent on a ligand without that reagent bonding within the coordination sphere. The reaction of electrophiles with iron acylate anions,²⁸ seen in **figure 5A**, and catalytic allylic alkylation utilizing palladium complexes,²⁹ seen in **figure 5B**, are a few

well-known examples. These correspondingly exhibit enriched reactivity and stereoselectivity via the contribution of organometallic complexes. In the second type, the new bond is fashioned amid ligated species and a supplementary subdivision is essential. The significant step may be cis-ligand movement, for which the most recognizable illustration is alkyl migration to coordinated carbon monoxide (CO) in catalytic hydroformylation. The C-C bond is established by coupling adjacent carbon-metal bonds associated with exclusion of the organic portion.¹⁷

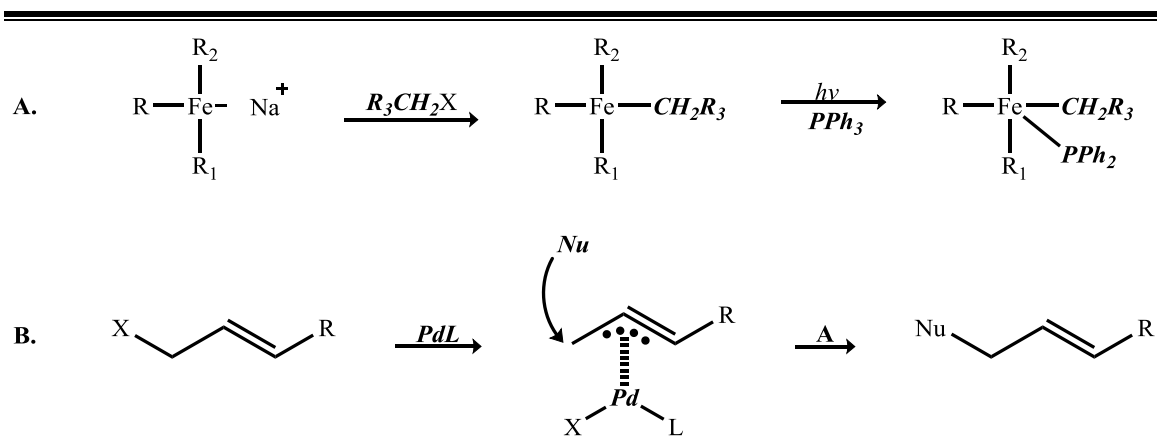


Figure 5 – Metal catalyst working as framework for C-C bond formation

Organometallics afford practical applications in many catalytic processes, most notably those applications involving CO and polymers originating from alkenes. Common manufacturing, such as polyethylene and polypropylene (types of rubber), are produced by means of organometallic catalysts, typically heterogeneously by the use of Ziegler-Natta³⁰ catalysis (**Figure 6**).³¹ The carbonylation of methanol catalyzed by iridium to acetic acid is an efficient process proclaimed by BP Chemicals using metal carbonyl catalysts as well.³²⁻³⁴ Generally, synthetic aldehydes are fabricated by means of

hydroformylation. Additionally, organic lithium (Li), magnesium (Mg), and aluminum (Al) compounds are highly basic reducing agents that catalyze various polymerization reactions.³⁵ Furthermore, organometallic compounds are also used in the fabrication of semiconductors.³¹ In addition to the diverse applications, organocatalysis often produces reactions with desirable quantitative yields.^{29, 36} Although, in organometallic reactions, the conversion of product is obtained in respectable yield, generally a mixture of isomers are obtained.^{29, 36, 37} However these processes use volatile compounds such as trimethyl-gallium, trimethyl-indium, trimethyl-aluminum, as well as related nitrogen, phosphorus, arsenic, and antimony compounds. Although found in the environment, they can be toxically hazardous when used in these quantities in industrial purposes.^{38, 39}

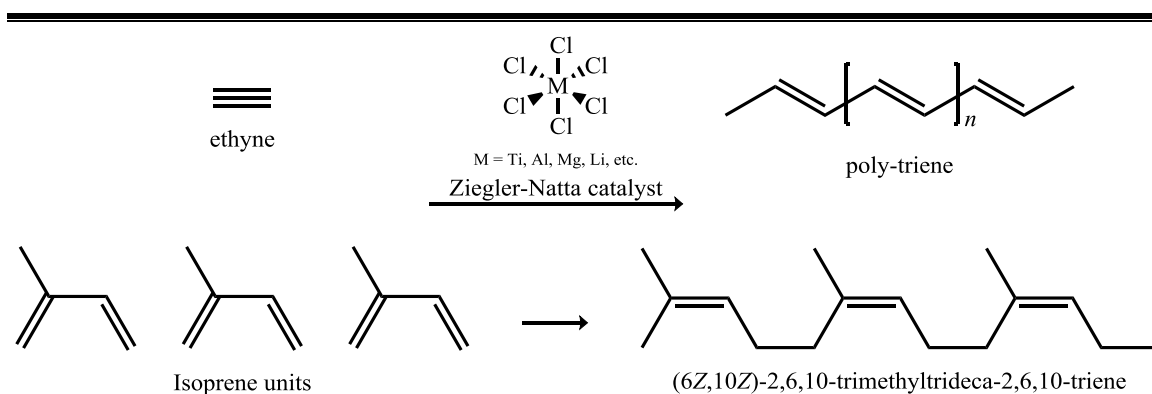


Figure 6 - Ziegler-Natta catalysis of isoprene units to form polymers such as rubber

Agricultural, as well as environmental chemistry, is also greatly impacted by organic chemical reactions. While nature has used monohydrogenase and other enzymes to functionalize alkanes in aqueous environments at ambient conditions,⁴⁰ alkanes are generally considered nonreactive in conventional organic chemistry.¹² The direct functionalization of alkanes is ubiquitously found in a variety of related fields including

the development of laboratory chemicals, energy, and medicine; therefore, chemical synthesis of alkanes has essential implications. Research in this area predominantly focuses on the conversion of a C-H bonds into a C-O bond. An example in **Figure 7** illustrates the coupling of methane with CO to produce acetic acid in aqueous conditions catalyzed by Ytterbium(III) acetate and sodium hypochlorite.⁴¹ Moreover, the application of organic synthesis of the catalytic reaction of C-H bonds adjacent to heteroatoms such as nitrogen and oxygen.⁴²

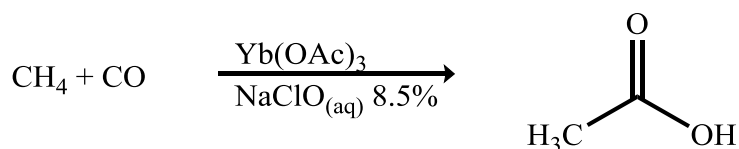


Figure 7 - Catalyzed carboxylation of methane to acetic acid with carbon monoxide in water

Another area where C-C bond formation is applied is in the utilization of carbon dioxide (CO₂). CO₂ constitutes a natural source of carbon and a one-carbon (C₁) synthetic component with a capacity for the functionalization of substrates.³⁷ Unfortunately, incorporation of CO₂ into unsaturated hydrocarbons is difficult because of its molecular stability and therefore requires activation that can be imparted through the use of transition metal catalysts.⁴³ **Figure 8** illustrates the activation of dienes by palladium complexes and direct incorporation of CO₂ into alkynes.

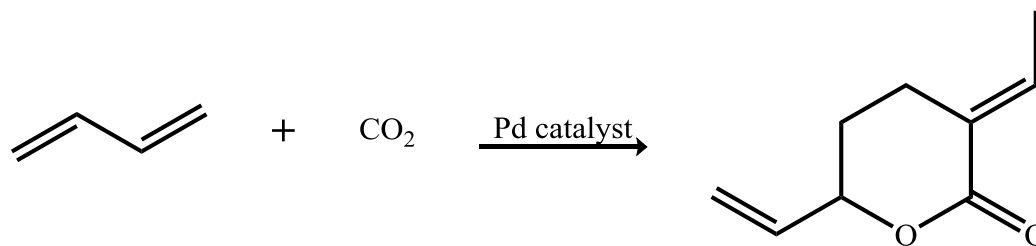


Figure 8 - Palladium catalyzed synthesis of Lactones using CO₂ and activated dienes

This is one catalytic route in which unsaturated lactones, a common intermediate in many synthetic schemes, are made.⁴⁴ Additionally, vinyl-carbamates can be regioselectively produced in one-step from terminal alkynes, CO₂, and secondary amines with ruthenium catalysts (**Figure 9**).⁴⁵

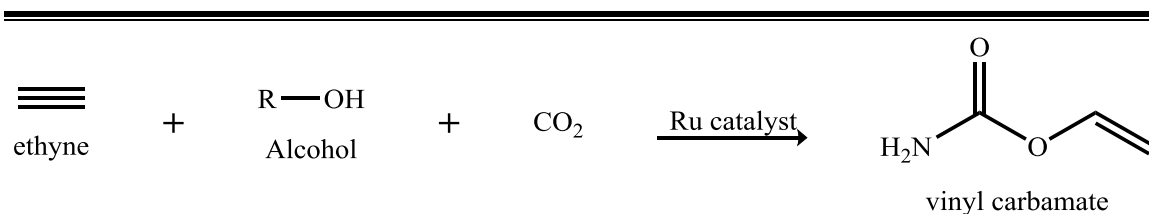


Figure 9 - Ruthenium catalyzed synthesis of Vinyl-carbamates

The Significance of a Broad Selection of Catalysts and Reagents

There are a wide variety of organic (non-metallic) catalytic reagents for traditional C-C bond formations. For example, Wittig reactions use phosphonium salts and phosphonates are used for Horner-Wadsworth-Emmons (HWE) reactions.⁴⁶ Both of these reactions are utilized to create alkene-containing products.⁴⁷ However, synthetic methods accessible for C-C bond formation are continually advancing.

There are various contributing factors that affect innovation, such as the expansion of stout and dependable protocols for cross-coupling, augmented obtainability

of various organometallic reagents, and the continued development of stoichiometric reagents that facilitate the addition of a specific carbon-containing moiety. The last category, depends on a diverse selection of reagents that can be employed under mild conditions with a broad substrate scope. Therefore, further development of reagents that permit potent routes to carbon-carbon bond formation is necessary. Cross-coupling reactions make use of substrates with favorable yields in diverse reaction conditions, as well as metal catalysts for various reactions. Research success hinges on the ability of the researcher to obtain the desired product, which is aided by the availability of reagents that consistently yield high specificity, when the experiment calls for it.⁴⁷

Though enzymatic processes in nature are obligated to occur in an aqueous environment by necessity, water has been a solvent to be evaded for conventional organic reactions. The increased acknowledgment that organic reactions can move forward suitably in aqueous media and extend improvements over those taking place in organic solvents is widespread in the scientific community.⁴⁸ This assertion was preceded by studies into Diels-Alder reactions forged by Breslow⁴⁹ and hydroformylation reactions.⁵⁰⁻
52

The advent of the field of green chemistry has encouraged the expansion of research activities in this subject matter.⁵³ Initial curiosity has developed into a lucrative discipline that companies have invested in with profound returns.⁵⁴ This takes form by way of an increase in stereoselectivity that benefits the researcher when designing synthetic routes for experimental protocols, as well as the added bonus of milder reaction conditions.⁵⁵ Also, contributing to a decrease in consumable materials that leads to increased profit margins.⁵³ Moreover, this affords the added benefit of decreasing the

amount of waste produced when manufacturing large scale chemical products, thereby limiting harmful effects to the environment.^{56, 57} This contributed to advancement toward comprehending the reactions of organic compounds in high-temperature water, which has obvious implications to chemical synthesis that extends to energy and fuels.⁵⁸ Green chemistry seeks to reduce chemical related impact on human health and the environment by the use of alternative, environmentally friendly processes and reaction media.⁵³

The decrease in consumable materials affects two areas: Solvent and reagent usage. The selection of solvents, the chemicals used to dissolve substances into a solution, are a significant aim for Green Chemistry programs. The foremost source of industrial waste in industrial chemical production comes from solvents, but meticulous selection can also raise reaction rates and reduce reaction temperatures. Reduction in the amount of organic solvent consumed in the synthesis of Viagra™ (Sildenafil Citrate) is a major triumph of Green Chemistry as well as shareholders at Pfizer in the UK.⁵⁹

Through innovation, organic chemists were able to make the synthesis of Sildenafil Citrate, the active ingredient in Viagra™ and Revatio™, more efficient. The improvements resulted in substantial environmental advantages, that brought about the decline in the amount of several organic solvents essential for the synthesis of sildenafil citrate.⁵⁵ The utter removal of all chlorinated and highly volatile solvents such as diethyl ether, dichloromethane, methanol and acetone. This innovation also allowed for the removal of tin (II) chloride from the synthesis, a known environmental polluter.⁵³ It was replaced by a catalytic hydrogenation reaction with water being the principal by-product. The new route was designed around a specific cyclisation reaction seen in the final step of the synthesis ensuring a higher quality product. The financial gains can be estimated

through the elimination of 30,000 tons of chemical solvent that are no longer needed and decrease in the chemical reagents and substrates necessary to produce the final product.⁵³ Essentially, the amount of product produced was increased with less reactants consumed.

Another example comes from the scale up of the synthesis of pregabalin (Lyrica™), a medication utilized in the treatment of neuropathic pain.⁵⁴ Organic chemists remodeled the route of several enzymatic reactions to allow for chemical reactions to be performed in water instead of organic solvents. In this occasion, a synthetically produced, endogenous catalyst, lipase, was used. Thereby reducing the amount of organic materials consumed. Environmentally this enzymatic process was calculated to eliminate more than 3 million tons of CO₂ emissions relative to the previous industrial process. This equates to the removal 1,000,000 cars per year off the road in the United Kingdom (UK).⁵³

Various Methods of Carbon-Carbon Bond Formation

In the field of natural product synthesis, there are a number of methods at our disposal to make C-C bonds. Chronologically, five separate reactions in the field of organic chemistry have facilitated the practical use of synthetic organic reactions in the scientific community: Michael Additions, Mannich reactions, Diels-Alder reactions, HWE reaction, and Suzuki-Negishi (S-N) coupling reactions.

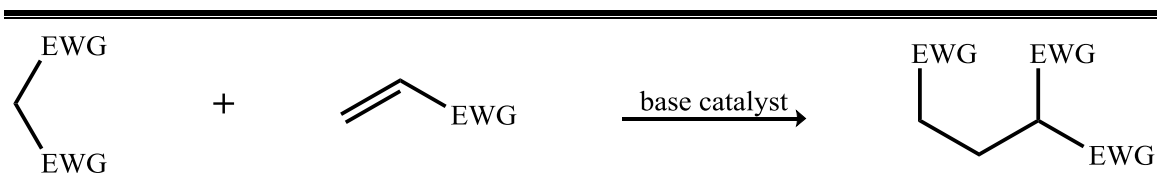
The Michael addition, introduced by Arthur Michael in 1887,⁶⁰ is a facile reaction for conjugate addition of a nucleophile and an activated olefin, or alkyne, for nucleophilic C-C multiple bond formation (**Figure 10**).⁶¹ The Michael addition has various advantages for the strategic planning of organic synthesis such as its use under mild reaction conditions and elevated functional group tolerance. It has a broad range of use for

polymerizable monomers and functional precursors as well as superior conversions with favorable reaction rates.⁶² Furthermore, its application in post-polymerization modification⁶³ and coupling of biological and synthetic polymers is well documented.⁶⁴ The Michael addition reactions versatility makes it well-suited to numerous types of laboratory disciplines to include biomedical applications such as gene transfection,⁶⁵ cell scaffolds,⁶⁶ and tissue replacements.⁶²

The convenience it affords over other reactions stems from facilitation of a wide range of polymers from assorted monomers, and analogous polymers are formulated in environments in which competing polymerization mechanisms will not function as well. This makes it valuable in biological applications, for instance, in protein derivitization the Michael additions mild reaction conditions are favorable since high temperatures, oxidizing radicals, and organic solvents are not possible.²¹

As aforementioned, the Michael addition encompasses the addition of a nucleophile, or 'donor,' to an activated electrophilic olefin, the 'acceptor,' resulting in a 'adduct.' It is generally considered in reactions where the addition of enolate nucleophiles to activated olefins is wanted; however, there are multiple functional groups that possess sufficient nucleophilicity to operate in the same capacity, as 'Michael' donors. Reactions containing non-enolate nucleophiles such as amines, thiols, and phosphines are classically referred to as 'Michael-type' additions. As long as the acceptor possesses an electron withdrawing and resonance stabilizing activating group that stabilizes the anionic intermediate, it can be considered a Michael addition.⁶⁷ There are many 'Michael-type' acceptors, because many functional groups have the electron withdrawing activating effect necessary to integrate seamlessly in Michael addition

reactions,⁶⁸ and are readily available commercially.⁴⁷ Examples are: Acrylamides, vinyl sulfones, α,β -unsaturated aldehydes, and azo compounds, to name a few.⁶⁷



EWG - Electron withdrawing group

Figure 10 - Michael addition reaction

The use of organic synthesis to produce natural endogenous compounds is quite prevalent and one such reaction employed to do so is the Mannich reaction, presented by Carl Mannich in 1912.⁶⁹ The synthesis of various compounds such as peptides,⁷⁰ nucleotides,⁷¹ antibiotics,⁷² and compounds that contain high concentrations of amines, such as alkaloids,¹¹ are all methods in which Mannich reactions are typically used.⁷³ Furthermore, it is commonly used in agrochemistry to synthesize endogenous auxins,¹¹ to establish quantitative structure-activity relationships, and analogous derivatives with improved properties to pioneer novel ligands compare pharmacophore model capacity.

The Mannich reaction is a condensation reaction considered to be a paradigm of nucleophilic addition of a primary or secondary amine to a carbonyl functional group, leading to subsequent dehydration to the Schiff base. The second step involves the electrophilic addition of the Schiff base with a compound possessing an acidic proton.⁷⁴ Essentially, it involves the addition of resonance-stabilized carbon nucleophiles to a substituted imines, or iminium salts. The carbonyl containing compound can undergo tautomerization to the enol form and subsequent attack of the protonated imine. The

Mannich reaction consists of three elements: (1) a primary or secondary amine; (2) an aldehyde; and (3) a methylene bridge,⁷⁵ a functional group that withdraws electrons by resonance.⁷¹ Condensation of the reactants takes place with concomitant discharge of H₂O. This leads to the production of a ‘Mannich base’, where the active hydrogen is supplanted by an amino-methyl group.⁷¹ A general reaction scheme can be seen in **figure 11**.

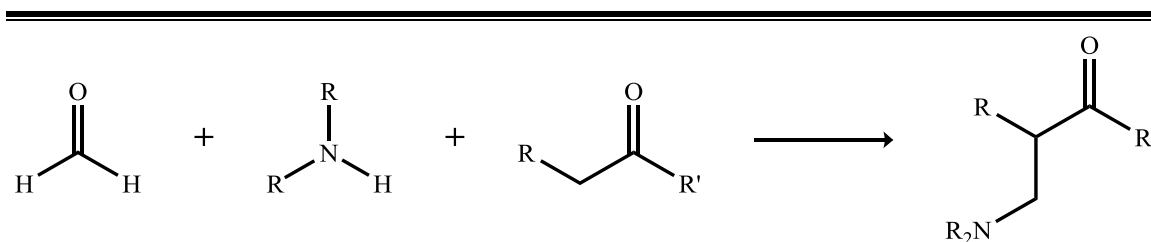


Figure 11 - Mannich reaction

The Diels–Alder reaction is yet another applicable form in which C-C bond formation is fundamental in research. It is the organic chemical reaction between a conjugated diene and a substituted alkene, ordinarily dubbed the dienophile, to form substituted cyclic systems.⁷⁶ In 1950, the Nobel Prize in Chemistry was awarded to Otto Diels and Kurt Alder for their introduction of this reaction in 1928.⁷⁷ Typically, the Diels–Alder reaction is acutely useful in synthetic organic chemistry as a dependable method for forming 6-membered systems with respectable management over regio- and stereochemical properties.⁷⁸ The underlying concept has also been applied to other π -systems, such as carbonyls and imines, to furnish the corresponding heterocycles, known as the hetero-Diels–Alder reaction.^{79, 80} A general reaction scheme can be seen in **figure 12**.

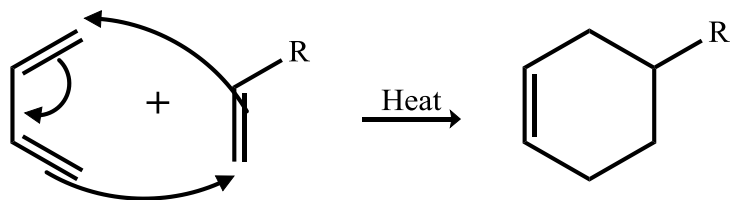


Figure 12 - Diels-Alder reaction

Diels–Alder reactions are another valuable tool for the formation of C-C bond formation used in total synthesis of endogenous steroids, such as cortisone and cholesterol.⁸¹ Butadiene’s reaction with quinone derivatives is essential to produce steroid skeleton rings with the sought after regiochemistry. Prostaglandins are another endogenous compound synthetically made that makes use of a Diels–Alder reaction early in its synthesis, thereby facilitating the relative stereochemistry of adjoining stereocenters on the prostaglandin core.⁸² The preceding applications justify the rational that C-C bond formation is scientifically fundamental and beneficial to the future development of laboratory research.

The HWE reaction is one of the tools of choice for olefination reactions in the field of organic chemistry. It stems from Leopold Horner’s publication in 1958, of a unique Wittig reaction that uses carbanions stabilized by phosphine-oxide and carbonyl compounds.⁸³ Eventually W.S. Wadsworth and W. D. Emmons were able to modify the reaction further by applying phosphonates.⁸⁴ It is prevalently used for elaborating on complex synthetic precursors. However, it also used as a method to strategically couple preformed sections of a target molecule. Based on the developed route it may also be used to otherwise introduce a newly formed olefin when a defined stereochemistry is preferred. A general reaction scheme can be seen in **figure 13**.

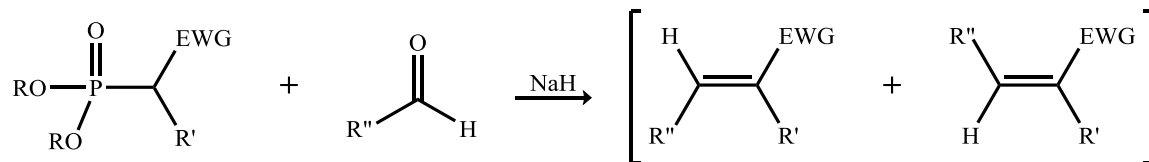


Figure 13 - HWE reaction

Although the prevailing employment of this reaction is as a dependable means for E-alkene formation, it must be noted that the stereochemical outcome of the reaction depends on both the structure of the reactants and on the reaction medium. These factors encompass the base, solvents, and the inclusion (or exclusion) of any congruent additives, such as salts and crown ethers.⁸⁵ However it has been demonstrated that Z-selectivity can be accomplished as well using either Phosphonic acid bis(2,2,2-trifluoroethyl) ester established by Still⁸⁶ or bis(O-aryl)phosphonates offered by Ando.⁸⁷ Furthermore, it is well documented that the standard conditions originally in place can be modified as well with adequate success.⁸⁵

The palladium-catalyzed cross coupling reaction of boronic acid in the presence of organic halides is labeled the “Suzuki coupling” and is another means by which organic chemists are able to accomplish C-C bonds.⁸⁸ The originator of this method, was Akira Suzuki in 1979.⁸⁹ Palladium-catalyzed cross couplings in organic synthesis were pioneered by Suzuki, Ei-ichi Negishi, as well as Richard Heck, and they were jointly awarded the Nobel Prize in chemistry in 2005 for their efforts.⁹⁰ One of the differences between the Suzuki and Negishi coupling reactions is the use of either Nickel (Ni) or Palladium (Pd).⁹¹ Moreover, Negishi reactions are more commonly used in the synthesis of acyclic di, tri, and higher order terpenoid systems, over Suzuki reactions.⁹²

Similar to HWE reactions, the Suzuki reaction is commonly employed to synthesize poly-olefins,⁸⁹ but with different substrate requirements. However, it is also used in reactions with styrenes, a precursor to plastic,⁹³ and substituted biphenyls are also coupled by this method.⁹⁴ It also shares the feature of its employment in the synthesis of complex compounds from smaller ones, which is advantageous for pharmaceutical agents in drug development.⁹⁵ For example, Caparratriene is an active compound isolated from the oil of *Ocotea caparrapi* tree, that is native to Colombia.⁹⁶ The oil is locally used in Colombia for remedies in treatment of a various ailments, and Cytotoxicity studies of the oil using human leukemia cells (CEM) showed considerable inhibition of growth at concentration when suspended in DMSO.⁹⁶ The key step in the synthesis of this compound uses the Suzuki reaction for coupling of the E-vinyl borane with E-2-bromo-2-butene that successfully generated isomerically pure caparratriene.⁹⁷ This infers the practicality of this reaction in chemical synthesis of C-C bond formation.

The general scheme for the Suzuki reaction (displayed in **figure 14**) employs a Pd catalyst, in the 0 oxidation state and a base, in the presence of a phosphine ligand (L_nPd^0) to facilitate the coupling of a organoboron species (RBR''_2) with a halide ($R'X$) to form a single carbon-carbon bond.⁹⁸ The reaction method is known to be less toxic and contain more functional group tolerance than its other organometallic predecessors. While having similar commercial availability options.⁹⁹ In addition, the Suzuki coupling is quite versatile with respect to the number of reaction conditions that it can be utilized in. For example, running the Suzuki coupling reaction in a micellar solution using TPGS-750-M, a designer surfactant, introduced by Bruce Lipshutz, enhances the yield and drastically diminishes the environmental contour it produces, or E factor, of the reaction.^{59, 100}

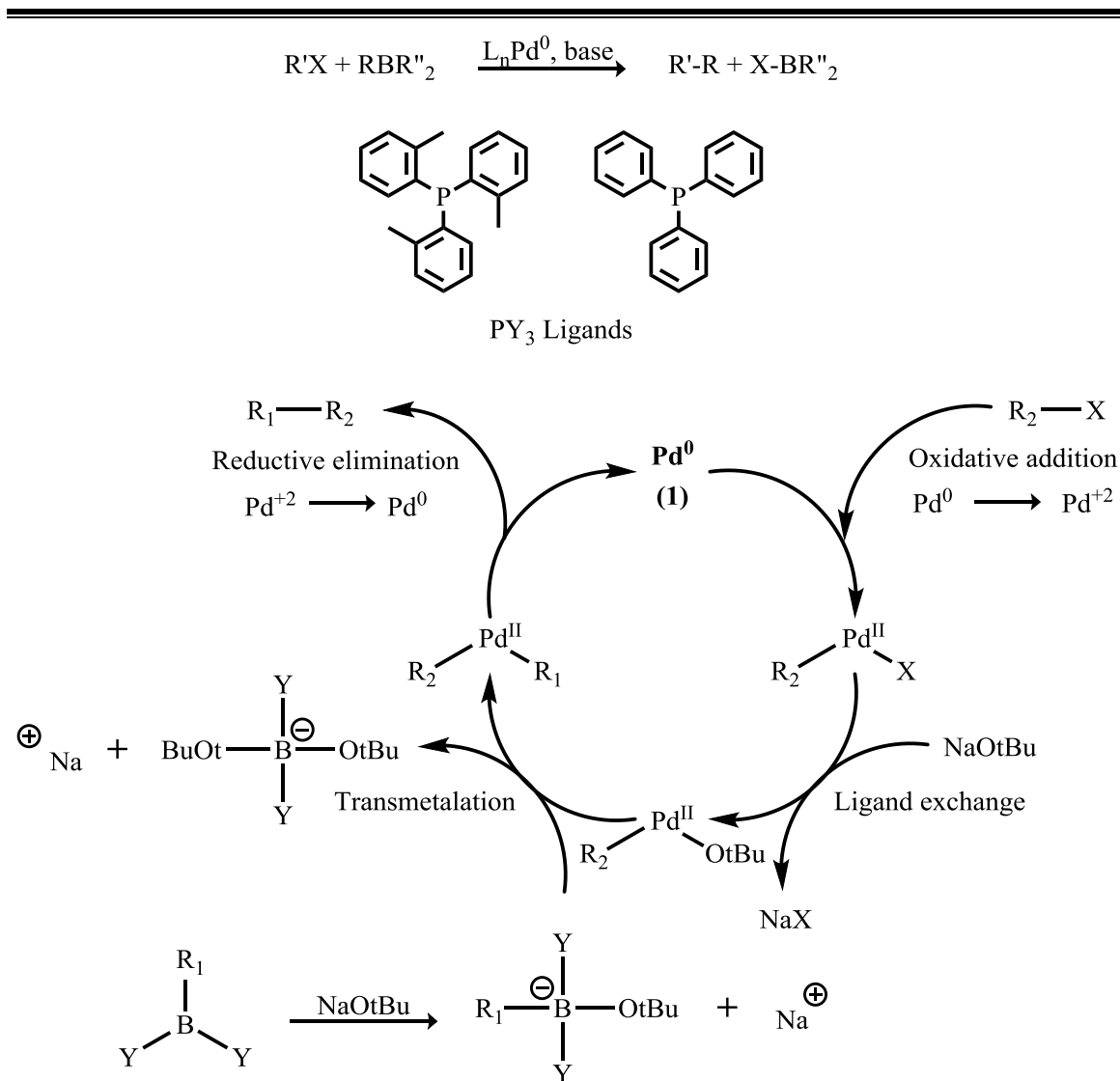
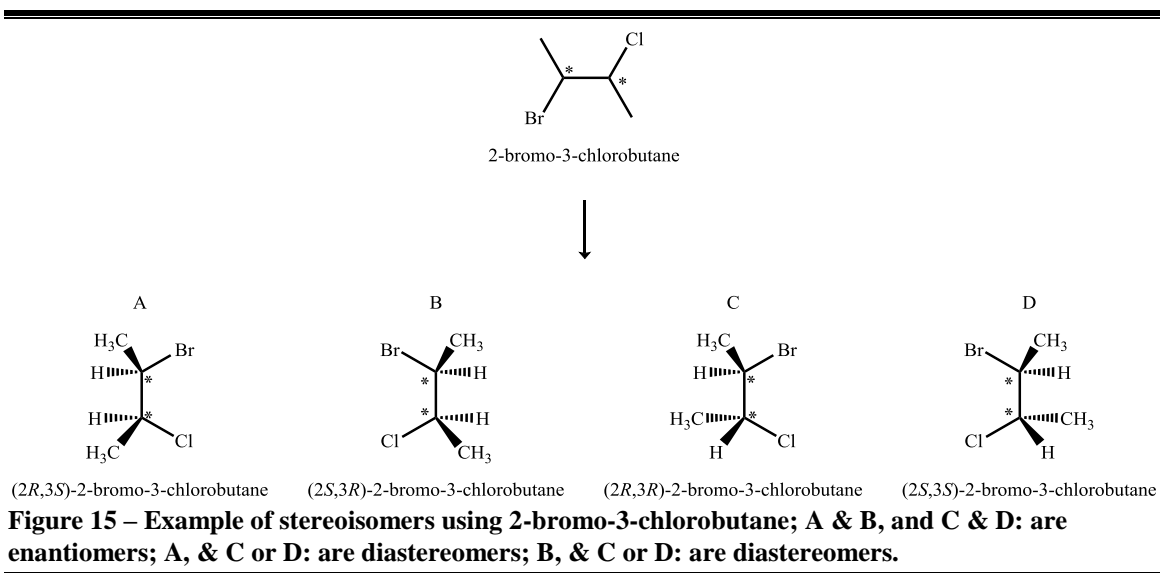


Figure 14 - General Suzuki reaction scheme with ligands below and catalytic cycle with Palladium

Stereochemistry and Regiochemistry

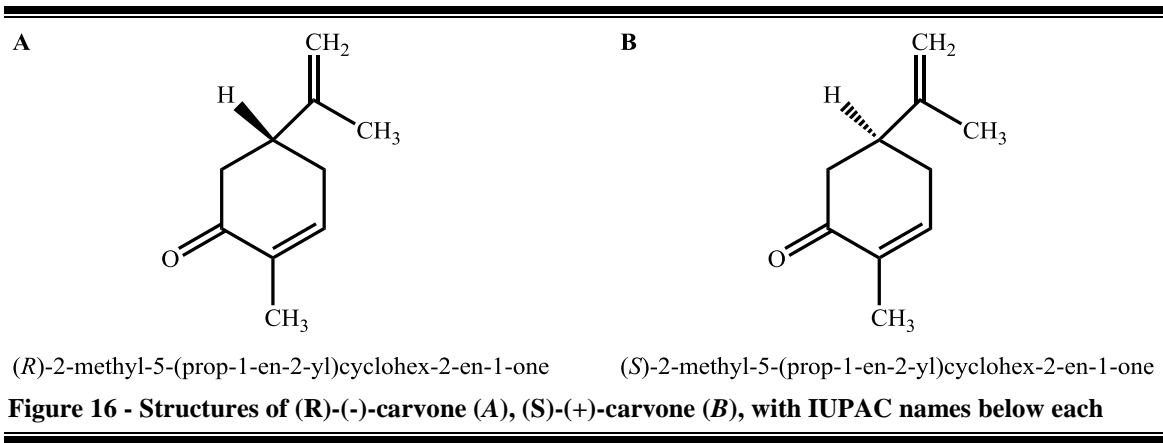
Although C-C bond formation is one of the foundations to organic chemical synthesis. It must be noted that physical and molecular properties can be expressed differently based on the stereochemistry of a compound. Furthermore how a compound participates in a reaction is a concept of regiochemistry.

A corollary of the tetrahedral arrangement of bonds to carbon is that two compounds may be different because the arrangement of their atoms in space is unlike. Stereoisomers have the same constitution but differ in their atomic spatial arrangement.¹⁰¹ For example, in **figure 15**, 2-bromo-3-chlorobutane have various confirmations in which it can assume, with some being enantiomers and others diastereomers.



Although the physical properties, such as density, melting point, and boiling point, can be relatively identical in most cases (*cis*- vs *trans*-2-butene being an exception¹⁰²). However, the difference in the relative spatial arrangement of atoms that

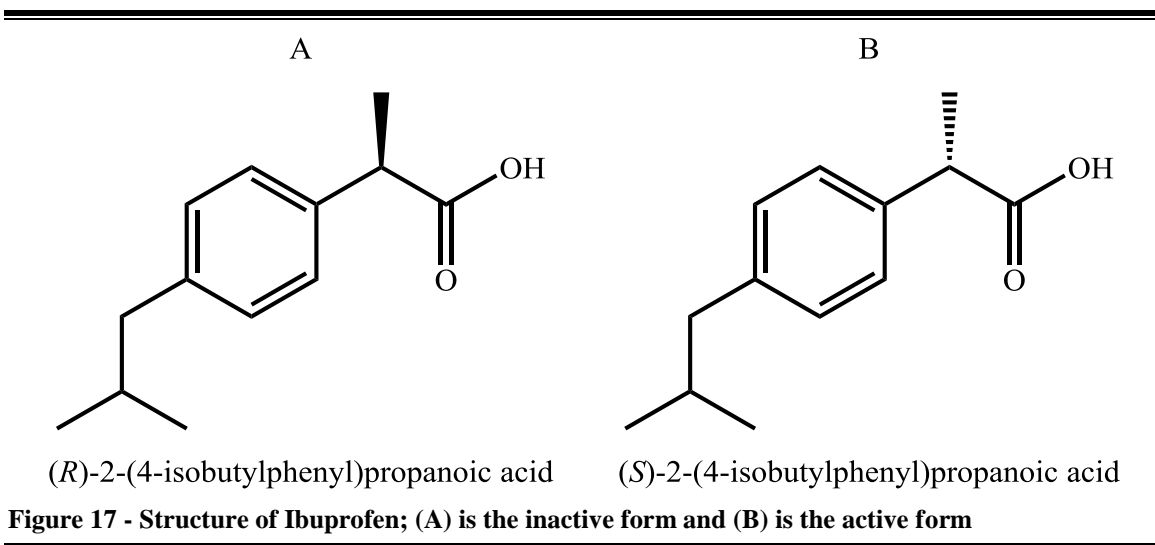
form the structure of molecules governs how molecules interact and their manipulation by other compounds in a reaction mixture.¹⁰³ The enantiomeric configurations of Carvone presents a comprehensible instance where this is made apparent (see **figure 16**).



The (S)-(+)-carvone, is a major component of caraway oil and its enantiomer conformation, (R)-(-)-carvone, is the primary constituent of Spearmint oil.¹⁰⁴ Although structurally similar, except at its chiral center, have different odors. The disparity in expression of these two enantiomers is due to the divergence in behavior toward receptor sites in the nose.¹⁰⁵ These receptor sites are themselves chiral and are innately stereoselective in the compounds that they will bind with.¹⁰¹ This illustration shows how the difference in stereoisomers modifies how two enantiomers accommodate to their environment.

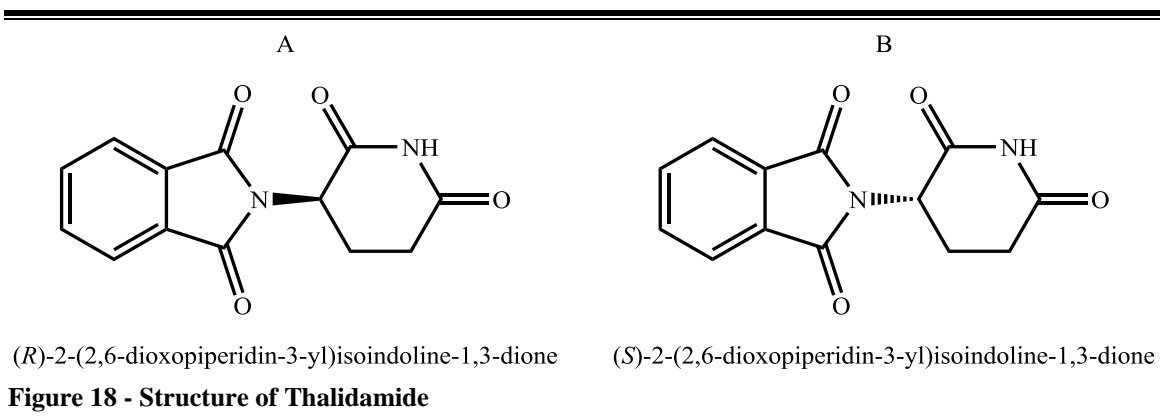
The high degree of chiral recognition inherent in most biological processes has prompted a number of considerations ranging from safety and efficacy to synthetic methodology, thereby requiring more chiral synthetic drugs become available in enantiomerically pure form.¹⁰⁶ Most naturally derived drugs are chiral and are already

extracted as a single enantiomer from the source instead of as a racemic mixture.¹⁰¹ Although the desired therapeutic activity resides in one of the enantiomers, many synthetically prepared drugs are administered as racemic mixtures. Although in some of these racemic drugs, the inert enantiomer is relatively benign. In the case of over the counter Ibuprofen, the (S) active form is responsible for the analgesic/anti-inflammatory effects and the (R) enantiomer is inert (see **figure 17** for structure). However, it is eventually metabolically converted through Lipase enzyme-catalysis in the body to the active (S) configuration.¹⁰⁷



However, this relatively benign effect is not always the case, as the frequently documented circumstance of thalidomide. Thalidomide is a pharmaceutical drug prescribed for the treatment of morning sickness in pregnant women¹⁰⁸ (see **figure 18** for structure). The drug was discovered to be teratogenic, producing harmful genetic modification to early embryonic development, leading to severe limb deformation in neonates.¹⁰⁹ There are various mechanisms proposed to explain the biological role for

both the (R)- and the (S)-thalidomide enantiomers.¹¹⁰ Pharmacokinetically thalidomide undergoes racemization: even if only one of the two enantiomers is administered as a drug, the other enantiomer is produced as a result of metabolism.¹¹¹ Thalidomide is currently used for the treatment of other diseases, most notably cancer.¹¹² This tragedy initiated the involvement of the Food and Drug Administration to develop strict guidelines requiring testing of drugs prior to making them accessible to the public.¹⁰⁶ These guidelines encouraged drug design that specifically focused on methods to synthesize the desired enantiomer, but left the option available for the approval of new drugs as racemic mixtures under special circumstances.¹¹³



The implications in synthetic organic chemical reactions is because during experiments, in the absence of other chiral molecules, reactions will generate achiral products or racemic mixtures.¹⁰¹ Functional groups such as Carbocations and alkenes, which are both planar, are attacked from either face in equal amounts generating racemic product mixtures.¹¹⁴ Since the faces of the systems are equivalent and there is nothing to distinguish them then the probability of interaction is generally the same. In order to

create non-racemic products, a chiral influence must be used in the form of the starting material, a reagent, a catalyst or even during purification.¹⁰¹ In either circumstance the general implication is that more reliable methods to produce higher yield of enantiomerically pure product is imperative to the organic synthesis.

Essentially, research into methods for executing syntheses of single stereoisomers is critical due to the obligation to produce optically pure pharmaceutical products, particularly where one enantiomer is more effective than the other.

In chemistry, regioselectivity is the process that favors bond formation at a particular atom over another possible atom.¹¹⁵ The concept concerns the various probable positions a reagent will affect a compound in a reaction procedure, such as which Hydrogen will be deprotonated by a strong base from an organic molecule, or the most favorable position of insertion of an additional substituent on an already substituted benzene ring.^{115, 116} This application of rules associated with reaction predictability based on the stability of a molecule relative to the point of incidence where two molecules possibly interact. The complexity of the topic is abstract and goes beyond the scope of this topic; therefore, the significance is better described by the description of what it implies in organic synthetic processes. Such as the potential to impact two adjacent carbons, like in addition reactions of C-C bond formation. In this instance, if two new single bonds are formed from two separate atoms, then the potential to form isomers exists and one isomeric configuration has priority over the other, or one form is the dominant form due to regioselectivity.

The most notable concept that applies is Markovnikov's rule¹¹⁷ that states, "With the addition of a protic acid (HX) to an unsymmetrical alkene, the acid hydrogen (H)

becomes attached to the carbon with fewer alkyl substituents, and the halide (X) group becomes attached to the carbon with more alkyl substituents.” The basis for this rule is the formation of the most stable carbocation during the addition process¹⁰¹ (see **figure 19**). Essentially, a positive charge is produced on the opposing carbon when a hydrogen ion undergoes addition to one carbon atom of an alkene, forming a carbocation intermediate. The more substituted carbon element has more stability due to induction and hyperconjugation. The major product of the addition reaction is predicted to be the carbocation with the most stable intermediate. However, the other less substituted, or less stable, carbocation will still be formed, but at less appreciable yield.

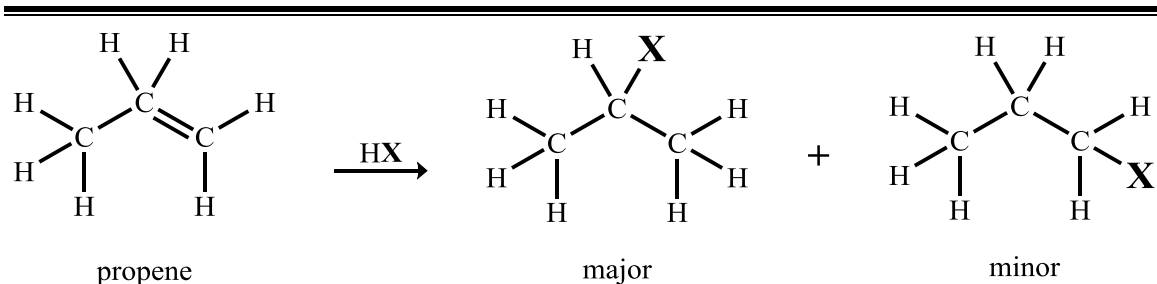


Figure 19 - General example of Markovnikov addition

An example can be ring-forming reactions using Baldwin’s rules, which are notably familiar processes in organic chemistry. The application of a set of simple rules (or predesignated constraints) is useful in predicting the relative capability of different ring closures; therefore, suitable preparation can negate potential problems to organic chemists, especially in planning syntheses.¹¹⁸ Furthermore, these rules help to specify that certain experiments are favored over others; which may be helpful to define more precisely their limits. The rules are of a stereochemical nature, thus these designs benefit

synthetic chemists in both planning syntheses and examination of unsuccessful constructs. Which is a common occurrence in all scientific disciplines, not solely limited to organocatalysis.

Regioselectivity extends to other disciplines as well. For example in molecular biology cyclin dependent kinases (CDK) are central for the processes of cell division and proliferation. Correspondingly, innovation into the development of synthetic CDK inhibitors for the treatment of cancer and other proliferative diseases is currently being done.¹¹⁹ More specifically, a report on the synthesis and inhibitory actions of purine derivatives against CDK₁ demonstrated that among these purines, the ortho hydroxyl substituted benzyl purine displayed greater activity towards the enzyme CDK₁ than its meta and para substituted counterparts.¹¹⁶ Therefore the synthetic approach was designed utilizing regioselective protection as the key step in the syntheses of the desired methyl benzoate.

This is shown in the reaction procedure by acylation of a compound predominating at hydroxyl groups that were meta and para to the carbomethoxy group and not the ortho substituted hydroxyl group of the benzoic acid substrate to be modified. Therefore, protecting groups¹²⁰ were introduced to the meta and para substituted hydroxyl groups to destabilize their reactive intermediates, ameliorating their regioselectivity in the reaction. The steric hindrance between the bulky protecting groups on the meta and para positions facilitated favorable conditions for O-methylation of the ortho-substituted hydroxyl group, converting it from the minor form to the dominant form. After this step the meta and para groups were deprotected yielding the desired methyl benzoate.¹²¹

Molecular regioselective predictability permitted for strategic planning to be used to ameliorate the inadequate yield of the desired product by revealing that the reaction conditions could be manipulated effectively to obtain the preferred construct. The ability to anticipate pitfalls in organic chemical synthesis in this approach is vital to generating the enantiomerically pure compounds required for pharmaceutical purposes and concomitant production of adequate quantitative yield of the preferred stereo- & regioselective product.¹²²

The Major Advantages of HuaCat®

A preponderance of chemical substances that are molded and fragmented in metabolic processes are optically active, and typically one specific enantiomer is shaped in these processes; therefore, affording their abundance in nature.¹²³ As a consequence of the stereoselectivity associated with these processes in biological systems, it is not mutually exclusive that it has also been observed on numerous circumstances that the physiological activity expressed of a particular compound resides almost exclusively in one of its optically active forms.¹²⁴ The scientific and the practical significance of methods for the research of specific optical isomers is relatively discernable.

The conventional chemical resolution system agonizes from the detriment of yielding theoretical maximums of approximately 50% of the required optically active isomer established by the racemic starting material. Treatment of the racemic mixture with reagents of biological origin such as, microbiological enzymes, is an alternate procedure that exists with relatively similar disadvantages.¹²⁴ Divergence from this regularity stems from the induction of an asymmetric synthesis that can theoretically

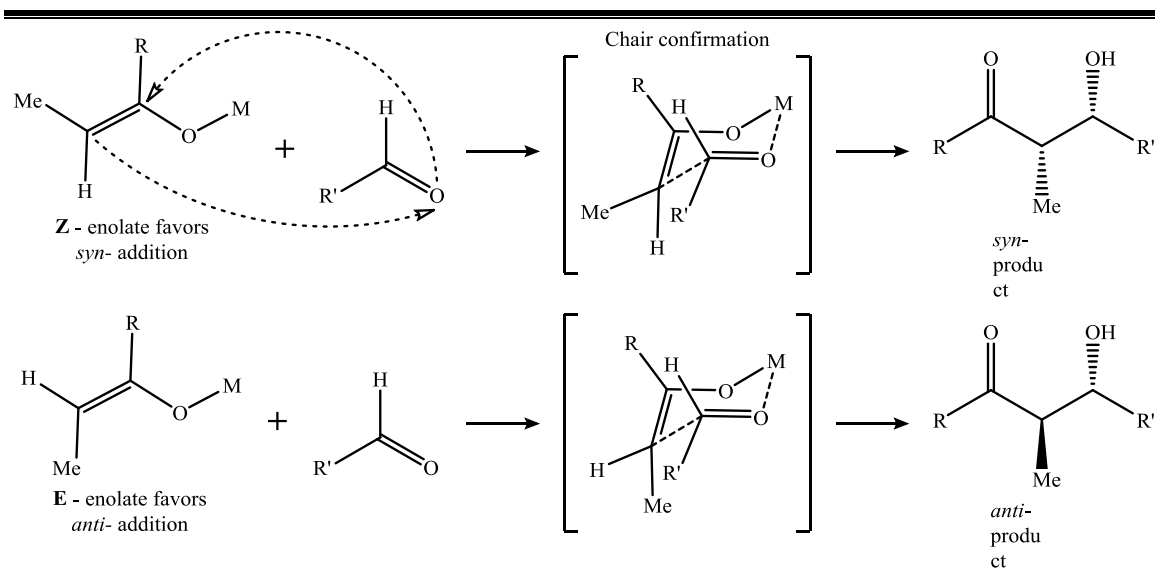
result in yields approaching 100% of simply one enantiomer.¹²⁵ Its significance is manifested through the copious amounts of journal articles and chemical literature demonstrating its magnitude.¹²⁶ The description of laboratory results with reactions producing one diastereoisomeric pair of a given structure is termed “stereoselective syntheses,” and is sometimes referred to as, “asymmetric syntheses” in some circles.¹²⁴

In parallel with the aforementioned concept that stereoselective reactions are critically important in the field of organic chemistry. There are numerous accounts of pharmaceutical therapeutics that have complex stereochemistry as key parts of their pharmacophore.¹²⁷⁻¹³⁰ Researching methods for forming selective carbon-carbon asymmetric bonds can have a large impact on drug discovery¹³¹ and human health.⁹

Considering this rational and that organocatalysis has gained the notice of the synthetic pharmaceutical population. Research in this area has been stimulated by stereoselectivity¹³² that can be produced in mild reaction conditions,¹³³ with relative ease of execution,¹³⁴ and extensive array of feasible chemical transformations.¹³⁵ Proline (Pro) as an organocatalyst,¹³⁶ has drawn noteworthy consideration in this area, markedly in the role of facilitating aldol reactions.¹³⁷ Pro has been used in the development of broad scope aldolase antibodies that show very high enantioselectivities¹³⁸ and it has been postulated that they proceed via an enamine mechanism.¹³⁹ Asymmetric small-molecule aldol catalysts that use an enamine mechanism have great potential in the discipline of organic chemical synthesis.¹⁴⁰

Explicitly, the proposed mechanism for Pro catalysis follows the Zimmerman-Traxler model for aldol reactions.¹⁴¹ This model suggests that the transition states of certain aldol reactions have six membered intermediates that display chair conformations

facilitated by intramolecular dipole-dipole bonding.¹⁴² **Figure 20** displays a general view of how the chair confirmation may look.



It is well documented that proline can undergo an assortment of reactions with aldehydes that are aliphatic¹⁴³ and aromatic¹⁴⁴ compounds. Although there are ketone side products this can be ameliorated with high concentration of a polar aprotic solvent, such as acetone or Dimethyl sulfoxide (DMSO);¹⁴⁵ however, this is problematic due to the high cost of solvents and the environmental difficulties that come with the removal of waste products.¹⁴⁶ Moreover, the yield is still relatively low at 68% as a racemic mixture.¹⁴⁵

The established reaction stereochemistry in the Zimmerman model, E-enolates (or trans for relative stereochemistry) have a tendency to generate anti-addition products with the two groups of higher priority added to opposite sides (or faces) of the newly formed carbon bond, essentially resulting in a reduction in bond order but a rise in the number of

substituents. In direct contrast, Z-enolates (cis) have a higher reaction propensity towards syn-addition products. The factors that control selectivity are the preference for placing substituents equatorially in six-membered transition states and the avoidance of syn-pentane interactions, respectively (See **figure 21** for proposed mechanism of interaction). Generally the use of metals such as lithium and boron are used for this enolate mechanism of aldol reactions and thereby reliably follow the Zimmerman–Traxler model.¹⁴⁷ However on occasion metals can be relatively unpredictable with respect to their stereochemical results.¹⁴⁸

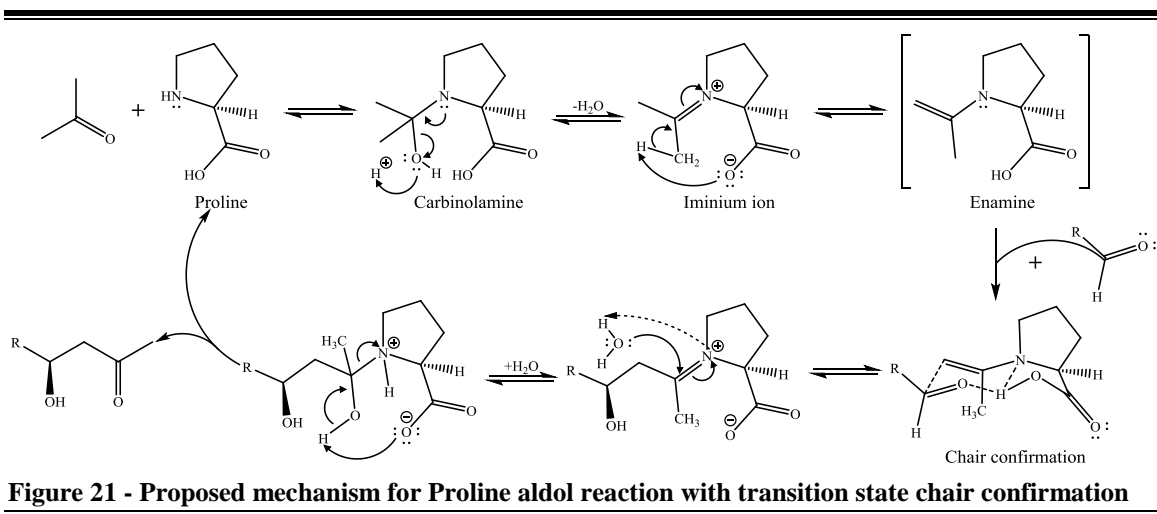


Figure 21 - Proposed mechanism for Proline aldol reaction with transition state chair confirmation

The exploration of Pro as an organocatalyst was initiated due to: (1) its nature for being an optically active pyrrolidine derivative. (2) The asymmetric carbon atom is in the same molecule next to the functional groups. (3) The asymmetric carbon atom is in a five-membered ring. The cyclic system provides amplified rigidity that typically augments the optical rotatory power; therefore, concomitant rise in the stereoselectivity of the asymmetric reagent can be anticipated. (4) The facile addition of the optically

active reagent on various positions of the reacting symmetrical construct facilitating differentiation of identical groups. This is facilitated by the addition of various functional group substituents to impart a transient disposition with respect to reaction conditions. (5) Furthermore, the isoelectric point of proline at pH 6.30 is ideal for limiting the formation of unwanted side products such as ketols.¹²⁴

The exploration of Pro as an organocatalyst was initiated due to: (1) its nature for being an optically active pyrrolidine derivative. (2) The asymmetric carbon atom is in the same molecule next to the functional groups. (3) The asymmetric carbon atom is in a five-membered ring. The cyclic system provides amplified rigidity that typically augments the optical rotatory power; therefore, concomitant rise in the stereoselectivity of the asymmetric reagent can be anticipated. (4) The facile addition of the optically active reagent on various positions of the reacting symmetrical construct facilitating differentiation of identical groups. This is facilitated by the addition of various functional group substituents to impart a transient disposition with respect to reaction conditions. (5) Furthermore, the isoelectric point of proline at pH 6.30 is ideal for limiting the formation of unwanted side products such as ketols.¹²⁴

Notwithstanding Pro's effective enabling of organocatalytic activity, it has its limitations.¹⁴⁹ Accordingly, an assortment of Pro mimetics are concomitantly being designed to furnish enhanced reactivity profiles.¹⁵⁰ Two frequently commissioned classes of note are the tetrazoles,¹⁵¹⁻¹⁵⁴ shown in **figure 22A**, and sulfonamides¹⁵⁵⁻¹⁶⁰ in **figure 22B**. The use of 4-trans-hydroxyproline derivatives is prevalent in organocatalysis;¹⁶¹ however, only one enantiomer of trans-hydroxyproline is facilely accessible which poses

another obstacle to these substrates; therefore, more considerably diverse structures are required for facile use.



Figure 22 – Tetrazole (A); Sulfonamides (B)

In addition, organocatalyzed reactions containing proline or proline surrogates utilize polar solvents such as DMF and DMSO.¹⁵⁷ Although universally employed in research laboratories, their polarity generates additional obstacles for product separation and purity. The industrial application of nonpolar solvents are valuable because they provide reliable phase splits with water and can be recycled to a limited scale.¹⁶²⁻¹⁶⁶

The use of solvents typically accounts for approximately 80% of the mass of a reaction in a conventional pharmaceutical batch chemical operation.¹⁶⁶ Furthermore, solvents are one of the principal players in the overall toxicity profile of a reaction procedure.⁵⁵ Yet, for synthetic organic chemists, solvents are classified as the medium in which a reaction takes place and are not typically included as reactants in the stoichiometric sense because the focus is in the formation of the anticipated compound, not in the instrument by which it is carried out.¹⁶⁶

It must be noted that the need for inexpensive materials is part of the bottom-line to any industrial and laboratory budget; therefore, proline mimetics should be reasonably priced and readily accessible in both enantiomeric forms. Thus, the development of a pragmatic solution for these tasks is persistently explored. However, there is a highly practical and readily available proline surrogate called HuaCat®, developed by Dr. Rich Carter of Oregon State University. It displays enhanced solubility properties in conventional nonpolar organic solvents.¹⁶⁷ HuaCat® is a proline mimetic sulfonamide-based catalyst.

HuaCat® has proven to be an effective catalyst for asymmetric aldol reactions (**A**), a reaction where the enolate of an aldehyde or ketone is alkylated at the α -carbon by a carbonyl of another molecule producing a β -hydroxy carbonyl compound with two newly formed stereocenters,¹⁶⁷ (**figure 23A**). HuaCat® can also mediate Mannich reactions (**B**), an organic reaction which consists of an amino alkylation of an acidic proton placed next to a carbonyl functional group by formaldehyde and a primary or secondary amine or ammonia,¹⁶⁸ (**figure 23B**). HuaCat® facilitates these reactions with high stereoselectivity in aqueous conditions. Additionally, intramolecular Michael additions (**C**), or cyclization of keto sulfones are also facilitated by HuaCat®, allowing for the synthesis of five and six-membered rings with good yield and stereoselectivity,¹⁶⁹ (**figure 23C**).

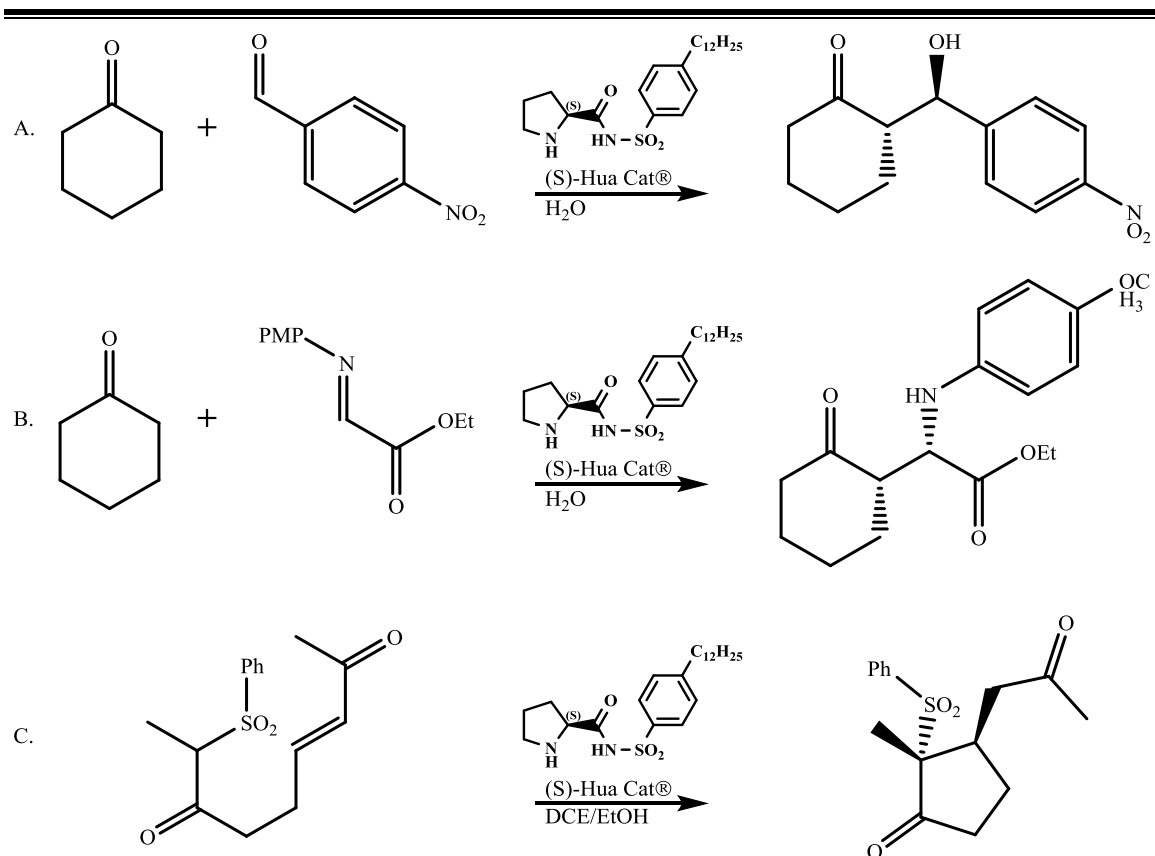


Figure 23 - HuaCat® facilitated asymmetric reactions: (A) Aldol reaction (B) Mannich reaction (C) intramolecular Michael addition

Since the goal of various research studies is to synthesize compounds with highly accurate stereo specificity through chiral affects from catalysts, reagents, and inexpensive solvent systems. It is prudent to discover more mechanistic avenues for selective addition of C-C Asymmetric bonds.

The major purpose of this experiment is to substitute select moieties on the Hua Cat catalyst with different electron withdrawing/donating groups and observe their Asymmetric induction of Carbon bonds in aqueous conditions. The hypothesis for the proposed research is that the substitution of the current alkyl moiety with a trifluoro, iodo, or dodecane functionality, in the Ortho position rather than the Para position, can

offer another mechanism and increase catalytic yield of stereospecific compounds in aqueous conditions for a wider range of substrate starting materials. (see **figure 24** for product structures)

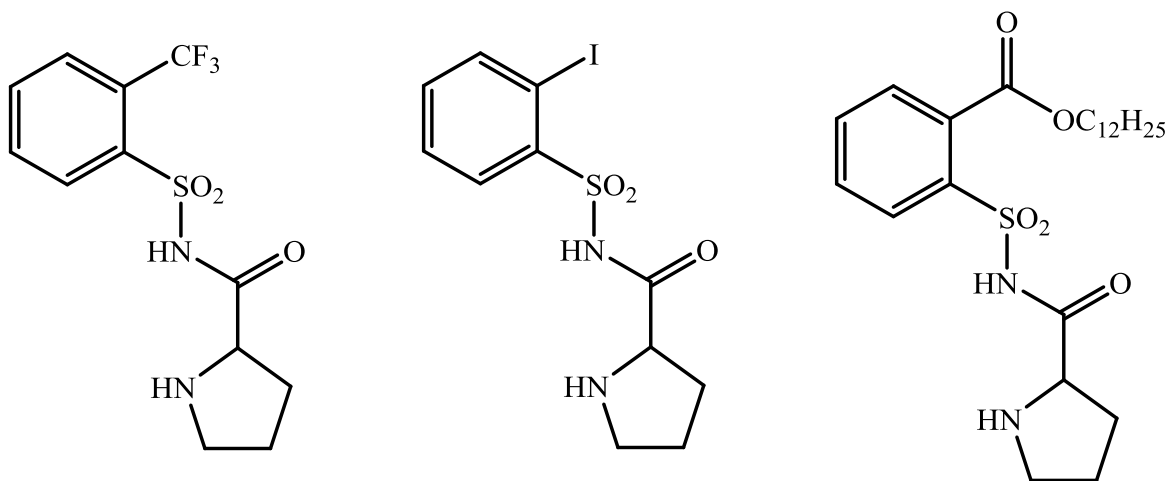


Figure 24 - Desired products

We hope to observe the effectiveness of the proposed catalyst through:

First, synthesizing the proposed compounds in high yield. Second, characterization of the compounds synthesized. Third, the use of the various catalysts in chemical reactions to observe their effectiveness relative to current compounds in use as reagents for chemical Asymmetric induction. The search for novel catalytic reagents is highly desired; with the aforementioned experiments we can preferentially formulate chemical reactions with one stereoisomer over another by broadening the chiral features that affect asymmetrically induced chemical reactions.

CHAPTER TWO

MATERIALS AND METHODS

General

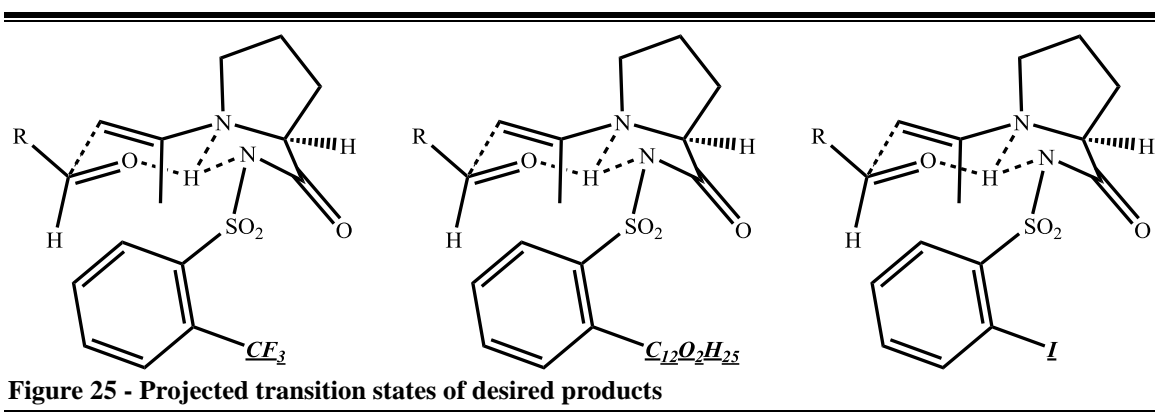
All reactions involving air- and moisture –sensitive compounds were carried out under a dried argon (Ar) atmosphere with standard Schlenk and vacuum-lines. All glassware was oven dried at $\geq 110^{\circ}\text{C}$ for ≥ 6 hrs or flame dried under vacuum and purged with Ar three times. Reactions were performed in Teflon tape sealed round bottom flasks and pigment-free, filler-free septa sleeve stoppers with reactions mixtures ensuing agitation via oven dried magnetic stir bars. Chemicals and solvents were purchased from commercial suppliers at $\geq 98.9\%$ purity as certified ACS reagent grade from Fisher Scientific (Fair Lawn, NJ) and Sigma Aldrich (Milwaukee, WI), without further purification. Thinlayer chromatography (TLC), was performed on silica gel plates (Merck, silica gel 60 F₂₅₄). Concentration of compounds was accomplished using a Büchi Rotary Evaporator (Rotovap) at appropriate solvent conditions with reduced atmospheric pressure and water bath at an average temperature of 40°C . Flash column chromatography was carried out with Grace Discoveries Reveleris flash purification system with Reveleris® silica gel with an average particle size of $39.1\ \mu\text{m}$ and a pore diameter of 65 angstrom. All compounds were visualized by irradiation with UV light and/or by treatment with a solution of phosphomolybdic acid (25 g), $\text{Ce}(\text{SO}_4)_2 \cdot \text{H}_2\text{O}$ (10 g), concentrated H_2SO_4 (60 mL), and H_2O (940 mL) followed by heating or by treatment with a solution of p-anisaldehyde (23 mL), concentrated H_2SO_4 (35 mL), acetic acid (10 mL), and ethanol (900 mL) followed by heating. ^1H NMR spectra were measured on a Bruker AM-300 spectrometer in CDCl_3 or acetone-d₆ with tetramethylsilane (TMS) as

the internal standard, where J (coupling constant) values are estimated in Hz. Spin multiples are given as s (singlet), d (doublet), t (triplet), q (quartet), m (multiplet), and br (broad).

CHAPTER THREE
SYNTHETIC STRATEGY, RESULTS, & DISCUSSION

Design Strategy

The main goal of the project is to make ortho-substituted HuaCat® derivatives with strong electron-withdrawing functional groups. Although a method has been established for making HuaCat® and other para-substituted HuaCat® derivatives, there is currently no reliable method for making the ortho-substituted analogous structures. The few relevant methods in the literature do not account for strong electron-withdrawing effects of the sulfonamide substrates rendering them much less nucleophilic than an unsubstituted sulfonamide. The development of the organocatalytic HuaCat® analogues began with the base proline structure and the attempted manipulation of the intramolecular forces that are displayed in the chair transition state model seen below in **figure 25**. The project had 3 different design phases based on the results of the respective previous designs.



Our initial experiments were based on the original synthetic route for a mainstream peptide coupling reaction with three marked regions of divergence that would serve to precede us through the design of further analogues after the initial brand originated from the master model of HuaCat®. The three building blocks, in **figure 26**, represent the areas where manipulation will occur. First, the substitution of an electron withdrawing/donating group at position 7 of building block 1. Second, is the rearrangement of the sulfonamide from para to ortho, or its movement from position 3 to position 5. Lastly, is the varying protecting groups at position 17 of building block 3.

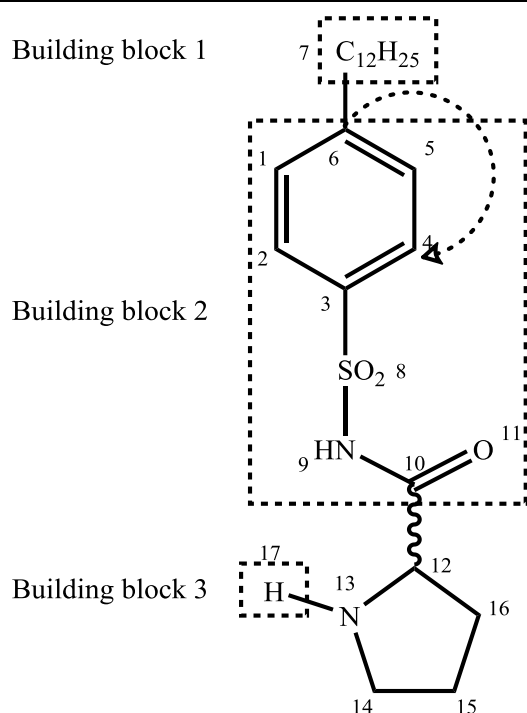
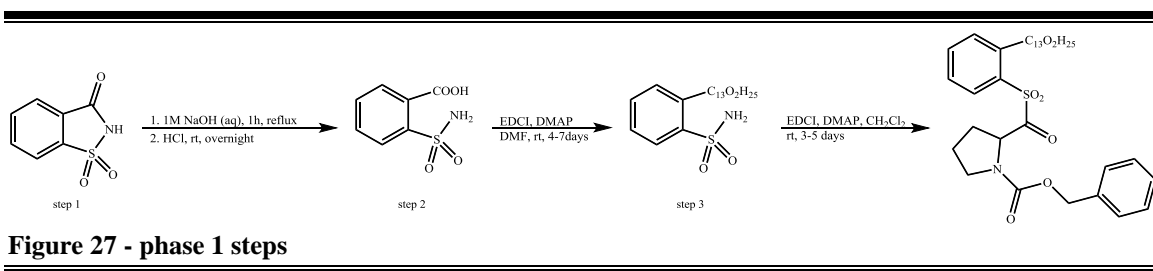


Figure 26 - Three building block regions of diversification

In the first design phase, we conducted base catalyzed break down of a larger molecule (compound 1/saccharin) in preparation for subsequent nucleophilic substitution

of the ester moiety to an activated iodododecane electrophile. Eventually leading to a standard peptide coupling on the activated Nitrogen (N) of the sulfonamide moiety to the electrophilic carbonyl portion of a Carboxybenzyl-protected L-proline (Cbz-L-Pro-OH), as outlined in the second step of **figure 27**. However, after attempted characterization of the final product, we concluded that this method was not efficient due to a lack of appreciable yield; therefore this route was abandoned and we proceeded on to our next phase of synthetic design.



In the second design phase, although it was understood that an ortho-substituted version would be appreciably less nucleophilic than the para-substituted compounds like HuaCat I & II. Moreover, it was noted that the steric hindrance would also be problematic to nucleophilic activation. However, to inductively rule out all possible barriers to success, we proceeded with the initial attempt utilizing similar reaction conditions to couple analogous starting materials to make the desired target compounds. As can be seen in **figure 28**, standard peptide coupling conditions were attempted.

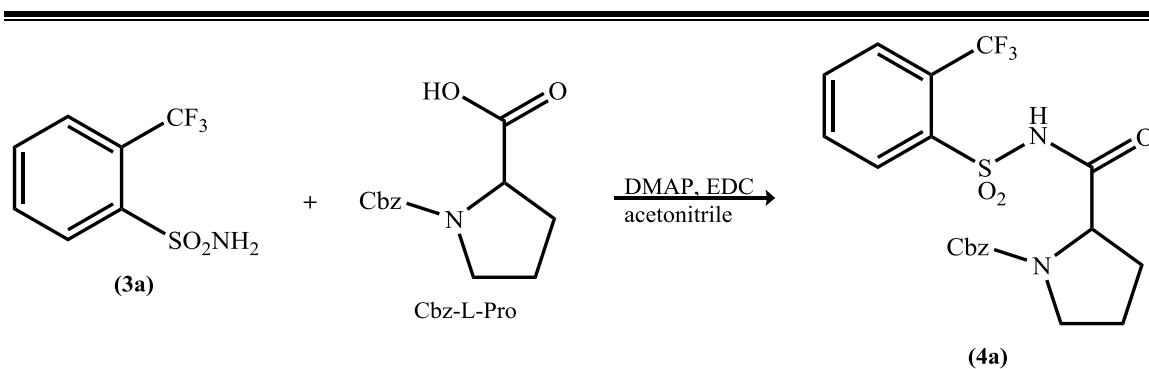


Figure 28 - Standard peptide coupling conditions

Essentially, this phase involved the purchase of sulfonamide, and corresponding carboxylic acid (Pro), starting materials to couple into the target compounds. Using NMR analysis of our product we concluded that the second design phase proved to be unsuccessful. We theorized that the CF₃ moiety created a heightened electron-withdrawing effect that deactivated the N portion of the sulfonamide nucleophile, thereby hindering its nucleophilic capability and preventing the reaction from moving forward. This led to the use of various coupling agents under the same reaction conditions to rule out the effectiveness of the reagents. This also comprised alternating various types of organic bases to ensure nucleophilic activation through deprotonation. This ruled out the propensity for one base over another under certain reaction conditions. It eventually came to include manipulation of reaction conditions in the form of temperature control, protic vs aprotic solvent usage, and various other strategies outlined in **Tables 1 & 2** referencing **figure 30**.

Despite copious manipulation of reaction procedure support elements, we were unable to ascertain the desired product and therefore aborted our second phase of experimental design strategy. Speculating that the ortho-substituted sulfonamide was

much less nucleophilic than the para-substituted sulfonamide, we moved towards an alternate design strategy. One that utilized the sulfonamide substrate as the electrophile rather than the nucleophile. In this phase, Thionyl chloride substituted starting material was coupled with the corresponding amido-substituted Prolinamide (Cbz-L-Pro-NH₂), as seen in **figure 29**.

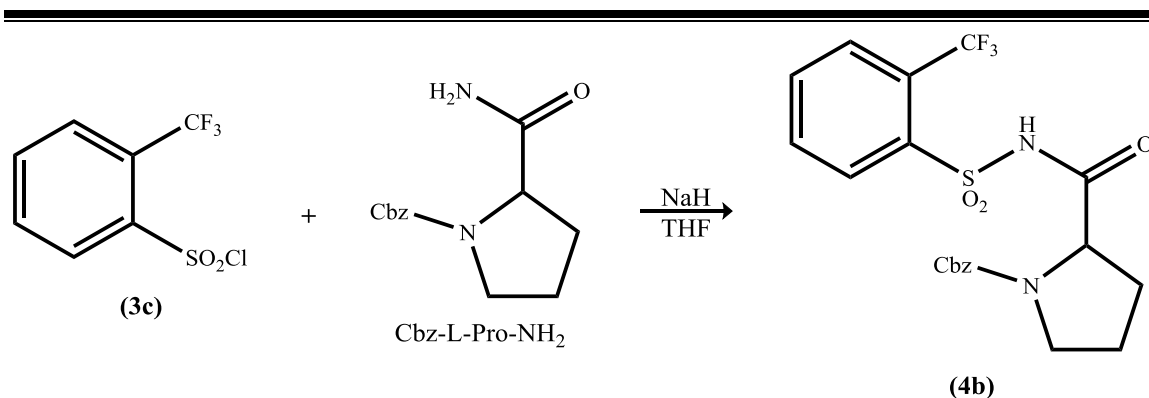


Figure 29 - Acid Chloride coupling reaction

As aforementioned, we attempted many different ways to construct the target derivatives. Some of the attempts included substrate changes from sulfonamides as nucleophiles to amides as nucleophiles, activating carboxylic acids for nucleophilic attack with many different peptide coupling agents¹⁷⁰ (EDCI, HOBt, HATU, etc.) and converting them to acid chlorides, the use of many different bases from mild to very strong, and increased reaction temperature with expanding reaction times.¹⁷¹⁻¹⁷⁵ To date, we have not been successful in constructing the target compound in appreciable yield.

The low yield of the product led to our third experimental design phase that involved a more indirect route through the use of a thiol substituted Benzene ring. Taking advantage of the increased electrophilic nature of the Thio-amine, relative to the

sulfonamide, we surmised that coupling the Carboxylic acid would be more feasible. Thereby allowing for higher yield of the target compound. After which we could oxidize the sulfur portion of the sulfo-amide converting it to the desired sulfonamide using a well-documented standard method with m-Chloroperoxybenzoic acid (MCPBA).^{176, 177}

We have attempted to synthesize HuaCat® ortho-substituted derivatives by reaction schemes outlined in **figure 30** following **Tables 1 & 2** reaction conditions. A more detailed explanation of each step will be presented in the experimental section.

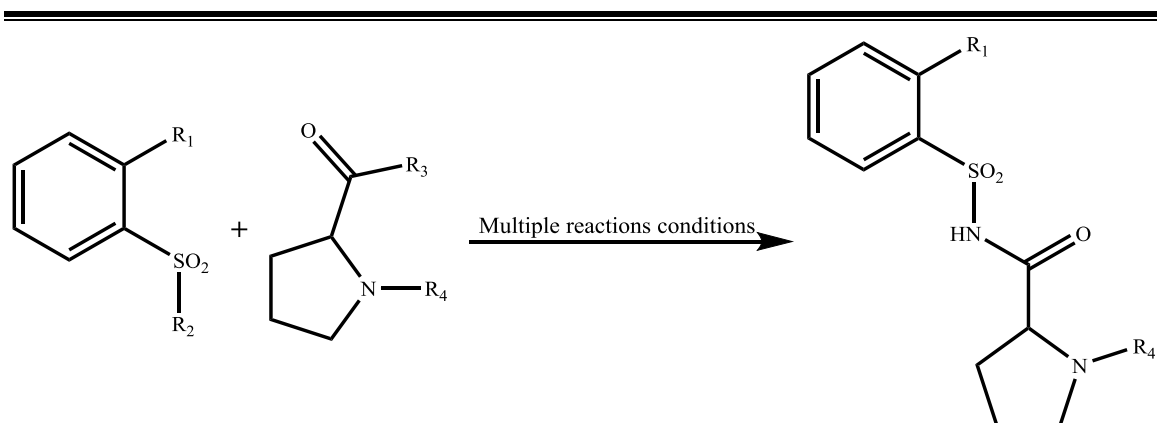


Figure 30 - General scheme for the formation of the desired organocatalysts

Table 1 - Sample of attempted reactions to achieve the desired final organocatalyst

R ₁	R ₂	R ₃	R ₄	Reaction Conditions
CF ₃	NH ₂	OH	Cbz, Boc, Fmoc	A, B, C, D
CF ₃	Cl	NH ₂	Cbz, Boc, Fmoc	B, D
CF ₃	NH ₂	Cl	Cbz, Boc, Fmoc	D, E
I	NH ₂	OH	Cbz, Boc, Fmoc	A, B, C, D
I	Cl	NH ₂	Cbz, Boc, Fmoc	B, D
I	NH ₂	OH	Cbz, Boc, Fmoc	D, E
C ₁₂ H ₂₅	NH ₂	OH	Cbz, Boc, Fmoc	A

Table 2 - Details of reaction conditions A-E

Reaction Condition A	Reaction Condition B	Reaction Condition C	Reaction Condition D	Reaction Condition E
EDC, DMAP, CH ₂ Cl ₂ rt, 72-120h	ZnCl ₂ , Benzoic anhydride MeCN, rt, 24h	H ₂ SO ₄ , Benzoic anhydride MeCN, rt, 24h	NaH, THF rt, 24h	Oxalochloride, MTBD Toluene, rt, 48h

Examination of Results & Discussion

The prevailing theory was that the common dynamics utilized to synthesize the original compound would again be applied to produce the analogue. Therefore, our initial protocol demonstrated as much; however, with different starting materials. Utilizing base catalysis that encompassed Saccharin as our starting material, with subsequent standard peptide coupling conditions¹⁷⁰ (EDC, DMAP, in DMF) of compounds that included Cbz-proline.¹⁷⁸ Followed by deprotection using activated charcoal as seen in **figure 31**.

However, this synthetic route was unsuccessful when we arrived at the third step that required the coupling of the Proline amino acid to the sulfonamide. Potentially due to the steric hindrance of the new position of the sulfonamide on the benzene ring. Rather than postulating the results with further experimentation we decided to explore other synthetic routes.

In light of this, we developed another unrelated synthetic scheme (**Figure 32**). First, a chemo-selective alkylation of a thiol using NaH followed by the formation of the thiol chloride and nucleophilic addition of ammonia should afford the benzenesulfamine.¹⁷⁹ The rationale behind this is that the thiohydroxylamine does not have the same acidic nature seen in the sulfonamide, potentially allowing for more reactivity that was hindered in previous experiments. We reasoned that the increased reactivity should tolerate the addition of the protected Proline-OH or Proline acid chloride peptide coupling.¹⁸⁰ Lastly, the oxidation of the thiol to the sulfone using *m*-chloroperoxybenzoic acid (MCPBA) yielding the desired product, before amino deprotection with Pd¹⁷⁸ on the Pro, is well documented.¹⁷⁶

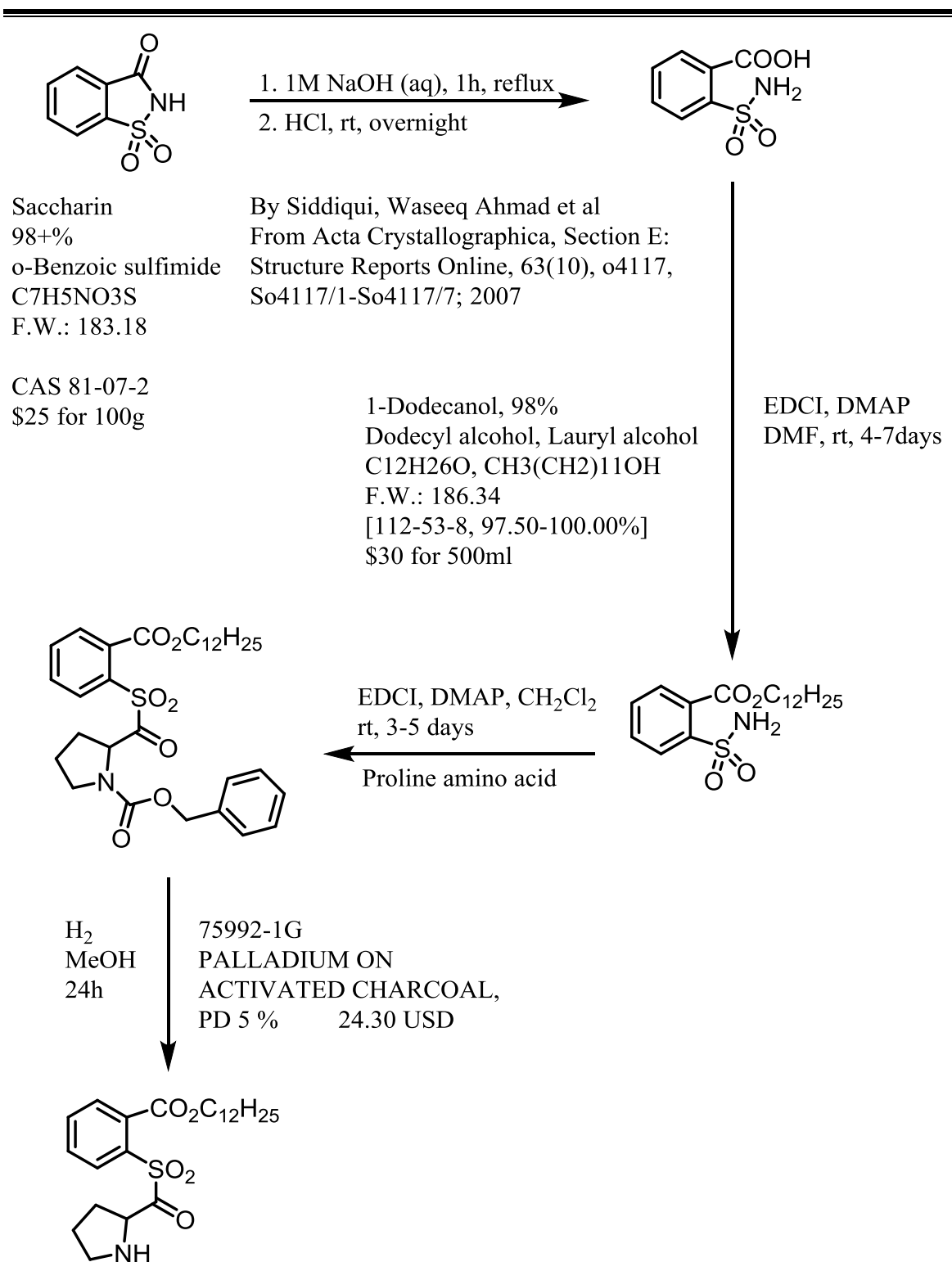


Figure 31 - Initial protocol for synthesis

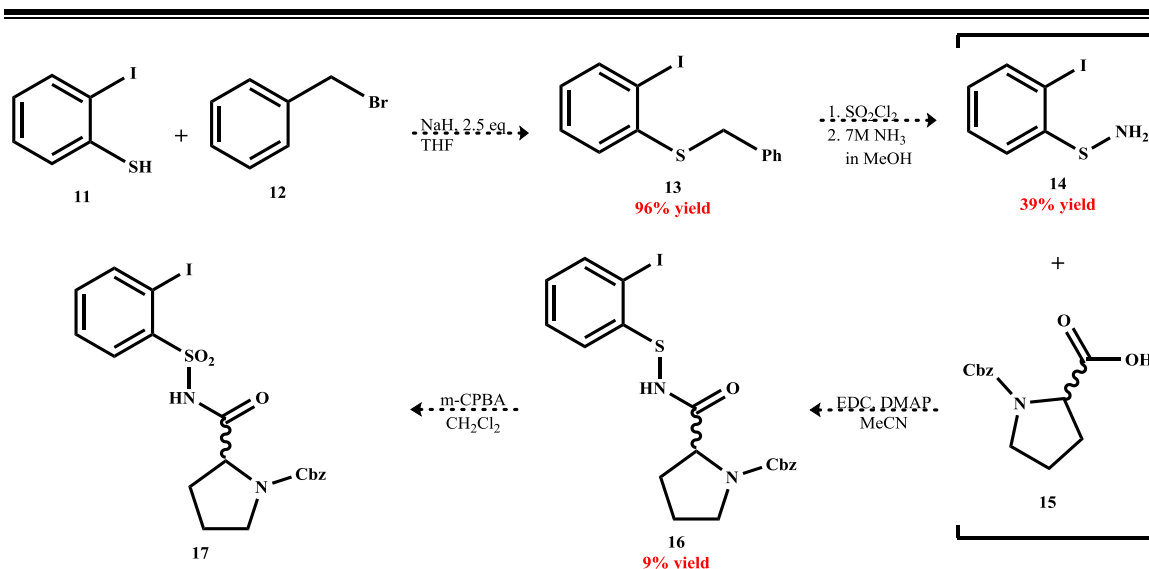


Figure 32 - Newly identified synthetic route to overcome the limitations of previous synthetic attempts

Conclusion

Although a method has been established for making HuaCat® and other para-substituted HuaCat® derivatives, there is currently no method for making the ortho-substituted analogous structures. The main goal of the project was to make HuaCat® derivatives with strong electron-withdrawing functional groups as a para-substituent. However we were unsuccessful at achieving this goal and are currently searching for other methods of obtaining this but are still deliberating on viable methods to accomplish this feat. The product can be synthesized via these routes however, the yield varies from 2-9 %. Unfortunately making it an undesirable amount relative to the cost, our test results vis-à-vis the desired standards for lucrative use in the laboratory.

Experimental Section

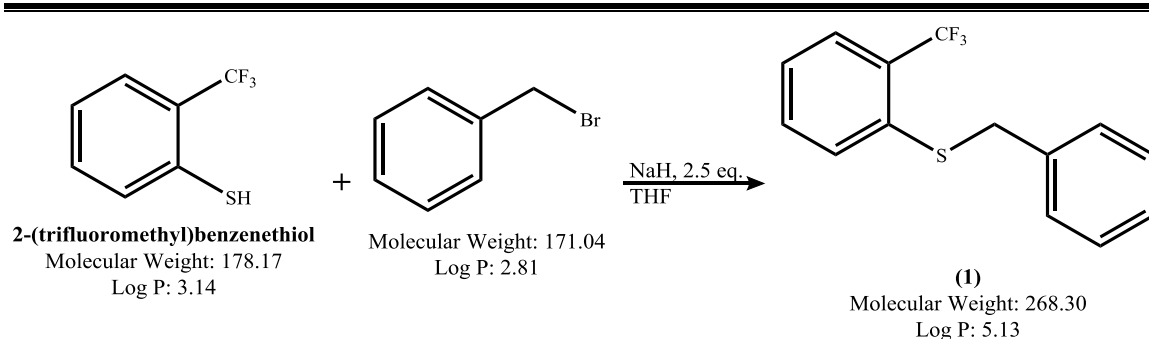


Figure 33 - Step one for production of compound 1

- Sodium hydride** (85% suspension in mineral oil, 280 mg, 2.5 mmol) was added to a solution of **2-(trifluoromethyl)benzenethiol** (500 mg, 2.8 mmol, 1 equiv) in **anhydrous THF** (5 mL). The mixture was stirred at room temperature for 10 min and treated with **benzyl bromide** (480 mg, 2.8 mmol, 1 equiv) for 1 h. After treatment with **acetic acid**, the reaction mixture was diluted with **EtOAc** and **brine**. The organic phase was separated and dried over **Na₂SO₄**. The filtrate was concentrated in vacuo and the resulting residue was purified by flash column chromatography on silica gel to obtain product. Product weight after purification: **2.017 mg**. $2.017/268.30=0.0075$; $1.438/178.17=0.0081$; $0.0075/0.0081=0.9259$
 $0.9259*100=$ **92.59% yield**.

Table 3 - Step one quantities

Compound	MW (g/mol)	D (g/mL)	mmol	mg	mL	Equiv
<u>2-(Trifluoromethyl) benzenethiol</u>	178.17	1.438	8.1	1.43	1.0	1
<u>Sodium Hydride</u>	23.9971	1.396		280.6		2.5
<u>THF</u>	72.11	0.948			5.61	0.5
<u>Benzyl bromide</u>	171.03	1.35	15.8	480.0	2	2

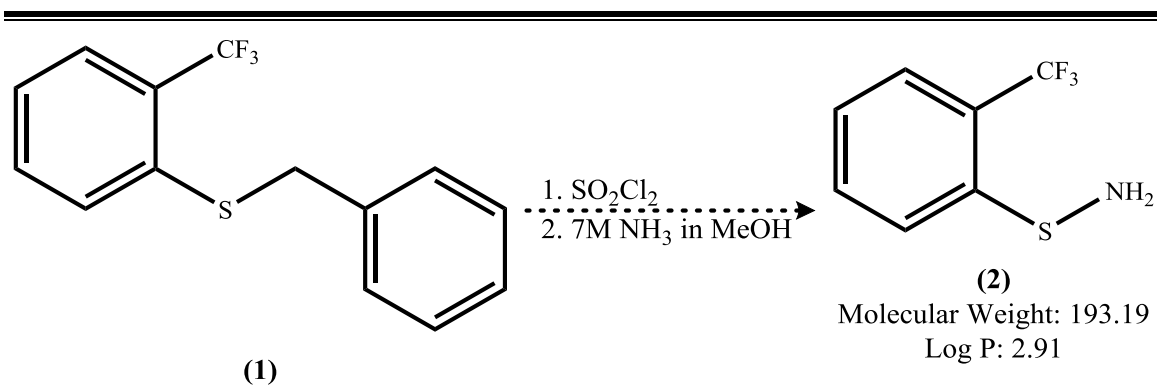
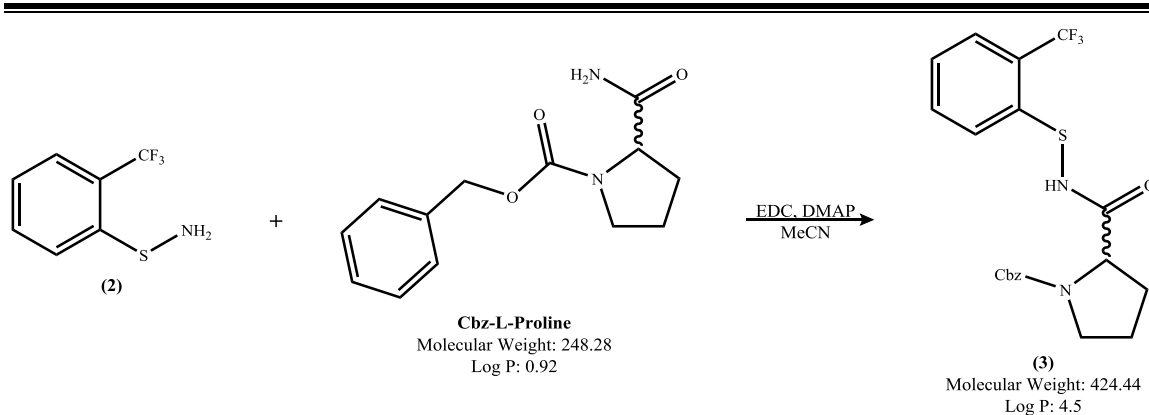


Figure 34 - Step two for compound 2

2. **Compound 1** (1.77 mg, 2 mmol) was dissolved in **CH₂Cl₂** (2 mL) and **SO₂Cl₂** (2 mL, 8 mmol) was added. The mixture was stirred at room temperature for 10 h and then concentrated to dryness. To the residue was added 7 M **NH₃** in **MeOH** 10 mL). The mixture was stirred 2 h at room temperature, then diluted with water, extracted with **EtOAc**, washed with **brine**, dried (**MgSO₄**), and concentrated to dryness. The residue was dissolved in a minimum amount of **EtOAc** and reprecipitated with **hexane**. The resulting solid was collected by filtration to afford the title compound as a light tan solid. Product weight after purification: **189.2 mg**. $189.2/193.19=0.9793$; $475/268.3=1.7704$; $0.9793/1.7704=0.5532$; $0.5532*100=$ **55.32% yield**.

Table 4 - Step two quantities

Compound	MW (g/mol)	D (g/mL)	mmol	mg	mL	Equiv
<u>Compound 1</u>	268.3		1.77	475.0		1
<u>Sulfonyl chloride</u>	118.97	1.631	8.85	1053.1	0.645	5
<u>Ammonia in MeOH</u>	50.07		3.54	177.3	10	2
<u>anhydrous DCM</u>	41.05	0.786	0.89		1.770	0.5



3. **EDCI** (176 mg, 1.14 mmol) and **4-dimethylaminopyridine** (189 mg, 1.55 mmol) were dissolved in **acetonitrile** (5 mL). The solution was then added to a mixture of **compound 2** (200 mg, 1.04 mmol) and **Cbz-L-Proline** (283 mg, 1.14 mmol) in a reaction flask cooled to 0° C. This reaction mixture was allowed to warm to room temperature and stir for 24 hours at which time it was diluted with **EtOAc** (50 mL) and washed with a saturated **NaHCO₃** solution (3x30 mL). The combined aqueous layers were back extracted with **EtOAc** (2x30 mL). All organic layers were combined, dried over **MgSO₄**, and concentrated to give 0.9507 mg of crude product mixture which was purified via flash chromatography (silica gel, 1:1 hexane: **EtOAc**) to give compound 14 (mg, % yield) as yellow oil. Product weight after purification: **38.1 mg**. $38.1/424.44=0.0898$; $200/193.19=1.0353$; $0.089/1.0353=0.086$; $0.086*100=$ **8.6 % yield**.

Table 5 - Step three quantities

Compound	MW (g/mol)	D (g/mL)	mmol	mg	mL	Equiv
<u>Cbz-L-Proline</u>	249.27		1.14	283.9		1.1
<u>EDCI</u>	155.24		1.14	176.8		1.1
<u>DMAP</u>	122.17		1.55	189.7		1.5
<u>Compound 3</u>	193.19		1.035	200.0		1
<u>Acetonitrile</u>	41.05	0.786	0.57		1.13	0.5

To a stirred solution of **Cbz-L-Proline** (500 mg, 2.01 mmol) in **Acetonitrile** (2 mL), were added **EDCI** (342 mg, 2.21 mmol), **DBU** (360 mg, 2.41 mmol), **HOBt** (338 mg, 2.21 mmol), and **2-(Trifloromethyl) benzenesulfonamide** (451 mg, 2.01 mmol), then left to stir for 3 days respectively. Daily, **EDC** and **HOBt** were added again (about 60% of original equivalents). After TLC verification, 15 mL **1M Citric Acid** was introduced to the reaction mixture (to neutralize the base), and then washed with **Brine** (3 X ~40 mL). The dried (**MgSO₄**) extract was concentrated in vacuo (after filtration) then purified by chromatography over silica gel, eluting with 5-10% **EtOAc / Hexane**.

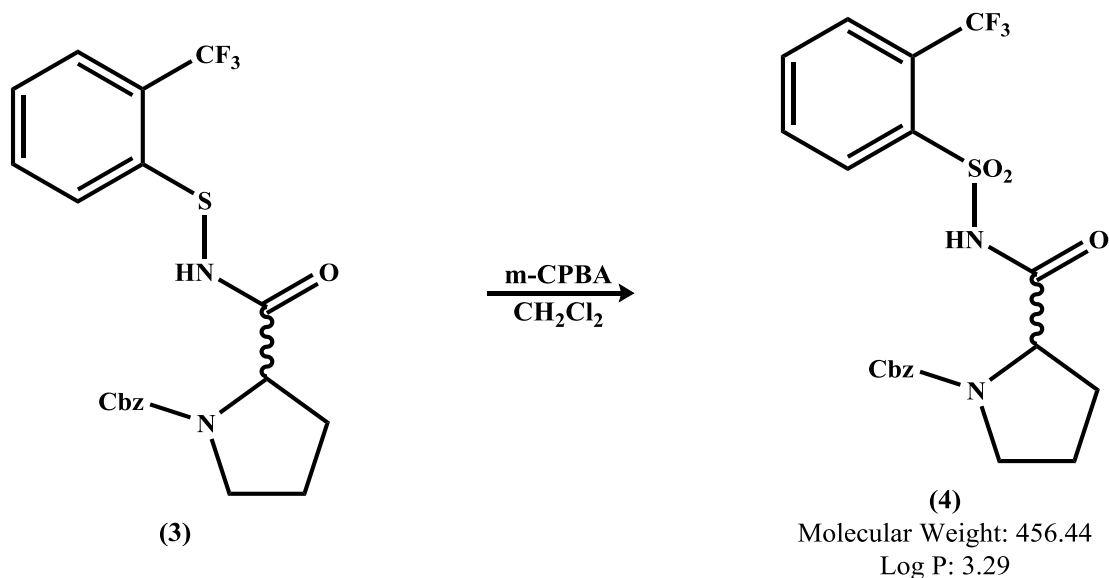


Figure 36 - Step four for compound 4

4. To a solution of **Compound 3** (500 mg, or 1 eq.) in **CH₂Cl₂** (3 mL) at 0 °C was added **m-CPBA** (142 mg, or 1.8 eq.). After the mixture is stirred at 0 °C for 39 h, the reaction is quenched with saturated aqueous **Na₂S₂O₃** and saturated aqueous **NaHCO₃**. The mixture was extracted with **EtOAc**, washed with saturated aqueous **NaCl**, dried over anhydrous **MgSO₄**, and concentrated to give the crude product mixture which is purified via flash chromatography (silica gel, 1:1 hexane: **EtOAc**) to give compound 14 (~59% yield) as a yellow oil.^{176, 177}

Various Attempted Experimental Procedures

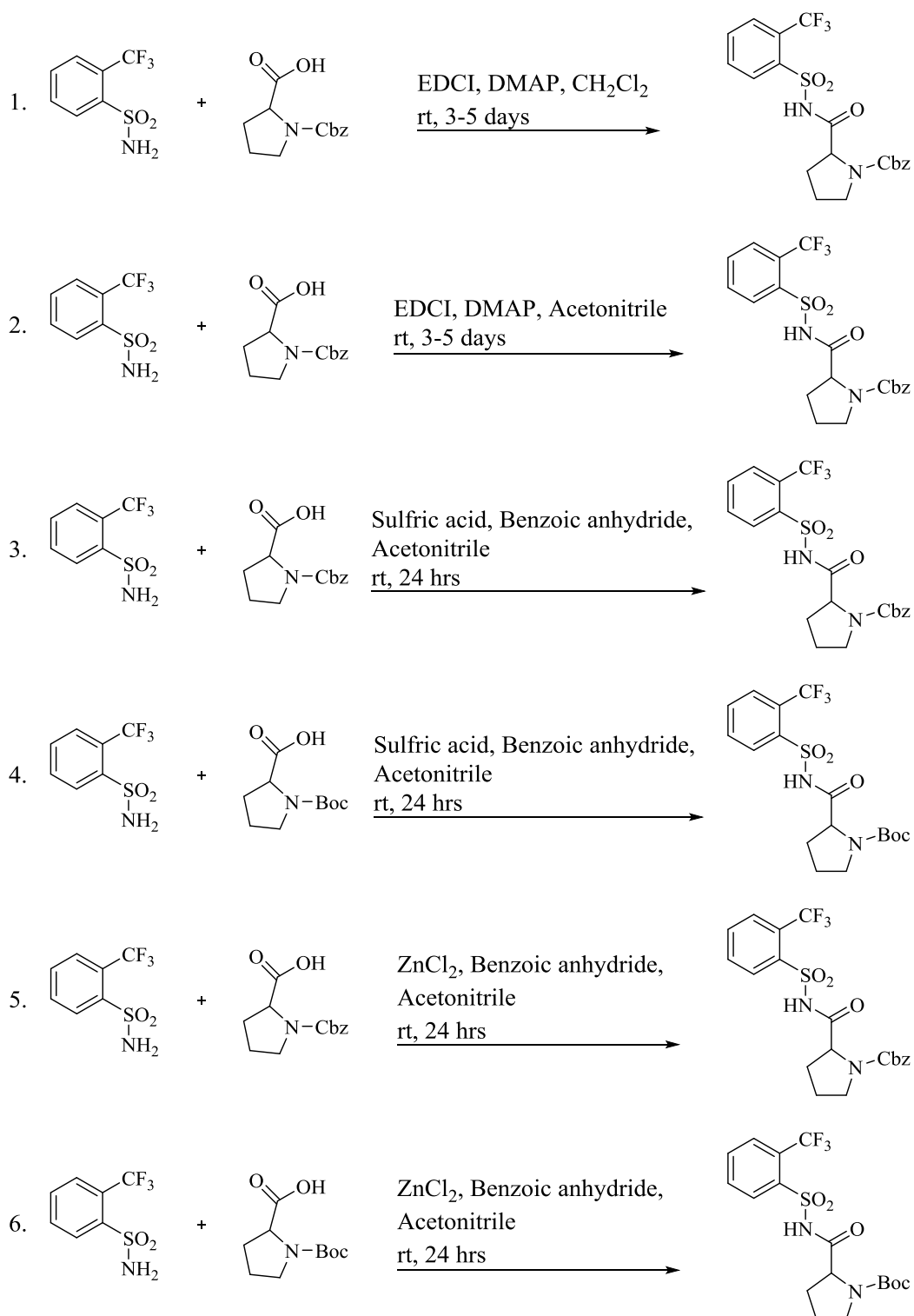


Figure 37 - Previous experimental procedures, 1-6 reactions

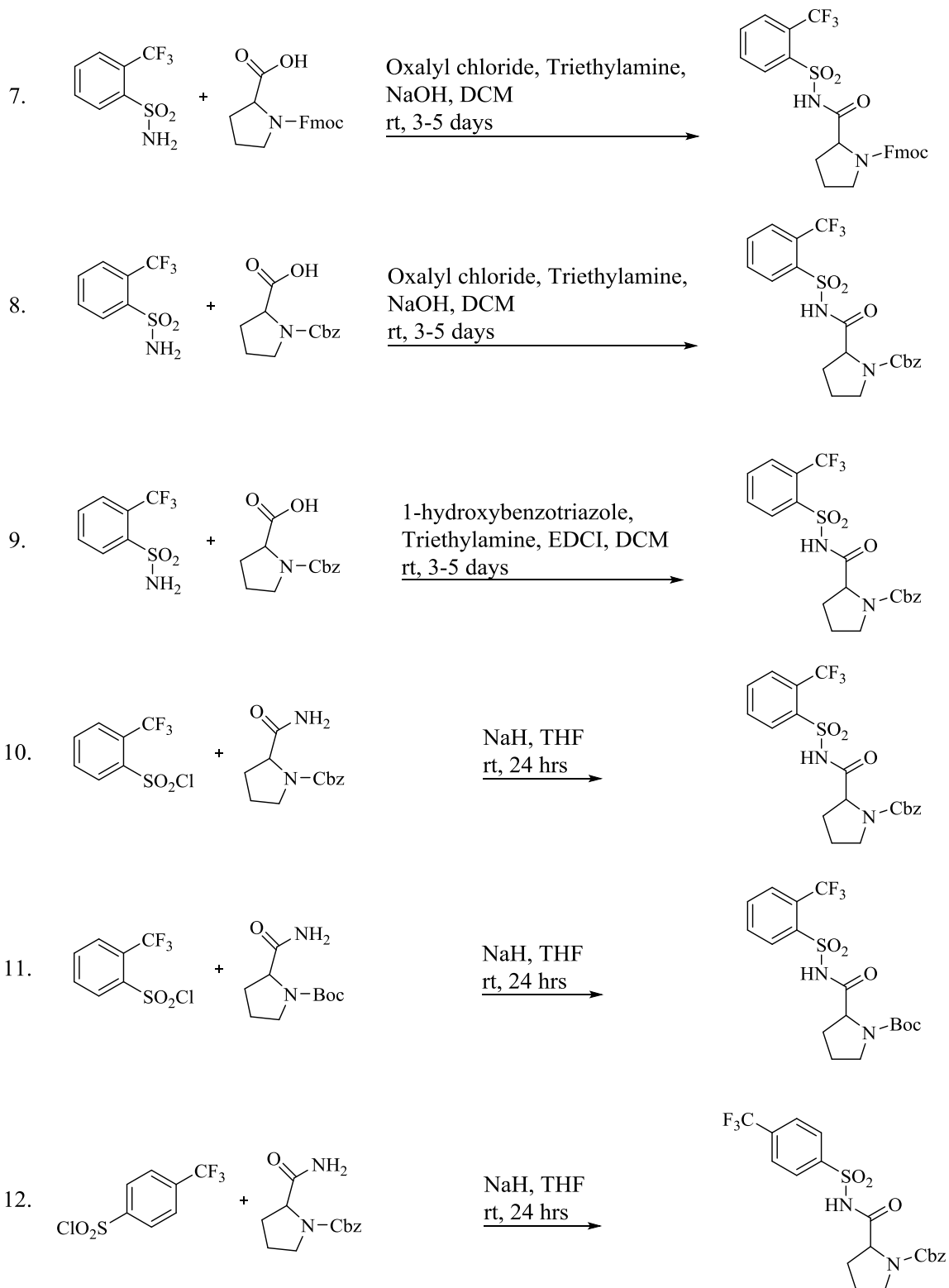


Figure 38 - Previous experimental procedures, 7-12 reactions

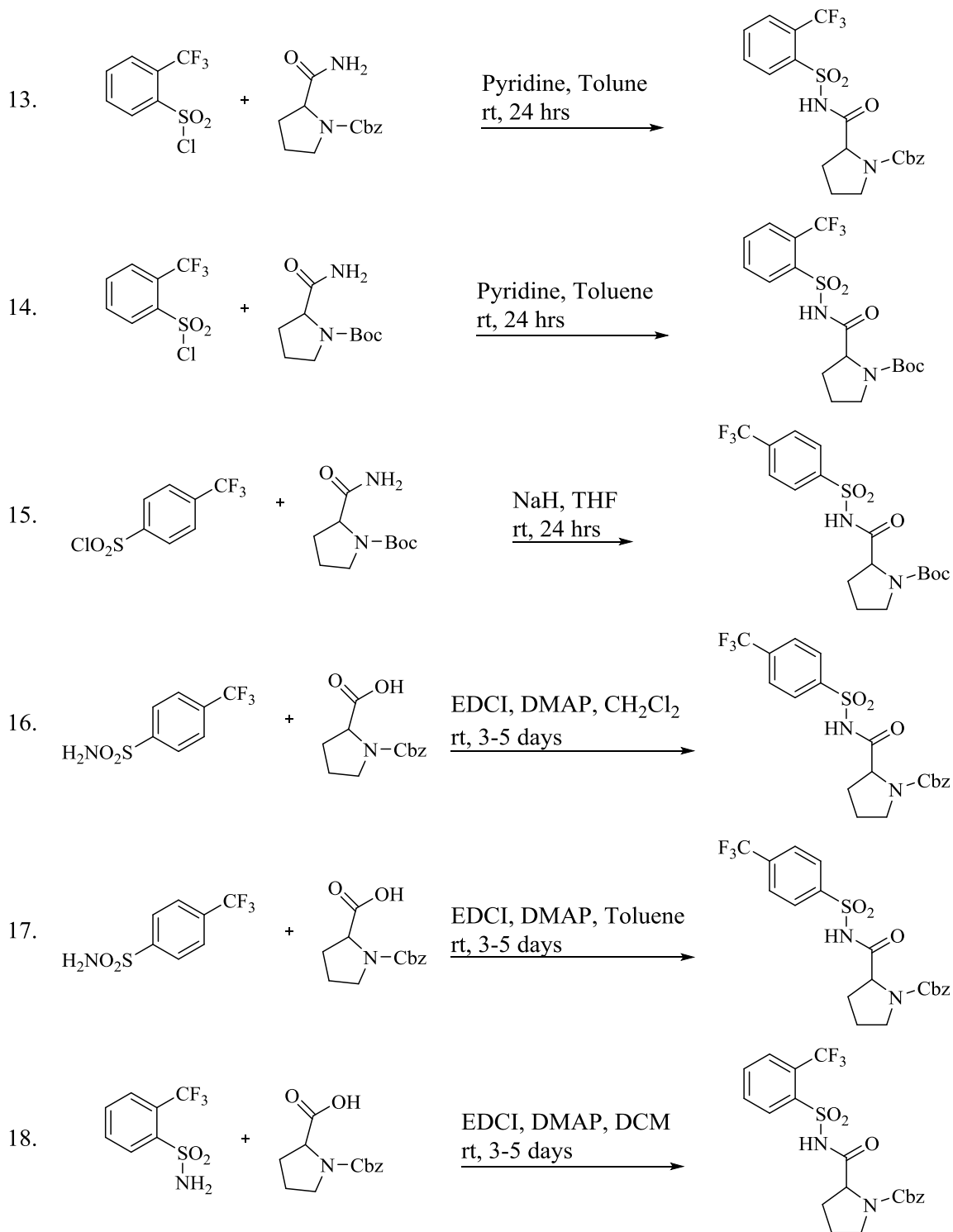


Figure 39 - Previous experimental procedures, 13-18 reactions

Typical procedure for the preparation of **Compound 2**:

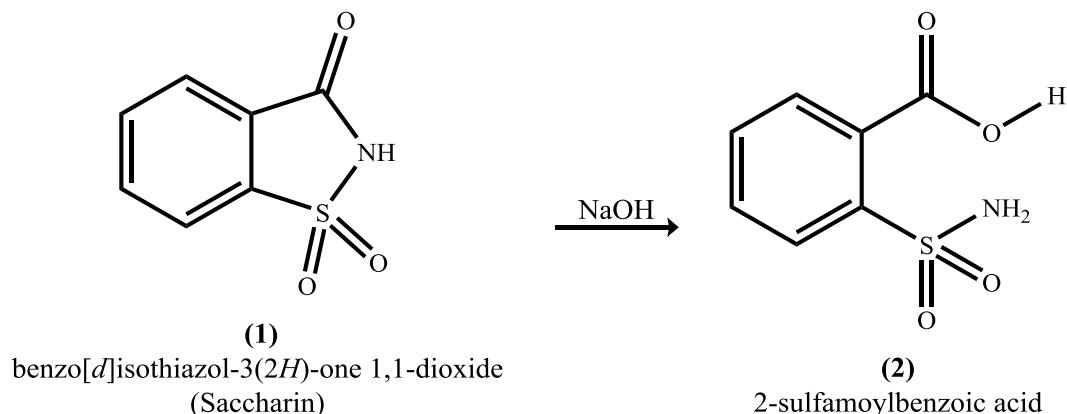


Figure 40 – Experimental procedure for 2.

General procedure:

A mixture of **saccharin** (0.997 g, 5.5 mmol.) and **sodium hydroxide (NaOH)** (0.5 g, 12.5 mmol.) in distilled water (25 ml) was heated to reflux (1 hr), cooled to room temperature and acidified to pH = 4 (15% **HCl**). The reaction mixture was subjected to cooling in freezer overnight and white flake-like product was filtered, washed with cold water and dried to yield 1.06 g of the title compound (5.3 mmol. 97%) which was recrystallized from a solution of **MeOH** and **CHCl₃** (1:1) at 40° C to obtain colorless crystals.^{180, 181}

Typical procedure for the preparation of **Compound 3a**:

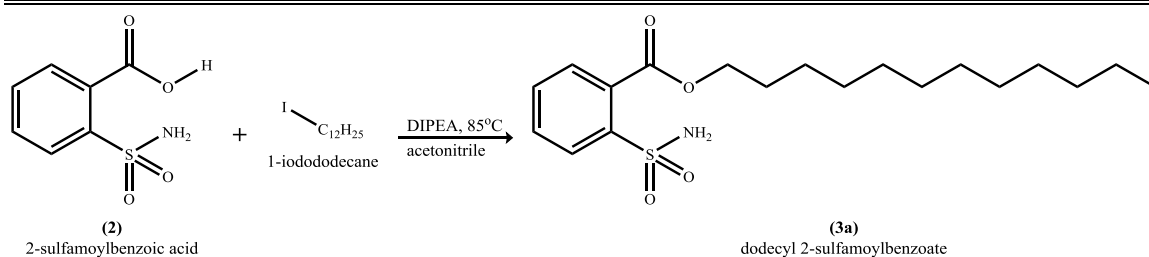


Figure 41 – Experimental procedure for 3a

General procedure:

To a mixture of **Compound 2** (304 mg, 1.51 mmol) and N, N-Diisopropylethyl amine (**DIPEA**) (214 mg, 1.66 mmol) that were dissolved in 13 mL of **acetonitrile**, was added **1-iodododecane** (492 mg, 1.66 mmol) at 85° C. The mixture was stirred overnight, then the reaction mixture was allowed to come to Room temperature. The mixture was then concentrated in vacuo to remove acetonitrile and then diluted with **EtOAc** (20 mL) and washed with 10% **KHSO₄** (2x5 mL), **NaHCO₃** sat (2x5 mL) and **brine**. The organic extracts were dried over **Na₂SO₄**, filtered and concentrated in vacuo. The crude was purified by flash column chromatography (5-20% EtOAc-hexanes) to yield 72 mg (0.10 mmol, 81%) of **3a** as a white solid.¹⁸²

Typical procedure for the preparation of **Compound 4a**:

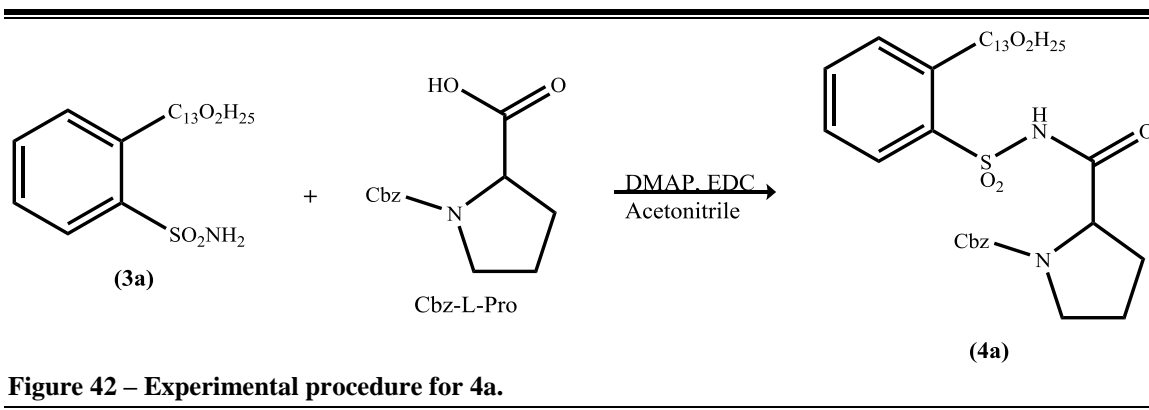


Figure 42 – Experimental procedure for 4a.

General Procedure:

A mixture of **EDCI** (176 mg, 1.14 mmol) and **4-dimethylaminopyridine** (189 mg, 1.55 mmol) were dissolved in **acetonitrile** (5 mL). The solution was then added to a mixture of **compound 1** (200 mg, 1.04 mmol) and **Z-Pro** (283 mg, 1.14 mmol) in a

reaction flask cooled to 0° C. The reaction mixture was allowed to warm to room temperature and stir for 24 hours at which time it was concentrated in vacuo to remove acetonitrile, then diluted with **EtOAc** (50 mL) and washed with a saturated **NaHCO₃** solution (3x30 mL). The combined aqueous layers were extracted with EtOAc (2x30 mL). All organic layers were combined, dried over **MgSO₄**, and concentrated to give 0.9507 mg of crude product mixture which was purified via flash chromatography (silica gel, 10:1 EtOAc:hexane) to give compound 4 (38.1 mg, % yield) as yellow oil.¹⁸³ Product weight after purification: **38.1 mg**.

Typical procedure for the preparation of **Compound 4b**:

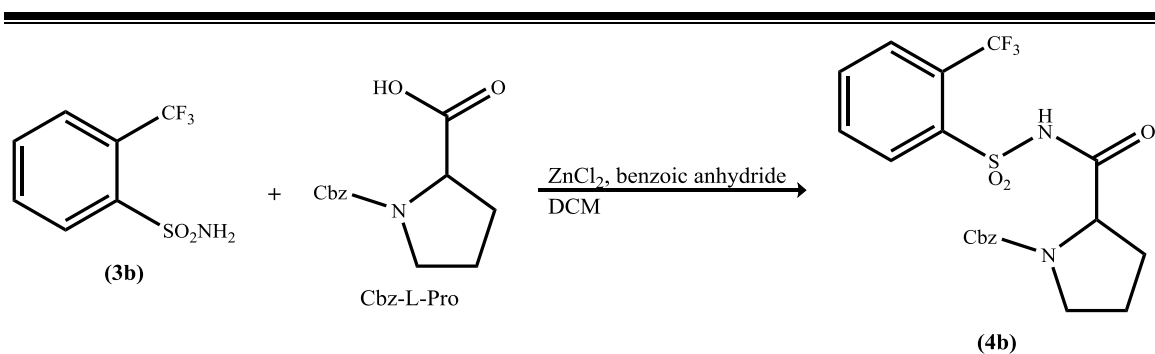


Figure 43 – Experimental procedure for 4b.

General experimental procedure for N-acylation of **sulfonamides** with **anhydrides**:

To a mixture of **Cbz-L-Proline** (1.0 mmol) and **Benzoic anhydride** (C₆H₅CO)₂O (1.5 mmol), 3 mol % of anhydrous **ZnCl₂** (1M in ether) was added and the reaction stirred in 20 mL **DCM** to allow for anhydride to form, then add **Sulfonamide** to reaction mixture and was allowed to stir for the given time. After completion of the reaction (monitored by TLC), the reaction mixture was diluted with dichloromethane and washed

with water and brine solution. The combined organic layers were dried over K_2SO_4 and evaporated in vacuo. The crude compound was purified by column chromatography (**hexanes** and **EtOAc**) to afford the corresponding N-acylated product.

General experimental procedure for N-acylation of **sulfonamides** with **carboxylic acids**:

To a stirred solution of 5 mol % anhydrous ZnCl_2 in anhydrous **dichloromethane**, **carboxylic acid** (1.2 mmol) was added followed by the addition of **benzoic anhydride** (1.2 mmol) under an **Argon** atmosphere at room temperature. After 10 min, a solution of **sulfonamide** in CH_2Cl_2 was added and the resulting reaction mixture was stirred for the given time. After completion, the reaction mixture was washed with water then brine and the combined organic layers were dried over Na_2SO_4 and evaporated in vacuo. The crude compound was purified by column chromatography (**hexanes** and **EtOAc**) to afford the corresponding **N-acylated** product.¹⁷⁴

Typical procedure for the preparation of **Compound 4c**:

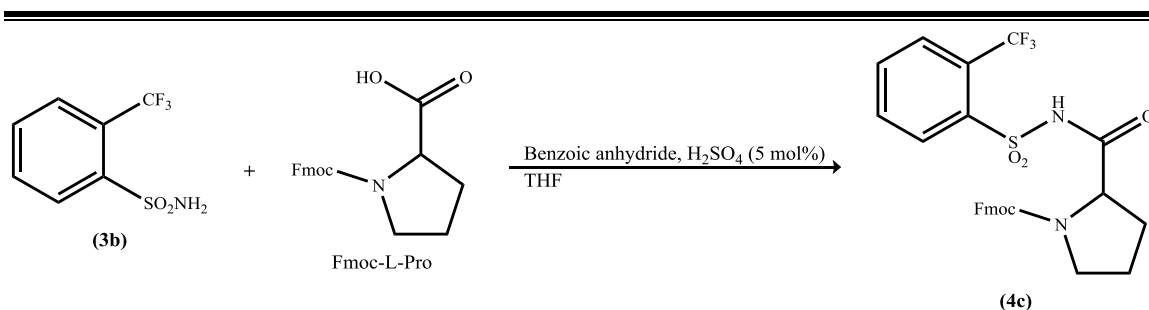


Figure 44 – Experimental procedure for 4c.

General procedure:

Under an **Argon** atmosphere, a mixture of **Fmoc-Proline** and **Benzoic anhydride** ($\text{C}_6\text{H}_5\text{CO}$) $_2\text{O}$, in **THF** (~8 ml) was stirred at 60°C and treated with 96% **sulfuric acid** (5

mol%) was added and the reaction stirred to allow for anhydride to form. The solution was maintained at 60°C for 4 hours until reaction was judged complete by TLC. Then **Benzenesulfonamide** (300 mg, 1.33 mmol), was added to reaction mixture drop-wise and was allowed to stir overnight @ 60°C. After completion of the reaction (monitored by TLC), the solvent was removed by distillation and then the solution was cooled to 24°C. Water (10–15 ml) was added dropwise to form a precipitate. The resulting mixture was stirred for 1 h at 20°C and then filtered. The crude solid was washed with deionized water (5–10 ml) and then dried in vacuo under nitrogen at 50°C for 18 h. Weight of white crystalline solid was 238 g. The reaction mixture was diluted with **dichloromethane** and washed with water and brine solution (3x15 mL). The combined organic layers were dried over **Na₂SO₄** and evaporated in vacuo. The crude compound was purified by column chromatography (10:1, EtOAc and hexanes) to afford the corresponding *N*-acylated product.¹⁷³

Typical procedure for the preparation of **Compound 4d**:

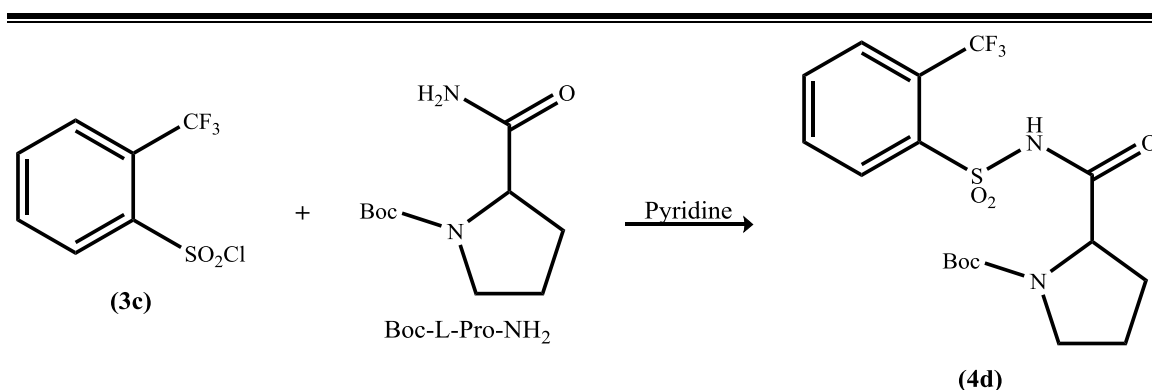


Figure 45 - Experimental procedure for 4d using Pyridine with acid chloride.

General Procedure:

Boc-Proline-NH₂ (2.04 mmol, 438 mg) was dissolved in 50 mL of **pyridine**; to this solution was added **2-(Trifluoromethyl) benzene sulfonyl chloride** (2.04 mmol, 315 μL). This mixture was stirred for 1–2 h and then left overnight without stirring. After completion of the reaction, **crushed ice** was added to this mixture and the mixture was stirred again to obtain a solid crude product; if the mixture was slightly acidified, we did not obtain any product. This crude product was washed with dichloromethane and ice cold water. The product was further purified using column chromatography to obtain crystals of compound.¹⁷²

Typical procedure for oxalyl chloride catalyzed preparation of **Compound 4b**:

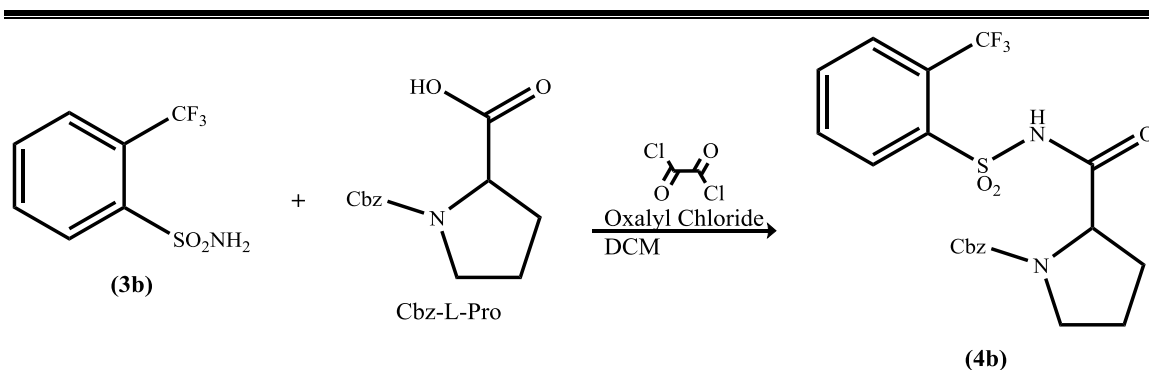


Figure 46 - Experimental procedure for 4b using oxalyl chloride.

General Procedure:

In a reaction mixture **Cbz-L-pro** (1.1 mg, 4.4 mmol) was suspended in dry **DCM** (10 mL) under Argon atmosphere. To this solution, **oxalyl chloride** (4.1 mL, 48 mmol) was slowly added and the mixture was stirred for 2 h (with TLC observation). Gas evolution was observed, and the system was allowed to stir at room temperature for 28 h. The system was connected to another flask of 6 M **NaOH** to react with the **HCl** gas that

is formed from the reaction of the Reactants. The **DCM** was removed under reduced pressure and the residue was suspended again in dry **CH₂Cl₂** (10 mL). After addition of **triethylamine** (0.74 mL, 5.2 mmol) to the reaction mixture, **2-(Trifluoromethyl) benzene sulfonamide** (1.2 mg, 5.2 mmol) in **DCM** (5 L) was slowly added. The reaction mixture was stirred at room temperature for 4 h and then the mixture was suspended in water to remove impurities. The organic phase separated and the solvent was removed under reduced pressure to obtain a brownish viscous oil.¹⁸⁴

Typical procedure for Amide peptide coupling reactions by various organocatalysts:

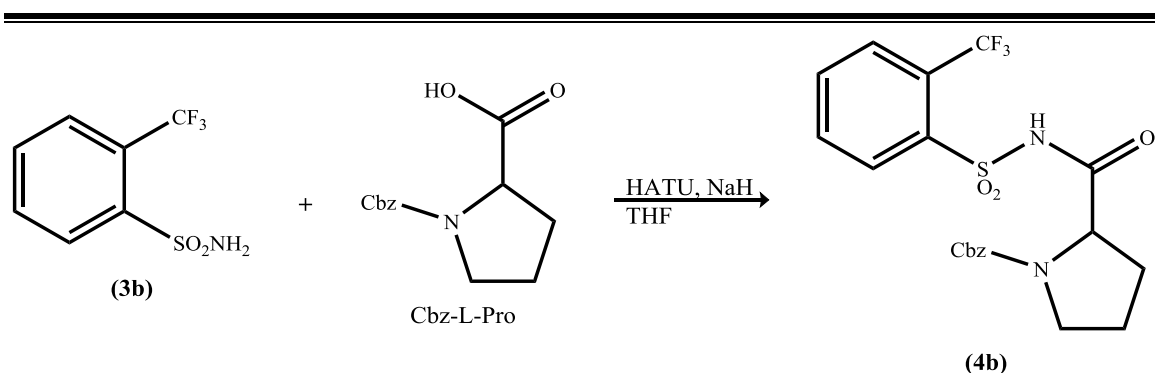


Figure 47 - Procedure for 4b using HATU

General Procedure:

To a stirred solution (after 4.0 hrs of stirring) of **Cbz-Pro-OH** (500 mg, 2.01 mmol) & **triethylamine** (0.300 mL, 2.21 mmol) in **THF** (2 mL), was added **HATU** (838 mg, 2.2 mmol). After 1hr a mixture of **2-(Trifluoro) benzene sulfonamide** (677 mg, 3.01 mmol) with 60% **NaH** (136 mg, 3.3 mmol) in **THF** (2mL) was added and left to stir for 2hrs respectively. After TLC verification, 5 mL **1M HCl** was introduced to the reaction mixture (to neutralize the base), and then washed with brine (3 X ~40 mL) and

the organic layer was washed again with **1M NaOH**. The dried (**Na₂SO₄**) extract was concentrated in vacuo (after filtration) then purified by chromatography over silica gel, eluting with 1-50% **EtOAc/hexanes**.¹⁸⁵

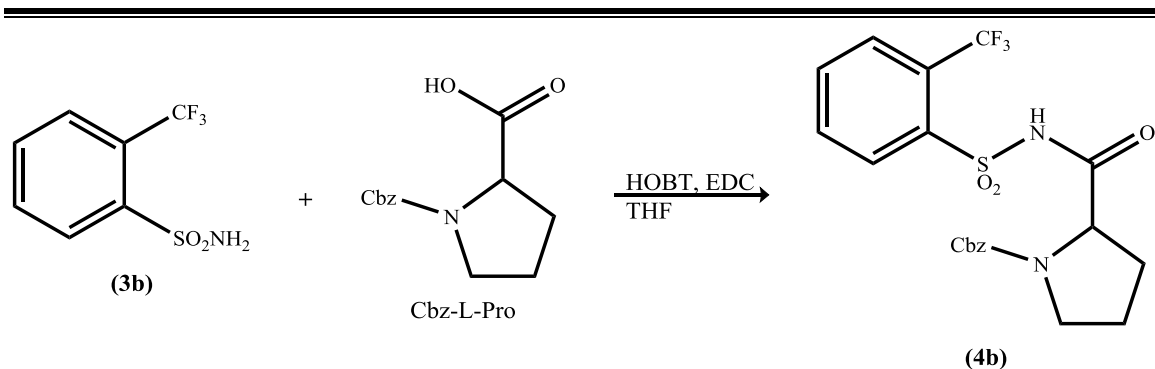


Figure 48 – Procedure for 4b using HOBT

General Procedure:

To a stirred solution of **Cbz-L-Pro** (0.166 g, 0.670 mmol) in **THF** (7 mL), were added **EDCI** (0.103 g, 0.670 mmol), **HOBT** (0.090 g, 0.670 mmol), and **2-(trifluoro)benzene sulfonamide** (0.300 g, 1.33 mmol) in **THF** (7 mL), then left to stir for 5 days respectively. After TLC verification, 15 mL **1M HCl** was introduced to the reaction mixture (to neutralize the base), and then washed with **brine** (3 X ~40 mL). The dried (**Na₂SO₄**) extract was concentrated in vacuo (after filtration) then purified by chromatography over silica gel, eluting with 5-20% **EtOAc/hexanes**.¹⁸⁶

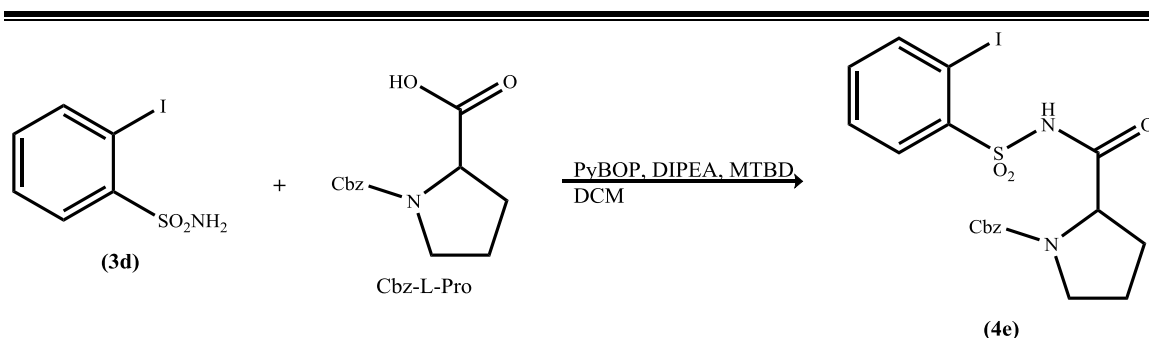


Figure 49 - Procedure for 4e using PyBOP and Iodo-benzene sulfonamide

General Procedure:

To a stirred solution (after 1.0 hr of stirring) of **Cbz-Pro-OH** (200 mg, 0.8 mmol) & **DIPEA** (0.4 mL, 2.4 mmol) in **THF** (2 mL), was added **PyBOP** (440 mg, 0.89 mmol). After 1hr a mixture of **MTBD** (0.150 mL, 0.96 mmol) **2-iodobenzene sulfonamide** (216 mg, 0.96 mmol) was added. After 10 min another equivalent of **PyBOP** was added and left to stir overnight, respectively. After TLC verification, 5 mL **1M HCl** was introduced to the reaction mixture (to neutralize the base), and then washed with brine (3 X ~40 mL). The dried (**Na₂SO₄**) extract was concentrated in vacuo (after filtration) then purified by chromatography over silica gel, eluting with 10% **MeOH/DCM**.¹⁸⁷

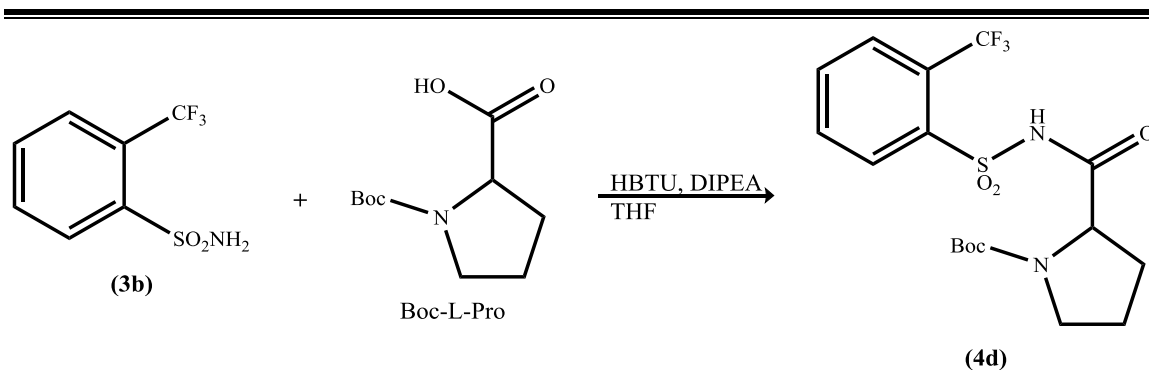


Figure 50 - Procedure for 4d using HBTU

General Procedure:

To a stirred solution (after 20 min of stirring) of **Boc-Pro-OH** (300 mg, 1.39 mmol) & **DIPEA** (0.728 mL, 4.18 mmol) in **THF** (2 mL), was added **HBTU** (581 mg, 1.53 mmol). After 1/2 hr, **2-(trifluoro) benzene sulfonamide** (313 mg, 1.39 mmol) was added and left to stir for 2hrs respectively. Reaction mixture was concentrated then extracted using **chloroform**. After TLC verification, 40 mL **1M HCl** was introduced to the reaction mixture (to neutralize the base), and then washed with **brine** (3 X ~40 mL). The dried (**Na₂SO₄**) extract was concentrated in vacuo (after filtration) then purified by chromatography over silica gel, eluting with 100% **EtOAc**. Product mass crude 976 mg.¹⁸⁸

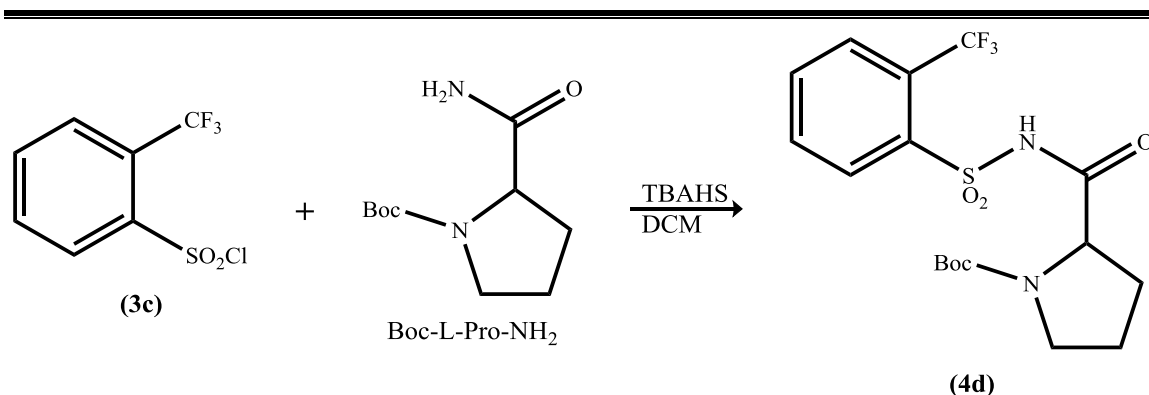


Figure 51 - Procedure for 4d using TBAHS and sulfonyl chloride through acid catalysis.

General Procedure:

To a stirred solution of **Boc-L-Pro-NH₂** (300 mg, 1.21 mmol) and NaOH (23 mg, 0.580 mmol) in **THF** (4 mL), were added tetrabutylammonium hydrogen sulfate (**TBAHS**) (40 mg, 0.121 mmol), and **2-(trifluoromethyl) benzene sulfonyl chloride** (0.37 mL, 2.4 mmol) in **DCM** (2 mL), then left to stir for 2 days respectively. After TLC

verification, 5 mL **1M HCl** was introduced to the reaction mixture (to neutralize the base), and then washed with brine (3 X ~40 mL). The dried (**Na₂SO₄**) extract was concentrated in vacuo (after filtration) then purified by chromatography over silica gel, eluting with 10% **MeOH/DCM**.¹⁸⁹

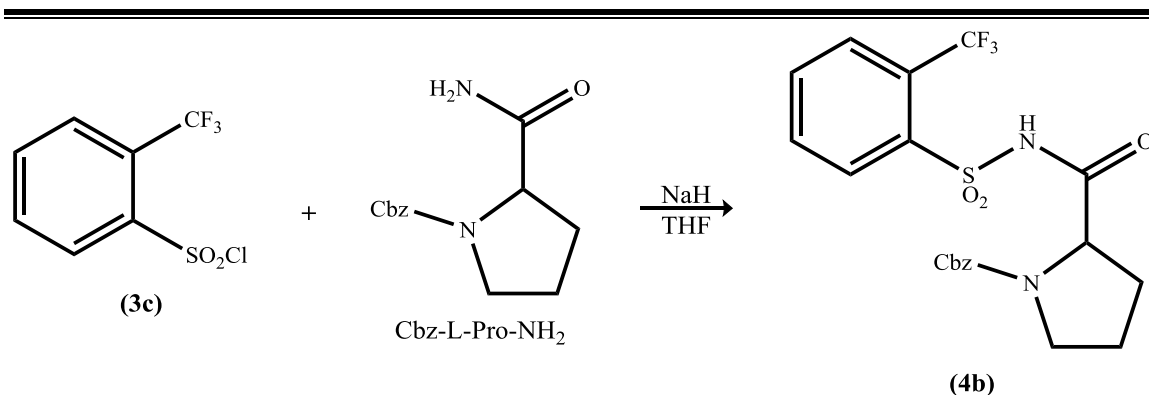


Figure 52 - Procedure using NaH and sulfonyl chloride

General Procedure:

To a stirred solution of **THF** and **sodium hydride (NaH)** (50 mg, 1.22 mmol), **Cbz-L-Pro-NH₂** (305 mg, 1.22 mmol) was added at 0° C. The solution was allowed to stir for **1 hr** at **rt** and then **2-(trifluoromethyl) benzene sulfonyl chloride** (315 µL, 2.0 mmol) was added drop-wise at 0° C, then allowed to stir for **1 hr**. The Reaction mixture was allowed to come to **rt** and left overnight. Then concentrated to remove **THF** and re-diluted with **EtOAc**. It was then separated using **brine, water, and EtOAc**. The organic layer was dried using **Na₂SO₄** anhydrous, then concentrated in vacuo. The product was weighed and purified using flash chromatography.¹⁹⁰

REFERENCES

1. You, S. L. (2015) *Asymmetric Functionalization of C-H Bonds*, Royal Society of Chemistry, Cambridge, UK.
2. Carter, R. G., Lingampally, R. and Yang, H. (2014) N-[(4-Dodecylphenyl)sulfonyl]-2-pyrrolidinecarboxamide (Hua Cat), In *e-EROS Encyclopedia of Reagents for Organic Synthesis*, pp 1-4, Oregon State University, Corvallis, OR, USA.
3. Carter, R. G., Lingampally, R. and Yang, H. (2014) Dodecyl 4-[[[(2S)-2-pyrrolidinyl-carbonyl]-amino]sulfonyl]benzoate (Hua CatII), In *e-EROS, Encyclopedia of Reagents for Organic Synthesis*, pp 1-2, Oregon State University, Corvallis, OR, USA.
4. Fife, W. K. (1983) Organic chemistry, *Journal of Chemical Education* 60, A239.
5. Johnson, A. W. (1990) The year-long first course in organic chemistry: A review, *Journal of Chemical Education* 67, 299.
6. Hanson, D. (2011) PREACHING CONVERGENCE, *Chemical & Engineering News Archive* 89, 29,33.
7. Mani, S. V., Connell, D. W., and Braddock, R. D. (1991) Structure activity relationships for the prediction of biodegradability of environmental pollutants, *Critical Reviews in Environmental Control* 21, 217-236.
8. Sims, G. K., and Sommers, L. E. (1986) Biodegradation of pyridine derivatives in soil suspensions, *Environmental Toxicology and Chemistry* 5, 503-509.
9. Yang, S.-Y. (2010) Pharmacophore modeling and applications in drug discovery: challenges and recent advances, *Drug Discovery Today* 15, 444-450.
10. Langer, T., and Wolber, G. (2004) Pharmacophore definition and 3D searches, *Drug Discovery Today: Technologies* 1, 203-207.
11. Rosa, F. A. F. d., Rebelo, R. A., and Nascimento, M. G. (2003) Synthesis of new indolecarboxylic acids related to the plant hormone indoleacetic acid IAA, *Journal of the Brazilian Chemical Society* 14, 11-15.

12. Li, C.-J. (2005) Organic Reactions in Aqueous Media with a Focus on Carbon–Carbon Bond Formations: A Decade Update, *Chemical Reviews* 105, 3095-3166.
13. Corey, E. J., and Cheng, X. M. (1989) *The logic of chemical synthesis*, Illustrated ed., John Willey & Sons, New York, USA.
14. Tkacz, J. S., and Lange, L. (2012) *Advances in Fungal Biotechnology for Industry, Agriculture, and Medicine*, Springer Science & Business Media, US.
15. Carruthers, W., and Coldham, I. (2004) *Modern Methods of Organic Synthesis*, 4th Edition ed., Cambridge University Press, Cambridge, UK.
16. G J Schroepfer, Jr. (1981) Sterol Biosynthesis, *Annual Review of Biochemistry* 50, 585-621.
17. Brown, J. M., and Cooley, N. A. (1988) Carbon-carbon bond formation through organometallic elimination reactions, *Chemical Reviews* 88, 1031-1046.
18. Kluger, R. (1992) 7 Mechanisms of Enzymic Carbon–Carbon Bond Formation and Cleavage, In *The Enzymes* (David, S. S., Ed.), pp 271-315, Academic Press.
19. Resch, V., Schrittwieser, J. H., Siirola, E., and Kroutil, W. (2011) Novel carbon–carbon bond formations for biocatalysis, *Current Opinion in Biotechnology* 22, 793-799.
20. Poulter, C. D. (2009) Bioorganic Chemistry. A Natural Reunion of the Physical and Life Sciences, *The Journal of organic chemistry* 74, 2631-2645.
21. Elbert, D. L., Pratt, A. B., Lutolf, M. P., Halstenberg, S., and Hubbell, J. A. (2001) Protein delivery from materials formed by self-selective conjugate addition reactions, *Journal of Controlled Release* 76, 11-25.
22. Smith, M. B., and March, J. (2007) *March's Advanced Organic Chemistry: Reactions, Mechanisms, and Structure*, Wiley.
23. Barnes, S. J., and Weitzman, P. D. J. (1986) Organization of citric acid cycle enzymes into a multienzyme cluster, *FEBS Letters* 201, 267-270.

24. Baliya, A. M., and Reynolds, A. M. (1982) A Mixed-Aldol Condensation Reaction with Unknown Aldehydes and Ketones: Employing Modern Methods To Improve the Learning Process for Second-Year Undergraduate Organic Chemistry Students, *Journal of Chemical Education* 90, 1100-1102.
25. Voet, D., and Voet, J. G. (2004) *Biochemistry*, 3rd ed., J. Wiley & Sons, New York.
26. Wood, E. J. (1999) Fundamentals of Biochemistry, *Trends in Biochemical Sciences* 24, 409-410.
27. Corey, E. J., Russey, W. E., and de Montellano, P. R. O. (1966) 2,3-Oxidosqualene, an Intermediate in the Biological Synthesis of Sterols from Squalene, *Journal of the American Chemical Society* 88, 4750-4751.
28. Davies, S. G., Dordor-Hedgecock, I. M., Sutton, K. H., and Whittaker, M. (1987) Conformational analysis for the pseudooctahedral complexes $(\eta^5\text{-C}_5\text{H}_5)\text{Fe}(\text{CO})(\text{PPh}_3)\text{CH}_2\text{R}$ [R = Me, Et, iso-Pr, tert-Bu, SiMe₃, (PMe₃)⁺, (PPh₃)⁺, mesityl, Ph, vinyl, 1-naphthyl]: x-ray crystal structures of $(\eta^5\text{-C}_5\text{H}_5)\text{Fe}(\text{CO})(\text{PPh}_3)\text{CH}_2\text{R}$ (R = Me, SiMe₃), *Journal of the American Chemical Society* 109, 5711-5719.
29. Abel, E. W., Adams, R. D., Stone, F. G. A., and Wilkinson, G. (1995) *Comprehensive Organometallic Chemistry II: A Review of the Literature 1982-1994. Heteronuclear metal-Metal bonds. Vol. 10*, Elsevier Science.
30. Hoff, R. (2010) Cobalt Ziegler–Natta Catalysts for Synthesis of Poly-cis-1,4-Butadiene, In *Handbook of Transition Metal Polymerization Catalysts*, pp 537-550, John Wiley & Sons, Inc.
31. Kissin, Y. V. (2008) Alkene polymerization reactions with transition metal catalysts.
32. Makaryan, I., Sedov, I., and Savchenko, V. (2015) Platinum Group Metal-Catalysed Carbonylation as the Basis of Alternative Gas-To-Liquids Processes, *Johnson Matthey Technology Review* 59, 14-25.
33. Haynes, A. (2006) Acetic Acid Synthesis by Catalytic Carbonylation of Methanol, In *Catalytic Carbonylation Reactions* (Beller, M., Ed.), pp 179-205, Springer Berlin Heidelberg, Berlin, Heidelberg.

34. Jones, J. H. (2000) The Cativa™ Process for the Manufacture of Acetic Acid, *Platinum Metals Review* 44, 94-105.
35. Rishina, L. A., Galashina, N. M., Gagieva, S. C., Tuskaev, V. A., and Kissin, Y. V. (2011) Polymerization of olefins catalyzed by a dichloride complex of titanium with a dioxolane dicarbonate ligand: The promoting effect of LiCl and MgCl₂, *Polymer Science Series B* 53, 42-51.
36. Alberts, A. H., and Wynberg, H. (1989) The role of the product in asymmetric carbon-carbon bond formation: stoichiometric and catalytic enantioselective autoinduction, *Journal of the American Chemical Society* 111, 7265-7266.
37. Pierre H. Dixneuf, C. B., Jean Fournier, Aresta, M., and Schloss, J. V. (2012) *Catalytic incorporation of CO₂ for the Synthesis of Organic compounds*, Springer Netherlands, Rennes, France.
38. Sigel, A., Sigel, H., Sigel, R. K. O., and Royal Society of, C. (2010) *Organometallics in Environment and Toxicology*, Royal Society of Chemistry, Cambridge, UK.
39. Netter, K. J. (2010) Metal Ions in Life Sciences, Vol. 7, Organometallics in Environment and Toxicology, A. Sigel, H. Sigel, R.K.O. Sigel (Eds.). The Royal Society of Chemistry (RSC Publishing), Cambridge (2010), ISBN: 978-1-84755-177-1, *Toxicology* 277, 86-87.
40. Vincent, J. B., Olivier-Lilley, G. L., and Averill, B. A. (1990) Proteins containing oxo-bridged dinuclear iron centers: a bioinorganic perspective, *Chemical Reviews* 90, 1447-1467.
41. Asadullah, M., Taniguchi, Y., Kitamura, T., and Fujiwara, Y. (1998) Direct carboxylation reaction of methane with CO by a Yb(OAc)₃/Mn(OAc)₂/NaClO/H₂O catalytic system under very mild conditions, *Applied Organometallic Chemistry* 12, 277-284.
42. Doye, S. (2001) Catalytic C–H Activation of sp³ C–H Bonds in α-Position to a Nitrogen Atom—Two New Approaches, *Angewandte Chemie International Edition* 40, 3351-3353.
43. Aresta, M., and Forti, G. (2012) *Carbon Dioxide as a Source of Carbon: Biochemical and Chemical Uses*, Springer Science & Business Media.

44. Braunstein, P., Matt, D., and Nobel, D. (1988) Carbon dioxide activation and catalytic lactone synthesis by telomerization of butadiene and carbon dioxide, *Journal of the American Chemical Society* 110, 3207-3212.
45. Murahashi, S., Naota, T., Ito, K., Maeda, Y., and Taki, H. (1987) Ruthenium-catalyzed oxidative transformation of alcohols and aldehydes to esters and lactones, *The Journal of organic chemistry* 52, 4319-4327.
46. Motoyoshiya, J., Kusaura, T., Kokin, K., Yokoya, S.-i., Takaguchi, Y., Narita, S., and Aoyama, H. (2001) The Horner–Wadsworth–Emmons reaction of mixed phosphonoacetates and aromatic aldehydes: geometrical selectivity and computational investigation, *Tetrahedron* 57, 1715-1721.
47. Chemistry, S. A. (2016) C-C bond formation, p 1, Sigma Aldrich, US.
48. Li, C. J. (1993) Organic reactions in aqueous media - with a focus on carbon-carbon bond formation, *Chemical Reviews* 93, 2023-2035.
49. Breslow, R. (1991) Hydrophobic effects on simple organic reactions in water, *Accounts of Chemical Research* 24, 159-164.
50. Borole, Y. L., and Chaudhari, R. V. (2005) New Route for the Synthesis of Propylene Glycols via Hydroformylation of Vinyl Acetate, *Industrial & Engineering Chemistry Research* 44, 9601-9608.
51. Franke, R., Selent, D., and Börner, A. (2012) Applied Hydroformylation, *Chemical Reviews* 112, 5675-5732.
52. Pogrzeba, T., Müller, D., Hamerla, T., Esche, E., Paul, N., Wozny, G., and Schomäcker, R. (2015) Rhodium-Catalyzed Hydroformylation of Long-Chain Olefins in Aqueous Multiphase Systems in a Continuously Operated Miniplant, *Industrial & Engineering Chemistry Research* 54, 11953-11960.
53. Horan, A. (2016) Organic Chemistry Contributing to Green Chemistry, In *Green Chemistry*, © Royal Society of Chemistry, Cambridge, UK.
54. Dunn, P. J. (2012) The importance of Green Chemistry in Process Research and Development, *Chemical Society Reviews* 41, 1452-1461.

55. Dunn, P. J., Wells, A. S., and Williams, M. T. (2010) Future Trends for Green Chemistry in the Pharmaceutical Industry, In *Green Chemistry in the Pharmaceutical Industry*, pp 333-355, Wiley-VCH Verlag GmbH & Co. KGaA.
56. Spargo, P. L. (2005) Aqueous-Phase Organometallic Catalysis: Concepts and Applications. 2nd, Completely Revised and Enlarged Edition Edited by Boy Cornils and Wolfgang A. Herrmann. Wiley-VCH: Weinheim. 2004. 750 pp. £160. ISBN 3-527-30712-5, *Organic Process Research & Development* 9, 1018-1019.
57. Goldman, A. S., and Goldberg, K. I. (2004) Organometallic C-H Bond Activation: An Introduction, In *Activation and Functionalization of C-H Bonds*, pp 1-43, American Chemical Society.
58. Siskin, M., and Katritzky, A. R. (1991) Reactivity of Organic Compounds in Hot Water: Geochemical and Technological Implications, *Science* 254, 231-237.
59. Ritter, S. K. (2016) Reducing Environmental Impact Of Organic Synthesis | April 15, 2013 Issue - Vol. 91 Issue 15 | Chemical & Engineering News, In *Chemical & Engineering News*, pp 22-23, American Chemical Society.
60. Michael, A. (1887) Ueber die Addition von Natriumacetessig- und Natriummalonsäureäthern zu den Aethern ungesättigter Säuren, *Journal für Praktische Chemie* 35, 349-356.
61. Michael, A. (1935) On the Mechanism of Reactions of Acetoacetic Ester, the Enolates and Structurally Related Compounds. I. C- and O-Alkylation, *Journal of the American Chemical Society* 57, 159-164.
62. Vernon, B., Tirelli, N., Bächli, T., Haldimann, D., and Hubbell, J. A. (2003) Water-borne, in situ crosslinked biomaterials from phase-segregated precursors, *Journal of Biomedical Materials Research Part A* 64A, 447-456.
63. Tokura, S., Nishi, N., Nishimura, S.-i., and Ikeuchi, Y. (1983) Studies on Chitin X. Cyanoethylation of Chitin, *Polym J* 15, 553-556.
64. Morpurgo, M., Veronese, F. M., Kachensky, D., and Harris, J. M. (1996) Preparation and Characterization of Poly(ethylene glycol) Vinyl Sulfone, *Bioconjugate Chemistry* 7, 363-368.

65. Richardson, S. C. W., Patrick, N. G., Stella Man, Y. K., Ferruti, P., and Duncan, R. (2001) Poly(Amidoamine)s as Potential Nonviral Vectors: Ability to Form Interpolyelectrolyte Complexes and to Mediate Transfection in Vitro, *Biomacromolecules* 2, 1023-1028.
66. Ferruti, P., Bianchi, S., Ranucci, E., Chiellini, F., and Caruso, V. (2005) Novel Poly(amido-amine)-Based Hydrogels as Scaffolds for Tissue Engineering, *Macromolecular Bioscience* 5, 613-622.
67. Mather, B. D., Viswanathan, K., Miller, K. M., and Long, T. E. (2006) Michael addition reactions in macromolecular design for emerging technologies, *Progress in Polymer Science* 31, 487-531.
68. Gimbert, C., Lumbierres, M., Marchi, C., Moreno-Mañas, M., Sebastián, R. M., and Vallribera, A. (2005) Michael additions catalyzed by phosphines. An overlooked synthetic method, *Tetrahedron* 61, 8598-8605.
69. Mannich, C., and Krösche, W. (1912) Ueber ein Kondensationsprodukt aus Formaldehyd, Ammoniak und Antipyrin, *Archiv der Pharmazie* 250, 647-667.
70. Córdova, A., Watanabe, S.-i., Tanaka, F., Notz, W., and Barbas, C. F. (2002) A Highly Enantioselective Route to Either Enantiomer of Both α - and β -Amino Acid Derivatives, *Journal of the American Chemical Society* 124, 1866-1867.
71. Kleinman, E. F. (1991) 4.1 - The Bimolecular Aliphatic Mannich and Related Reactions A2 - Trost, Barry M, In *Comprehensive Organic Synthesis* (Fleming, I., Ed.), pp 893-951, Pergamon, Oxford.
72. Quevedo, R., and Moreno-Murillo, B. (2009) One-step synthesis of a new heterocyclophane family, *Tetrahedron Letters* 50, 936-938.
73. Arend, M., Westermann, B., and Risch, N. (1998) Modern Variants of the Mannich Reaction, *Angewandte Chemie International Edition* 37, 1044-1070.
74. Blicke, F. F., and Burckhalter, J. H. (1942) The Preparation of β -Keto Amines by the Mannich Reaction, *Journal of the American Chemical Society* 64, 451-454.
75. Geiger, W. E., Gennett, T., McVicar, W. K., and Herrmann, W. A. (1987) Transition metal methylene complexes. 65. Electrochemical oxidation and reduction of

methylene-bridged complexes of manganese, cobalt, and rhodium, *Organometallics* 6, 1634-1639.

76. Wang, T., Naredla, R. R., Thompson, S. K., and Hoye, T. R. (2016) The pentadehydro-Diels-Alder reaction, *Nature advance online publication*.
77. Nobelprize.org. (2016) The Nobel Prize in Chemistry 1950, Nobel Media AB.
78. Gatzemeier, T., van Gemmeren, M., Xie, Y., Höfler, D., Leutzsch, M., and List, B. (2016) Asymmetric Lewis acid organocatalysis of the Diels–Alder reaction by a silylated C–H acid, *Science* 351, 949-952.
79. Nantz, M. (2007) *Modern Organic Synthesis*, W. H. Freeman, USA.
80. Maruoka, K., Itoh, T., Shirasaka, T., and Yamamoto, H. (1988) Asymmetric hetero-Diels-Alder reaction catalyzed by a chiral organoaluminum reagent, *Journal of the American Chemical Society* 110, 310-312.
81. Woodward, R. B., Sondheimer, F., Taub, D., Heusler, K., and McLamore, W. M. (1952) The Total Synthesis of Steroids¹, *Journal of the American Chemical Society* 74, 4223-4251.
82. Corey, E. J., Weinshenker, N. M., Schaaf, T. K., and Huber, W. (1969) Stereo-controlled synthesis of dl-prostaglandins F₂.alpha. and E₂, *Journal of the American Chemical Society* 91, 5675-5677.
83. Horner, L., Hoffmann, H., and Wippel, H. G. (1958) Phosphororganische Verbindungen, XII. Phosphinoxyde als Olefinierungsreagenzien, *Chemische Berichte* 91, 61-63.
84. Wadsworth, W. S., and Emmons, W. D. (1961) The Utility of Phosphonate Carbanions in Olefin Synthesis, *Journal of the American Chemical Society* 83, 1733-1738.
85. Juan, A. B., and Liliana, R. O. (2012) Recent Applications of the Horner-Wadsworth-Emmons Reaction to the Synthesis of Natural Products, *Current Organic Chemistry* 16, 2206-2230.

86. Still, W. C., and Gennari, C. (1983) Direct synthesis of Z-unsaturated esters. A useful modification of the horner-emmons olefination, *Tetrahedron Letters* 24, 4405-4408.
87. Ando, K., Oishi, T., Hirama, M., Ohno, H., and Ibuka, T. (2000) Z-Selective Horner–Wadsworth–Emmons Reaction of Ethyl (Diarylphosphono)acetates Using Sodium Iodide and DBU, *The Journal of organic chemistry* 65, 4745-4749.
88. Suzuki, A. (1999) Recent advances in the cross-coupling reactions of organoboron derivatives with organic electrophiles, 1995–1998, *Journal of Organometallic Chemistry* 576, 147-168.
89. Miyaura, N., Yamada, K., and Suzuki, A. (1979) A new stereospecific cross-coupling by the palladium-catalyzed reaction of 1-alkenylboranes with 1-alkenyl or 1-alkynyl halides, *Tetrahedron Letters* 20, 3437-3440.
90. Nobelprize.org. (2014) The Nobel Prize in Chemistry 2010, In *Nobelprize.org*, Nobel Media AB
91. Negishi, E., King, A. O., and Okukado, N. (1977) Selective carbon-carbon bond formation via transition metal catalysis. 3. A highly selective synthesis of unsymmetrical biaryls and diarylmethanes by the nickel- or palladium-catalyzed reaction of aryl- and benzylzinc derivatives with aryl halides, *The Journal of organic chemistry* 42, 1821-1823.
92. Negishi, E.-i., Liou, S.-Y., Xu, C., and Huo, S. (2002) A Novel, Highly Selective, and General Methodology for the Synthesis of 1,5-Diene-Containing Oligoisoprenoids of All Possible Geometrical Combinations Exemplified by an Iterative and Convergent Synthesis of Coenzyme Q10, *Organic Letters* 4, 261-264.
93. Harold, G., Huckins, J. H. A., and Stein, T. W. (1967) Process for producing styrene, Google Patents, US.
94. Suzuki, A. (2002) Cross-coupling reactions via organoboranes, *Journal of Organometallic Chemistry* 653, 83-90.
95. Liu, J., Lotesta, S. D., and Sorensen, E. J. (2011) A concise synthesis of the molecular framework of pleuromutilin, *Chemical Communications* 47, 1500-1502.

96. Palomino, E., Maldonado, C., Kempff, M. B., and Ksebati, M. B. (1996) Caparratriene, an Active Sesquiterpene Hydrocarbon from *Ocotea caparrapi*, *Journal of Natural Products* 59, 77-79.
97. Vyvyan, J. R., Peterson, E. A., and Stephan, M. L. (1999) An expedient total synthesis of (\pm)-caparratriene, *Tetrahedron Letters* 40, 4947-4949.
98. Miyaura, N., and Suzuki, A. (1995) Palladium-Catalyzed Cross-Coupling Reactions of Organoboron Compounds, *Chemical Reviews* 95, 2457-2483.
99. Suzuki, A. (1991) Synthetic studies via the cross-coupling reaction of organoboron derivatives with organic halides, In *Pure and Applied Chemistry*, p 419.
100. Lipshutz, B. H., and Ghorai, S. (2012) Organocatalysis in Water at Room Temperature with In-Flask Catalyst Recycling, *Organic Letters* 14, 422-425.
101. Carey, F. A., Carey, F. A., and Giuliano, R. M. (2011) *Organic Chemistry*, McGraw-Hill.
102. Woodworth, R. C., and Skell, P. S. (1959) Methylene, CH₂. Stereospecific Reaction with cis- and trans-2-Butene, *Journal of the American Chemical Society* 81, 3383-3386.
103. Rabinovitch, B. S., and Michel, K. W. (1959) The Thermal Unimolecular cis-trans Isomerization of cis-Butene-2, *Journal of the American Chemical Society* 81, 5065-5071.
104. Miles, W. H., Nutaitis, C. F., and Berreth, C. L. (1994) Hydrochlorination of (R)-Carvone, *Journal of Chemical Education* 71, 1097.
105. Pathirana, S., Neely, W. C., and Vodyanoy, V. (1998) Condensing and Expanding Effects of the Odorants (+)- and (-)-Carvone on Phospholipid Monolayers, *Langmuir* 14, 679-682.
106. Tomaszewski, J., and Rumore, M. M. (1994) Stereoisomeric Drugs: FDA'S Policy Statement and the Impact on Drug Development, *Drug Development and Industrial Pharmacy* 20, 119-139.

107. Sie Yon, L., Gonawan, F. N., Kamaruddin, A. H., and Uzir, M. H. (2013) Enzymatic Deracemization of (R,S)-Ibuprofen Ester via Lipase-catalyzed Membrane Reactor, *Industrial & Engineering Chemistry Research* 52, 9441-9453.
108. Tseng, S., Pak, G., Washenik, K., Keltz Pomeranz, M., and Shupack, J. L. (1996) Rediscovering thalidomide: A review of its mechanism of action, side effects, and potential uses, *Journal of the American Academy of Dermatology* 35, 969-979.
109. Calabrese, L., and Fleischer Jr, A. B. (2000) Thalidomide: current and potential clinical applications, *The American Journal of Medicine* 108, 487-495.
110. Stephens, T. D., Bunde, C. J. W., and Fillmore, B. J. (2000) Mechanism of action in thalidomide teratogenesis, *Biochemical Pharmacology* 59, 1489-1499.
111. Melchert, M., and List, A. (2007) The thalidomide saga, *The International Journal of Biochemistry & Cell Biology* 39, 1489-1499.
112. Franks, M. E., Macpherson, G. R., and Figg, W. D. (2004) Thalidomide, *The Lancet* 363, 1802-1811.
113. Administration, F. a. D. (1992) FDA's policy statement for the development of new stereoisomeric drugs, *Chirality* 4, 338-340.
114. Carey, F. A., and Sundberg, R. J. (2000) *Advanced Organic Chemistry*, Springer US.
115. Andersh, B., Kilby, K. N., Turnis, M. E., and Murphy, D. L. (2008) Regioselectivity in Organic Synthesis: Preparation of the Bromohydrin of alpha-Methylstyrene, *Journal of Chemical Education* 85, 102.
116. Legrand, S., and Högskolan i Kalmar. Institutionen för kemi och biomedicinsk, v. (2006) *Stereoselectivity and Regioselectivity in Organic Chemistry: Novel Systems and Applications*, Department of Chemistry and Biomedical Sciences, University of Kalmar.
117. Markownikoff, W. (1870) I. Ueber die Abhängigkeit der verschiedenen Vertretbarkeit des Radicalwasserstoffs in den isomeren Buttersäuren, *Justus Liebigs Annalen der Chemie* 153, 228-259.

118. Baldwin, J. E. (1976) Rules for ring closure, *Journal of the Chemical Society, Chemical Communications*, 734-736.
119. Sielecki, T. M., Boylan, J. F., Benfield, P. A., and Trainor, G. L. (2000) Cyclin-Dependent Kinase Inhibitors: Useful Targets in Cell Cycle Regulation, *Journal of Medicinal Chemistry* 43, 1-18.
120. Greene, T. W., and Wuts, P. G. M. (2002) Protection for the Hydroxyl Group, Including 1,2- and 1,3-Diols, In *Protective Groups in Organic Synthesis*, pp 17-245, John Wiley & Sons, Inc.
121. Legrand, S., Nordlander, G., Nordenhem, H., Borg-Karlson, A.-K., and Unelius, C. R. (2004) Hydroxy-Methoxybenzoic Methyl Esters: Synthesis and Antifeedant Activity on the Pine Weevil, *Hylobius abietis*, In *Zeitschrift für Naturforschung B*, p 829.
122. Greene, T. W., and Wuts, P. G. M. (2002) The Role of Protective Groups in Organic Synthesis, In *Protective Groups in Organic Synthesis*, pp 1-16, John Wiley & Sons, Inc.
123. Coqueiro, A., and Verpoorte, R. (2015) Alkaloids☆, In *Reference Module in Chemistry, Molecular Sciences and Chemical Engineering*, Elsevier.
124. Hajos, Z. G., and Parrish, D. R. (1974) Asymmetric synthesis of bicyclic intermediates of natural product chemistry, *The Journal of organic chemistry* 39, 1615-1621.
125. McMurry, J., and Miller, R. B. (2013) *Annual Reports in Organic Synthesis — 1970*, Elsevier Science, New York, US.
126. Jarvis, L. M. (2014) Anatomy Of An Academic Drug Discovery Program, *Chemical & Engineering News Archive* 92, 28-29.
127. Qiu, S., Sun, H., Zhang, A.-H., Xu, H.-Y., Yan, G.-L., Han, Y., and Wang, X.-J. (2014) Natural alkaloids: basic aspects, biological roles, and future perspectives, *Chinese Journal of Natural Medicines* 12, 401-406.
128. Patel, R. N. (2011) Biocatalysis: Synthesis of Key Intermediates for Development of Pharmaceuticals, *ACS Catalysis* 1, 1056-1074.

129. Russo, P., Frustaci, A., Bufalo, A. D., Fini, M., and Cesario, A. (2013) Multitarget Drugs of Plants Origin Acting on Alzheimer's Disease, *Current Medicinal Chemistry* 20, 1686-1693.
130. Anand, S. (2006) *Medical textiles and biomaterials for healthcare : incorporating proceedings of MEDTEX03 International Conference and Exhibition on Healthcare and Medical Textiles*, Woodhead ; CRC Press, Cambridge; Boca Raton, FL.
131. Thirumurugan, P., Matosiuk, D., and Jozwiak, K. (2013) Click Chemistry for Drug Development and Diverse Chemical–Biology Applications, *Chemical Reviews* 113, 4905-4979.
132. Eliel, E. L., and Wilen, S. H. (2008) *Stereochemistry of Organic Compounds*, Wiley India Pvt. Limited.
133. Houk, K. N., and List, B. (2004) Asymmetric Organocatalysis, *Accounts of Chemical Research* 37, 487-487.
134. Enders, D., Grondal, C., and Hüttl, M. R. M. (2007) Asymmetric Organocatalytic Domino Reactions, *Angewandte Chemie International Edition* 46, 1570-1581.
135. Longbottom, D. A., Franckevicius, V., Kumarn, S., Oelke, A. J., Wascholowski, V., and Ley, S. V. (2008) Practical organocatalysis with (S)- and (R)-5-pyrrolidin-2-yl-1H-tetrazoles, *Aldrichimica Acta* 41, 3-11.
136. Bui, T., and Barbas Iii, C. F. (2000) A proline-catalyzed asymmetric Robinson annulation reaction, *Tetrahedron Letters* 41, 6951-6954.
137. Kotsuki, H., Ikishima, H., and Okuyama, A. (2008) Organocatalytic asymmetric synthesis using proline and related molecules. Part 1, *Heterocycles* 75, 493-529.
138. Wagner, J., Lerner, R. A., and Barbas, C. F. (1995) Efficient Aldolase Catalytic Antibodies That Use the Enamine Mechanism of Natural Enzymes, *Science* 270, 1797-1800.
139. Agami, C., Puchot, C., and Sevestre, H. (1986) Is the mechanism of the proline-catalyzed enantioselective aldol reaction related to biochemical processes ?, *Tetrahedron Letters* 27, 1501-1504.

140. Jarvo, E. R., and Miller, S. J. (2002) Amino acids and peptides as asymmetric organocatalysts, *Tetrahedron* 58, 2481-2495.
141. List, B. (2002) Proline-catalyzed asymmetric reactions, *Tetrahedron* 58, 5573-5590.
142. Zimmerman, H. E., and Traxler, M. D. (1957) The Stereochemistry of the Ivanov and Reformatsky Reactions. I, *Journal of the American Chemical Society* 79, 1920-1923.
143. Seebach, D., Boes, M., Naef, R., and Schweizer, W. B. (1983) Alkylation of amino acids without loss of the optical activity: preparation of .alpha.-substituted proline derivatives. A case of self-reproduction of chirality, *Journal of the American Chemical Society* 105, 5390-5398.
144. Rizzi, G. P. (1970) Evidence for an azomethine ylide intermediate in the carbonyl-assisted decarboxylation of sarcosine. Novel synthesis of dl-phenylephrine hydrochloride, *The Journal of organic chemistry* 35, 2069-2072.
145. List, B., Lerner, R. A., and Barbas, C. F. (2000) Proline-Catalyzed Direct Asymmetric Aldol Reactions, *Journal of the American Chemical Society* 122, 2395-2396.
146. Sheldon, R. (2010) Introduction to Green Chemistry, Organic Synthesis and Pharmaceuticals, In *Green Chemistry in the Pharmaceutical Industry*, pp 1-20, Wiley-VCH Verlag GmbH & Co. KGaA.
147. Heathcock, C. H., Buse, C. T., Kleschick, W. A., Pirrung, M. C., Sohn, J. E., and Lampe, J. (1980) Acyclic stereoselection. 7. Stereoselective synthesis of 2-alkyl-3-hydroxy carbonyl compounds by aldol condensation, *The Journal of organic chemistry* 45, 1066-1081.
148. Heathcock, C. H. (1981) Acyclic Stereocontrol Through the Aldol Condensation, *Science* 214, 395-400.
149. Kano, T., Takai, J., Tokuda, O., and Maruoka, K. (2005) Design of an Axially Chiral Amino Acid with a Binaphthyl Backbone as an Organocatalyst for a Direct Asymmetric Aldol Reaction, *Angewandte Chemie International Edition* 44, 3055-3057.

150. Nakadai, M., Saito, S., and Yamamoto, H. (2002) Diversity-based strategy for discovery of environmentally benign organocatalyst: diamine–protonic acid catalysts for asymmetric direct aldol reaction, *Tetrahedron* 58, 8167-8177.
151. Hartikka, A., and Arvidsson, P. I. (2004) Rational design of asymmetric organocatalysts—increased reactivity and solvent scope with a tetrazolic acid, *Tetrahedron: Asymmetry* 15, 1831-1834.
152. Arnó, M., Zaragoza, R. J., and Domingo, L. R. (2005) Density functional theory study of the 5-pyrrolidin-2-yltetrazole-catalyzed aldol reaction, *Tetrahedron: Asymmetry* 16, 2764-2770.
153. Mirabal-Gallardo, Y., Piérola, J., Shankaraiah, N., and Santos, L. S. (2012) Enantioselective total synthesis of (S)-(+)-lennoxamine through asymmetric hydrogenation mediated by l-proline-tetrazole ruthenium catalyst, *Tetrahedron Letters* 53, 3672-3675.
154. Knudsen, K. R., Mitchell, C. E. T., and Ley, S. V. (2006) Asymmetric organocatalytic conjugate addition of malonates to enones using a proline tetrazole catalyst, *Chemical Communications*, 66-68.
155. Zu, L., Xie, H., Li, H., Wang, J., and Wang, W. (2008) Highly Enantioselective Aldol Reactions Catalyzed by a Recyclable Fluorous (S) Pyrrolidine Sulfonamide on Water, *Organic Letters* 10, 1211-1214.
156. Wang, X.-J., Zhao, Y., and Liu, J.-T. (2007) Regiospecific Organocatalytic Asymmetric Aldol Reaction of Methyl Ketones and α,β -Unsaturated Trifluoromethyl Ketones, *Organic Letters* 9, 1343-1345.
157. Wu, Y., Zhang, Y., Yu, M., Zhao, G., and Wang, S. (2006) Highly Efficient and Reusable Dendritic Catalysts Derived from N-Prolylsulfonamide for the Asymmetric Direct Aldol Reaction in Water, *Organic Letters* 8, 4417-4420.
158. Sundén, H., Dahlin, N., Ibrahim, I., Adolfsson, H., and Córdova, A. (2005) Novel organic catalysts for the direct enantioselective α -oxidation of carbonyl compounds, *Tetrahedron Letters* 46, 3385-3389.
159. Engqvist, M., Casas, J., Sundén, H., Ibrahim, I., and Córdova, A. (2005) Direct organocatalytic asymmetric α -oxidation of ketones with iodosobenzene and N-sulfonyloxaziridines, *Tetrahedron Letters* 46, 2053-2057.

160. Wang, W., Wang, J., Li, H., and Liao, L. (2004) An amine sulfonamide organocatalyst for promoting direct, highly enantioselective α -aminooxylation reactions of aldehydes and ketones, *Tetrahedron Letters* 45, 7235-7238.
161. Hayashi, Y., Sumiya, T., Takahashi, J., Gotoh, H., Urushima, T., and Shoji, M. (2006) Highly diastereo- and enantioselective direct aldol reactions in water, *Angew Chem Int Ed Engl* 45, 958-961.
162. Aycock, D. F. (2007) Solvent Applications of 2-Methyltetrahydrofuran in Organometallic and Biphasic Reactions, *Organic Process Research & Development* 11, 156-159.
163. Fuenfschilling, P. C., Hoehn, P., and Mutz, J.-P. (2007) An Improved Manufacturing Process for Fluvastatin, *Organic Process Research & Development* 11, 13-18.
164. Butters, M., Catterick, D., Craig, A., Curzons, A., Dale, D., Gillmore, A., Green, S. P., Marziano, I., Sherlock, J.-P., and White, W. (2006) Critical Assessment of Pharmaceutical Processes A Rationale for Changing the Synthetic Route, *Chemical Reviews* 106, 3002-3027.
165. Delhaye, L., Ceccato, A., Jacobs, P., Köttgen, C., and Merschaert, A. (2007) Removal of Reaction Solvent by Extractive Workup: Survey of Water and Solvent Co-extraction in Various Systems, *Organic Process Research & Development* 11, 160-164.
166. Constable, D. J. C., Jimenez-Gonzalez, C., and Henderson, R. K. (2007) Perspective on Solvent Use in the Pharmaceutical Industry, *Organic Process Research & Development* 11, 133-137.
167. Yang, H., and Carter, R. G. (2008) N-(p-Dodecylphenylsulfonyl)-2-pyrrolidinecarboxamide: A Practical Proline Mimetic for Facilitating Enantioselective Aldol Reactions, *Organic Letters* 10, 4649-4652.
168. Yang, H., and Carter, R. G. (2009) Enantioselective Mannich Reactions with the Practical Proline Mimetic N-(p-Dodecylphenyl-sulfonyl)-2-pyrrolidinecarboxamide, *The Journal of organic chemistry* 74, 2246-2249.

169. Saha, M., and Carter, R. G. (2013) Toward a Unified Approach for the Lycopodines: Synthesis of 10-Hydroxylycopodine, Deacetylpaniculine, and Paniculine, *Organic Letters* 15, 736-739.
170. Dunetz, J. R., Magano, J., and Weisenburger, G. A. (2016) Large-Scale Applications of Amide Coupling Reagents for the Synthesis of Pharmaceuticals, *Organic Process Research & Development* 20, 140-177.
171. Hartikka, A., Ślósarczyk, A. T., and Arvidsson, P. I. (2007) Application of novel sulfonamides in enantioselective organocatalyzed cyclopropanation, *Tetrahedron: Asymmetry* 18, 1403-1409.
172. Thorat, P. B., Goswami, S. V., Khade, B. C., and Bhusare, S. R. (2012) Organocatalyzed Baylis–Hillman reaction: an enantioselective approach, *Tetrahedron: Asymmetry* 23, 1320-1325.
173. Martin, M. T., Roschangar, F., and Eaddy, J. F. (2003) Practical acid-catalyzed acylation of sulfonamides with carboxylic acid anhydrides, *Tetrahedron Letters* 44, 5461-5463.
174. Raji Reddy, C., Mahipal, B., and Yaragorla, S. R. (2007) A new and efficient method for the facile synthesis of N-acyl sulfonamides under Lewis acid catalysis, *Tetrahedron Letters* 48, 7528-7532.
175. Allman, J. M., and Kauffman, J. (2016) Method for making methyl methacrylate from propionaldehyde and formaldehyde via oxidative esterification, US2014/0206897 A1 ed., Google Patents.
176. Tsuruda, T., Ebine, M., Umeda, A., and Oishi, T. (2015) Stereoselective Synthesis of the C1–C29 Part of Amphidinol 3, *The Journal of organic chemistry* 80, 859-871.
177. Wu, J., Zhao, W., and Cao, S. (2012) Synthesis of Difluoromethyl-Containing α -Acylloxycarboxamide Derivatives through a Passerini Reaction and Desulfonylation, *European Journal of Organic Chemistry* 2012, 1380-1387.
178. Greene, T. W., and Wuts, P. G. M. (2002) Protection for the Amino Group, In *Protective Groups in Organic Synthesis*, pp 494-653, John Wiley & Sons, Inc.

179. Salvatore, R. N., Smith, R. A., Nischwitz, A. K., and Gavin, T. (2005) A mild and highly convenient chemoselective alkylation of thiols using Cs₂CO₃-TBAI, *Tetrahedron Letters* 46, 8931-8935.
180. Zhiqin Ji, † Asma A. Ahmed, ‡ Daniel H. Albert, † Jennifer J. Bouska, † Peter F. Bousquet, ‡ George, A. Cunha, ‡ Gilbert Diaz, †, Keith B. Glaser, J. G., † Christopher M. Harris, ‡ Junling Li, † Patrick A. Marcotte, † Maria D. Moskey, ‡ Tetsuro Oie, †, and Lori Pease, N. B. S., † Kent D. Stewart, † Steven K. Davidsen, † and Michael R. Michaelides †. (2008) 3-Amino-benzo[d]isoxazoles as Novel Multitargeted Inhibitors of Receptor Tyrosine Kinases, *Journal of Medicinal Chemistry* 51, 1231-1241.
181. Solà, J., Fletcher, S. P., Castellanos, A., and Clayden, J. (2010) Nanometer-Range Communication of Stereochemical Information by Reversible Switching of Molecular Helicity, *Angewandte Chemie International Edition* 49, 6836-6839.
182. Golden, M., Legg, D., Milne, D., Bharadwaj M, A., Deepthi, K., Gopal, M., Dokka, N., Nambiar, S., Ramachandra, P., Santhosh, U., Sharma, P., Sridharan, R., Sultur, M., Linderberg, M., Nilsson, A., Sohlberg, R., Kremers, J., Oliver, S., and Patra, D. (2016) The Development of a Manufacturing Route to an MCHR1 Antagonist, *Organic Process Research & Development* 20, 675-682.
183. Rensing, D. T., Uppal, S., Blumer, K. J., and Moeller, K. D. (2015) Toward the Selective Inhibition of G Proteins: Total Synthesis of a Simplified YM-254890 Analog, *Organic Letters* 17, 2270-2273.
184. Tayebee, R., Amini, M. M., Akbari, M., and Aliakbari, A. (2015) A novel inorganic-organic nanohybrid material H₄SiW₁₂O₄₀/pyridino-MCM-41 as efficient catalyst for the preparation of 1-amidoalkyl-2-naphthols under solvent-free conditions, *Dalton Transactions* 44, 9596-9609.
185. Han, S.-Y., and Kim, Y.-A. (2004) Recent development of peptide coupling reagents in organic synthesis, *Tetrahedron* 60, 2447-2467.
186. Albericio, F. (2004) Developments in peptide and amide synthesis, *Current Opinion in Chemical Biology* 8, 211-221.
187. Gabriel, C. M., Keener, M., Gallou, F., and Lipshutz, B. H. (2015) Amide and Peptide Bond Formation in Water at Room Temperature, *Organic Letters* 17, 3968-3971.

188. Montalbetti, C. A. G. N., and Falque, V. (2005) Amide bond formation and peptide coupling, *Tetrahedron* 61, 10827-10852.
189. Kotha, S. (2003) The Building Block Approach to Unusual α -Amino Acid Derivatives and Peptides, *Accounts of Chemical Research* 36, 342-351.
190. Liu, C., Tan, J.-L., Xiao, S.-Y., Liao, J.-F., Zou, G.-R., Ai, X.-X., Chen, J.-B., Xiang, Y., Yang, Q., and Zuo, H. (2014) 1,4-Benzoxazine-3(4H)-ones as potent inhibitors of platelet aggregation: design, synthesis and structure-activity relations, *Chem Pharm Bull (Tokyo)* 62, 915-920.

APPENDIX A

FLASH CHROMATOGRAPHER PURIFICATION REPORTS



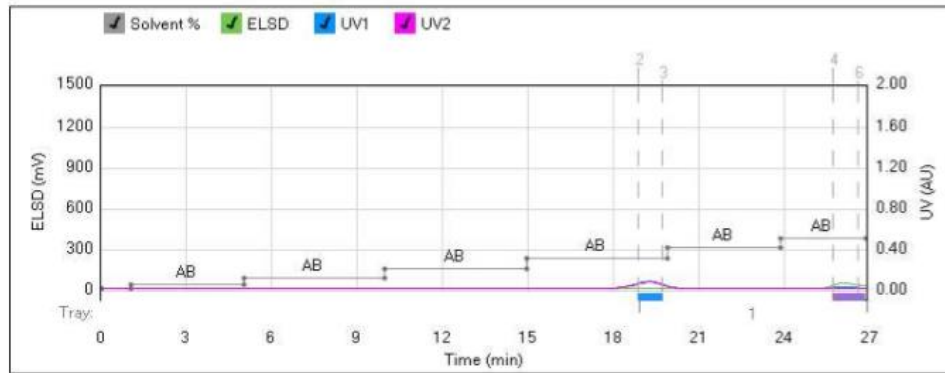
Method Name:
Run Name: 2014-08-11_h-b2-c-2nd
Run Date: 2014-08-11 13:05

Column: Reveleris® Silica 12g
Flow Rate: 30 mL/min
Equilibration: 4.8 min
Run Length: 27.0 min
Air Purge Time: 0.5 min

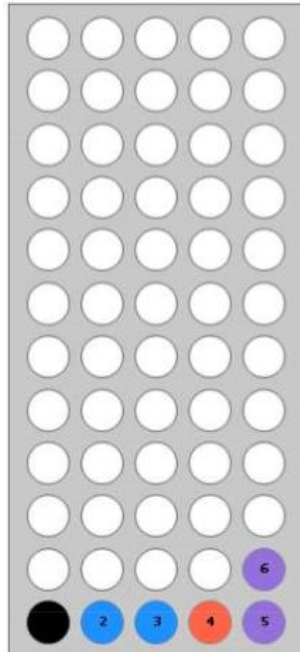
Slope Detection: Off
ELSD Threshold: 20 mV
UV Threshold: 0.05 AU
UV1 Wavelength: 254 nm
UV2 Wavelength: 280 nm

Collection Mode: Collect Peaks
Per-Vial Volume: 25 mL
Non-Peaks: 25 mL
Injection Type: Dry

ELSD Carrier: Iso-propanol
Solvent A: Hexane
Solvent B: Ethyl acetate
Solvent C: <No solvent chose
Solvent D: <No solvent chose



1 - 7B19



Gradient Table

	Min	Solvents	% 2nd
1	0.0	AB	0
2	1.0	AB	0
3	0.0	AB	2
4	4.0	AB	2
5	0.0	AB	5
6	5.0	AB	5
7	0.0	AB	10
8	5.0	AB	10
9	0.0	AB	15
10	5.0	AB	15
11	0.0	AB	20
12	4.0	AB	20
13	0.0	AB	25
14	3.0	AB	25

Vial Mapping Table

Peak #	Start Tray/Vial	End Tray/Vial
1	1:2	1:3
2	1:4	1:4
3	1:5	1:6



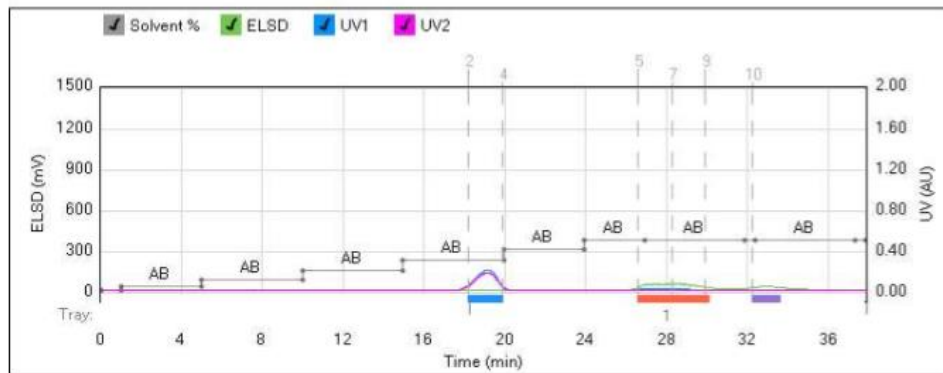
Method Name:
Run Name: 2014-08-11_h-b2-c
Run Date: 2014-08-11 10:34

Column: Reveleris® Silica 12g
Flow Rate: 30 mL/min
Equilibration: 4.8 min
Run Length: 38.0 min
Air Purge Time: 0.5 min

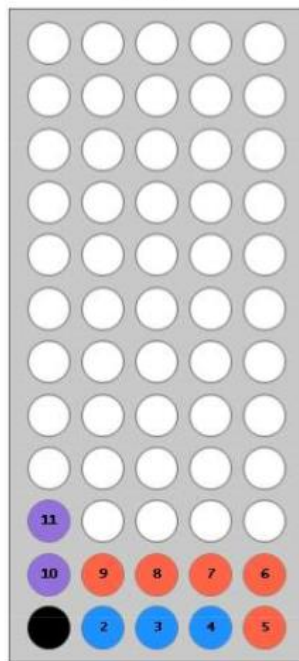
Slope Detection: Off
ELSD Threshold: 20 mV
UV Threshold: 0.05 AU
UV1 Wavelength: 254 nm
UV2 Wavelength: 280 nm

Collection Mode: Collect Peaks
Per-Vial Volume: 25 mL
Non-Peaks: 25 mL
Injection Type: Dry

ELSD Carrier: Iso-propanol
Solvent A: Hexane
Solvent B: Ethyl acetate
Solvent C: <No solvent chose
Solvent D: <No solvent chose



1-7B19



Gradient Table

	Min	Solvents	% 2nd
1	0.0	AB	0
2	1.0	AB	0
3	0.0	AB	2
4	4.0	AB	2
5	0.0	AB	5
6	5.0	AB	5
7	0.0	AB	10
8	5.0	AB	10
9	0.0	AB	15
10	5.0	AB	15
11	0.0	AB	20
12	4.0	AB	20
13	0.0	AB	25
14	3.0	AB	25
15	5.0	AB	25
16	0.5	AB	25
17	5.0	AB	25
18	0.5	AB	25

Vial Mapping Table

Peak #	Start Tray/Vial	End Tray/Vial
1	1:2	1:4
2	1:5	1:9
3	1:10	1:11



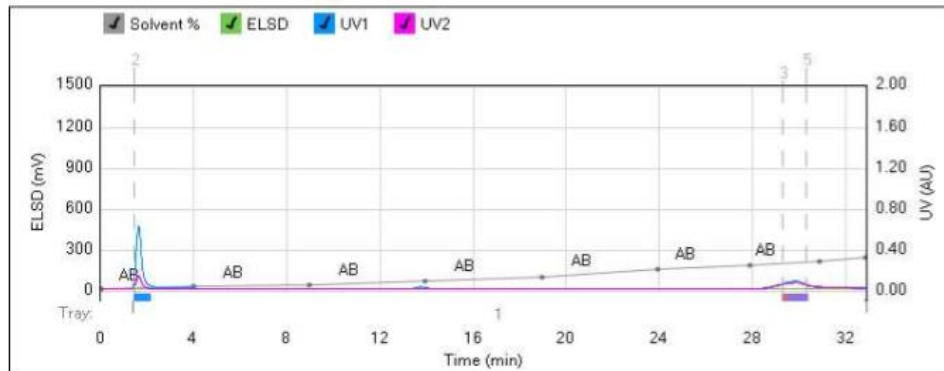
Method Name:
Run Name: 2014-07-30_KL-H-B5-A
Run Date: 2014-07-30 15:37

Column: Reveleris® Silica 12g
 Flow Rate: 30 mL/min
 Equilibration: 4.8 min
 Run Length: 33.0 min
 Air Purge Time: 0.5 min

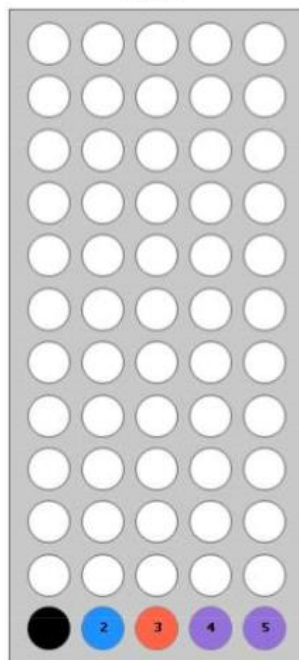
Slope Detection: Off
 ELSD Threshold: 20 mV
 UV Threshold: 0.05 AU
 UV1 Wavelength: 254 nm
 UV2 Wavelength: 280 nm

Collection Mode: Collect Peaks
 Per-Vial Volume: 25 mL
 Non-Peaks: 25 mL
 Injection Type: Manual

ELSD Carrier: Iso-propanol
 Solvent A: Hexane
 Solvent B: Ethyl acetate
 Solvent C: <No solvent chose
 Solvent D: <No solvent chose



1-7B19



Gradient Table

	Min	Solvents	% 2nd
1	0.0	AB	0
2	4.0	AB	1
3	5.0	AB	2
4	5.0	AB	4
5	5.0	AB	6
6	5.0	AB	10
7	4.0	AB	12
8	3.0	AB	14
9	2.0	AB	16

Vial Mapping Table

Peak #	Start Tray/Vial	End Tray/Vial
1	1:2	1:2
2	1:3	1:3
3	1:4	1:5



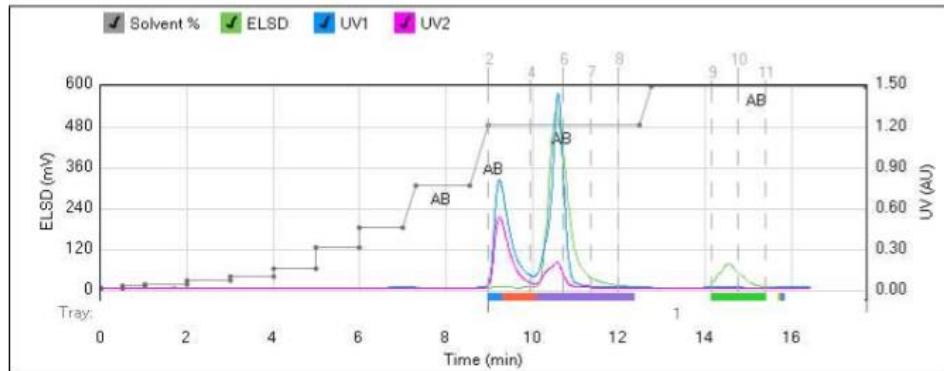
Method Name:
Run Name: KL-H-B2-H
Run Date: 2015-11-16 11:42

Column: Generic Silica 40g
Flow Rate: 40 mL/min
Equilibration: 6.0 min
Run Length: 17.8 min
Air Purge Time: 1 min

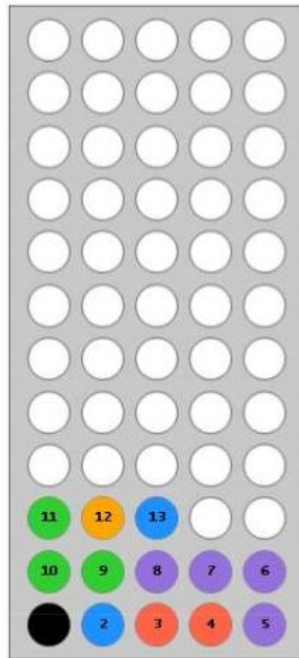
Slope Detection: High
ELSD Threshold: 5 mV
UV Threshold: 0.02 AU
UV1 Wavelength: 254 nm
UV2 Wavelength: 280 nm

Collection Mode: Collect Peaks
Per-Vial Volume: 25 mL
Non-Peaks: 25 mL
Injection Type: Dry

ELSD Carrier: Iso-propanol
Solvent A: Hexane
Solvent B: Ethyl acetate
Solvent C: <No solvent chosen>
Solvent D: <No solvent chosen>



1-7B19



Gradient Table

	Min	Solvents	% 2nd
1	0.0	AB	0
2	0.5	AB	0
3	0.0	AB	1
4	0.5	AB	1
5	0.0	AB	2
6	1.0	AB	2
7	0.0	AB	4
8	1.0	AB	4
9	0.0	AB	6
10	1.0	AB	6
11	0.0	AB	10
12	1.0	AB	10
13	0.0	AB	20
14	1.0	AB	20
15	0.0	AB	30
16	1.0	AB	30
17	0.3	AB	51
18	1.3	AB	51
19	0.4	AB	81
20	3.5	AB	81
21	0.3	AB	100
22	5.0	AB	100

Vial Mapping Table

Peak #	Start Tray Vial	End Tray Vial
1	1:2	1:2
2	1:3	1:4
3	1:5	1:8



Method Name:
Run Name: KL-H-B2-H
Run Date: 2015-11-16 11:42

Vial Mapping Table

Peak #	Start Tray/Vial	End Tray/Vial
4	1:9	1:11
5	1:12	1:12
6	1:13	1:13



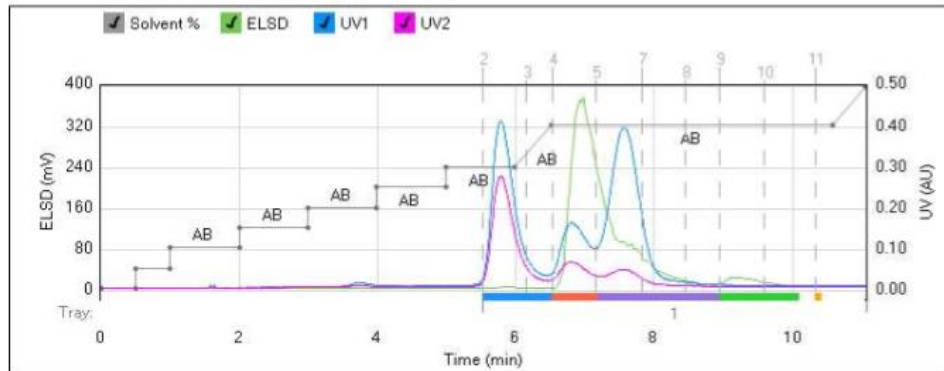
Method Name:
Run Name: KL-H-B2-H_2
Run Date: 2015-11-17 07:33

Column: Generic Silica 40g
Flow Rate: 40 mL/min
Equilibration: 6.0 min
Run Length: 11.1 min
Air Purge Time: 1 min

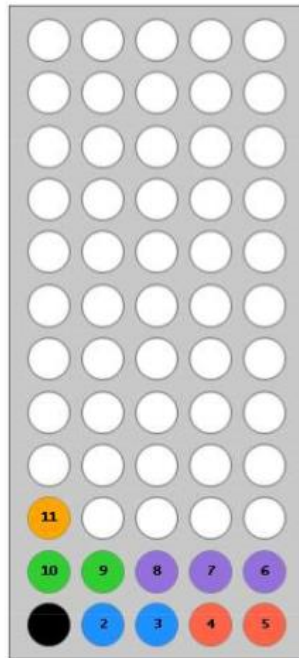
Slope Detection: High
ELSD Threshold: 5 mV
UV Threshold: 0.02 AU
UV1 Wavelength: 254 nm
UV2 Wavelength: 280 nm

Collection Mode: Collect Peaks
Per-Vial Volume: 25 mL
Non-Peaks: 25 mL
Injection Type: Dry

ELSD Carrier: Iso-propanol
Solvent A: Hexane
Solvent B: Ethyl acetate
Solvent C: <No solvent chosen>
Solvent D: <No solvent chosen>



1-7B19



Gradient Table

	Min	Solvents	% 2nd
1	0.0	AB	0
2	0.5	AB	0
3	0.0	AB	10
4	0.5	AB	10
5	0.0	AB	20
6	1.0	AB	20
7	0.0	AB	30
8	1.0	AB	30
9	0.0	AB	40
10	1.0	AB	40
11	0.0	AB	50
12	1.0	AB	50
13	0.0	AB	60
14	1.0	AB	60
15	0.5	AB	81
16	4.1	AB	81
17	0.5	AB	100

Vial Mapping Table

Peak #	Start Tray/Vial	End Tray/Vial
1	1:2	1:3
2	1:4	1:5
3	1:6	1:8
4	1:9	1:10
5	1:11	1:11



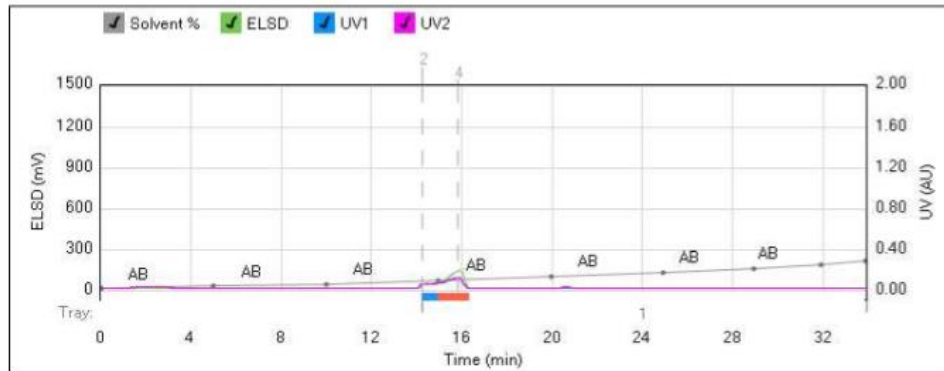
Method Name:
Run Name: 2014-08-01_KL-H-B5-B
Run Date: 2014-08-01 06:21

Column: Reveleris® Silica 12g
 Flow Rate: 30 mL/min
 Equilibration: 4.8 min
 Run Length: 34.0 min
 Air Purge Time: 0.5 min

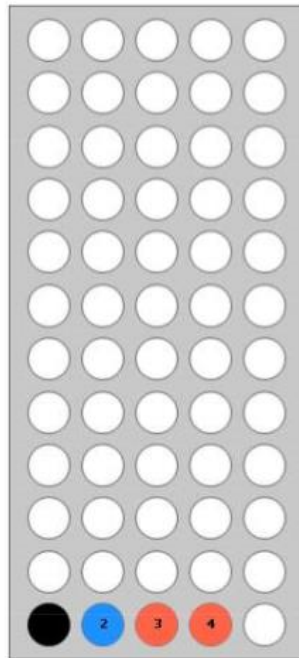
Slope Detection: Off
 ELSD Threshold: 20 mV
 UV Threshold: 0.05 AU
 UV1 Wavelength: 254 nm
 UV2 Wavelength: 280 nm

Collection Mode: Collect Peaks
 Per-Vial Volume: 25 mL
 Non-Peaks: 25 mL
 Injection Type: Dry

ELSD Carrier: Iso-propanol
 Solvent A: Hexane
 Solvent B: Ethyl acetate
 Solvent C: <No solvent chose
 Solvent D: <No solvent chose



1-7B19



Gradient Table

	Min	Solvents	% 2nd
1	0.0	AB	0
2	5.0	AB	1
3	5.0	AB	2
4	5.0	AB	4
5	5.0	AB	6
6	5.0	AB	8
7	4.0	AB	10
8	3.0	AB	12
9	2.0	AB	14

Vial Mapping Table

Peak #	Start Tray Vial	End Tray Vial
1	1.2	1.2
2	1.3	1.4



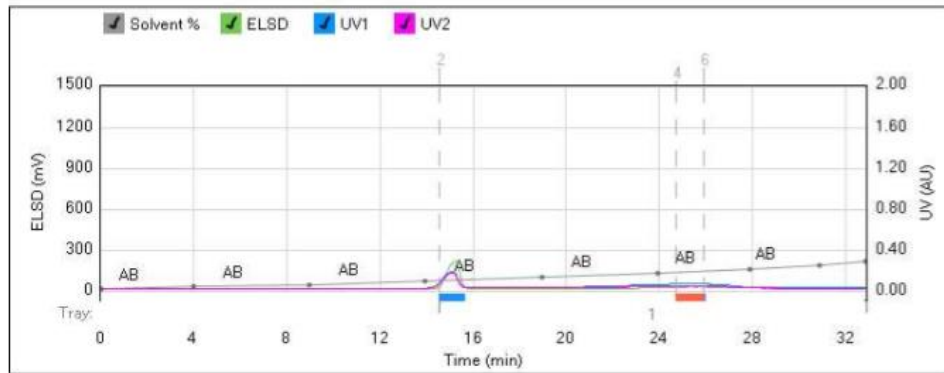
Method Name:
Run Name: 2014-08-01_KL-H-B5-C
Run Date: 2014-08-01 07:10

Column: Reveleris® Silica 12g
Flow Rate: 30 mL/min
Equilibration: 4.8 min
Run Length: 33.0 min
Air Purge Time: 0.5 min

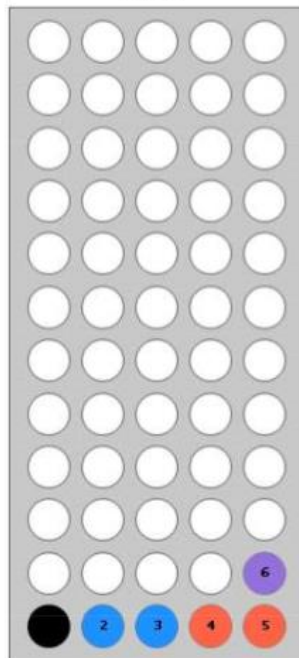
Slope Detection: Off
ELSD Threshold: 20 mV
UV Threshold: 0.05 AU
UV1 Wavelength: 254 nm
UV2 Wavelength: 280 nm

Collection Mode: Collect Peaks
Per-Vial Volume: 25 mL
Non-Peaks: 25 mL
Injection Type: Dry

ELSD Carrier: Iso-propanol
Solvent A: Hexane
Solvent B: Ethyl acetate
Solvent C: <No solvent chose
Solvent D: <No solvent chose



1-7B19



Gradient Table

	Min	Solvents	% 2nd
1	0.0	AB	0
2	4.0	AB	1
3	5.0	AB	2
4	5.0	AB	4
5	5.0	AB	6
6	5.0	AB	8
7	4.0	AB	10
8	3.0	AB	12
9	2.0	AB	14

Vial Mapping Table

Peak #	Start Tray/Vial	End Tray/Vial
1	1:2	1:3
2	1:4	1:5
3	1:6	1:6



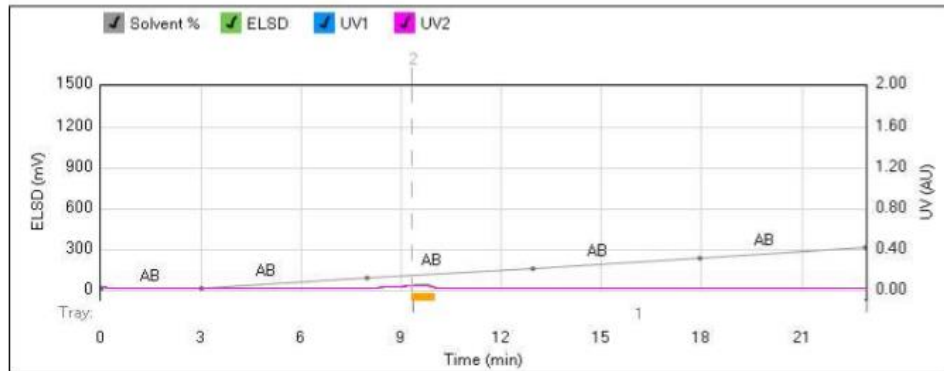
Method Name:
Run Name: 2014-08-04_H-B5-D2
Run Date: 2014-08-05 12:33

Column: Reveleris® Silica 12g
Flow Rate: 30 mL/min
Equilibration: 4.8 min
Run Length: 23.0 min
Air Purge Time: 0.5 min

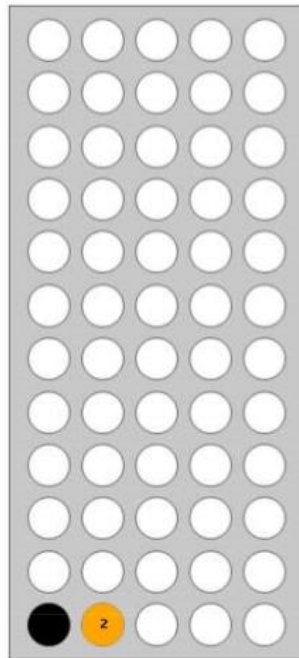
Slope Detection: Off
ELSD Threshold: 20 mV
UV Threshold: 0.05 AU
UV1 Wavelength: 254 nm
UV2 Wavelength: 280 nm

Collection Mode: Collect Peaks
Per-Vial Volume: 25 mL
Non-Peaks: 25 mL
Injection Type: Dry

ELSD Carrier: Iso-propanol
Solvent A: Hexane
Solvent B: Ethyl acetate
Solvent C: <No solvent chose
Solvent D: <No solvent chose



1-7B19



Gradient Table

	Min	Solvents	% 2nd
1	0.0	AB	0
2	3.0	AB	0
3	5.0	AB	5
4	5.0	AB	10
5	5.0	AB	15
6	5.0	AB	20

Vial Mapping Table

Peak #	Start Tray Vial	End Tray Vial
1	1,2	1,2



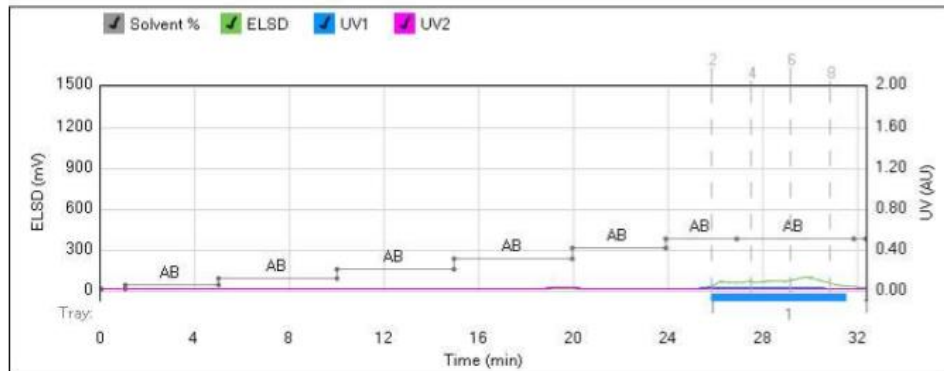
Method Name:
Run Name: 2014-08-11_h-b2-d1
Run Date: 2014-08-11 14:03

Column: Reveleris® Silica 12g
Flow Rate: 30 mL/min
Equilibration: 4.8 min
Run Length: 32.5 min
Air Purge Time: 0.5 min

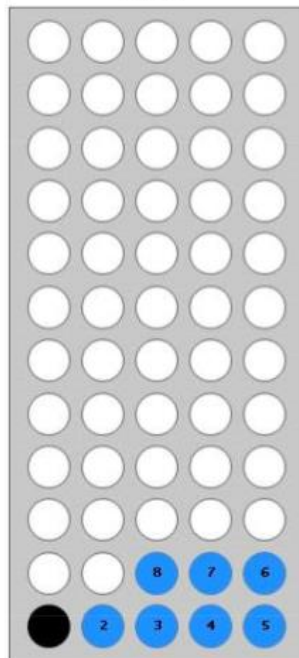
Slope Detection: Off
ELSD Threshold: 20 mV
UV Threshold: 0.05 AU
UV1 Wavelength: 254 nm
UV2 Wavelength: 280 nm

Collection Mode: Collect Peaks
Per-Vial Volume: 25 mL
Non-Peaks: 25 mL
Injection Type: Dry

ELSD Carrier: Iso-propanol
Solvent A: Hexane
Solvent B: Ethyl acetate
Solvent C: <No solvent chose
Solvent D: <No solvent chose



1-7B19



Gradient Table

	Min	Solvents	% 2nd
1	0.0	AB	0
2	1.0	AB	0
3	0.0	AB	2
4	4.0	AB	2
5	0.0	AB	5
6	5.0	AB	5
7	0.0	AB	10
8	5.0	AB	10
9	0.0	AB	15
10	5.0	AB	15
11	0.0	AB	20
12	4.0	AB	20
13	0.0	AB	25
14	3.0	AB	25
15	5.0	AB	25
16	0.5	AB	25

Vial Mapping Table

Peak #	Start Tray Vial	End Tray Vial
1	1:2	1:8



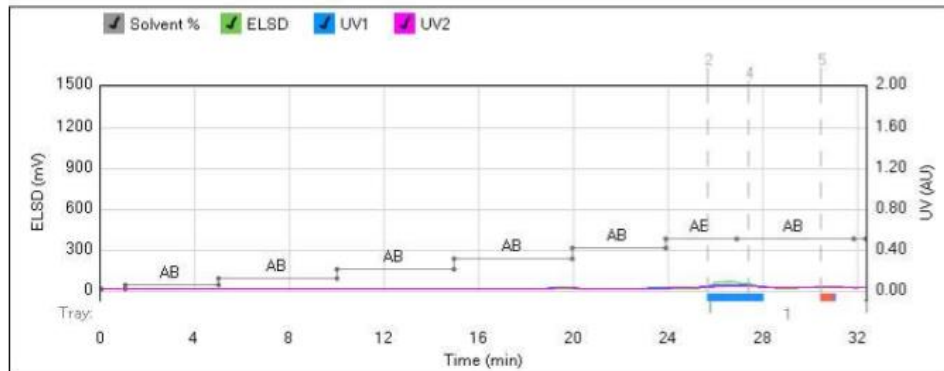
Method Name:
Run Name: 2014-08-11_h-b2-d2
Run Date: 2014-08-11 15:01

Column: Reveleris® Silica 12g
Flow Rate: 30 mL/min
Equilibration: 4.8 min
Run Length: 32.5 min
Air Purge Time: 0.5 min

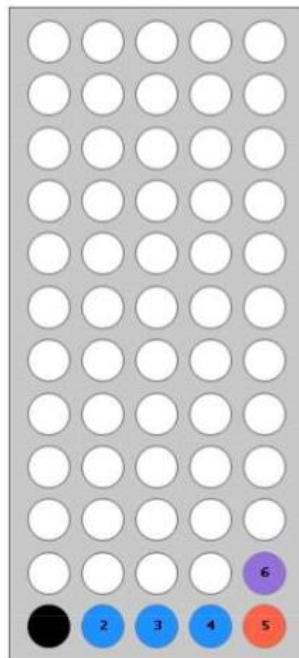
Slope Detection: Off
ELSD Threshold: 20 mV
UV Threshold: 0.05 AU
UV1 Wavelength: 254 nm
UV2 Wavelength: 280 nm

Collection Mode: Collect Peaks
Per-Vial Volume: 25 mL
Non-Peaks: 25 mL
Injection Type: Dry

ELSD Carrier: Iso-propanol
Solvent A: Hexane
Solvent B: Ethyl acetate
Solvent C: <No solvent chose
Solvent D: <No solvent chose



1-7B19



Gradient Table

	Min	Solvents	% 2nd
1	0.0	AB	0
2	1.0	AB	0
3	0.0	AB	2
4	4.0	AB	2
5	0.0	AB	5
6	5.0	AB	5
7	0.0	AB	10
8	5.0	AB	10
9	0.0	AB	15
10	5.0	AB	15
11	0.0	AB	20
12	4.0	AB	20
13	0.0	AB	25
14	3.0	AB	25
15	5.0	AB	25
16	0.5	AB	25

Vial Mapping Table

Peak #	Start Tray Vial	End Tray Vial
1	1:2	1:4
2	1:5	1:5
3	1:6	1:6



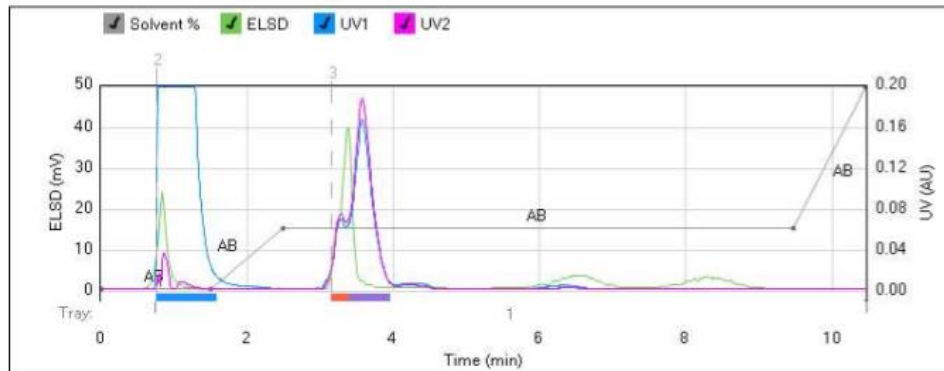
Method Name:
Run Name: KL-H-B6-E
Run Date: 2015-03-19 11:14

Column: Reveleris® Silica 12g
Flow Rate: 30 mL/min
Equilibration: 4.8 min
Run Length: 10.5 min
Air Purge Time: 0.5 min

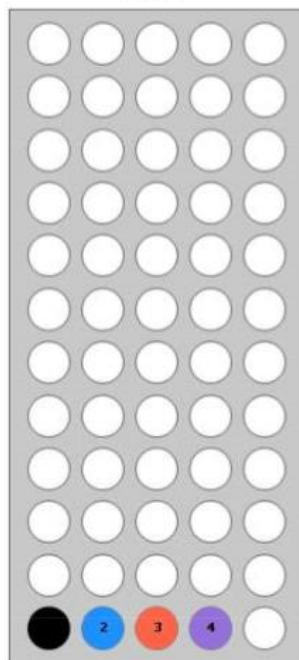
Slope Detection: High
ELSD Threshold: 5 mV
UV Threshold: 0.02 AU
UV1 Wavelength: 254 nm
UV2 Wavelength: 280 nm

Collection Mode: Collect Peaks
Per-Vial Volume: 25 mL
Non-Peaks: 25 mL
Injection Type: Manual

ELSD Carrier: Iso-propanol
Solvent A: Hexane
Solvent B: Ethyl acetate
Solvent C: <No solvent chose
Solvent D: <No solvent chose



1-7B19



Gradient Table

	Min	Solvents	% 2nd
1	0.0	AB	0
2	1.5	AB	0
3	1.0	AB	30
4	7.0	AB	30
5	1.0	AB	100

Vial Mapping Table

Peak #	Start Tray/Vial	End Tray/Vial
1	1:2	1:2
2	1:3	1:3
3	1:4	1:4



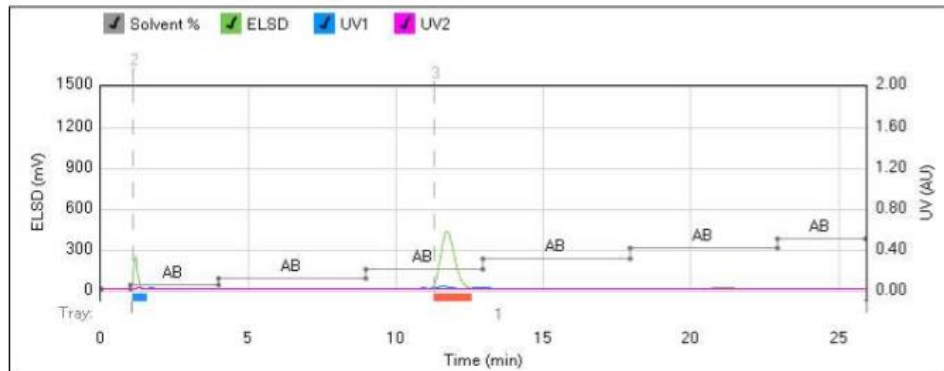
Method Name:
Run Name: 2014-08-12_h-b7-a
Run Date: 2014-08-12 07:23

Column: Reveleris® Silica 4g
Flow Rate: 15 mL/min
Equilibration: 2.4 min
Run Length: 26.0 min
Air Purge Time: 0.5 min

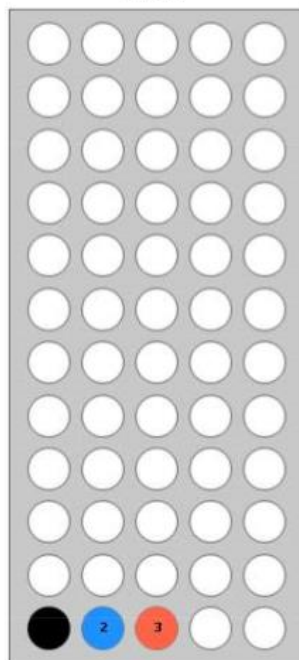
Slope Detection: Off
ELSD Threshold: 20 mV
UV Threshold: 0.05 AU
UV1 Wavelength: 254 nm
UV2 Wavelength: 280 nm

Collection Mode: Collect Peaks
Per-Vial Volume: 25 mL
Non-Peaks: 25 mL
Injection Type: Dry

ELSD Carrier: Iso-propanol
Solvent A: Hexane
Solvent B: Ethyl acetate
Solvent C: <No solvent chosen
Solvent D: <No solvent chosen



1 - 7B19



Gradient Table

	Min	Solvents	% 2nd
1	0.0	AB	0
2	1.0	AB	0
3	0.0	AB	2
4	3.0	AB	2
5	0.0	AB	5
6	5.0	AB	5
7	0.0	AB	10
8	4.0	AB	10
9	0.0	AB	15
10	5.0	AB	15
11	0.0	AB	20
12	5.0	AB	20
13	0.0	AB	25
14	3.0	AB	25

Vial Mapping Table

Peak #	Start Tray Vial	End Tray Vial
1	1:2	1:2
2	1:3	1:3



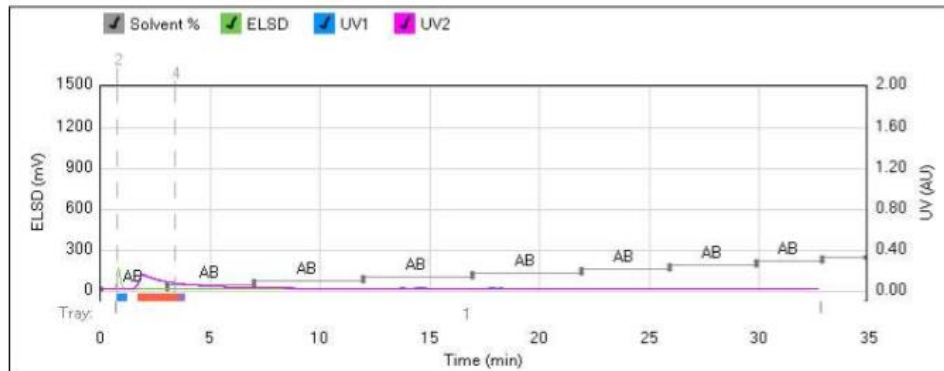
Method Name:
Run Name: 2014-08-14_h-b7-b
Run Date: 2014-08-14 11:03

Column: Reveleris® Silica 4g
Flow Rate: 15 mL/min
Equilibration: 2.4 min
Run Length: 35.0 min
Air Purge Time: 0.5 min

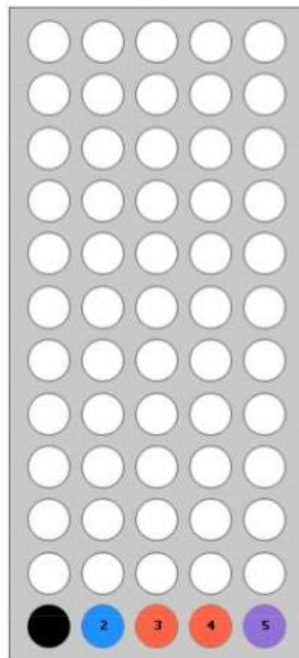
Slope Detection: Off
ELSD Threshold: 20 mV
UV Threshold: 0.05 AU
UV1 Wavelength: 254 nm
UV2 Wavelength: 280 nm

Collection Mode: Collect Peaks
Per-Vial Volume: 25 mL
Non-Peaks: 25 mL
Injection Type: Manual

ELSD Carrier: Iso-propanol
Solvent A: Hexane
Solvent B: Ethyl acetate
Solvent C: <No solvent chosen
Solvent D: <No solvent chosen



1-7B19



Gradient Table

	Min	Solvents	% 2nd
1	0.0	AB	0
2	3.0	AB	0
3	0.0	AB	2
4	4.0	AB	2
5	0.0	AB	4
6	5.0	AB	4
7	0.0	AB	6
8	5.0	AB	6
9	0.0	AB	8
10	5.0	AB	8
11	0.0	AB	10
12	4.0	AB	10
13	0.0	AB	12
14	4.0	AB	12
15	0.0	AB	14
16	3.0	AB	14
17	0.0	AB	16
18	2.0	AB	16

Vial Mapping Table

Peak #	Start Tray Vial	End Tray Vial
1	1:2	1:2
2	1:3	1:4
3	1:5	1:5



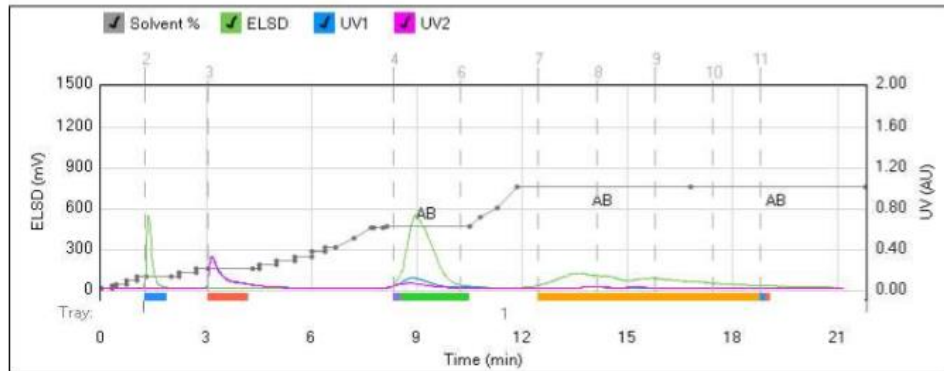
Method Name:
Run Name: 2014-08-29_h-b7-c
Run Date: 2014-08-29 14:53

Column: Reveleris® Silica 4g
Flow Rate: 15 mL/min
Equilibration: 2.4 min
Run Length: 21.9 min
Air Purge Time: 0.5 min

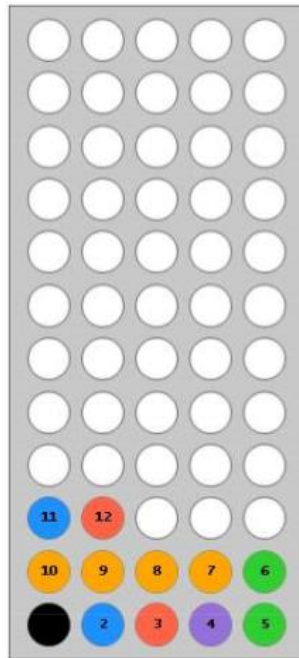
Slope Detection: Off
ELSD Threshold: 20 mV
UV Threshold: 0.05 AU
UV1 Wavelength: 254 nm
UV2 Wavelength: 280 nm

Collection Mode: Collect Peaks
Per-Vial Volume: 25 mL
Non-Peaks: 25 mL
Injection Type: Dry

ELSD Carrier: Iso-propanol
Solvent A: Hexane
Solvent B: Ethyl acetate
Solvent C: <No solvent chosen
Solvent D: <No solvent chosen



1-7B19



Gradient Table

	Min	Solvents	% 2nd
1	0.0	AB	0
2	0.3	AB	0
3	0.0	AB	1
4	0.1	AB	1
5	0.0	AB	2
6	0.3	AB	2
7	0.0	AB	4
8	0.3	AB	4
9	0.0	AB	6
10	0.3	AB	6
11	0.7	AB	6
12	0.2	AB	6
13	0.0	AB	8
14	0.5	AB	8
15	0.0	AB	10
16	0.3	AB	10
17	1.3	AB	10
18	0.2	AB	10
19	0.0	AB	12
20	0.5	AB	12
21	0.0	AB	14
22	0.5	AB	14
23	0.0	AB	16
24	0.5	AB	16
25	0.0	AB	18
26	0.4	AB	18
27	0.0	AB	20
28	0.3	AB	20



Method Name:
Run Name: 2014-08-29_h-b7-c
Run Date: 2014-08-29 14:53

Gradient Table

	Min	Solvents	% 2nd
29	0.5	AB	25
30	0.5	AB	30
31	0.1	AB	30
32	0.3	AB	30
33	0.1	AB	31
34	2.4	AB	31
35	0.3	AB	35
36	0.5	AB	40
37	0.5	AB	50
38	5.0	AB	50
39	5.0	AB	50

Vial Mapping Table

Peak #	Start Tray/Vial	End Tray/Vial
1	1:2	1:2
2	1:3	1:3
3	1:4	1:4
4	1:5	1:6
5	1:7	1:10
6	1:11	1:11
7	1:12	1:12



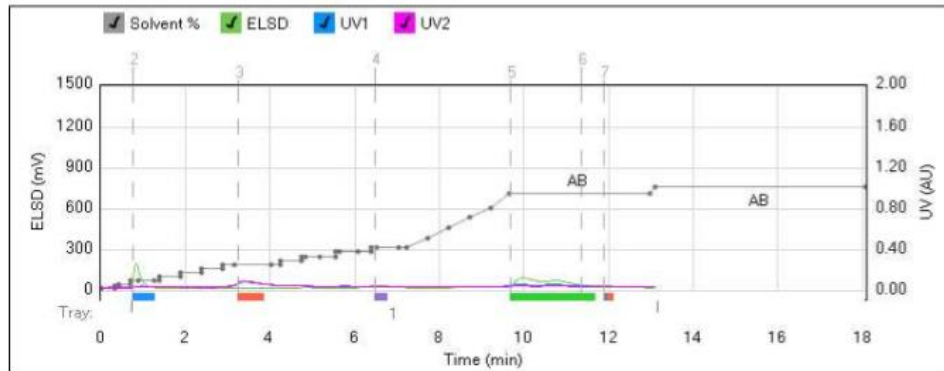
Method Name:
Run Name: 2014-08-29_h-b7-d
Run Date: 2014-08-29 15:35

Column: Reveleris® Silica 4g
Flow Rate: 15 mL/min
Equilibration: 2.4 min
Run Length: 18.1 min
Air Purge Time: 0.5 min

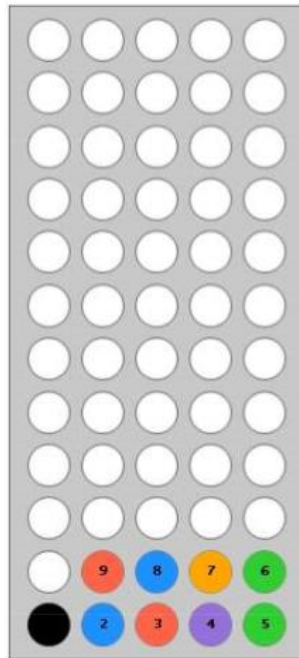
Slope Detection: Off
ELSD Threshold: 20 mV
UV Threshold: 0.05 AU
UV1 Wavelength: 254 nm
UV2 Wavelength: 280 nm

Collection Mode: Collect Peaks
Per-Vial Volume: 25 mL
Non-Peaks: 25 mL
Injection Type: Manual

ELSD Carrier: Iso-propanol
Solvent A: Hexane
Solvent B: Ethyl acetate
Solvent C: <No solvent chosen
Solvent D: <No solvent chosen



1-7B19



Gradient Table

	Min	Solvents	% 2nd
1	0.0	AB	0
2	0.3	AB	0
3	0.0	AB	1
4	0.1	AB	1
5	0.0	AB	2
6	0.3	AB	2
7	0.0	AB	4
8	0.2	AB	4
9	0.4	AB	4
10	0.1	AB	4
11	0.0	AB	6
12	0.5	AB	6
13	0.0	AB	8
14	0.5	AB	8
15	0.0	AB	10
16	0.5	AB	10
17	0.0	AB	12
18	0.3	AB	12
19	0.9	AB	12
20	0.2	AB	12
21	0.0	AB	14
22	0.5	AB	14
23	0.0	AB	16
24	0.1	AB	16
25	0.4	AB	16
26	0.4	AB	16
27	0.0	AB	18
28	0.1	AB	18



Method Name:
Run Name: 2014-08-29_h-b7-d
Run Date: 2014-08-29 15:35

Gradient Table

	Min	Solvents	% 2nd
29	0.5	AB	18
30	0.3	AB	18
31	0.0	AB	20
32	0.1	AB	20
33	0.5	AB	20
34	0.2	AB	20
35	0.5	AB	25
36	0.5	AB	30
37	0.5	AB	35
38	0.5	AB	40
39	0.4	AB	47
40	3.4	AB	47
41	0.1	AB	50
42	5.0	AB	50

Vial Mapping Table

Peak #	Start Tray/Vial	End Tray/Vial
1	1:2	1:2
2	1:3	1:3
3	1:4	1:4
4	1:5	1:6
5	1:7	1:7
6	1:8	1:8
7	1:9	1:9



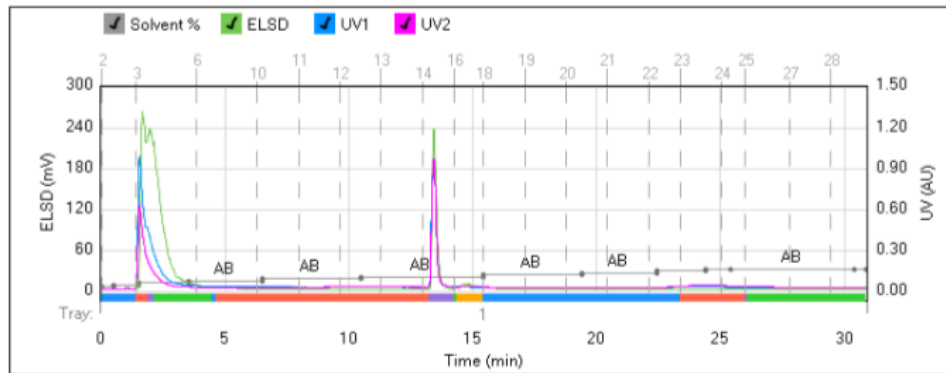
Method Name:
Run Name: KL-H-C3-B; 10-13-2014
Run Date: 2014-10-13 16:02

Column: Reveleris® Silica 4g
 Flow Rate: 15 mL/min
 Equilibration: 2.4 min
 Run Length: 31.0 min
 Air Purge Time: 0.5 min

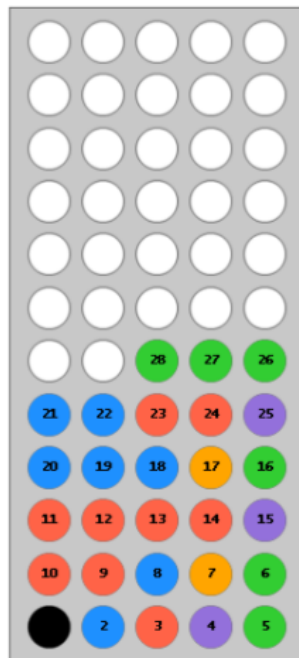
Slope Detection: High
 ELSD Threshold: 3 mV
 UV Threshold: 0.02 AU
 UV1 Wavelength: 254 nm
 UV2 Wavelength: 280 nm

Collection Mode: Collect All
 Per-Vial Volume: 25 mL
 Non-Peaks: 25 mL
 Injection Type: Dry

ELSD Carrier: Iso-propanol
 Solvent A: Methylene chloride
 Solvent B: Methanol
 Solvent C: <No solvent chosen>
 Solvent D: <No solvent chosen>



1-7B19



Gradient Table

	Min	Solvents	% 2nd
1	0.0	AB	1
2	0.5	AB	1
3	0.0	AB	2
4	1.0	AB	2
5	0.0	AB	3
6	2.0	AB	3
7	0.0	AB	4
8	3.0	AB	4
9	0.0	AB	5
10	4.0	AB	5
11	0.0	AB	6
12	5.0	AB	6
13	0.0	AB	7
14	4.0	AB	7
15	0.0	AB	8
16	3.0	AB	8
17	0.0	AB	9
18	2.0	AB	9
19	0.0	AB	10
20	1.0	AB	10
21	5.0	AB	10
22	0.5	AB	10

Vial Mapping Table

Peak #	Start Tray:Vial	End Tray:Vial
1	1:3	1:3
2	1:4	1:4
3	1:5	1:6



Method Name:
Run Name: KL-H-C3-B; 10-13-2014
Run Date: 2014-10-13 16:02

Vial Mapping Table

Peak #	Start Tray/Vial	End Tray/Vial
4	1:7	1:7
5	1:8	1:8
6	1:15	1:15
7	1:16	1:16
8	1:17	1:17
9	1:23	1:24
10	1:25	1:25



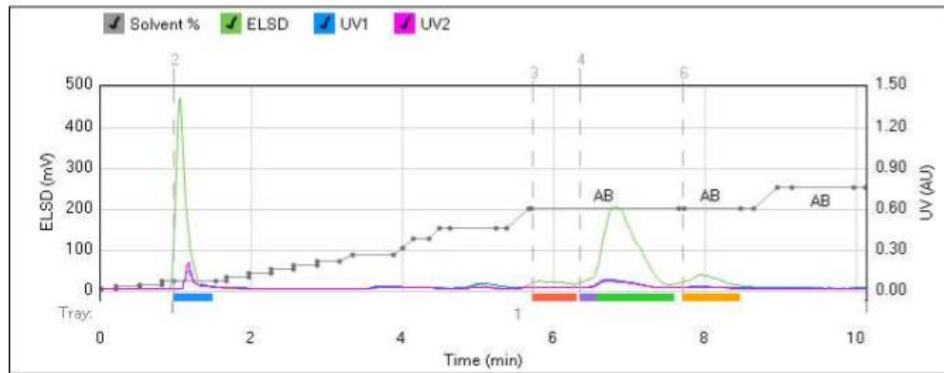
Method Name:
Run Name: 2014-09-08_h-c1-a,#2
Run Date: 2014-09-08 15:50

Column: Reveleris® Silica 4g
Flow Rate: 15 mL/min
Equilibration: 2.4 min
Run Length: 10.2 min
Air Purge Time: 0.5 min

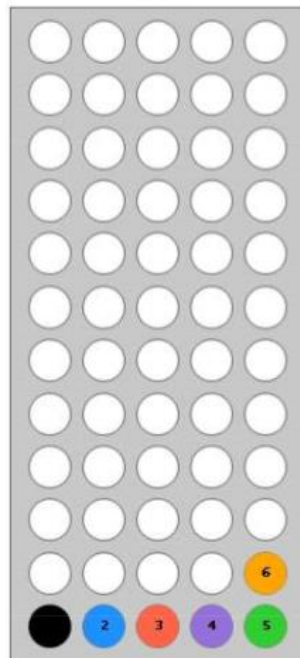
Slope Detection: Off
ELSD Threshold: 15 mV
UV Threshold: 0.04 AU
UV1 Wavelength: 254 nm
UV2 Wavelength: 280 nm

Collection Mode: Collect Peaks
Per-Vial Volume: 25 mL
Non-Peaks: 25 mL
Injection Type: Dry

ELSD Carrier: Iso-propanol
Solvent A: Hexane
Solvent B: Ethyl acetate
Solvent C: <No solvent chosen
Solvent D: <No solvent chosen



1-7B19



Gradient Table

	Min	Solvents	% 2nd
1	0.0	AB	0
2	0.2	AB	0
3	0.0	AB	1
4	0.3	AB	1
5	0.0	AB	2
6	0.3	AB	2
7	0.0	AB	4
8	0.2	AB	4
9	0.6	AB	4
10	0.1	AB	4
11	0.0	AB	6
12	0.3	AB	6
13	0.0	AB	8
14	0.3	AB	8
15	0.0	AB	10
16	0.3	AB	10
17	0.0	AB	12
18	0.3	AB	12
19	0.0	AB	14
20	0.3	AB	14
21	0.2	AB	17
22	0.6	AB	17
23	0.1	AB	20
24	0.2	AB	25
25	0.2	AB	25
26	0.1	AB	30
27	0.1	AB	30
28	0.6	AB	30



Method Name:
Run Name: 2014-09-08_h-c1-a,#2
Run Date: 2014-09-08 15:50

Gradient Table

	Min	Solvents	% 2nd
29	0.2	AB	30
30	0.3	AB	40
31	0.0	AB	40
32	2.0	AB	40
33	0.1	AB	40
34	0.8	AB	40
35	0.2	AB	40
36	0.3	AB	50
37	0.2	AB	50
38	0.8	AB	50
39	0.2	AB	50

Vial Mapping Table

Peak #	Start Tray/Vial	End Tray/Vial
1	1:2	1:2
2	1:3	1:3
3	1:4	1:4
4	1:5	1:5
5	1:6	1:6



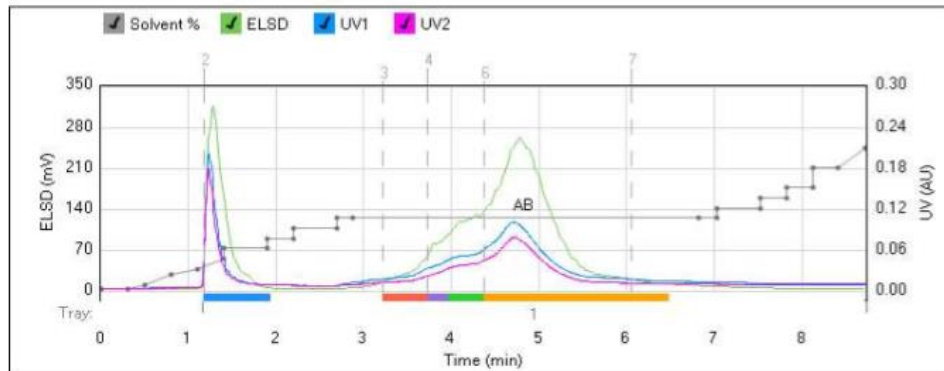
Method Name: h-c2-a
 Run Name: 2014-09-09_h-c1-a; #'s 4, 5, & 6
 Run Date: 2014-09-09 17:45

Column: Reveleris® Silica 4g
 Flow Rate: 15 mL/min
 Equilibration: 2.4 min
 Run Length: 8.8 min
 Air Purge Time: 0.5 min

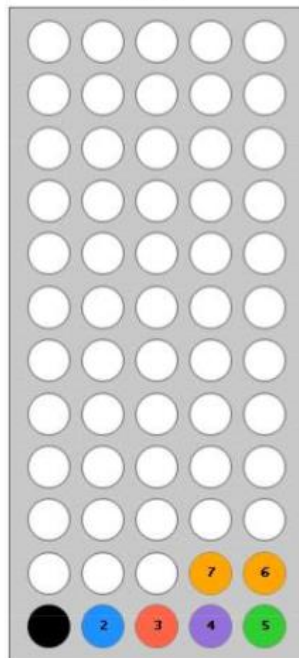
Slope Detection: High
 ELSD Threshold: 10 mV
 UV Threshold: 0.03 AU
 UV1 Wavelength: 254 nm
 UV2 Wavelength: 280 nm

Collection Mode: Collect Peaks
 Per-Vial Volume: 25 mL
 Non-Peaks: 25 mL
 Injection Type: Dry

ELSD Carrier: Iso-propanol
 Solvent A: Hexane
 Solvent B: Ethyl acetate
 Solvent C: <No solvent chosen
 Solvent D: <No solvent chosen



1-7B19



Gradient Table

	Min	Solvents	% 2nd
1	0.0	AB	0
2	0.3	AB	0
3	0.2	AB	2
4	0.3	AB	7
5	0.3	AB	10
6	0.3	AB	15
7	0.0	AB	20
8	0.5	AB	20
9	0.0	AB	25
10	0.3	AB	25
11	0.0	AB	30
12	0.5	AB	30
13	0.0	AB	35
14	0.2	AB	35
15	4.0	AB	35
16	0.2	AB	35
17	0.0	AB	40
18	0.5	AB	40
19	0.0	AB	45
20	0.3	AB	45
21	0.0	AB	50
22	0.3	AB	50
23	0.0	AB	60
24	0.3	AB	60
25	0.3	AB	70

Vial Mapping Table

Peak #	Start Tray Vial	End Tray Vial
--------	-----------------	---------------



Method Name: h-c2-a
Run Name: 2014-09-09_h-c1-a; #'s 4, 5, & 6
Run Date: 2014-09-09 17:45

Vial Mapping Table

Peak #	Start Tray/Vial	End Tray/Vial
1	1:2	1:2
2	1:3	1:3
3	1:4	1:4
4	1:5	1:5
5	1:6	1:7



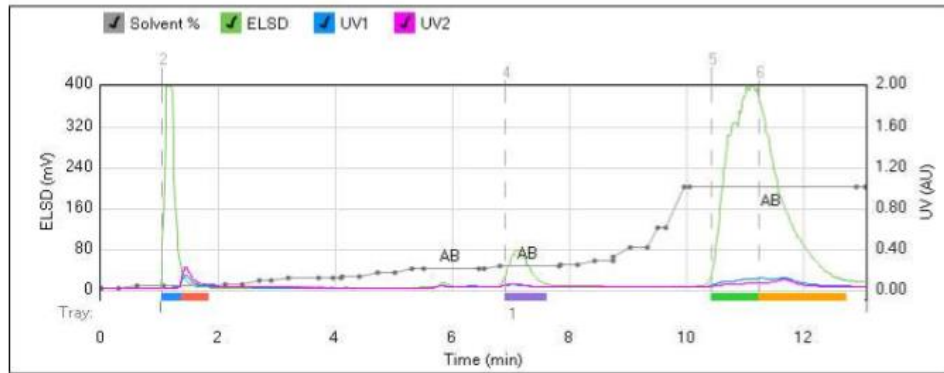
Method Name:
Run Name: 2014-09-08_h-c-2-a
Run Date: 2014-09-08 10:21

Column: Reveleris® Silica 4g
Flow Rate: 15 mL/min
Equilibration: 2.4 min
Run Length: 13.1 min
Air Purge Time: 0.5 min

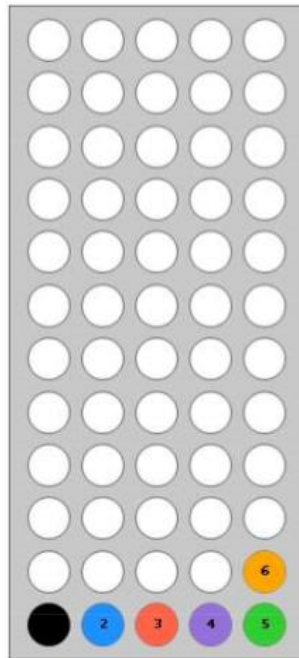
Slope Detection: Off
ELSD Threshold: 20 mV
UV Threshold: 0.05 AU
UV1 Wavelength: 254 nm
UV2 Wavelength: 280 nm

Collection Mode: Collect Peaks
Per-Vial Volume: 25 mL
Non-Peaks: 25 mL
Injection Type: Dry

ELSD Carrier: Iso-propanol
Solvent A: Hexane
Solvent B: Ethyl acetate
Solvent C: <No solvent chosen
Solvent D: <No solvent chosen



1-7B19



Gradient Table

	Min	Solvents	% 2nd
1	0.0	AB	0
2	0.3	AB	0
3	0.3	AB	1
4	0.5	AB	1
5	0.8	AB	1
6	0.0	AB	1
7	0.2	AB	2
8	0.3	AB	2
9	0.3	AB	4
10	0.2	AB	4
11	0.3	AB	5
12	0.5	AB	5
13	0.3	AB	5
14	0.1	AB	5
15	0.0	AB	6
16	0.3	AB	6
17	0.3	AB	8
18	0.3	AB	8
19	0.3	AB	10
20	0.2	AB	10
21	0.9	AB	10
22	0.1	AB	10
23	0.3	AB	11
24	1.0	AB	11
25	0.0	AB	12
26	0.3	AB	12
27	0.3	AB	14
28	0.3	AB	14



Method Name:
Run Name: 2014-09-08_h-c2-a
Run Date: 2014-09-08 10:21

Gradient Table

	Min	Solvents	% 2nd
29	0.0	AB	16
30	0.3	AB	20
31	0.3	AB	20
32	0.2	AB	30
33	0.1	AB	30
34	0.3	AB	30
35	0.1	AB	30
36	2.9	AB	30
37	0.2	AB	30

Vial Mapping Table

Peak #	Start Tray/Vial	End Tray/Vial
1	1:2	1:2
2	1:3	1:3
3	1:4	1:4
4	1:5	1:5
5	1:6	1:6



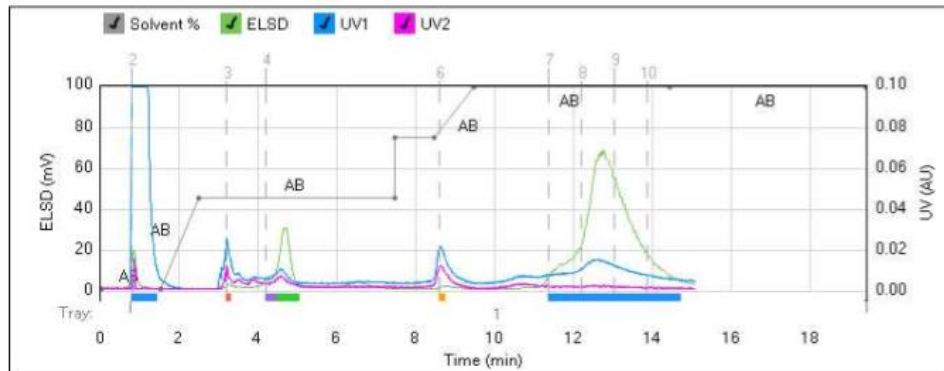
Method Name:
Run Name: KL-H-D4-D
Run Date: 2015-03-25 09:01

Column: Reveleris® Silica 12g
Flow Rate: 30 mL/min
Equilibration: 4.8 min
Run Length: 19.5 min
Air Purge Time: 0.5 min

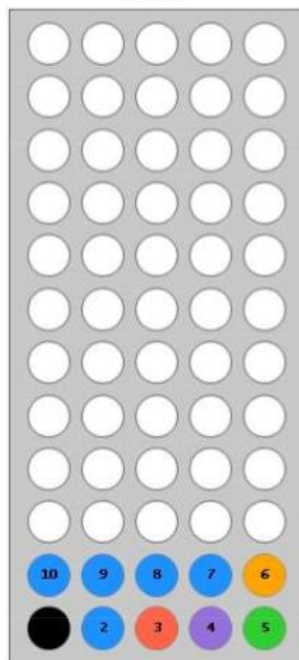
Slope Detection: High
ELSD Threshold: 5 mV
UV Threshold: 0.02 AU
UV1 Wavelength: 254 nm
UV2 Wavelength: 280 nm

Collection Mode: Collect Peaks
Per-Vial Volume: 25 mL
Non-Peaks: 25 mL
Injection Type: Manual

ELSD Carrier: Iso-propanol
Solvent A: Hexane
Solvent B: Ethyl acetate
Solvent C: <No solvent chose
Solvent D: <No solvent chose



1-7B19



Gradient Table

	Min	Solvents	% 2nd
1	0.0	AB	0
2	1.5	AB	0
3	1.0	AB	45
4	5.0	AB	45
5	0.0	AB	75
6	1.0	AB	75
7	1.0	AB	100
8	5.0	AB	100
9	5.0	AB	100

Vial Mapping Table

Peak #	Start Tray/Vial	End Tray/Vial
1	1:2	1:2
2	1:3	1:3
3	1:4	1:4
4	1:5	1:5
5	1:6	1:6
6	1:7	1:10



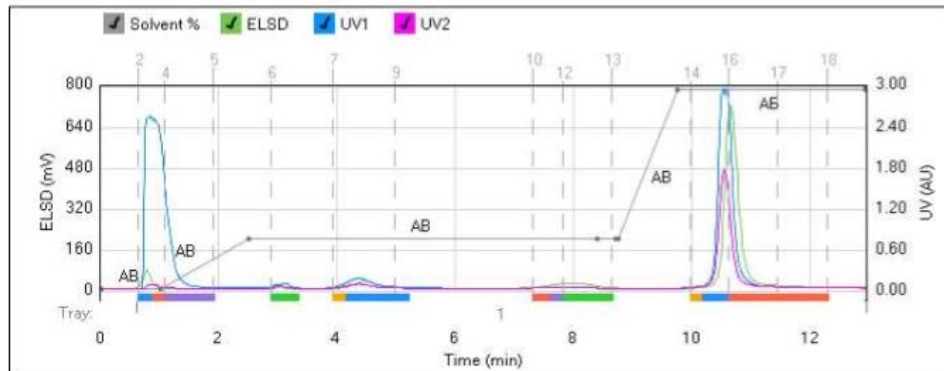
Method Name:
 Run Name: KL-H-D4-E; 2
 Run Date: 2015-03-04 10:31

Column: Reveleris® Silica 12g
 Flow Rate: 30 mL/min
 Equilibration: 4.8 min
 Run Length: 13.0 min
 Air Purge Time: 0.5 min

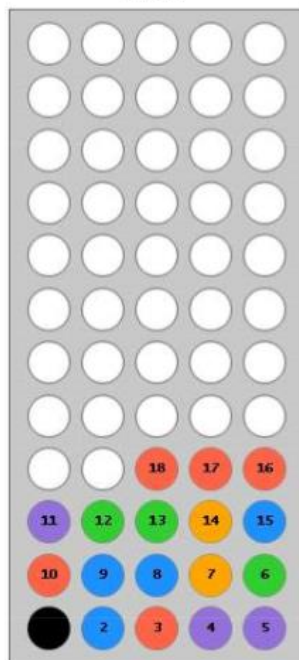
Slope Detection: High
 ELSD Threshold: 5 mV
 UV Threshold: 0.02 AU
 UV1 Wavelength: 254 nm
 UV2 Wavelength: 280 nm

Collection Mode: Collect Peaks
 Per-Vial Volume: 25 mL
 Non-Peaks: 25 mL
 Injection Type: Manual

ELSD Carrier: Iso-propanol
 Solvent A: Hexane
 Solvent B: Ethyl acetate
 Solvent C: <No solvent chose
 Solvent D: <No solvent chose



1-7B19



Gradient Table

	Min	Solvents	% 2nd
1	0.0	AB	0
2	1.0	AB	0
3	1.5	AB	25
4	5.9	AB	25
5	0.3	AB	25
6	0.1	AB	25
7	1.0	AB	99
8	3.2	AB	99
9	0.0	AB	100

Vial Mapping Table

Peak #	Start Tray/Vial	End Tray/Vial
1	1:2	1:2
2	1:3	1:3
3	1:4	1:5
4	1:6	1:6
5	1:7	1:7
6	1:8	1:9
7	1:10	1:10
8	1:11	1:11
9	1:12	1:13
10	1:14	1:14
11	1:15	1:15
12	1:16	1:18



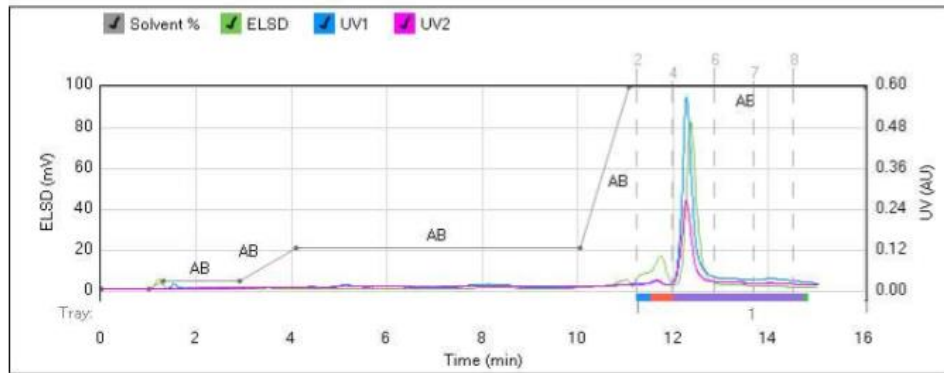
Method Name:
Run Name: KL-H-D4-E; 3
Run Date: 2015-03-04 13:59

Column: Reveleris® Silica 12g
 Flow Rate: 30 mL/min
 Equilibration: 4.8 min
 Run Length: 16.1 min
 Air Purge Time: 0.5 min

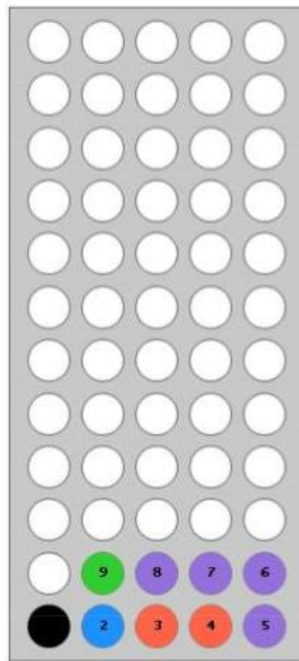
Slope Detection: High
 ELSD Threshold: 5 mV
 UV Threshold: 0.02 AU
 UV1 Wavelength: 254 nm
 UV2 Wavelength: 280 nm

Collection Mode: Collect Peaks
 Per-Vial Volume: 25 mL
 Non-Peaks: 25 mL
 Injection Type: Dry

ELSD Carrier: Iso-propanol
 Solvent A: Hexane
 Solvent B: Ethyl acetate
 Solvent C: <No solvent chose
 Solvent D: <No solvent chose



1-7B19



Gradient Table

	Min	Solvents	% 2nd
1	0.0	AB	0
2	1.0	AB	0
3	0.3	AB	4
4	1.6	AB	4
5	1.2	AB	20
6	6.0	AB	20
7	1.0	AB	100
8	5.0	AB	100

Vial Mapping Table

Peak #	Start Tray/Vial	End Tray/Vial
1	12	12
2	13	14
3	15	18
4	19	19



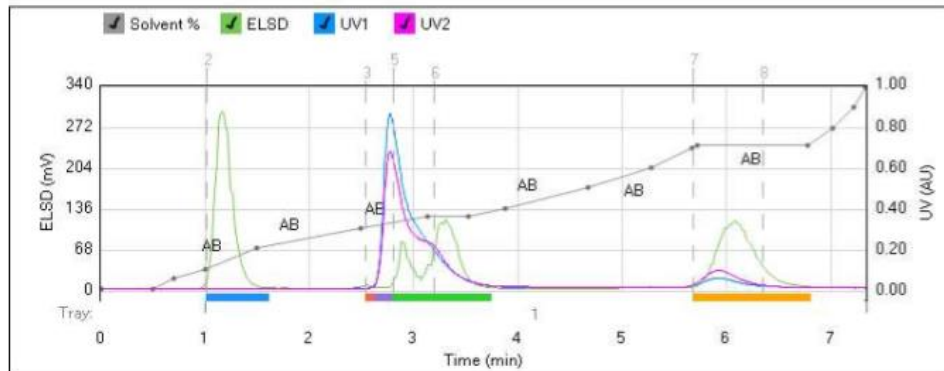
Method Name:
Run Name: KL-H-D2-A
Run Date: 2015-01-29 15:28

Column: Reveleris® Silica 12g
Flow Rate: 30 mL/min
Equilibration: 4.8 min
Run Length: 7.4 min
Air Purge Time: 0.5 min

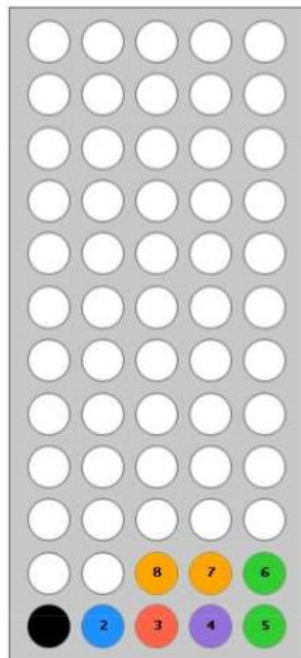
Slope Detection: Off
ELSD Threshold: 5 mV
UV Threshold: 0.02 AU
UV1 Wavelength: 254 nm
UV2 Wavelength: 280 nm

Collection Mode: Collect Peaks
Per-Vial Volume: 25 mL
Non-Peaks: 25 mL
Injection Type: Dry

ELSD Carrier: Iso-propanol
Solvent A: Hexane
Solvent B: Ethyl acetate
Solvent C: <No solvent chose
Solvent D: <No solvent chose



1-7B19



Gradient Table

	Min	Solvents	% 2nd
1	0.0	AB	0
2	0.5	AB	0
3	0.2	AB	5
4	0.3	AB	10
5	0.5	AB	20
6	1.0	AB	30
7	0.6	AB	36
8	0.4	AB	36
9	0.4	AB	40
10	0.8	AB	50
11	0.6	AB	60
12	0.4	AB	70
13	0.1	AB	71
14	1.1	AB	71
15	0.2	AB	80
16	0.2	AB	90
17	0.1	AB	100

Vial Mapping Table

Peak #	Start Tray/Vial	End Tray/Vial
1	1:2	1:2
2	1:3	1:3
3	1:4	1:4
4	1:5	1:6
5	1:7	1:8



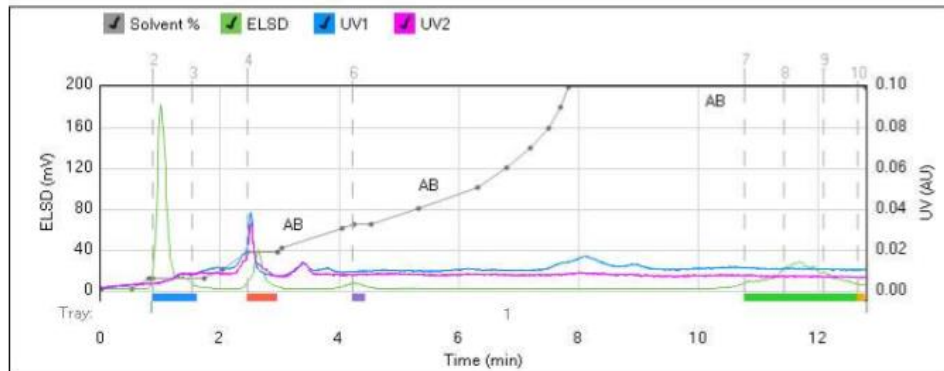
Method Name:
Run Name: KL-H-D3-A
Run Date: 2015-02-01 15:47

Column: Reveleris® Silica 12g
Flow Rate: 30 mL/min
Equilibration: 3.0 min
Run Length: 12.9 min
Air Purge Time: 0.5 min

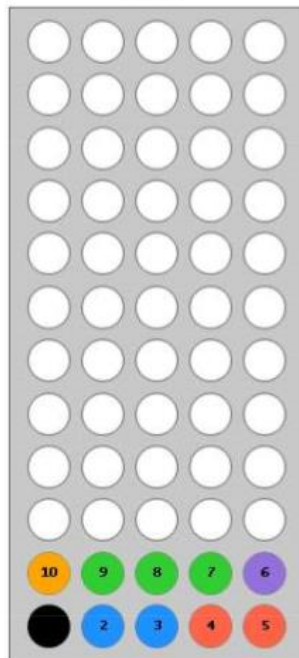
Slope Detection: Off
ELSD Threshold: 5 mV
UV Threshold: 0.02 AU
UV1 Wavelength: 254 nm
UV2 Wavelength: 280 nm

Collection Mode: Collect Peaks
Per-Vial Volume: 20 mL
Non-Peaks: 25 mL
Injection Type: Manual

ELSD Carrier: Iso-propanol
Solvent A: Hexane
Solvent B: Ethyl acetate
Solvent C: <No solvent chose
Solvent D: <No solvent chose



1-7B19



Gradient Table

	Min	Solvents	% 2nd
1	0.0	AB	0
2	0.5	AB	0
3	0.3	AB	5
4	0.1	AB	5
5	0.9	AB	5
6	0.3	AB	10
7	0.4	AB	18
8	0.5	AB	18
9	0.1	AB	20
10	1.0	AB	30
11	0.2	AB	32
12	0.3	AB	32
13	0.8	AB	40
14	1.0	AB	50
15	0.5	AB	60
16	0.4	AB	70
17	0.3	AB	80
18	0.2	AB	90
19	0.1	AB	100
20	5.0	AB	100

Vial Mapping Table

Peak #	Start Tray Vial	End Tray Vial
1	1:2	1:3
2	1:4	1:5
3	1:6	1:6
4	1:7	1:9
5	1:10	1:10



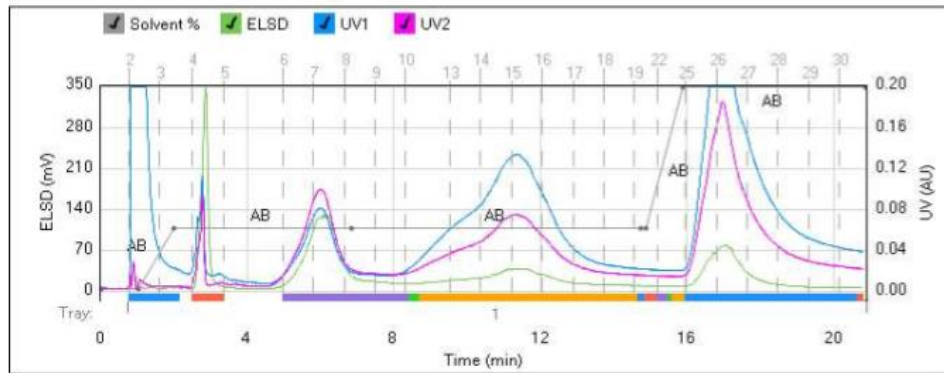
Method Name:
Run Name: KL-H-D2-C
Run Date: 2015-03-17 10:33

Column: Reveleris® Silica 12g
Flow Rate: 30 mL/min
Equilibration: 4.8 min
Run Length: 20.9 min
Air Purge Time: 0.5 min

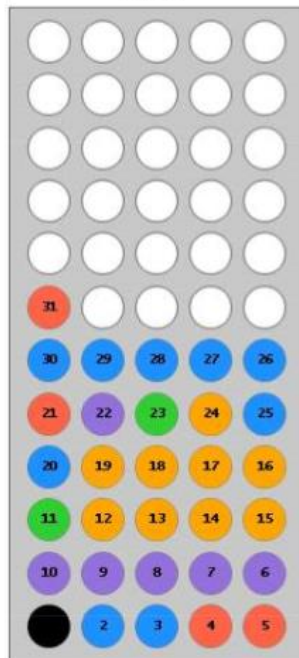
Slope Detection: Off
ELSD Threshold: 5 mV
UV Threshold: 0.02 AU
UV1 Wavelength: 254 nm
UV2 Wavelength: 280 nm

Collection Mode: Collect Peaks
Per-Vial Volume: 25 mL
Non-Peaks: 25 mL
Injection Type: Manual

ELSD Carrier: Iso-propanol
Solvent A: Hexane
Solvent B: Ethyl acetate
Solvent C: <No solvent chose
Solvent D: <No solvent chose



1-7B19



Gradient Table

	Min	Solvents	% 2nd
1	0.0	AB	0
2	1.0	AB	0
3	1.0	AB	30
4	4.9	AB	30
5	7.9	AB	30
6	0.1	AB	30
7	1.0	AB	100
8	5.0	AB	100

Vial Mapping Table

Peak #	Start Tray/Vial	End Tray/Vial
1	1:2	1:3
2	1:4	1:5
3	1:6	1:10
4	1:11	1:11
5	1:12	1:19
6	1:20	1:20
7	1:21	1:21
8	1:22	1:22
9	1:23	1:23
10	1:24	1:24
11	1:25	1:30
12	1:31	1:31



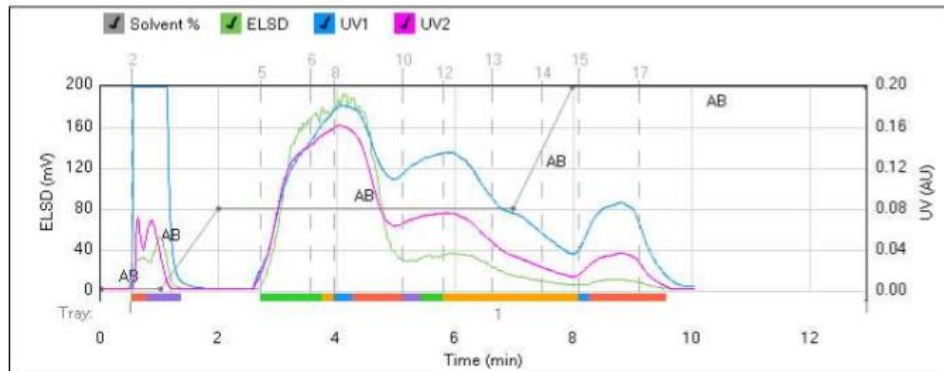
Method Name:
Run Name: KL-H-D2-C; #2
Run Date: 2015-03-24 08:05

Column: Reveleris® Silica 12g
Flow Rate: 30 mL/min
Equilibration: 4.8 min
Run Length: 13.0 min
Air Purge Time: 0.5 min

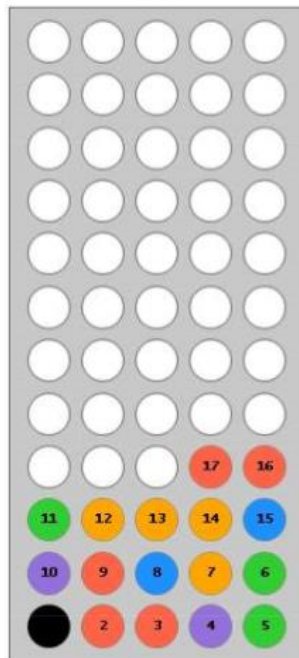
Slope Detection: High
ELSD Threshold: 5 mV
UV Threshold: 0.02 AU
UV1 Wavelength: 254 nm
UV2 Wavelength: 280 nm

Collection Mode: Collect Peaks
Per-Vial Volume: 25 mL
Non-Peaks: 25 mL
Injection Type: Manual

ELSD Carrier: Iso-propanol
Solvent A: Hexane
Solvent B: Ethyl acetate
Solvent C: <No solvent chose
Solvent D: <No solvent chose



1-7B19



Gradient Table

	Min	Solvents	% 2nd
1	0.0	AB	0
2	1.0	AB	0
3	1.0	AB	40
4	5.0	AB	40
5	1.0	AB	100
6	5.0	AB	100

Vial Mapping Table

Peak #	Start Tray Vial	End Tray Vial
1	1:2	1:3
2	1:4	1:4
3	1:5	1:6
4	1:7	1:7
5	1:8	1:8
6	1:9	1:9
7	1:10	1:10
8	1:11	1:11
9	1:12	1:14
10	1:15	1:15
11	1:16	1:17



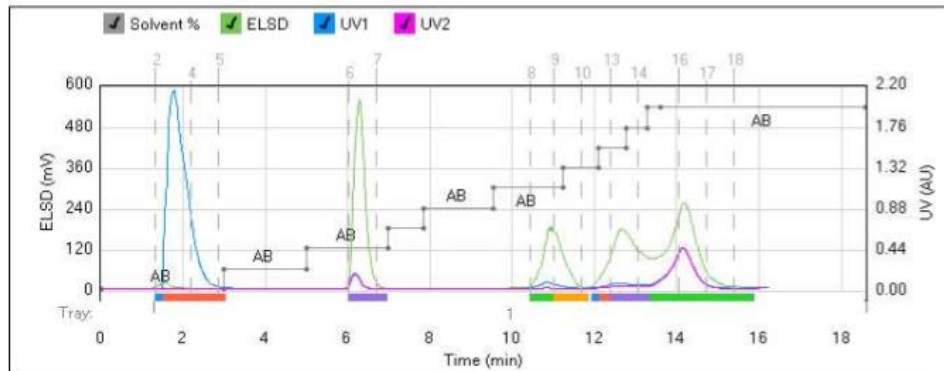
Method Name:
Run Name: KL-H-EI-C
Run Date: 2014-11-21 11:13

Column: Reveleris® Silica 12g
Flow Rate: 15 mL/min
Equilibration: 2.4 min
Run Length: 18.7 min
Air Purge Time: 0.5 min

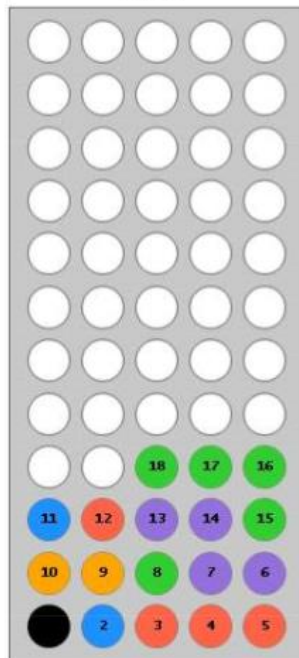
Slope Detection: High
ELSD Threshold: 5 mV
UV Threshold: 0.02 AU
UV1 Wavelength: 254 nm
UV2 Wavelength: 280 nm

Collection Mode: Collect Peaks
Per-Vial Volume: 10 mL
Non-Peaks: 25 mL
Injection Type: Manual

ELSD Carrier: Iso-propanol
Solvent A: Hexane
Solvent B: Ethyl acetate
Solvent C: <No solvent chose
Solvent D: <No solvent chose



1-7B19



Gradient Table

	Min	Solvents	% 2nd
1	0.0	AB	0
2	3.0	AB	0
3	0.0	AB	10
4	2.0	AB	10
5	0.0	AB	20
6	2.0	AB	20
7	0.0	AB	30
8	0.9	AB	30
9	0.0	AB	40
10	1.7	AB	40
11	0.0	AB	50
12	1.7	AB	50
13	0.0	AB	60
14	0.9	AB	60
15	0.0	AB	70
16	0.7	AB	70
17	0.0	AB	80
18	0.5	AB	80
19	0.0	AB	90
20	0.3	AB	90
21	5.0	AB	90

Vial Mapping Table

Peak #	Start Tray/Vial	End Tray/Vial
1	12	12
2	13	15
3	16	17
4	18	18



Method Name:
Run Name: KL-H-EI-C
Run Date: 2014-11-21 11:13

Vial Mapping Table

Peak #	Start Tray/Vial	End Tray/Vial
5	1:9	1:10
6	1:11	1:11
7	1:12	1:12
8	1:13	1:14
9	1:15	1:18



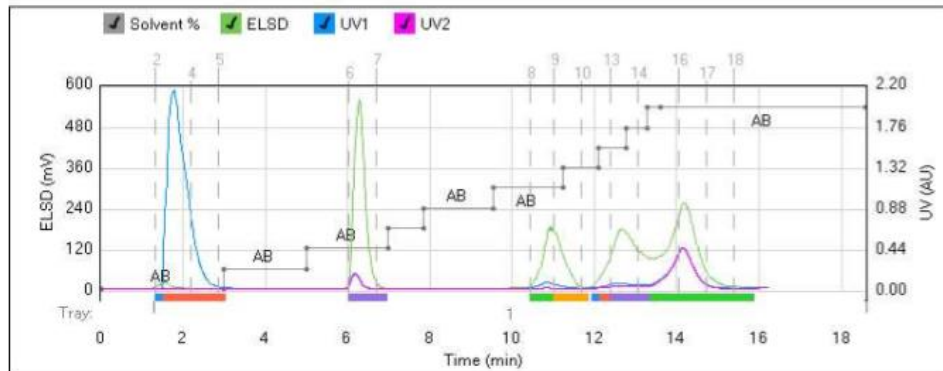
Method Name:
Run Name: KL-H-EI-C
Run Date: 2014-11-21 11:13

Column: Reveleris® Silica 12g
Flow Rate: 15 mL/min
Equilibration: 2.4 min
Run Length: 18.7 min
Air Purge Time: 0.5 min

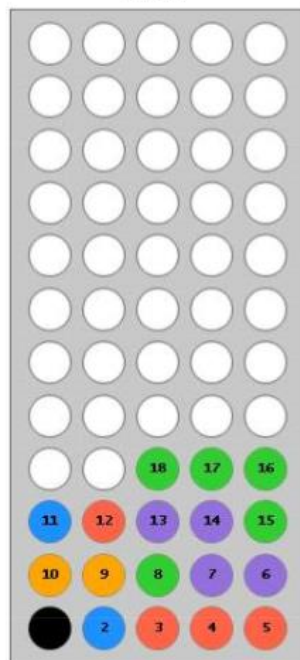
Slope Detection: High
ELSD Threshold: 5 mV
UV Threshold: 0.02 AU
UV1 Wavelength: 254 nm
UV2 Wavelength: 280 nm

Collection Mode: Collect Peaks
Per-Vial Volume: 10 mL
Non-Peaks: 25 mL
Injection Type: Manual

ELSD Carrier: Iso-propanol
Solvent A: Hexane
Solvent B: Ethyl acetate
Solvent C: <No solvent chose
Solvent D: <No solvent chose



1-7B19



Gradient Table

	Min	Solvents	% 2nd
1	0.0	AB	0
2	3.0	AB	0
3	0.0	AB	10
4	2.0	AB	10
5	0.0	AB	20
6	2.0	AB	20
7	0.0	AB	30
8	0.9	AB	30
9	0.0	AB	40
10	1.7	AB	40
11	0.0	AB	50
12	1.7	AB	50
13	0.0	AB	60
14	0.9	AB	60
15	0.0	AB	70
16	0.7	AB	70
17	0.0	AB	80
18	0.5	AB	80
19	0.0	AB	90
20	0.3	AB	90
21	5.0	AB	90

Vial Mapping Table

Peak#	Start Tray/Vial	End Tray/Vial
1	12	12
2	13	15
3	16	17
4	18	18

Page 1



Method Name:
Run Name: KL-H-EI-C
Run Date: 2014-11-21 11:13

Vial Mapping Table

Peak #	Start Tray/Vial	End Tray/Vial
5	1:9	1:10
6	1:11	1:11
7	1:12	1:12
8	1:13	1:14
9	1:15	1:18



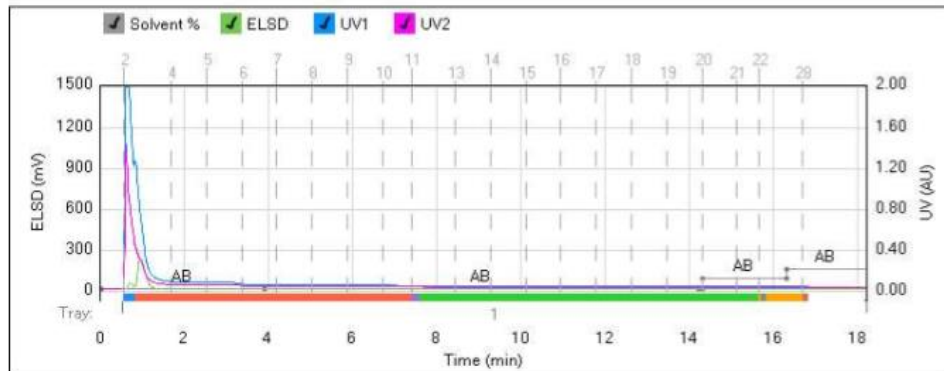
Method Name:
Run Name: KL-H-F1-A2
Run Date: 2015-06-30 10:27

Column: Reveleris® Silica 12g
Flow Rate: 30 mL/min
Equilibration: 4.8 min
Run Length: 18.3 min
Air Purge Time: 0.5 min

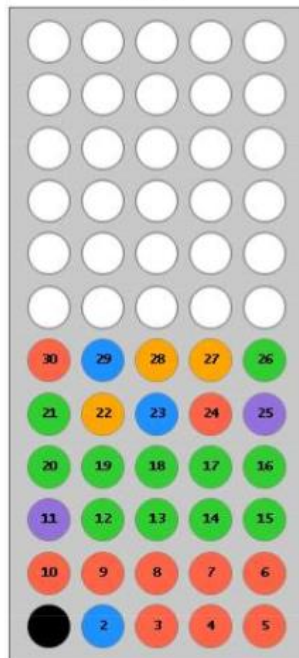
Slope Detection: High
ELSD Threshold: 5 mV
UV Threshold: 0.02 AU
UV1 Wavelength: 254 nm
UV2 Wavelength: 280 nm

Collection Mode: Collect Peaks
Per-Vial Volume: 25 mL
Non-Peaks: 25 mL
Injection Type: Manual

ELSD Carrier: Iso-propanol
Solvent A: Hexane
Solvent B: Ethyl acetate
Solvent C: <No solvent chose
Solvent D: <No solvent chose



1-7B19



Gradient Table

	Min	Solvents	% 2nd
1	0.0	AB	0
2	3.9	AB	0
3	10.4	AB	0
4	0.1	AB	0
5	0.0	AB	5
6	2.0	AB	5
7	0.0	AB	10
8	3.0	AB	10
9	5.0	AB	100

Vial Mapping Table

Peak #	Start Tray Vial	End Tray Vial
1	1.2	1.2
2	1.3	1.10
3	1.11	1.11
4	1.12	1.21
5	1.22	1.22
6	1.23	1.23
7	1.24	1.24
8	1.25	1.25
9	1.26	1.26
10	1.27	1.28
11	1.29	1.29
12	1.30	1.30



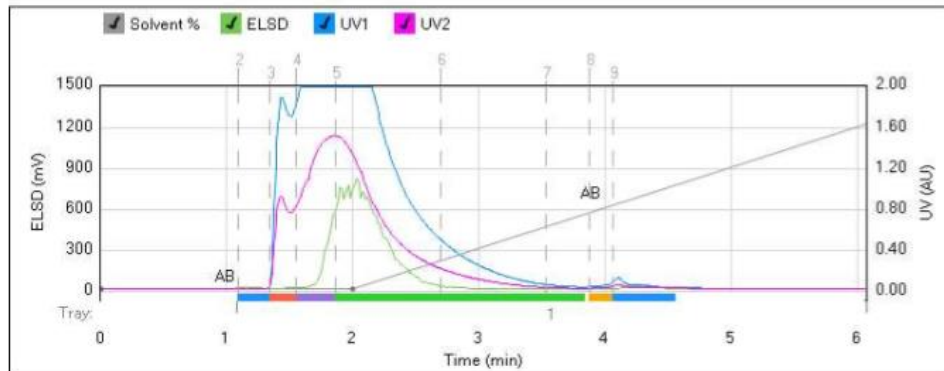
Method Name:
Run Name: KL-H-F1-A4
Run Date: 2015-07-03 08:22

Column: Reveleris® Silica 12g
 Flow Rate: 30 mL/min
 Equilibration: 4.8 min
 Run Length: 6.1 min
 Air Purge Time: 0.5 min

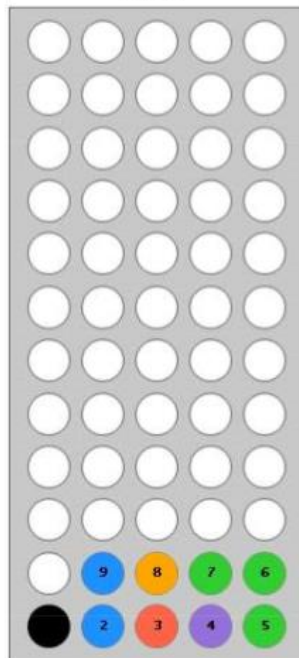
Slope Detection: High
 ELSD Threshold: 5 mV
 UV Threshold: 0.02 AU
 UV1 Wavelength: 254 nm
 UV2 Wavelength: 280 nm

Collection Mode: Collect Peaks
 Per-Vial Volume: 25 mL
 Non-Peaks: 25 mL
 Injection Type: Dry

ELSD Carrier: Iso-propanol
 Solvent A: Hexane
 Solvent B: Ethyl acetate
 Solvent C: <No solvent chose
 Solvent D: <No solvent chose



1-7B19



Gradient Table

	Min	Solvents	% 2nd
1	0.0	AB	0
2	2.0	AB	0
3	5.0	AB	100

Vial Mapping Table

Peak #	Start Tray Vial	End Tray Vial
1	12	12
2	13	13
3	14	14
4	15	17
5	18	18
6	19	19



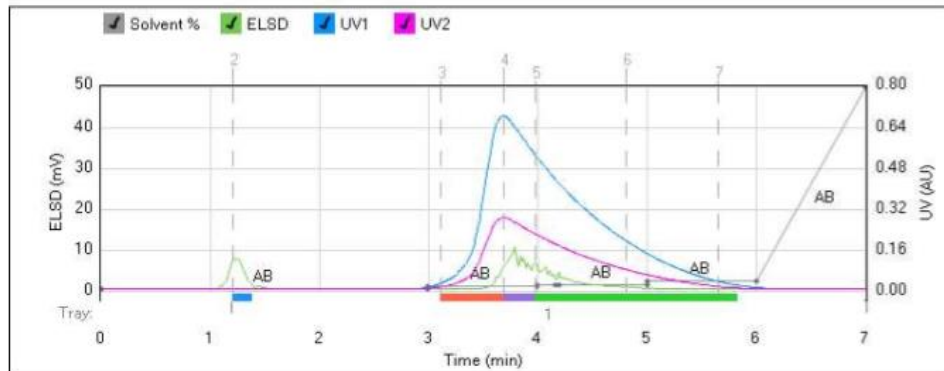
Method Name:
Run Name: KL-H-F1-B
Run Date: 2015-07-21 10:32

Column: Reveleris® Silica 12g
Flow Rate: 30 mL/min
Equilibration: 4.8 min
Run Length: 7.0 min
Air Purge Time: 0.5 min

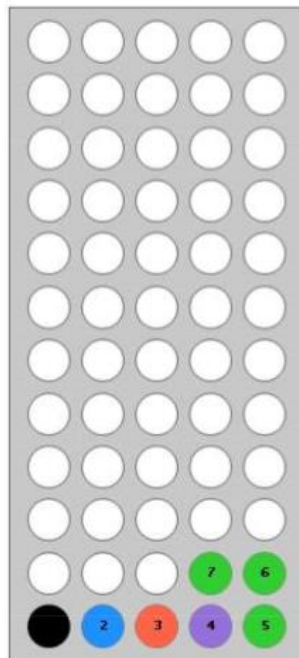
Slope Detection: High
ELSD Threshold: 5 mV
UV Threshold: 0.02 AU
UV1 Wavelength: 254 nm
UV2 Wavelength: 280 nm

Collection Mode: Collect Peaks
Per-Vial Volume: 25 mL
Non-Peaks: 25 mL
Injection Type: Dry

ELSD Carrier: Iso-propanol
Solvent A: Hexane
Solvent B: Ethyl acetate
Solvent C: <No solvent chose
Solvent D: <No solvent chose



1-7B19



Gradient Table

	Min	Solvents	% 2nd
1	0.0	AB	0
2	3.0	AB	0
3	0.0	AB	1
4	1.0	AB	1
5	0.0	AB	2
6	0.2	AB	2
7	0.0	AB	2
8	0.8	AB	2
9	0.0	AB	4
10	1.0	AB	4
11	1.0	AB	100

Vial Mapping Table

Peak #	Start Tray/Vial	End Tray/Vial
1	1:2	1:2
2	1:3	1:3
3	1:4	1:4
4	1:5	1:7



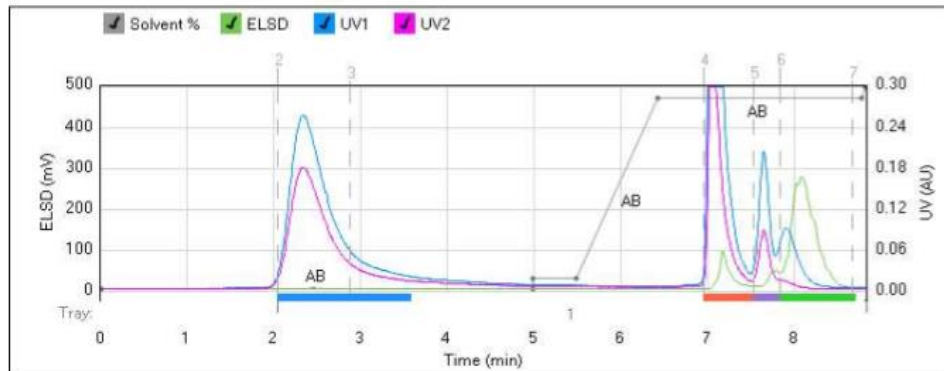
Method Name:
Run Name: KL-H-F1-C
Run Date: 2015-11-03 07:55

Column: Reveleris® Silica 12g
Flow Rate: 30 mL/min
Equilibration: 4.8 min
Run Length: 8.9 min
Air Purge Time: 0.5 min

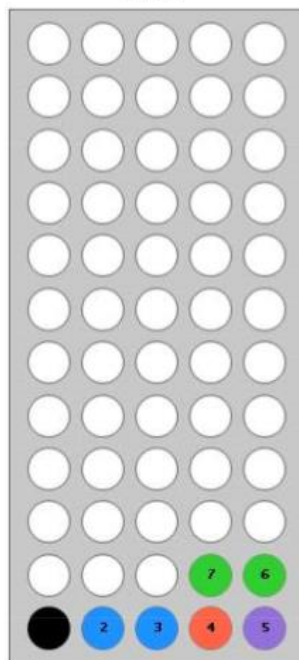
Slope Detection: High
ELSD Threshold: 5 mV
UV Threshold: 0.02 AU
UV1 Wavelength: 254 nm
UV2 Wavelength: 280 nm

Collection Mode: Collect Peaks
Per-Vial Volume: 25 mL
Non-Peaks: 25 mL
Injection Type: Dry

ELSD Carrier: Iso-propanol
Solvent A: Hexane
Solvent B: Ethyl acetate
Solvent C: <No solvent chose
Solvent D: <No solvent chose



1-7B19



Gradient Table

	Min	Solvents	% 2nd
1	0.0	AB	0
2	5.0	AB	0
3	0.0	AB	5
4	0.5	AB	5
5	1.0	AB	95
6	2.4	AB	95
7	0.1	AB	100

Vial Mapping Table

Peak #	Start Tray-Vial	End Tray-Vial
1	1:2	1:3
2	1:4	1:4
3	1:5	1:5
4	1:6	1:7



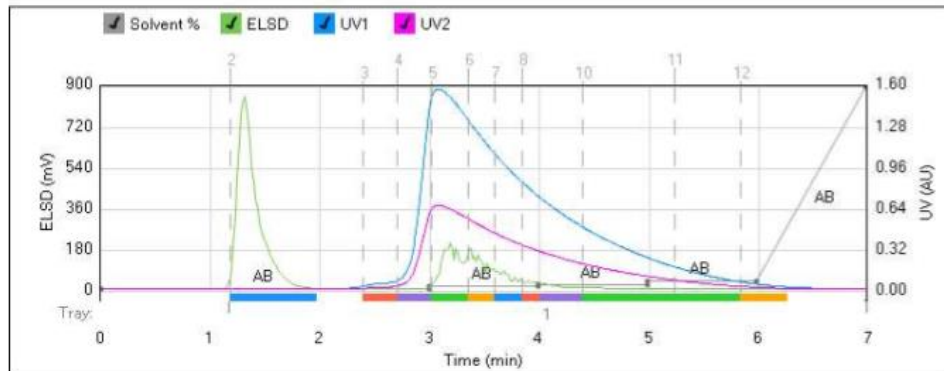
Method Name:
Run Name: KL-H-F2-A
Run Date: 2015-07-28 07:28

Column: Reveleris® Silica 12g
Flow Rate: 30 mL/min
Equilibration: 4.8 min
Run Length: 7.0 min
Air Purge Time: 0.5 min

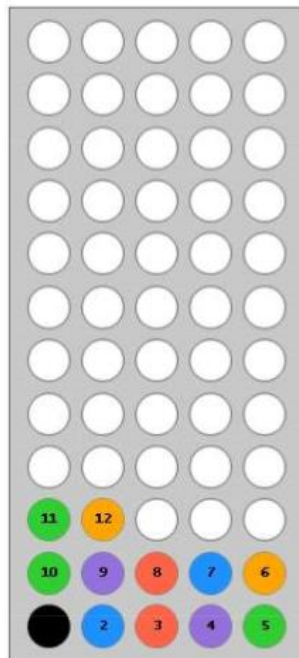
Slope Detection: High
ELSD Threshold: 5 mV
UV Threshold: 0.02 AU
UV1 Wavelength: 254 nm
UV2 Wavelength: 280 nm

Collection Mode: Collect Peaks
Per-Vial Volume: 25 mL
Non-Peaks: 25 mL
Injection Type: Dry

ELSD Carrier: Iso-propanol
Solvent A: Hexane
Solvent B: Ethyl acetate
Solvent C: <No solvent chose
Solvent D: <No solvent chose



1-7B19



Gradient Table

	Min	Solvents	% 2nd
1	0.0	AB	0
2	3.0	AB	0
3	0.0	AB	1
4	1.0	AB	1
5	0.0	AB	2
6	1.0	AB	2
7	0.0	AB	4
8	1.0	AB	4
9	1.0	AB	100

Vial Mapping Table

Peak #	Start Tray Vial	End Tray Vial
1	1:2	1:2
2	1:3	1:3
3	1:4	1:4
4	1:5	1:5
5	1:6	1:6
6	1:7	1:7
7	1:8	1:8
8	1:9	1:9
9	1:10	1:11
10	1:12	1:12



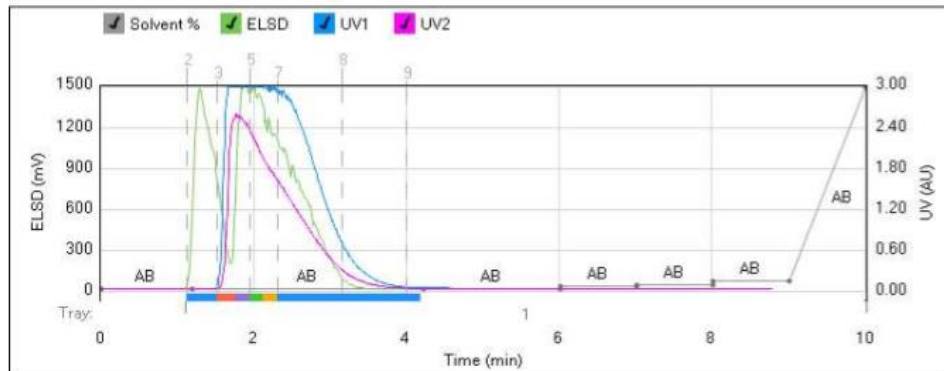
Method Name:
Run Name: KL-H-F2-B
Run Date: 2015-08-10 16:57

Column: Reveleris® Silica 12g
Flow Rate: 30 mL/min
Equilibration: 4.8 min
Run Length: 10.0 min
Air Purge Time: 0.5 min

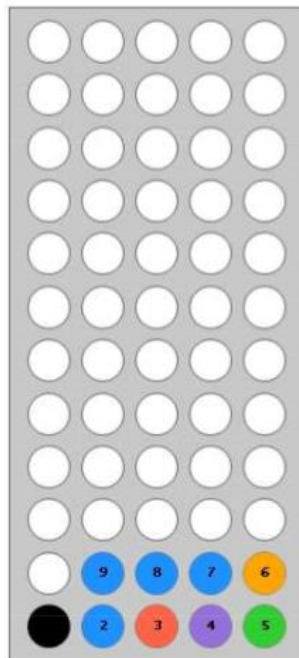
Slope Detection: High
ELSD Threshold: 5 mV
UV Threshold: 0.02 AU
UV1 Wavelength: 254 nm
UV2 Wavelength: 280 nm

Collection Mode: Collect Peaks
Per-Vial Volume: 25 mL
Non-Peaks: 25 mL
Injection Type: Dry

ELSD Carrier: Iso-propanol
Solvent A: Hexane
Solvent B: Ethyl acetate
Solvent C: <No solvent chose
Solvent D: <No solvent chose



1-7B19



Gradient Table

	Min	Solvents	% 2nd
1	0.0	AB	0
2	1.2	AB	0
3	3.0	AB	0
4	1.8	AB	0
5	0.0	AB	1
6	1.0	AB	1
7	0.0	AB	2
8	1.0	AB	2
9	0.0	AB	4
10	1.0	AB	4
11	1.0	AB	100

Vial Mapping Table

Peak #	Start Tray/Vial	End Tray/Vial
1	1:2	1:2
2	1:3	1:3
3	1:4	1:4
4	1:5	1:5
5	1:6	1:6
6	1:7	1:9



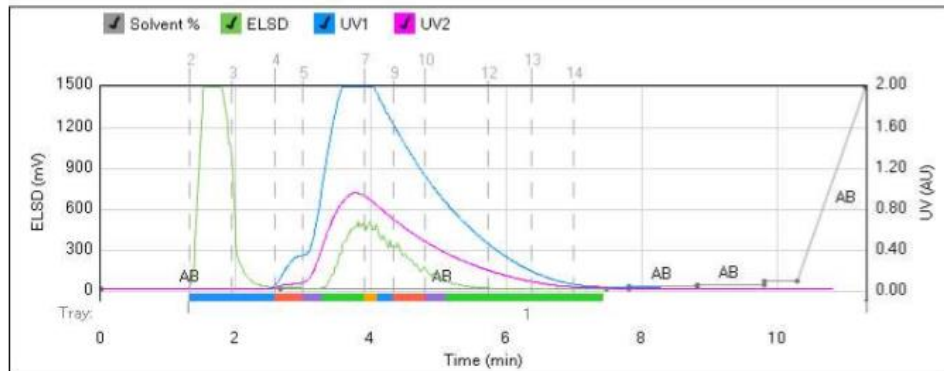
Method Name:
Run Name: KL-H-F2-B2
Run Date: 2015-08-25 14:27

Column: Reveleris® Silica 40g
Flow Rate: 40 mL/min
Equilibration: 7.1 min
Run Length: 11.4 min
Air Purge Time: 1 min

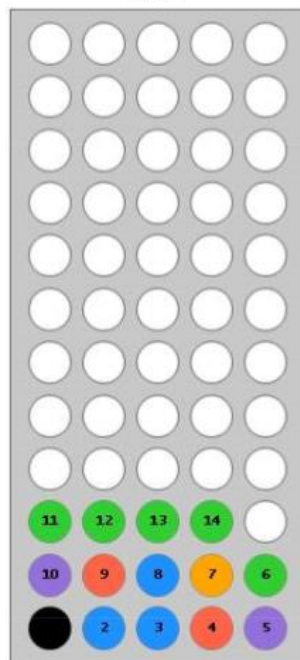
Slope Detection: High
ELSD Threshold: 5 mV
UV Threshold: 0.02 AU
UV1 Wavelength: 254 nm
UV2 Wavelength: 280 nm

Collection Mode: Collect Peaks
Per-Vial Volume: 25 mL
Non-Peaks: 25 mL
Injection Type: Manual

ELSD Carrier: Iso-propanol
Solvent A: Hexane
Solvent B: Ethyl acetate
Solvent C: <No solvent chose
Solvent D: <No solvent chose



1-7B19



Gradient Table

	Min	Solvents	% 2nd
1	0.0	AB	0
2	2.7	AB	0
3	4.9	AB	0
4	0.3	AB	0
5	0.0	AB	1
6	1.0	AB	1
7	0.0	AB	2
8	1.0	AB	2
9	0.0	AB	4
10	0.5	AB	4
11	1.0	AB	100

Vial Mapping Table

Peak #	Start Tray/Vial	End Tray/Vial
1	1:2	1:3
2	1:4	1:4
3	1:5	1:5
4	1:6	1:6
5	1:7	1:7
6	1:8	1:8
7	1:9	1:9
8	1:10	1:10
9	1:11	1:14



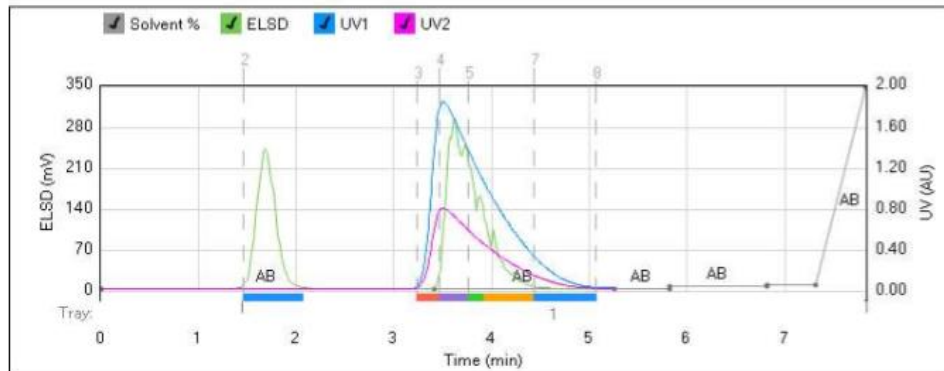
Method Name:
Run Name: KL-H-F2-B3
Run Date: 2015-08-27 11:12

Column: Reveleris® Silica 40g
Flow Rate: 40 mL/min
Equilibration: 7.1 min
Run Length: 7.9 min
Air Purge Time: 1 min

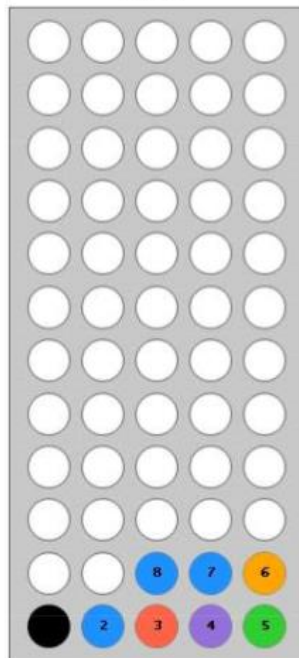
Slope Detection: High
ELSD Threshold: 5 mV
UV Threshold: 0.02 AU
UV1 Wavelength: 254 nm
UV2 Wavelength: 280 nm

Collection Mode: Collect Peaks
Per-Vial Volume: 25 mL
Non-Peaks: 25 mL
Injection Type: Dry

ELSD Carrier: Iso-propanol
Solvent A: Hexane
Solvent B: Ethyl acetate
Solvent C: <No solvent chose
Solvent D: <No solvent chose



1-7B19



Gradient Table

	Min	Solvents	% 2nd
1	0.0	AB	0
2	3.4	AB	0
3	1.9	AB	0
4	0.6	AB	0
5	0.0	AB	1
6	1.0	AB	1
7	0.0	AB	2
8	0.5	AB	2
9	0.5	AB	100

Vial Mapping Table

Peak #	Start Tray Vial	End Tray Vial
1	1:2	1:2
2	1:3	1:3
3	1:4	1:4
4	1:5	1:5
5	1:6	1:6
6	1:7	1:8



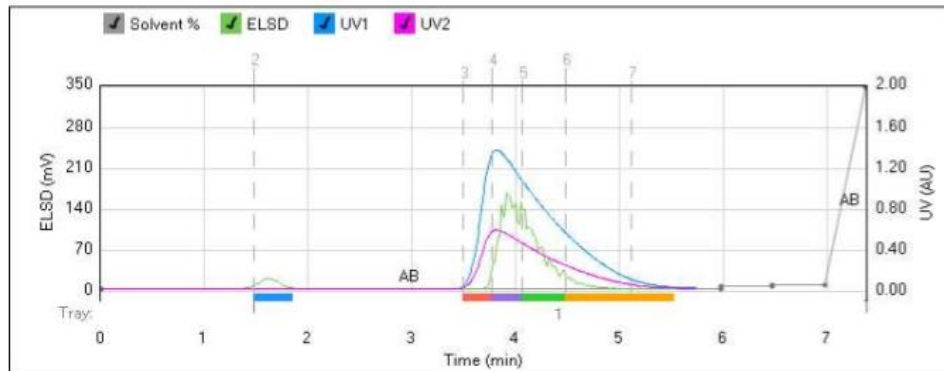
Method Name:
 Run Name: KL-H-F2-B4
 Run Date: 2015-08-27 11:30

Column: Reveleris® Silica 40g
 Flow Rate: 40 mL/min
 Equilibration: 7.1 min
 Run Length: 7.4 min
 Air Purge Time: 1 min

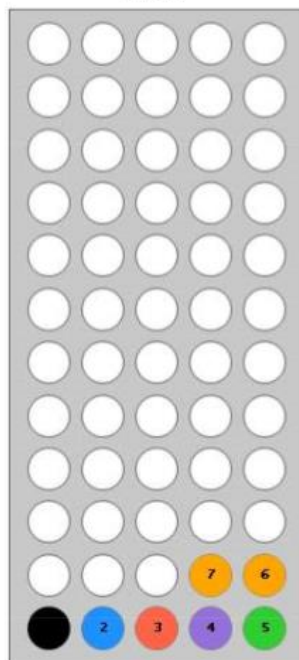
Slope Detection: High
 ELSD Threshold: 5 mV
 UV Threshold: 0.02 AU
 UV1 Wavelength: 254 nm
 UV2 Wavelength: 280 nm

Collection Mode: Collect Peaks
 Per-Vial Volume: 25 mL
 Non-Peaks: 25 mL
 Injection Type: Dry

ELSD Carrier: Iso-propanol
 Solvent A: Hexane
 Solvent B: Ethyl acetate
 Solvent C: <No solvent chose
 Solvent D: <No solvent chose



1-7B19



Gradient Table

	Min	Solvents	% 2nd
1	0.0	AB	0
2	6.0	AB	0
3	0.0	AB	1
4	0.5	AB	1
5	0.0	AB	2
6	0.5	AB	2
7	0.4	AB	100

Vial Mapping Table

Peak #	Start Tray-Vial	End Tray-Vial
1	1,2	1,2
2	1,3	1,3
3	1,4	1,4
4	1,5	1,5
5	1,6	1,7



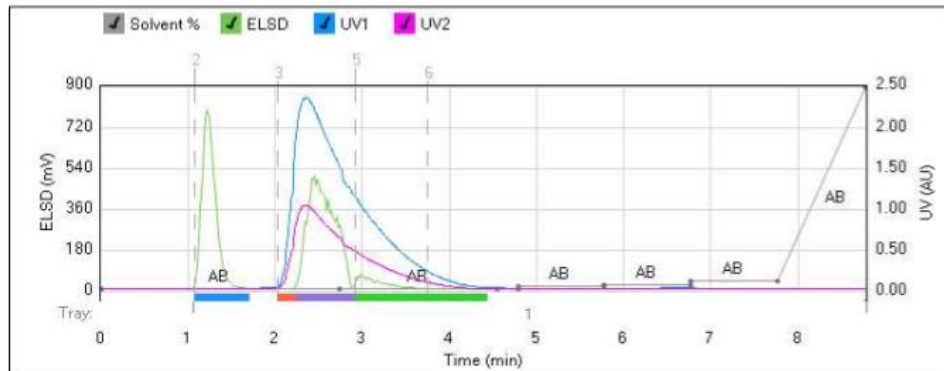
Method Name:
Run Name: KL-H-F3-A
Run Date: 2015-07-13 10:49

Column: Reveleris® Silica 12g
 Flow Rate: 30 mL/min
 Equilibration: 4.8 min
 Run Length: 8.8 min
 Air Purge Time: 0.5 min

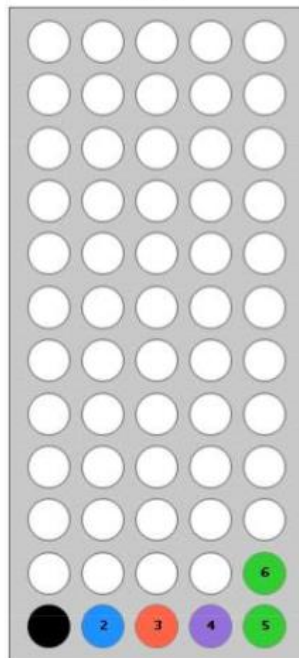
Slope Detection: High
 ELSD Threshold: 5 mV
 UV Threshold: 0.02 AU
 UV1 Wavelength: 254 nm
 UV2 Wavelength: 280 nm

Collection Mode: Collect Peaks
 Per-Vial Volume: 25 mL
 Non-Peaks: 25 mL
 Injection Type: Dry

ELSD Carrier: Iso-propanol
 Solvent A: Hexane
 Solvent B: Ethyl acetate
 Solvent C: <No solvent chose
 Solvent D: <No solvent chose



1-7B19



Gradient Table

	Min	Solvents	% 2nd
1	0.0	AB	0
2	2.8	AB	0
3	1.8	AB	0
4	0.2	AB	0
5	0.0	AB	1
6	1.0	AB	1
7	0.0	AB	2
8	1.0	AB	2
9	0.0	AB	4
10	1.0	AB	4
11	1.0	AB	100

Vial Mapping Table

Peak #	Start Tray/Vial	End Tray/Vial
1	1:2	1:2
2	1:3	1:3
3	1:4	1:4
4	1:5	1:6



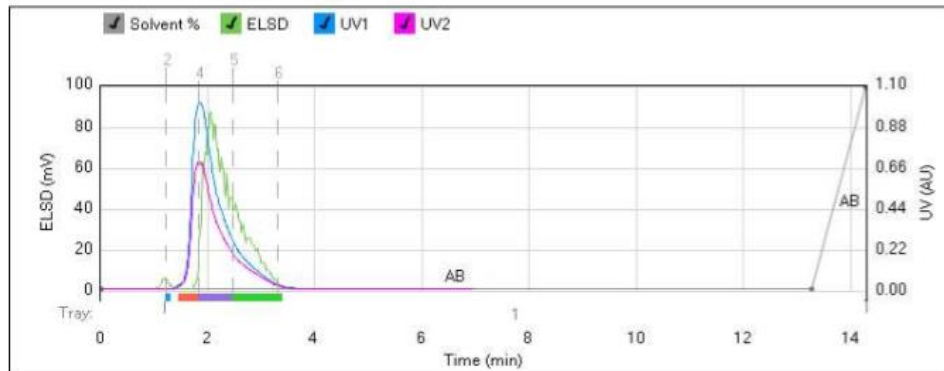
Method Name:
Run Name: KL-H-F4-B
Run Date: 2015-11-03 07:36

Column: Reveleris® Silica 12g
Flow Rate: 30 mL/min
Equilibration: 4.8 min
Run Length: 14.3 min
Air Purge Time: 0.5 min

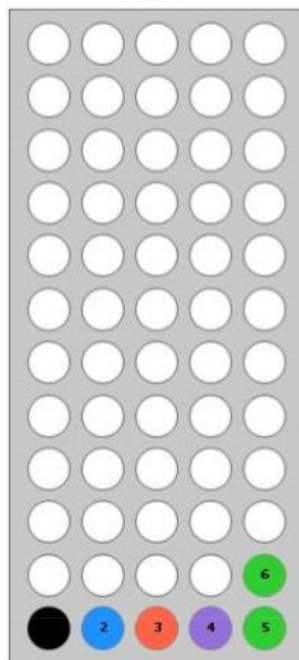
Slope Detection: High
ELSD Threshold: 5 mV
UV Threshold: 0.02 AU
UV1 Wavelength: 254 nm
UV2 Wavelength: 280 nm

Collection Mode: Collect Peaks
Per-Vial Volume: 25 mL
Non-Peaks: 25 mL
Injection Type: Dry

ELSD Carrier: Iso-propanol
Solvent A: Hexane
Solvent B: Ethyl acetate
Solvent C: <No solvent chose
Solvent D: <No solvent chose



1-7B19



Gradient Table

	Min	Solvents	% 2nd
1	0.0	AB	0
2	13.3	AB	0
3	1.0	AB	100

Vial Mapping Table

Peak #	Start Tray Vial	End Tray Vial
1	1.2	1.2
2	1.3	1.3
3	1.4	1.4
4	1.5	1.6



Method Name:
Run Name: KL-H-F2-E
Run Date: 2015-10-25 08:27

Vial Mapping Table

Peak #	Start Tray/Vial	End Tray/Vial
15	1:17	1:17
16	1:18	1:18
17	1:19	1:19
18	1:20	1:20
19	1:21	1:21
20	1:22	1:22
21	1:23	1:23
22	1:24	1:24
23	1:25	1:25
24	1:26	1:26
25	1:27	1:27
26	1:28	1:28
27	1:29	1:29
28	1:30	1:30
29	1:31	1:31
30	1:32	1:33
31	1:34	1:35
32	1:36	1:36



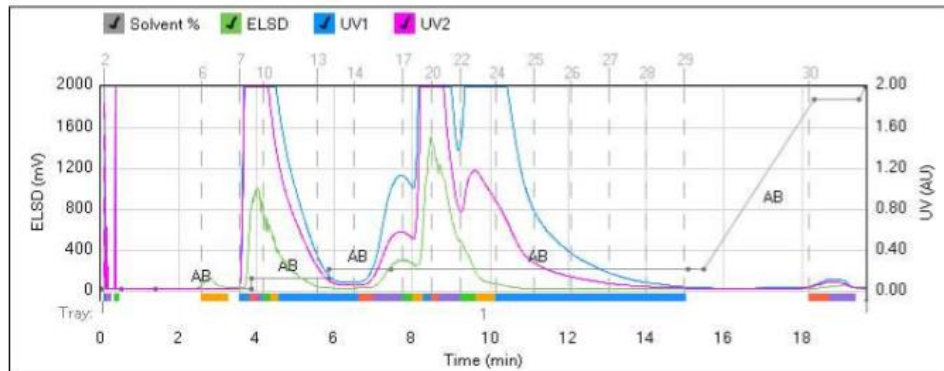
Method Name:
Run Name: KL-H-F2-E2
Run Date: 2015-10-26 06:25

Column: Generic Silica 40g
Flow Rate: 40 mL/min
Equilibration: 6.0 min
Run Length: 19.7 min
Air Purge Time: 1 min

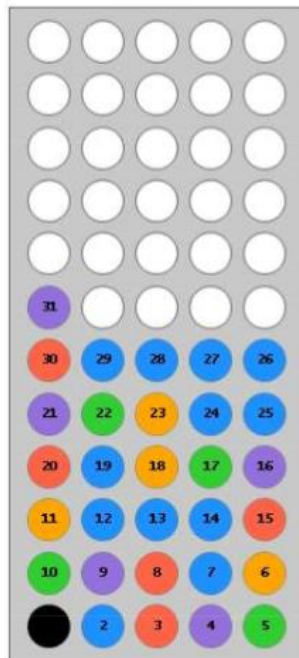
Slope Detection: High
ELSD Threshold: 20 mV
UV Threshold: 0.02 AU
UV1 Wavelength: 254 nm
UV2 Wavelength: 280 nm

Collection Mode: Collect Peaks
Per-Vial Volume: 25 mL
Non-Peaks: 25 mL
Injection Type: Manual

ELSD Carrier: Iso-propanol
Solvent A: Hexane
Solvent B: Ethyl acetate
Solvent C: <No solvent chosen>
Solvent D: <No solvent chosen>



1-7B19



Gradient Table

	Min	Solvents	% 2nd
1	0.0	AB	0
2	0.5	AB	0
3	0.9	AB	0
4	2.5	AB	0
5	0.0	AB	5
6	2.0	AB	5
7	0.0	AB	10
8	1.6	AB	10
9	7.7	AB	10
10	0.4	AB	10
11	2.8	AB	94
12	1.2	AB	94
13	0.2	AB	100

Vial Mapping Table

Peak #	Start Tray Vial	End Tray Vial
1	1:2	1:2
2	1:3	1:3
3	1:4	1:4
4	1:5	1:5
5	1:6	1:6
6	1:7	1:7
7	1:8	1:8
8	1:9	1:9
9	1:10	1:10
10	1:11	1:11
11	1:12	1:14
12	1:15	1:15



Method Name:
Run Name: KL-HF2-E2
Run Date: 2015-10-26 06:25

Vial Mapping Table

Peak #	Start Tray/Vial	End Tray/Vial
13	1:16	1:16
14	1:17	1:17
15	1:18	1:18
16	1:19	1:19
17	1:20	1:20
18	1:21	1:21
19	1:22	1:22
20	1:23	1:23
21	1:24	1:29
22	1:30	1:30
23	1:31	1:31

APPENDIX B
NMR ANALYSIS REPORTS
Carbon NMR

KL-H-F2-A

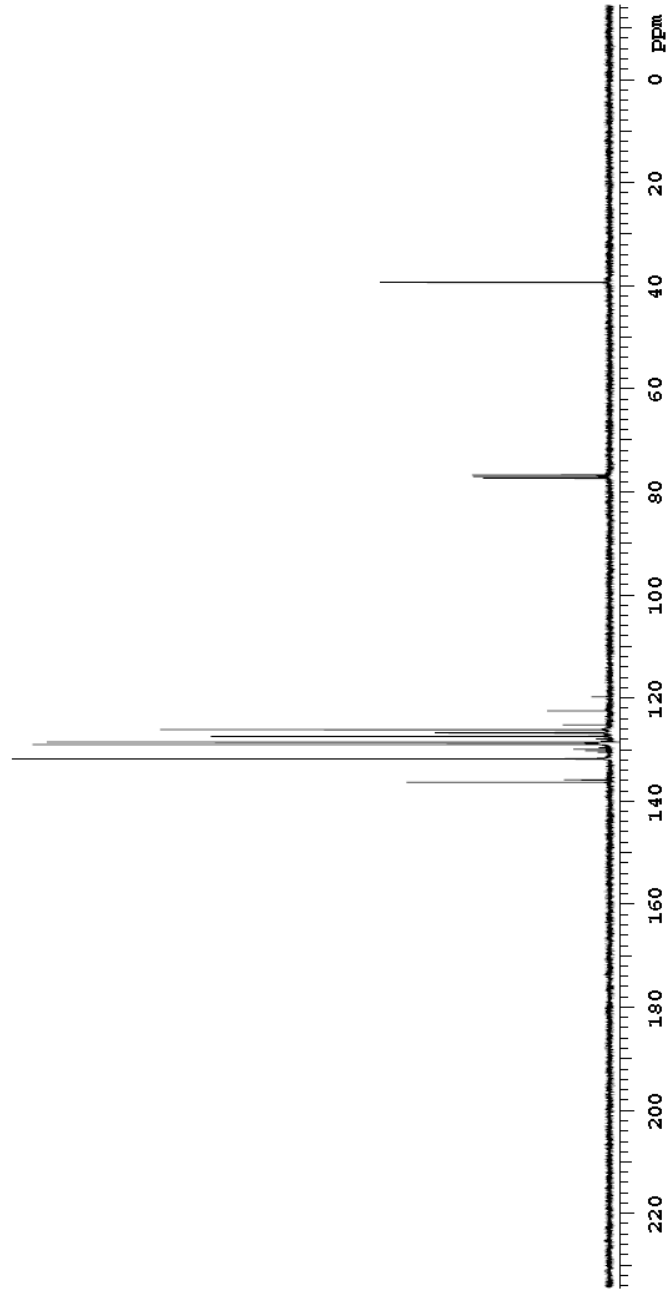


Sample Name KL-H-F2-A
Data collected 2015-07-28

Pulse sequence CARBON
Solvent cdd3

Temperature 28
Spectrometer Agilent-NMR-vnmrsl00

Study owner veldon
Operator veldon



Data file I:\ome\LLU\vnmsys\data\me\dm\kl-h-f2-a_20150728_01\CARBON_01.fid

Plot date 2015-07-28

KL-HF2-A



Agilent Technologies

Sample Name KL-HF2-A
Date collected 2015-07-28

Pulse sequence CARBON
Solvent cdcl3

Temperature 28
Spectrometer agilent-NMR-vnmrs400

Study owner weldon
Operator weldon



SAMPLE	SPECIAL
date	temp 28.0
solvent	gain 30
file	spin 0
cdcl3	flatt 0.008
/home/lluvnmrs/	pw90 3.500
data/weldon/KL-HF2-A_20	alpha 10.000
150728_01CARBON_01.fid	
ACQUISITION	FLAGS
sw 25000.0	il n
at 1.311	in n
np 65536	dp y
tb 17000	hs nn
bs 64	
d1 1.000	PROCESSING
nt 512	lb 0.50
ct 512	fn not used
TRANSMITTER	DISPLAY
tn C13	sp -1442.2
stfq 100.530	wp 24999.2
to f 1530.6	rf 1442.9
tp wr 55	rp 0
pw 4.750	rp -79.8
DECOUPLER	lp 0
dn HI	PLOT
dof 0	wc 234
dm 399	sc 8
deco wave w	vs 10382
dpuir 39	th 4
dmf 8850	ai odo ph
PRESATURATION	
satmode n	
wet n	

Plot name: CARBON_01_p1o101

Data file /home/lluvnmrs/data/weldon/KL-HF2-A_20150728_01CARBON_01.fid

Plot date 2015-07-28

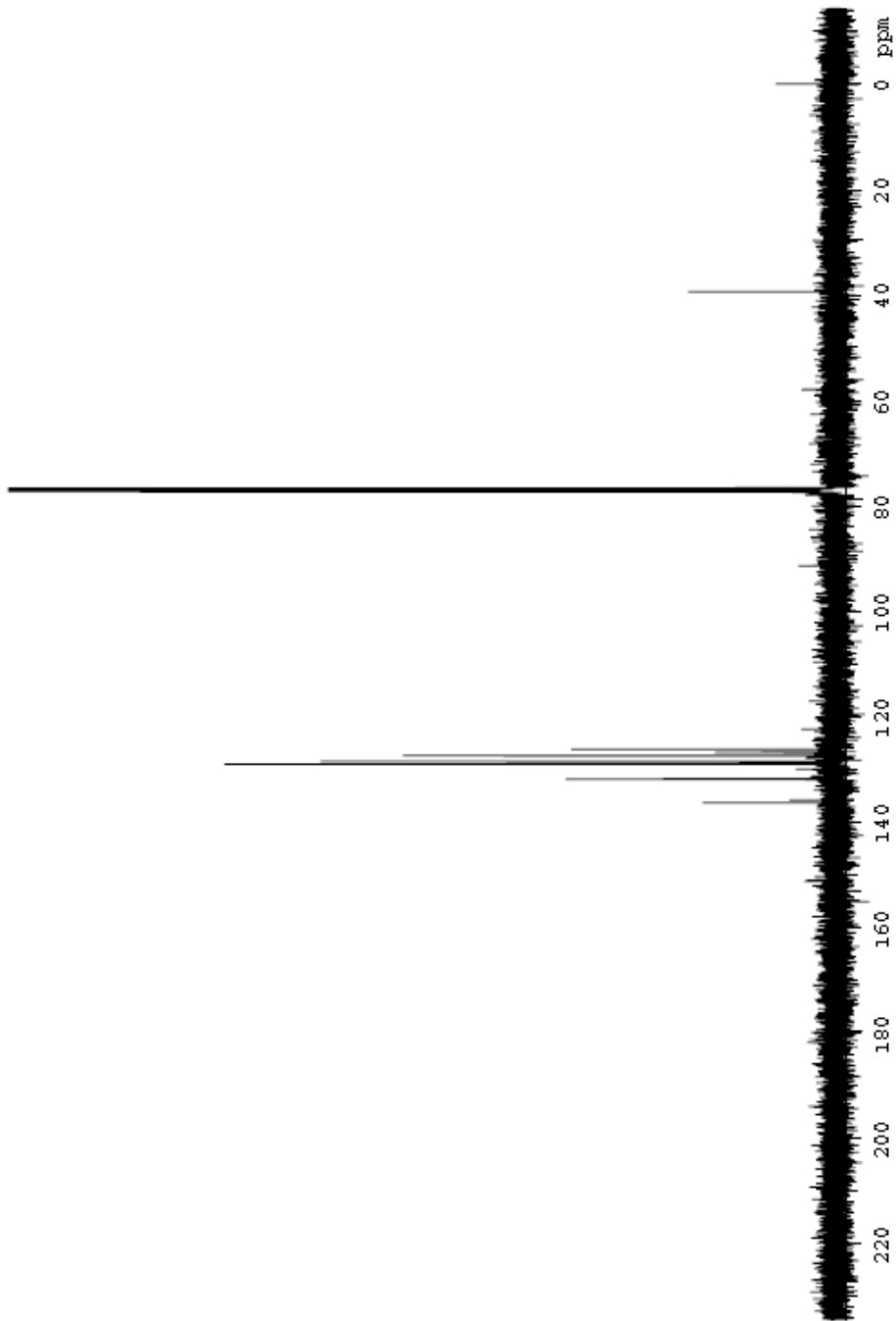
KL-H-F2-C

Sample Name: KL-H-F2-C
Date collected: 2016-08-20

Pulse sequence: CARBON
Solvent: ddh₂O

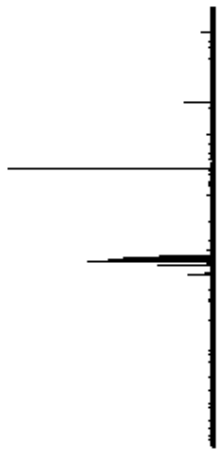
Temperature: 23
Spectrometer: Agilent MMR-mm r400

Study owner: vvidan
Operator: vvidan



KL-H-F2-C

Sample Name: **KL-H-F2-C** Pulse sequence: **COARBO M** Temperature: **23** Study owner: **veldon**
 Date collected: **2016-03-20** Solvent: **addis** Spectrometer: **agilent MM R-vm r400** Operator: **veldon**



SAMPLE		SPECIAL	
date	Aug 20 2016	temp	23.0
solvent	addis	gain	30
file	Home\LU\vm\rcv\ddata\veldon\KL-H-F2-C_20160320_01\COARBO_M_01.f2	spin	0
		h1	0.003
		pw50	8.875
		stb5	10.000
ACQUISITION		FLASH	
zfu	28000.0	ll	n
sf	13.11	ln	n
rp	8628	dp	y
tb	9.000	hz	nn
bs	84		
d1	1.000		
nl	612		
cl	612	lb	0.60
		tn	not used
TRANSMITTER		DISPLAY	
in	C18	sp	-1442.2
stq	100.829	wp	2.4898.2
ky	620.8	rl	1442.0
lpx	66	rp	0
pw	4.322	ip	-175.7
		lp	0
DECOUPLER		PLOT	
dn	H1	WC	284
dof	0	SC	2
dm	111	us	116726
decouple	0	in	16
dpor	38	st	adc ph
dm1	3250		
PREPARATION			
zaincode	n		
ue1	n		

Filename: **COARBO_01_Plot01**

Date: Home\LU\vm\rcv\ddata\veldon\KL-H-F2-C_20160320_01\COARBO_M_01.f2

Rollback: 20160320

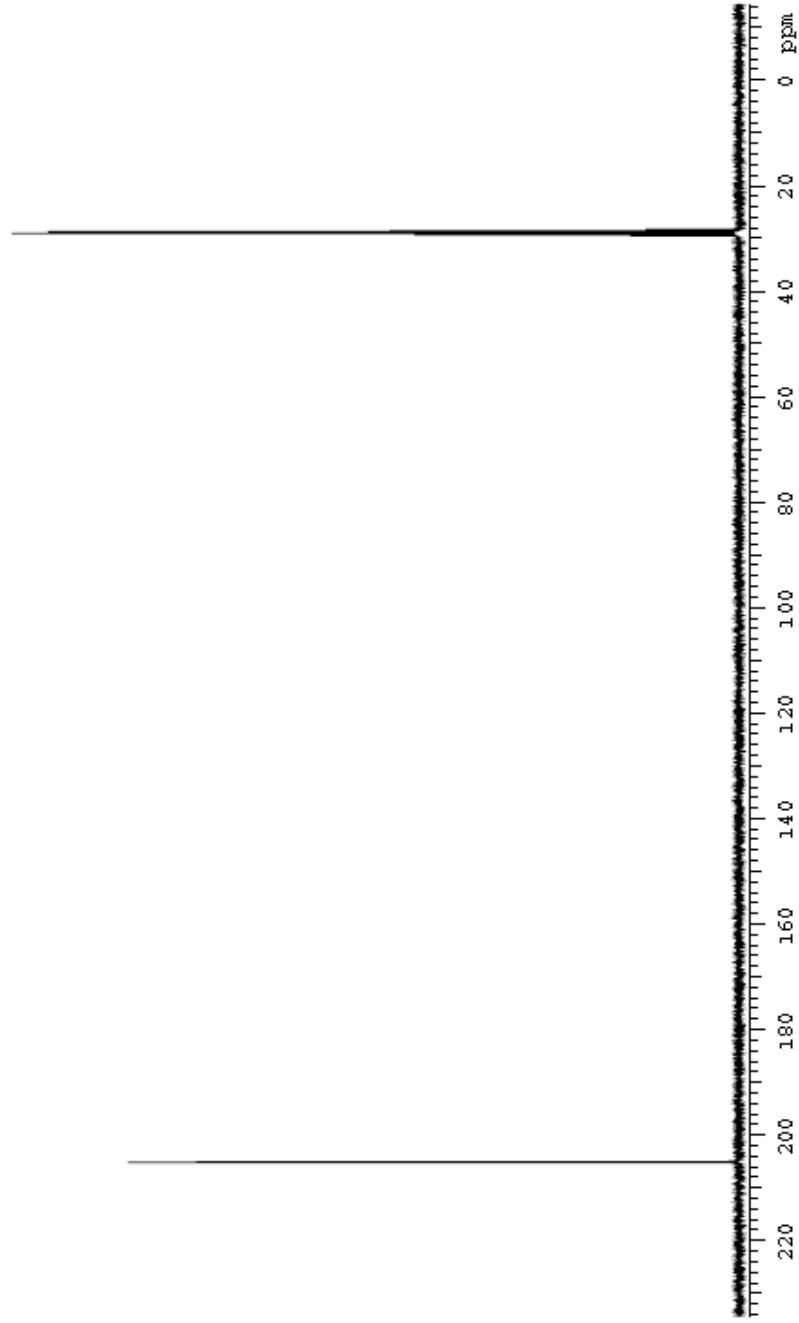
KL-H-F2-D1

Sample Name KL-H-F2-D1
Date collected 2016-09-02

Pulse sequence CARBON
Solvent acetone

Temperature 23
Spectrometer spectrometer400

Study owner veldan
Operator veldan



Path: /home/lu/Armsisys/Database/kl-h-f2-01_20160902_01V-CARBON_H2O.D1.f2

Revised: 2016-09-02

KL-K-P2-01

Sample Name: KL-K-P2-01 Run Sequence: CARBON Temperature: 25 Study Owner: waldan
Date Collected: 2016-08-06 Source: acetone Spectrometer: Agilent 4400 Operator: waldan



SAMPLE

date	08p 22016	temp	23.0
solvent	acetone	gain	30
file	home\LU\mmr\p2\438\waldan\KL-K-P2-01_2	zoff	0
	0160002_D\CARBON_01_10	hsl	0.008
		puiso	9.876
		zfs	10.000

ACQUISITION

sw	2000.0	fl ags	n
ai	1.311	in	n
rp	6658	dp	v
tb	5000	hs	nn
bs	84		
d1	1.000		
n1	612	lb	0.60
cl	612	th	not used

TRANSMITTER

in	C12
freq	100.620
lot	680.8
bw	66
pw	4.822

DECOUPLER

din	H1
dot	0
din	100
decouple	20
dout	3580
dout	

PREATTENUATION

gain	n
wet	n

SPECIAL

ii	n
in	n
dp	v
hs	nn

PROCESSING

lb	0.60
th	not used

DISPLAY

sp	-1442.1
wp	24889.2
rl	1442.8
rp	0
lp	-178.2
ip	0

PLOT

usc	284
sc	3
us	12861
sh	2
sh	adc.ph

Plotname: CARBON_01_plot01

Path: home\LU\mmr\p2\438\waldan\KL-K-P2-01_20160806_D1\CARBON_01_10

Print Date: 2016-08-08

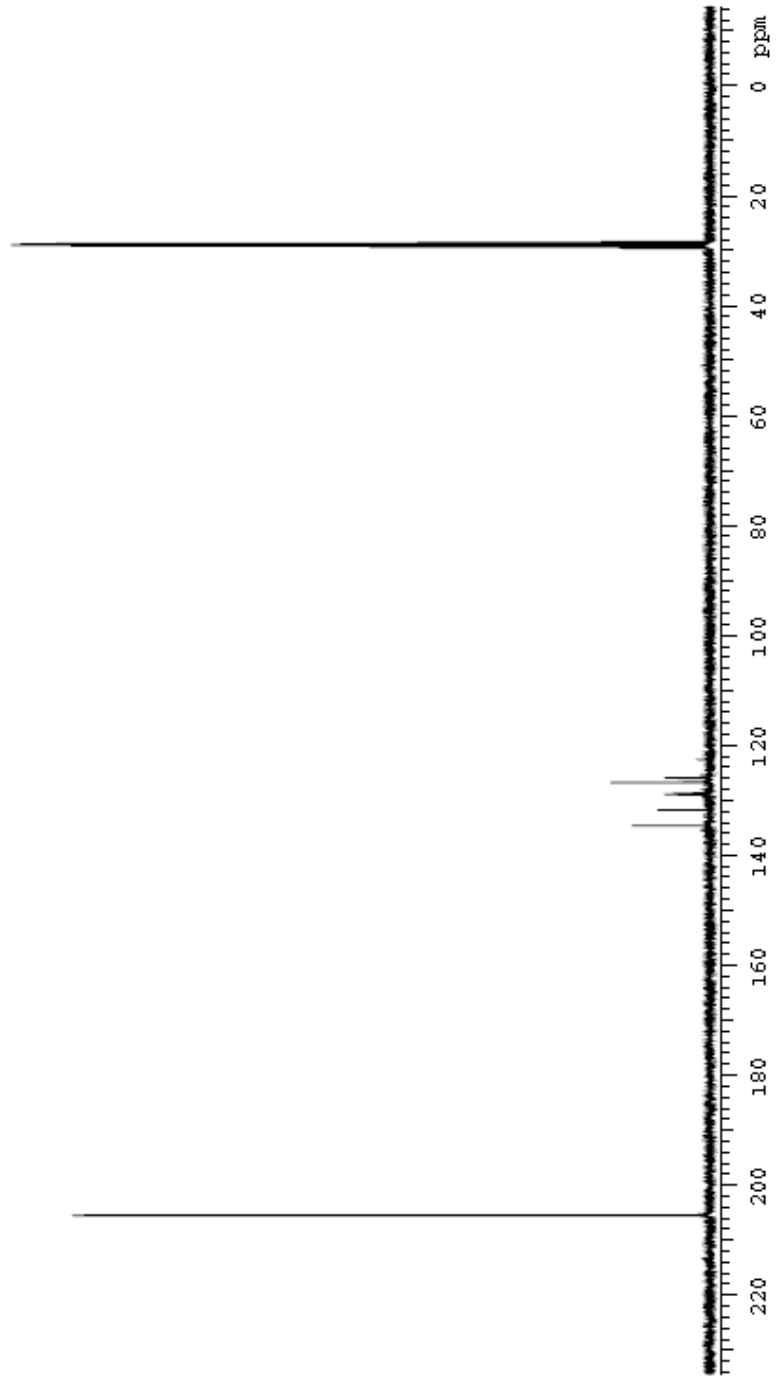
K1-H-F2-06

Sample Name **K1-H-F2-06**
Date collected **2016-08-11**

Pulse sequence **CARBON**
Solvent **acetone**

Temperature **28**
Spectrometer **Agilent MM R-Vnm rxd400**

Study owner **veldan**
Operator **veldan**



K1-H-F2-06

Sample Name: K1-H-F2-06
 Date Collected: 2016-08-11
 Pulse sequence: CARBON
 Solution: acetone
 Temperature: 28
 Spectrometer: agilent-nmr-rnm-r400
 Study owner: weldan
 Operator: weldan



```

SAMPLE
date      Bp 112016
solution  acetone
file      Name/LU/Name/2016
          d33A:weldan/K1-H-F2-06_2
          0160811_01CARBON_0116

ACQUISITION
SI 0
SI 28000.0
SI 1.311
SI 0
SI 6658
SI 17000
SI 84
SI 1.000
SI 612
SI 612

TRANSMITTER
SI C16
SI 100.630
SI 630.8
SI 66
SI 4.322

DECOUPLER
SI H1
SI 0
SI 177
SI 0
SI 89
SI 3350

PREPARATION
SI mode
SI n
SI wet
SI n

SPECIAL
SI temp 28.0
SI gain 30
SI spin 0
SI h1 0.002
SI pwr 6.876
SI sb 10.000

FLAGS
SI ll n
SI ln n
SI op y
SI ps nn
SI pr n
SI rb n
SI tp 0.60
SI tn notu end

DISPLAY
SI sp -1442.1
SI up 24896.2
SI rl 1442.8
SI rp 0
SI tp -168.8
SI lp 0

PLOT
SI WC 284
SI SC 2
SI US 12848
SI In 2
SI atc ph

PLOTNAME: CARBON_01_plot01
  
```

DATA FILE HOME/13C/Name/ps/3d/3d/weldan/K1-H-F2-06_20160811_01CARBON_0116

File Date 2016-08-11

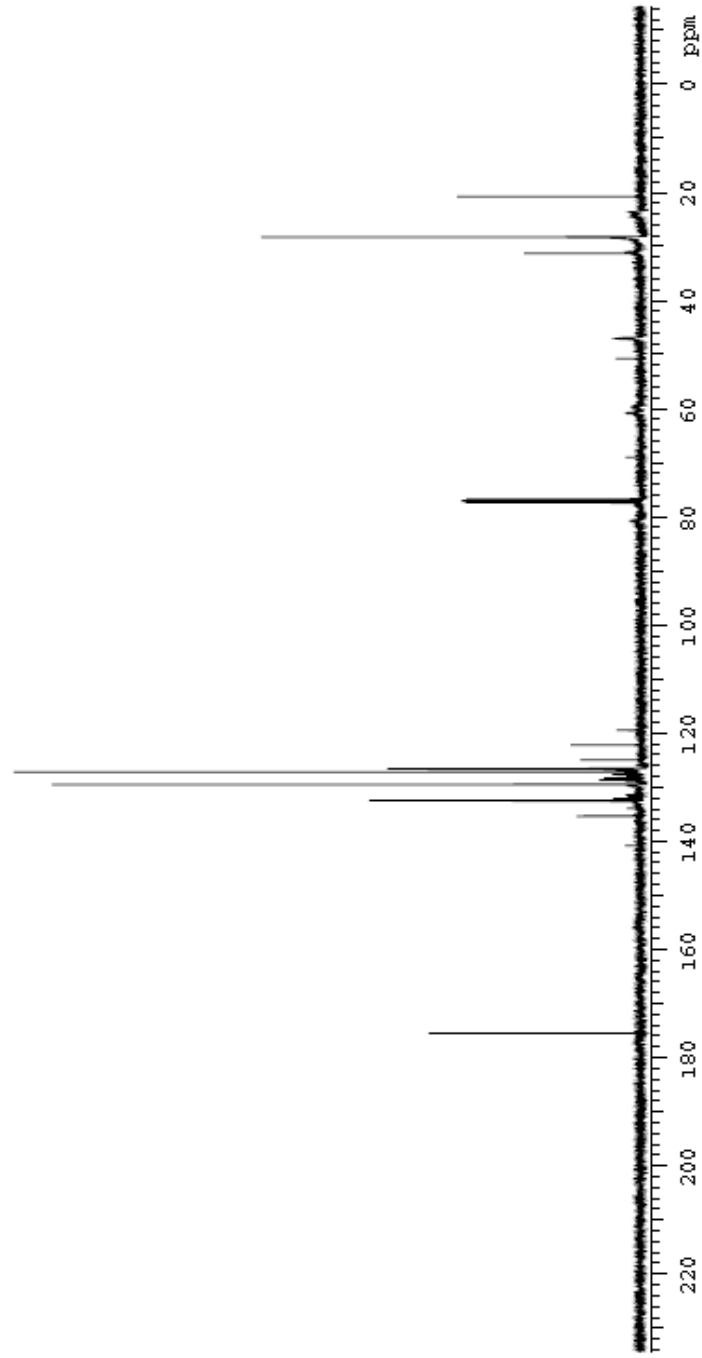
K1-R-F4-A

Sample Name K1-R-F4-A
Date collected 2016-10-03

Pulse sequence CARBON
Solvent ddh2o

Temperature 23
Spectrometer 300mmMNRmmr400

Study owner veldan
Operator veldan



Data file: home\LU\Arms\sys\NMR\K1-R-F4-A_20161003_01\CARBO #_D116

Release 2015-10-05

KL-H-F4-A

Sample Name: KL-H-F4-A
 Date Collected: 2016-10-08
 Pulse sequence: CARBON
 Solvent: ddh2o
 Temperature: 28
 Spectrometer: zg30nt1M1R-vmrncd00
 Study owner: waldon
 Operator: waldon



SAMPLE

date: Oct 20 16
 solvent: ddh2o
 file: Home/LU/umrncd/435/waldon/KL-H-F4-A_20161008_01CARBON_M_01.fid

SPECIAL

temp: 28.0
 gain: 30
 sph: 0
 h1: 0.008
 p160: 8.876
 s160: 10.000

ACQUISITION

sw: 26000.0
 al: 1.311
 rg: 66688
 tb: 9000
 bs: 84
 d1: 1.000
 n1: 612
 cl: 612

FLAGS

ll: n
 ln: n
 dp: y
 h1: nn
 PROCESSING
 lb: 0.60
 th: not used

TRANSMITTER

fr: C18
 frq: 100.628
 lot: 630.8
 pow: 66
 pw: 4.323

DISPLAY

sp: -1442.2
 up: 24889.2
 rl: 1443.0
 rp: 0
 lp: -142.6
 ip: 0

DECOUPLER

dn: H1
 dot: 0
 dm: w
 decoupl: w
 dpr: 28
 dnt: 2660

PLOT

wc: 284
 sic: 2
 us: 12816
 fr: 6
 sf: calc.ph

PREPARATION

solmode: n
 wcl: n

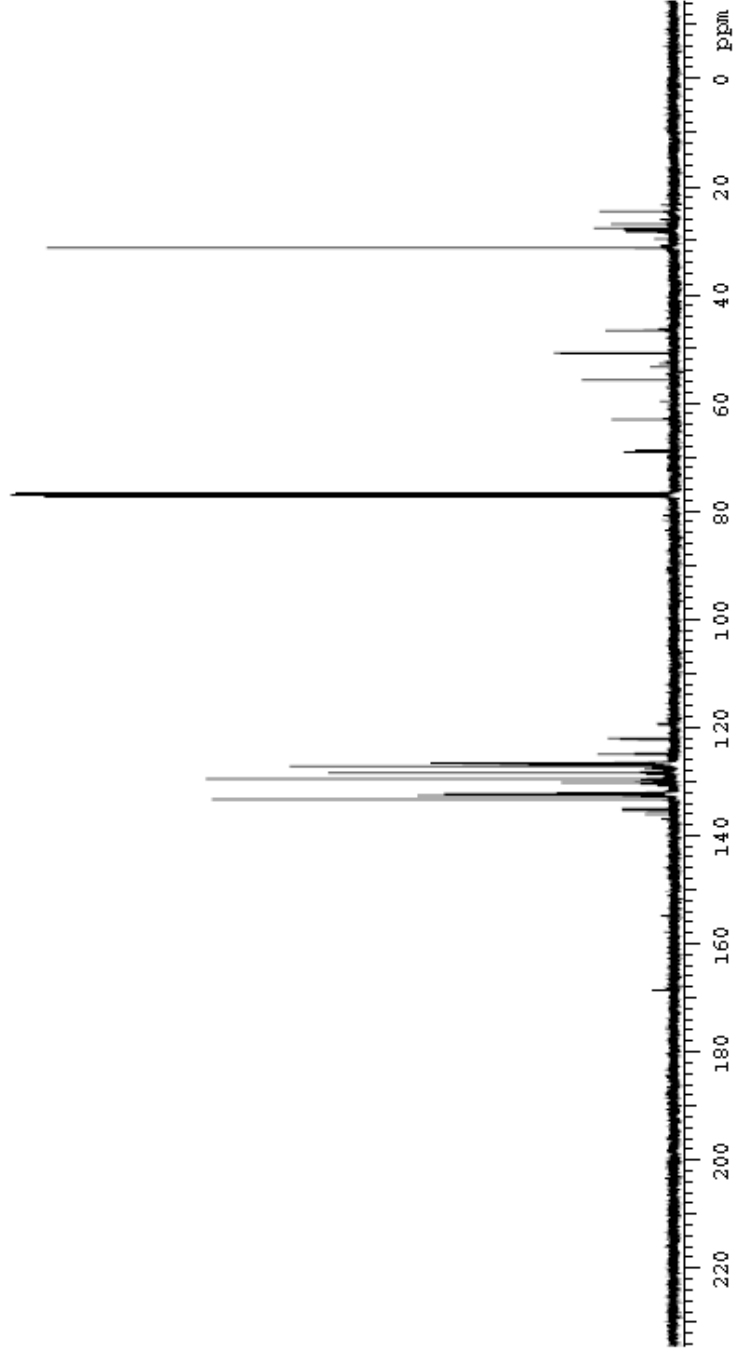
Plotname: CARBON_01_plot01

0435 Home/LU/umrncd/435/waldon/KL-H-F4-A_20161008_01CARBON_M_01.fid

Rollback 2016-10-08

KL-H-F4-B

Sample Name	KL-H-F4-B	Pulse sequence	CARBO 1	Temperature	28	Study owner	Walden
Date collected	2016-10-14	Solvent	ddt2	Spectrometer	agilent NMR-ann r300	Operator	Walden



K1-R-F4-B

Sample Name: K1-R-F4-B
 Date Collected: 2016-10-14
 Pulse Sequence: CARBON
 Spectrometer: Agilent 4401
 Study Owner: weldon
 Operator: weldon



```

SAMPLE
date      Oct 14 2016
solvent   C6H14
file      Home\11\unm\rez\c
          data\weldon\K1-R-F4-B_20
          161014_01\CARBON_01.d
SPECIAL
temp      23.0
dsh       30
sdrh      0
hs1       0.003
pulsed    8.876
sfs       10.000
ACQUISITION
sw        20000.0
ai         1.811
rp        65628
to        70000
bs        84
d1        1.000
f1        612
f2        612
TRANSMITTER
In        C18
sfq       100.628
koff      550.8
lpwr      66
pw        4.832
DECOUPLER
dn        H1
dof       0
dm        0
decoupler 0
dprw      38
dmT       3260
PREPARATION
salmode   n
wet       n
  
```

Plotname: CARBON_01_Plot01

Date: Home\11\unm\systems\weldon\K1-R-F4-B_20161014_01\CARBON_01.d

Roll date: 2015-10-14

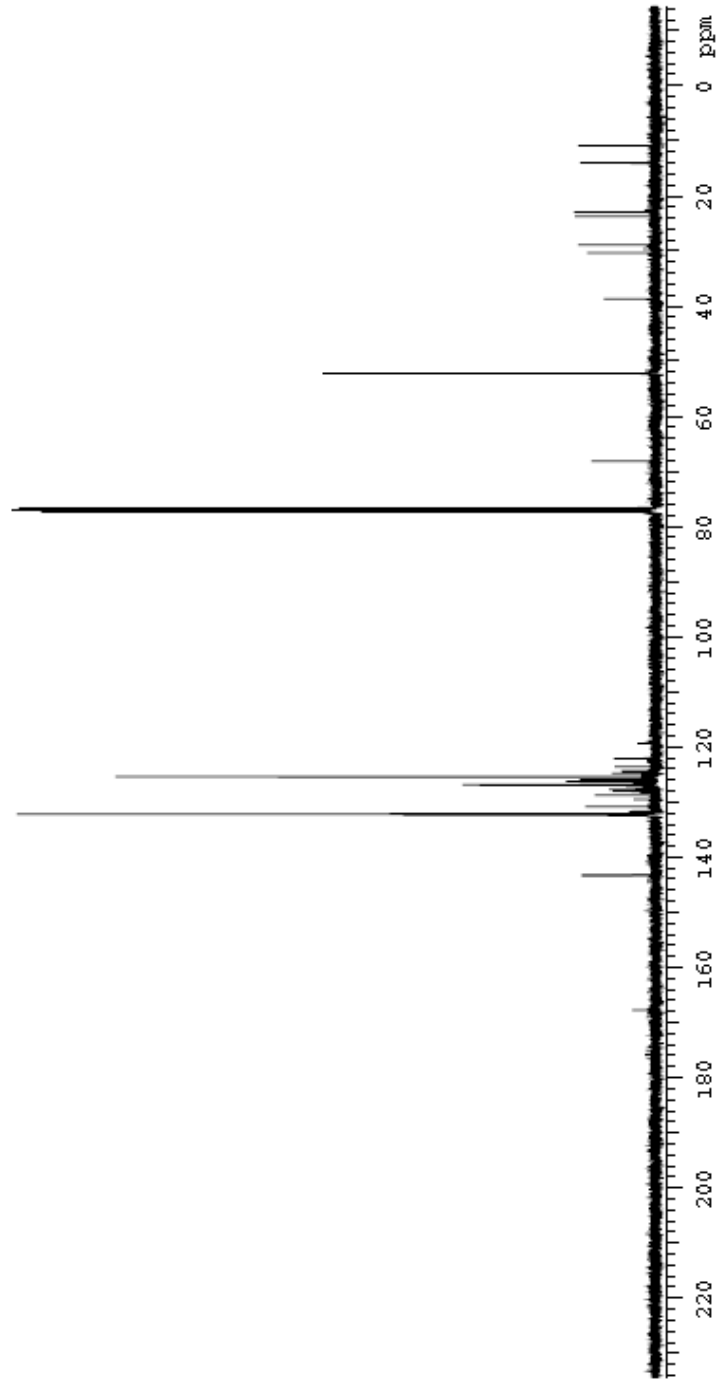
KL-RP2-E

Sample Name **KL-RP2-E**
Date collected **2016-10-28**

Pulse sequence **CARBON**
Solvent **ddis**

Temperature **23**
Spectrometer **Agilent MM R-nmr400**

Study owner **:wldan**
Operator **:wldan**



K1-H-F2-E

Sample Name: K1-H-F2-E Temperature: 23 Study owner: weldon
 Date collected: 2016-10-28 Spectrometer: Agilent MMF-ann-rs400 Operator: weldon



SAMPLE

date: Oct 28 2016
 solvent: ddh2o
 file: Name: K1-H-F2-E_20
 data: weldon\K1-H-F2-E_20
 161028_01\CARBON_M_0116

SPECIAL

temp: 23.0
 gain: 30
 gain: 0
 hel: 0.002
 prog: P.075
 size: 10.000

ACQUISITION

sw: 2600.0
 al: 1.311
 no: 66528
 to: 7000
 bz: 84
 d1: 1.000
 n1: 612
 c1: 612

FLAG

ll: n
 ln: n
 dp: y
 hc: nn
 PROCERRING

TRANSMITTER

in: C18
 s1q: 100.628
 lot: 1620.8
 lpar: 66
 pw: 4.333

DB PLAY

sp: -1442.2
 wp: 24888.2
 rd: 1443.0
 rd: 0
 rd: -176.2
 rd: 0

DECOUPLER

dn: H1
 cor: 0
 dm: vvv
 devalue: w
 dpar: 28
 dmt: 3250

PLOT

wc: 234
 sc: 3
 us: 28202
 in: 10
 al: calc pH

PREBATHURATION

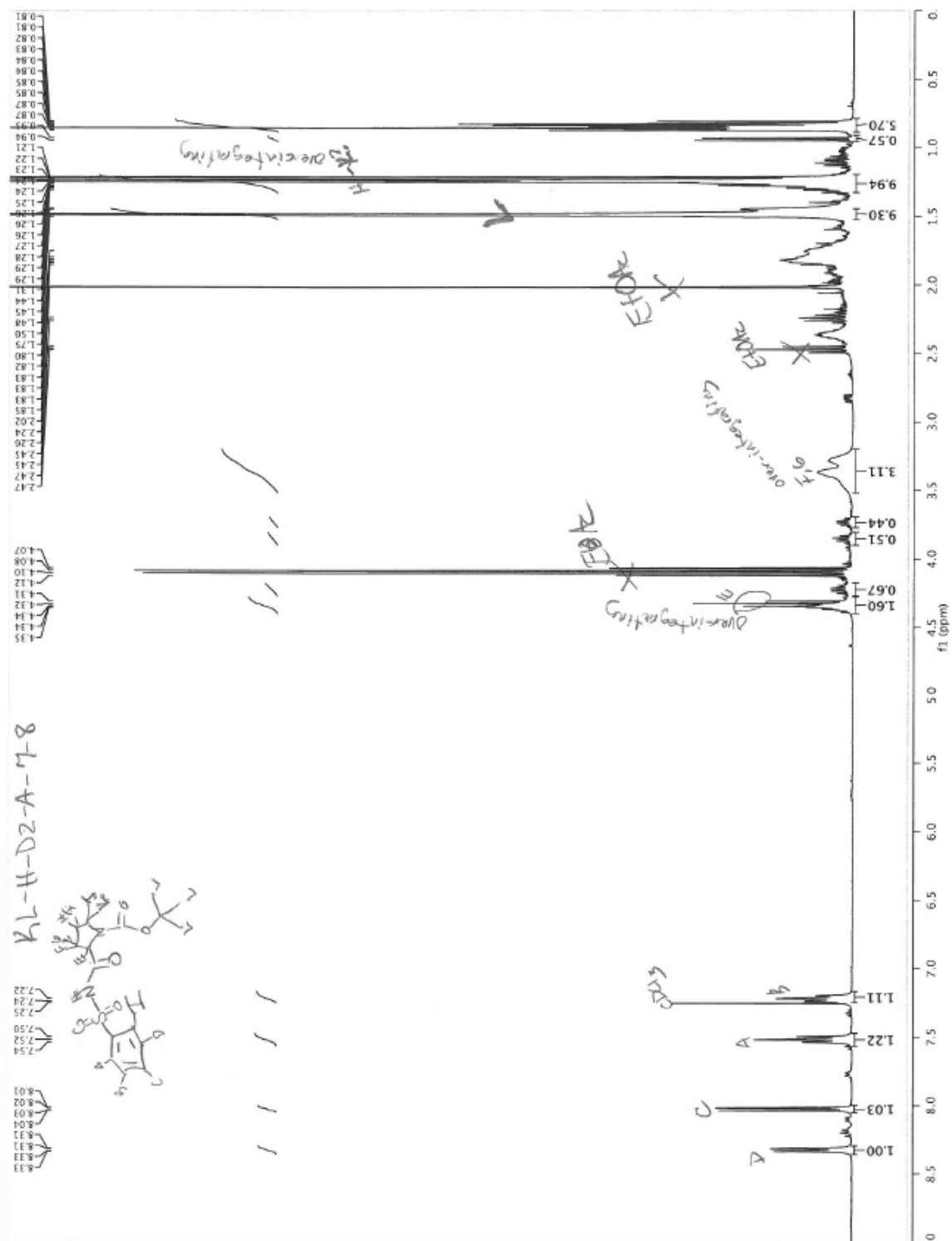
calmode: n
 wet: n

Filename: CARBON_01_Plot01

Date: /home/llw/admin/systems/batch/K1-H-F2-E_20161028_01\CARBON_M_0116

Roll date: 2016-10-26

Proton NMR



KL-H-F2-A



Agilent Technologies

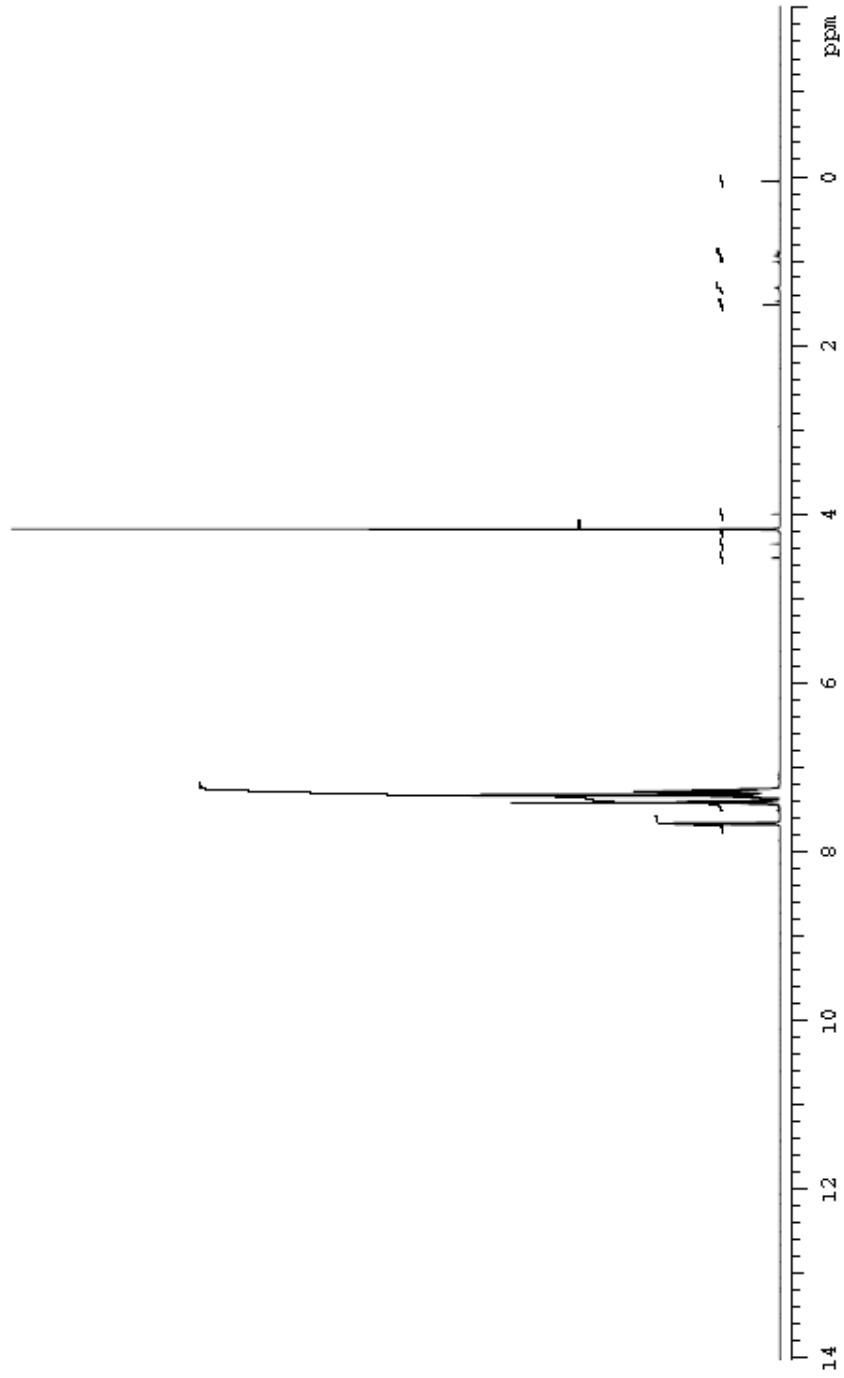
Sample Name: KL-H-F2-A
Date Collected: 2016-07-28

Pulse sequence:
SQUASH

PROTON

Temperature: 28
Spectrometer: agilent MM R-mm rdd00

Study owner: wida n
Operator: wida n



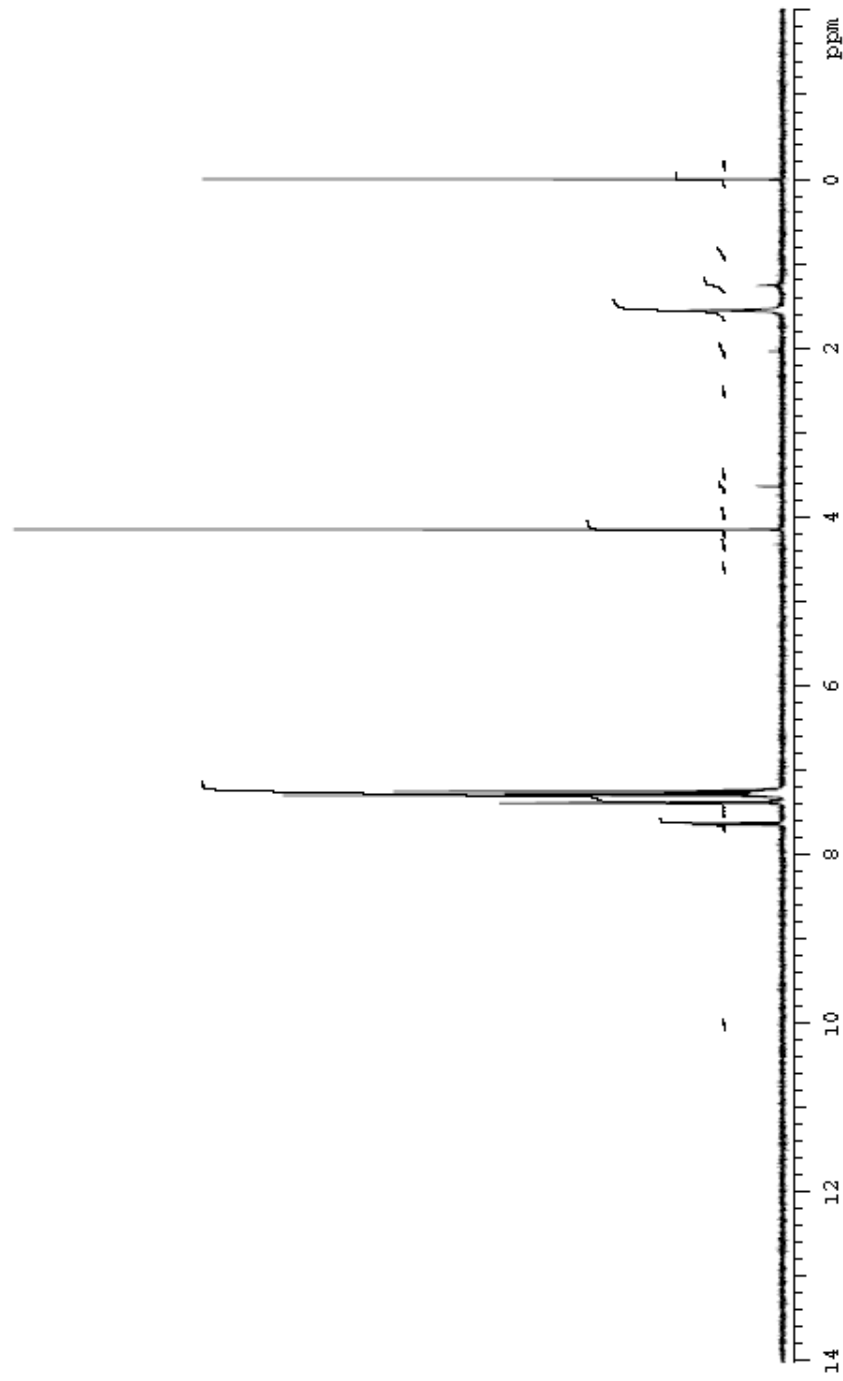
KL-H-F2-C

Sample Name KL-H-F2-C
Date collected 2016-05-20

Pulse sequence PROTON
Solvent ddh₂O

Temperature 23
Spectrometer Agilent MMR-mm-rsd00

Study owner veldon
Operator veldon



05816 ThermoFisher\Instruments\Agilent\KL-H-F2-C_20160520_01\PROTON_H_01.f2

Rollback 2016-05-20

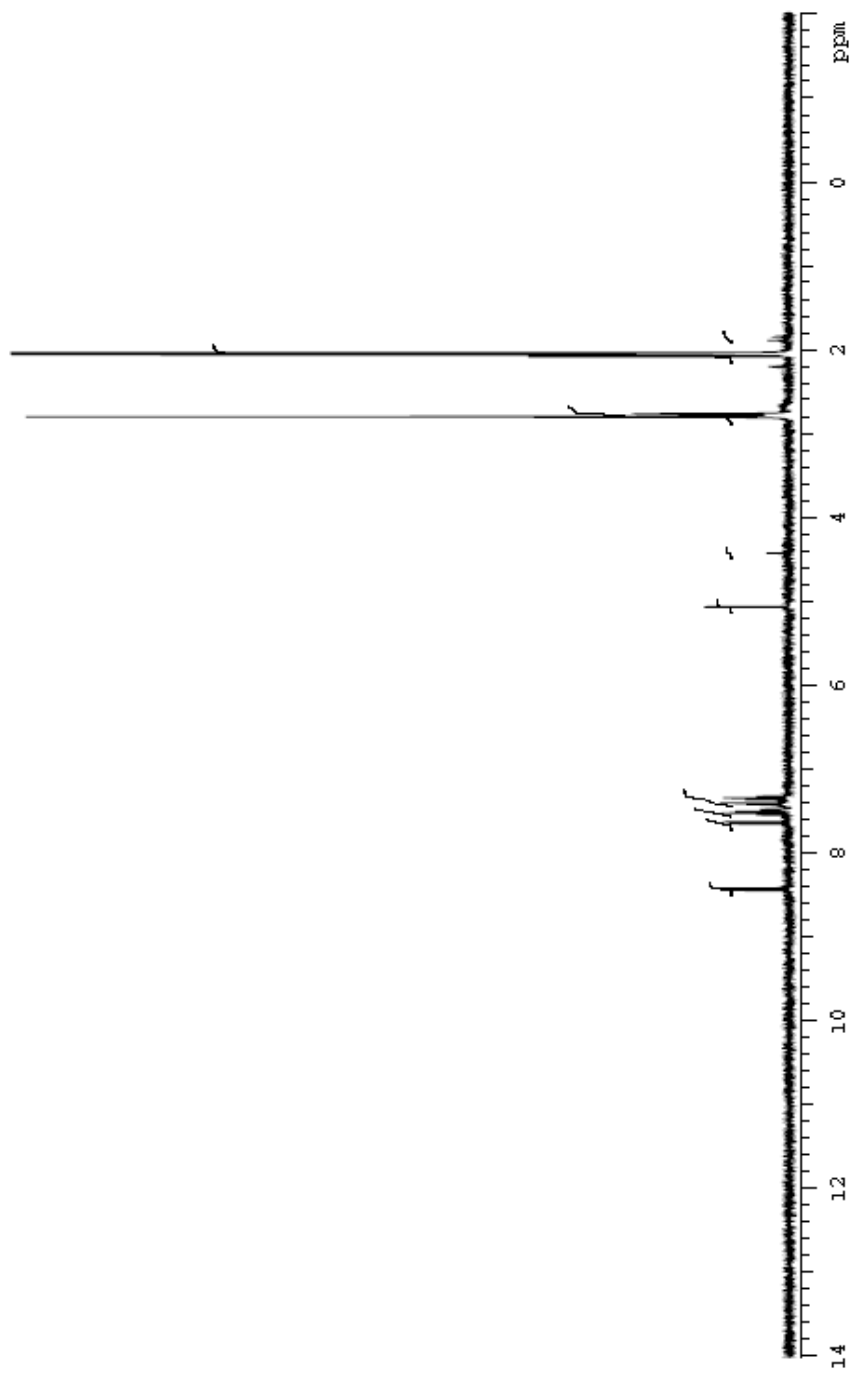
KL-H-F2-D1

Sample Name: KL-H-F2-D1
Date collected: 2016-08-08

Pulse sequence: PROTON
Solvent: acetone

Temperature: 23
Spectrometer: spect 400

Study owner: widon
Operator: widon

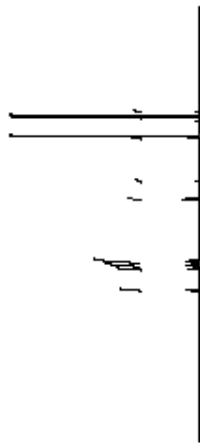


000016: /home/llw/numrisys/ataxweb/000/kl-h-f2-d1_20160808_01/PROTON_H_01.fid

Point: 20160808

KL-H-P2-D1

Sample Name: KL-H-P2-D1
 Date collected: 2016-09-08
 Pulse sequence: PROTON
 Solvent: acetone
 Temperature: 28
 Spectrometer: agilent MM-RNM1400
 Study owner: waldon
 Operator: waldon



```

SAMPLE                                wt1      n
-----
date      Sep 08 2016
solvent1  acetone
file      /home/lu/waldon/20160908/kl-h-p2-d1_2
          0160908_01PROTON_01.fid
ACQUISITION
sw        6410.3
sf        2.568
rg        327.93
rb        4000
bs        32
d1        1.000
n1        3
c1        3

TRANSMITTER
In        H1
sfreq    399.759
lof      399.3
pwr      59
pw       6.660

DECOUPLER
dfn      C13
dot      0
dm       nnn
decouple WALTZ16
dpuw     34
dmr      28412

PREPARATION
salmode  n
  
```

Filename: PROTON_01_plot01

Path: /home/lu/waldon/20160908/kl-h-p2-d1_20160908_01PROTON_01.fid

Printed: 2016-09-08

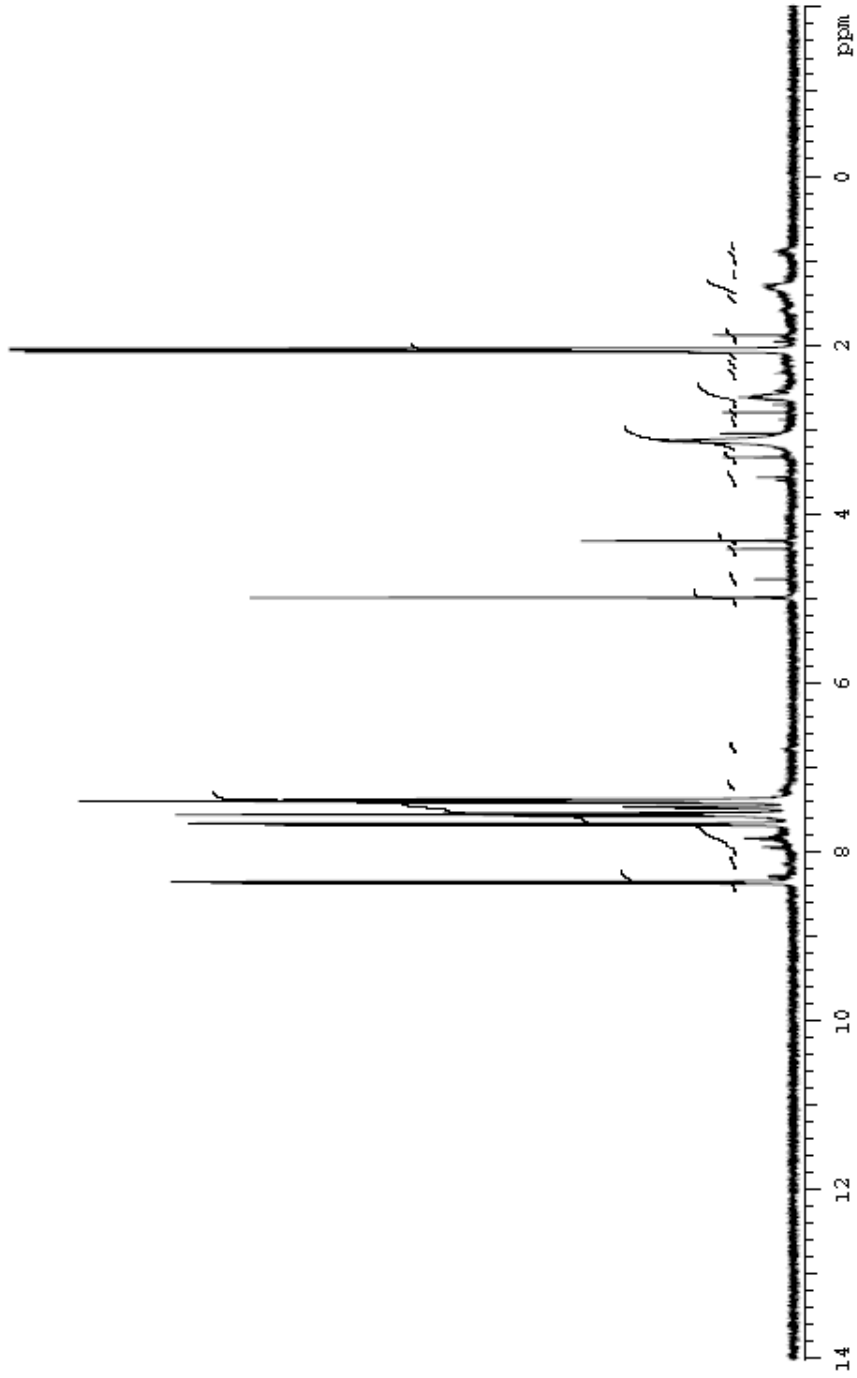
KL-RP2-08

Sample Name KL-RP2-08
Date Collected 20-16-08-11

Pulse sequence: **PROTON**
Solvent: **aceton**

Temperature: **23**
Spectrometer: **agilent MM R-nm rcd00**

Study owner: **vidan**
Operator: **vidan**

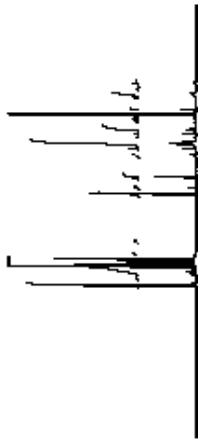


data file: home\lun\mms\stata\work\KL-RP2-03_20160811_DIVPROTON_M_D1_08

File Date: 2016/08/11

KL-H-F2-06

Sample Name: KL-H-F2-06
Date collected: 2016-08-11
Pulse sequence: PROTON
Solvent: acetone
Temperature: 25
Spec: chemist
Study owner: veldan
Operator: veldan



SAMPLE		wei	n
date	Exp_112016		
solvent	acetone		
file	h:\home\luj\vm\proj\0160811_U\PROTON_0160		
dir	0160811_U\PROTON_0160		
temp	23.0		
gain	40		
spin	0		
rel	0.005		
pw50	11.100		
strs	10.000		
ACQUISITION			
sw	8410.2		
al	2.668		
rp	32782		
to	4000		
bs	22		
d1	1.000		
m1	2		
cl	2		
TRANSMITTER			
in	H1		
str	288.768		
ref	288.2		
low	58		
pw	6.660		
DECOUPLER			
dn	C18		
dof	0		
dm	non		
decouple	W40_KC16mm		
dpor	24		
dm1	28412		
PREHEATING			
solmode	n		
DISPLAY			
sp	-308.2		
wp	8408.8		
rl	208.6		
rp	0		
rp	-52.8		
lp	0		
PILOT			
wc	284		
rc	2		
us	200		
in	2		
st	adc.ph		

Plotname: PROTON_01_plot01

base: h:\home\luj\vm\sys\data\velon\KL-H-F2-03_20160811_DI\PROTO_M_01.d

Roll date: 2016-09-11

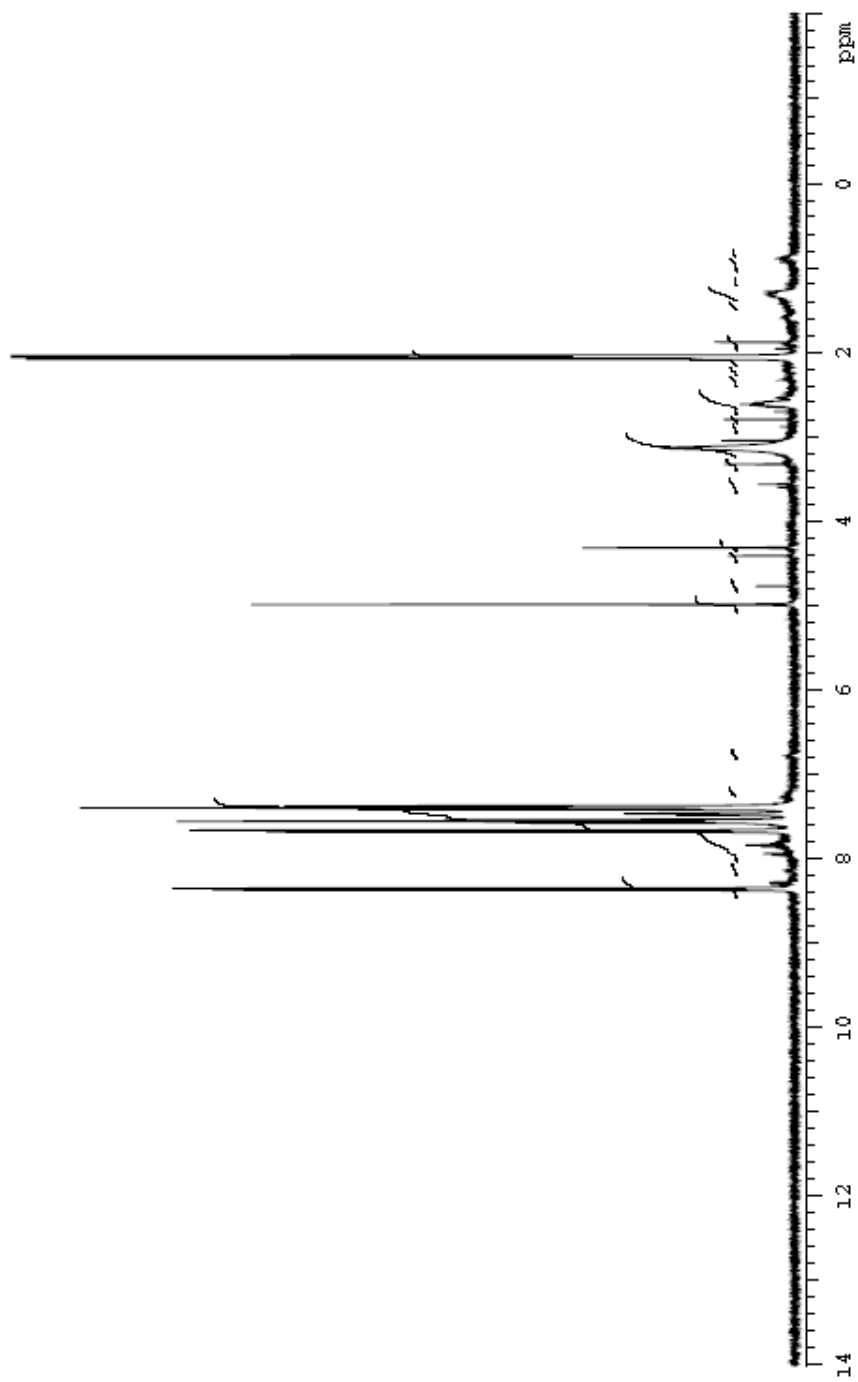
KL-H-F2-D8

Sample Name KL-H-F2-D8
Date collected 2016-08-11

Pulse sequence PROTON
Solvent acetonitrile

Temperature 23
Spectrometer 300 MHz MM RNM R400

Study owner wjdon
Operator wjdon

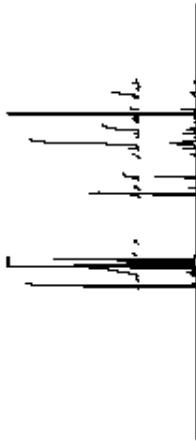


DATA: /home/llui/arnesys/data/bwedit/KL-H-F2-D8_20160811_01/PROTON_KL_D11.D

Rollback 2016-08-11

KL-H-F2-08

Sample Name: KL-H-F2-08 Pulse sequence: PROTON Temperature: 23 Study owner: weldon
 Date collected: 2016-08-11 Solvent: acetone Spectrometer: 300lentMMR-nmr400 Operator: weldon



SAMPLE vel n

SPECIAL

temp	23.0
gain	40
spin	0
hel	0.003
pw50	11.100
st20	10.000

ACQUISITION

sw	640.0
rl	2.666
rb	32785
rb	4000
bs	82
d1	1.000
nl	3
cl	3

TRANSMITTER

fn	not used
----	----------

DISPLAY

zp	508.2
wp	6400.8
rl	308.6
rb	0
rp	-62.8
lp	0

PLOT

vc	284
sc	3
us	300
th	2
si	dic ph

satmode n

Filename: PROTON_01_plot01

Date: /home/luu/arniesys/database/velon/KL-H-F2-08_20160811_01/PROTON_01.D1.01

Rollback: 2016-08-11

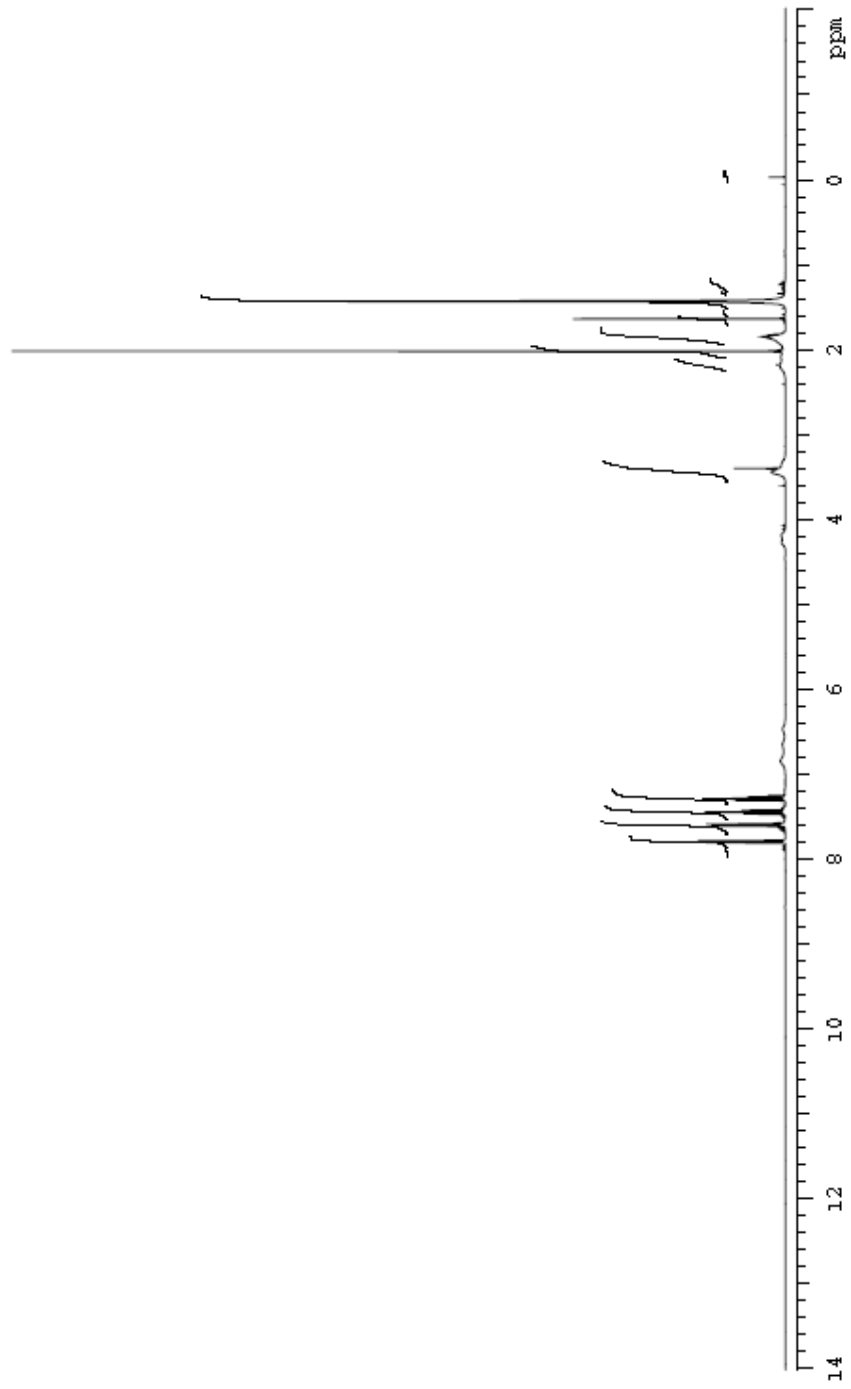
K1-R-F4-A

Sample Name K1-R-F4-A
Date collected 20 16-10-08

Pulse sequence PROTON
Solvent ddh₂O

Temperature 28
Spectrometer agilent NMR-vmr r400

Study owner veldan
Operator veldan

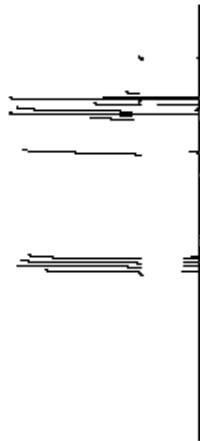


Path: /home/luu/Armsys/Database/K1-R-F4-A_20161008_01/PRO TO K_01.td

Rollback 2016-10-08

KL-H-F4-A

Sample Name: KL-H-F4-A Pulse sequence: PROTON Temperature: 28 Study owner: vwidon
Date collected: 2016-10-08 Solvent: ddh2o Spectrometer: agilent MM R-nmr0800 Operator: vwidon



SAMPLE Wt1 n

date Oct 20 16 SPECIAL

solvent ddh2o
file Name/LU/immrec/
 d3h2oimmrec/kl-h-f4-a_20
 161008_0_VPROTON_01.fid
temp 28.0
puls 24
spin 0
hs1 0.002
pused 11.100
sfs 10.000

ACQUISITION

zvw 6410.3
a1 2.668
rp 32782
fb 4000
bs 32
d1 1.000
n1 8
c1 8

FLA08

ii n
in n
dp y
hs nn

PROCBING

th not used

DISPLAY

sp -308.2
wp 8408.8
rl 308.8
rp 0
lp -47.6
ip 0

DECOUPLER

bin C13
bocf 0
bin nnn
decouple vwd_rc kimm
dpor 24
dmt 28412

PILOT

wc 284
sc 8
us 44
in 44

PREBATHRATION

zaincode n

Plotname: PROTON_01_plot01

Date # Home/LU/immrec/kl-h-f4-a_20161008_01_VPROTON_01.fid

Roll date 2016-10-08

KL-H-F4-B

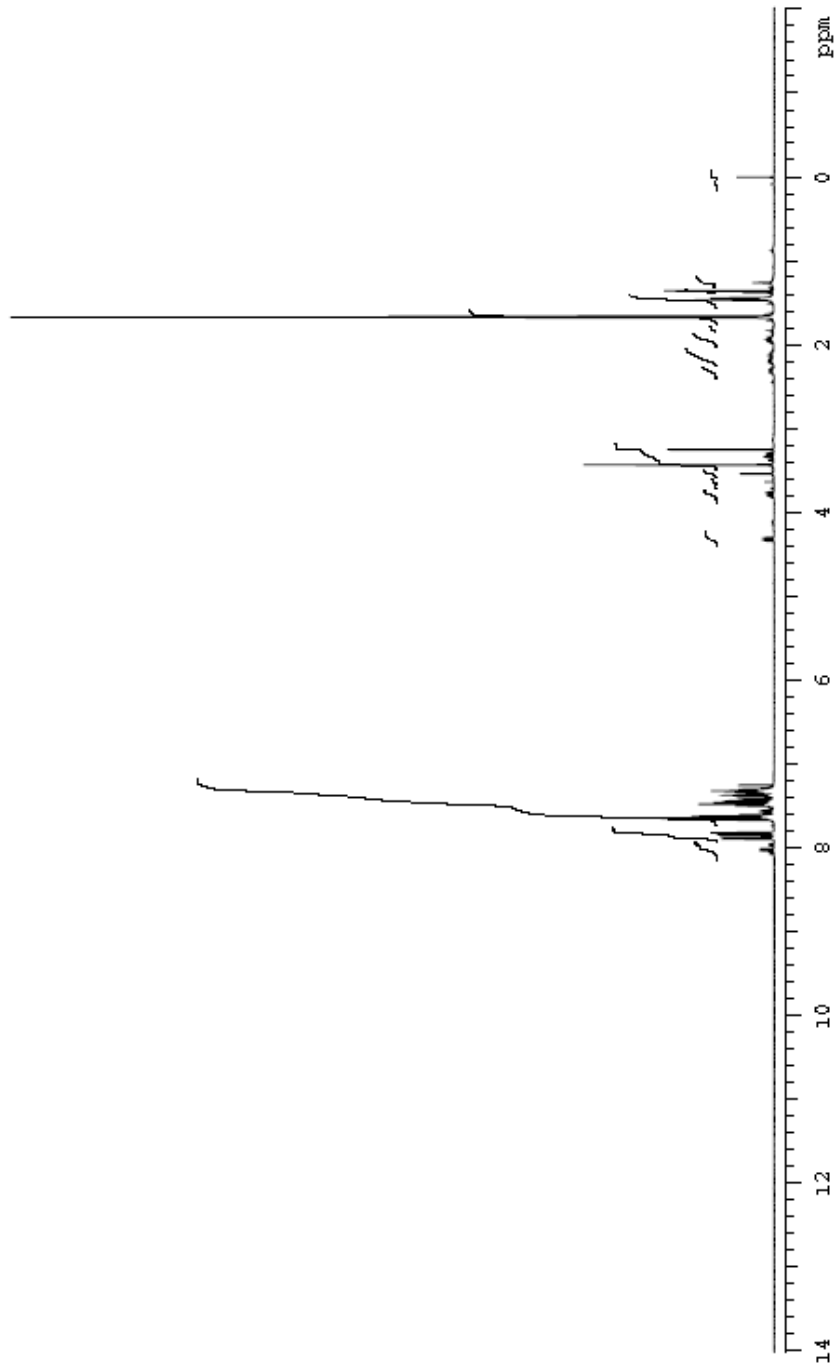
Sample Name: KL-H-F4-B
Date collected: 2016-10-14

Pulse sequence:
Solen

PROTON

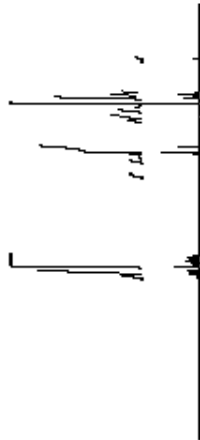
Temperature Spectrometer
23 agilent's MM5-mm-rsd00

Study owner: weldon
Operator: weldon



KL-H-F4-B

Sample Name: **KL-H-F4-B** Temperature: **28** Study owner: **Walden**
 Date collected: **2016-10-14** Spectrometer: **Agilent 8860mmr0400** Operator: **Walden**



SAMPLE		wt1	n
date	Oct 14 2016		
solvent	CDCl3		
file	home\LU\NMR\proj\data\Walden\KL-H-F4-B_20161014_BVPROTON_01.fid		
ACQUISITION			
sw	8410.2		
al	2.668		
rp	32782		
to	4000		
bs	22		
d1	1.000		
m1	2		
cl	2		
TRANSMITTER			
fr	H1		not used
freq	388.767		
ky	288.7		
bw	69		
pw	6.660		
DECOUPLER			
dr	C18		
dot	0		
dm	nm		
decoupl	VMD_16mm		
dpuw	24		
dm1	28412		
PREPARATION			
solmode			n

Plotname: **PROTON_01_plot01**

Date: **home\LU\NMR\proj\data\Walden\KL-H-F4-B_20161014_BVPROTON_01.fid**

Filedate: **2016-10-14**

KL-H-F2-E

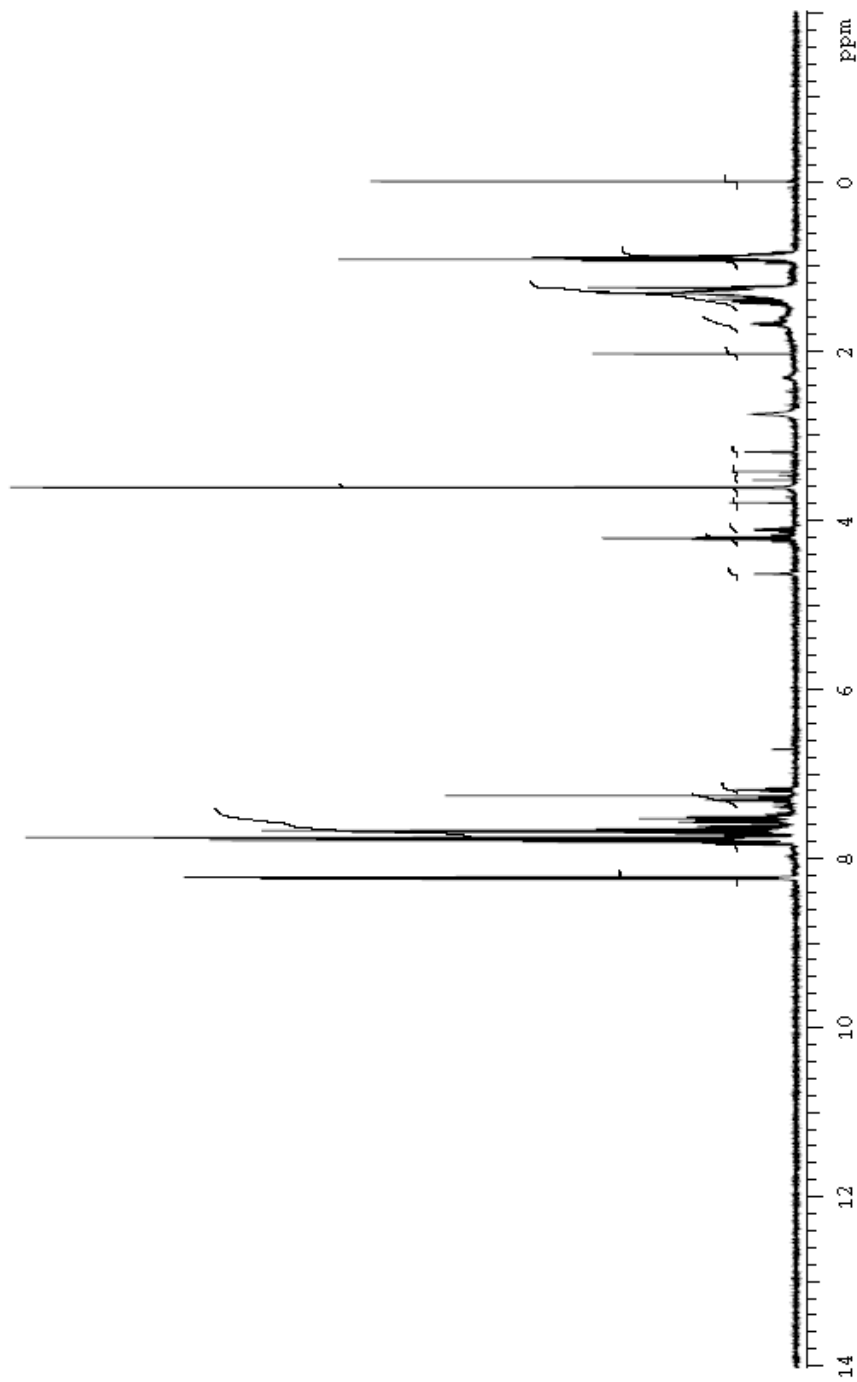
Sample Name KL-H-F2-E
Date collected 2015-10-26

Pulse sequence
SOLVENT

PROTON

Temperature 28
Spectrometer agilent-nmr-vnmr400

Study owner weldon
Operator weldon



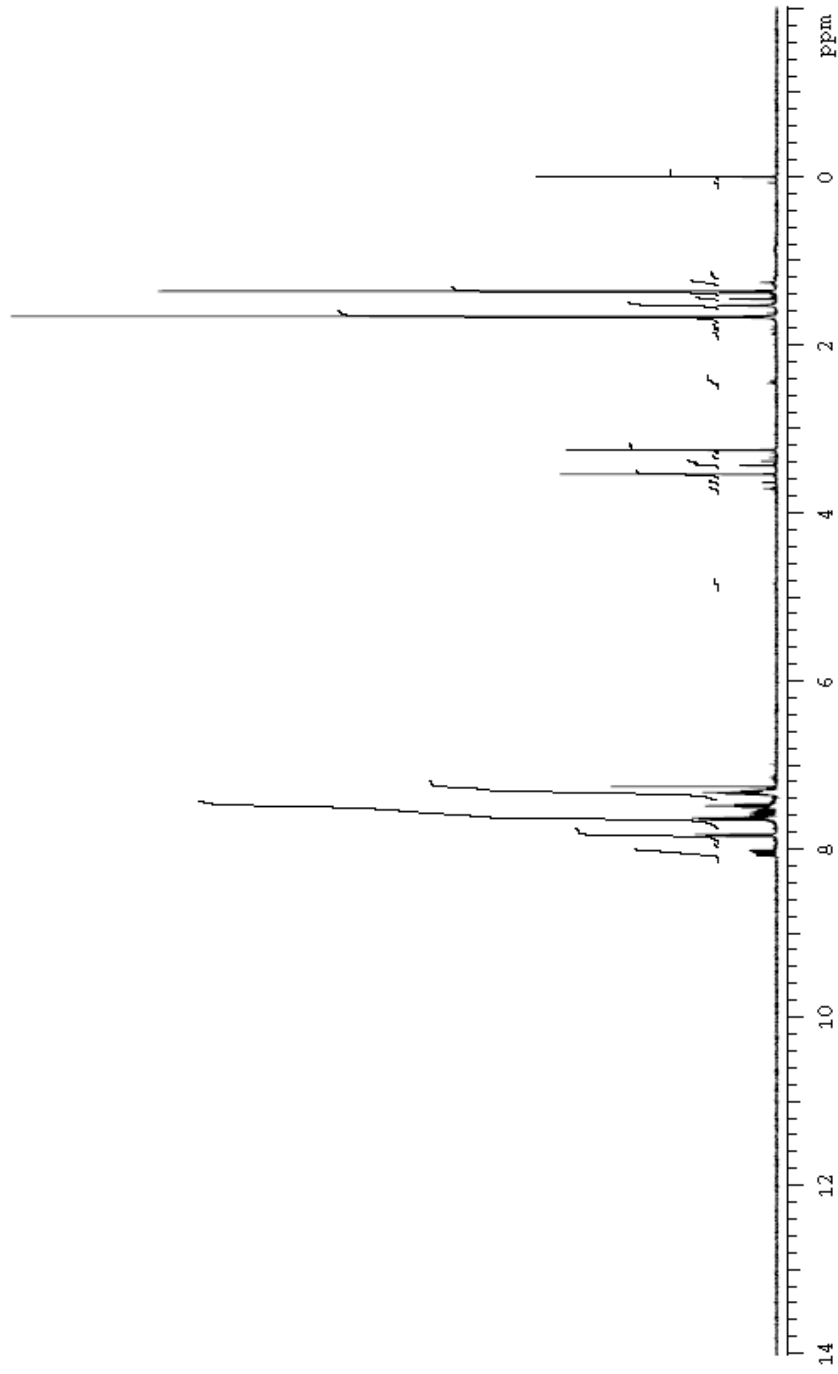
KL-H-F4-B3

Sample Name: KL-H-F4-B3
Date collected: 20 10-11-03

Plate sequence: PROTON
Solvent: CDCl3

Temperature: 23
Spectrometer: agilent-HMR-mm1400

Study owner: waldon
Operator: waldon

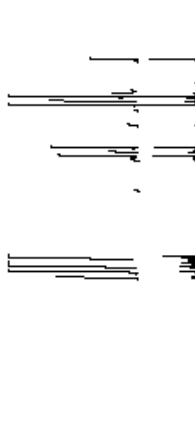


DATA FILE: A:\ome\11\001\msys\DATA\me100a\F4-B3_201010103_01\PROTON_01.f02

PLOT DATE: 2010-11-03

KL-H-R-B3

Sample Name: KL-H-R-B3
 Date collected: 2015-11-03
 Plate sequence: PROTON
 Temperature: 23
 Spec: 0615
 Operator: veldon
 Operator: veldon



SAMPLE

date: Nov 3 2015
 solvent: 0615
 file: /home/llw/vmmr/4/
 datafile/kl-h-r-b3
 20151103_01PROTON_01.f
 d

ACQUISITION

sw: 6410.3
 at: 2.556
 sp: 32758
 to: 4000
 bs: 32
 d1: 1.000
 st: 8
 ct: 8

TRANSMITTER

h: H1
 stq: 353.757
 txr: 355.7
 pwr: 55
 pw: 5.550

DECOUPLER

dt: C13
 dof: 0
 dm: nmr
 decouple: %40_HC45mm
 dpwr: 34
 dimr: 28412

PRESATURATION

acqmode: n
 wet: n
 SPECIAL
 temp: 23.0
 gain: 44
 dph: 0
 tzt: 0.005
 pwr50: 11.100
 aiba: 10.000

FLAGS

l: n
 h: n
 q: .
 k: nmr

PROCESSING

h: not used

DIS PLAY

sp: -80.62
 wp: 6408.9
 m: 20.6.5
 np: 0
 p: -53.5
 b: 0

PLOT

wc: 254
 sc: 8
 uc: 45
 u: 44
 ai: odd: p1

Plotname: PROTON_01_plot01

Datafile: /home/llw/vmmr/4/kl-h-r-b3_20151103_01PROTON_01.f

PLATE: 2015-11-03

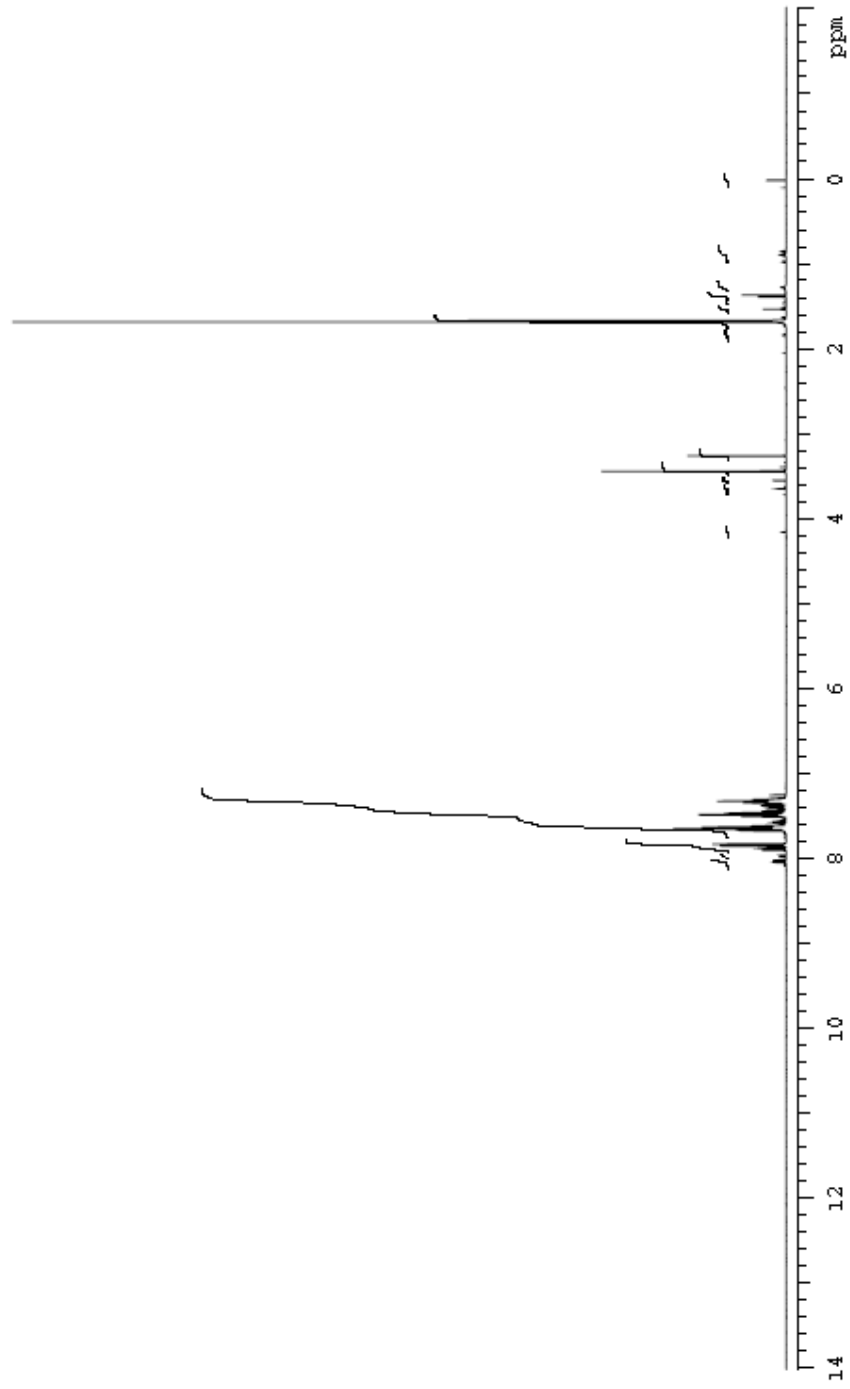
KL-R-4-B4

Sample Name KL-R-4-B4
Date collected 2016-11-03

Pulse sequence PROTON
Solvent acdms

Temperature 23
Spectrometer agilent MM R-nmr400

Study owner veldon
Operator veldon



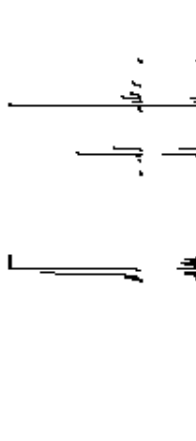
KL-H-F4-B-4

Sample Name: KL-H-F4-B-4
 Date collected: 2016-11-03

Temperature Spectrometer: 23
 Study owner: weldon
 Operator: weldon

Pulse sequence: PROTON
 Solvent: ad018

File: A:\home\LU\wmm\p\o\data\wldon\KL-H-F4-B-4-20161103_01\PROTO_K_013



SAMPLE

date: Mo v 2016
 solvent: ad018
 file: A:\home\LU\wmm\p\o\data\wldon\KL-H-F4-B-4-20161103_01\PROTO_K_013

ACQUISITION

sw: 6410.2
 zl: 2.568
 fq: 327.82
 ta: 4000
 bz: 32
 d1: 1.000
 ni: 3
 ci: 3

TRANSMITTER

h1: HI
 s1q: 386.767
 tot: 386.7
 tpr: 68
 pw: 6.660

DECOUPLER

dh: C18
 dot: 0
 dm: nnn
 decou: WAG_HC16mm
 dpr: 34
 dm1: 28412

PREPARATION

solmode: n
 wet: n
 SPECIAL

FLAGS

ll: n
 ln: n
 dp: .
 hc: nnn

PROCESSING

th: not used
 DBPLAY

PILOT

sp: -308.2
 wp: 6408.9
 rl: 308.8
 rp: 0
 lp: -88.3
 ip: 0

WC

sc: 284
 sz: 3
 us: 32
 tn: 44
 ai: calc ph

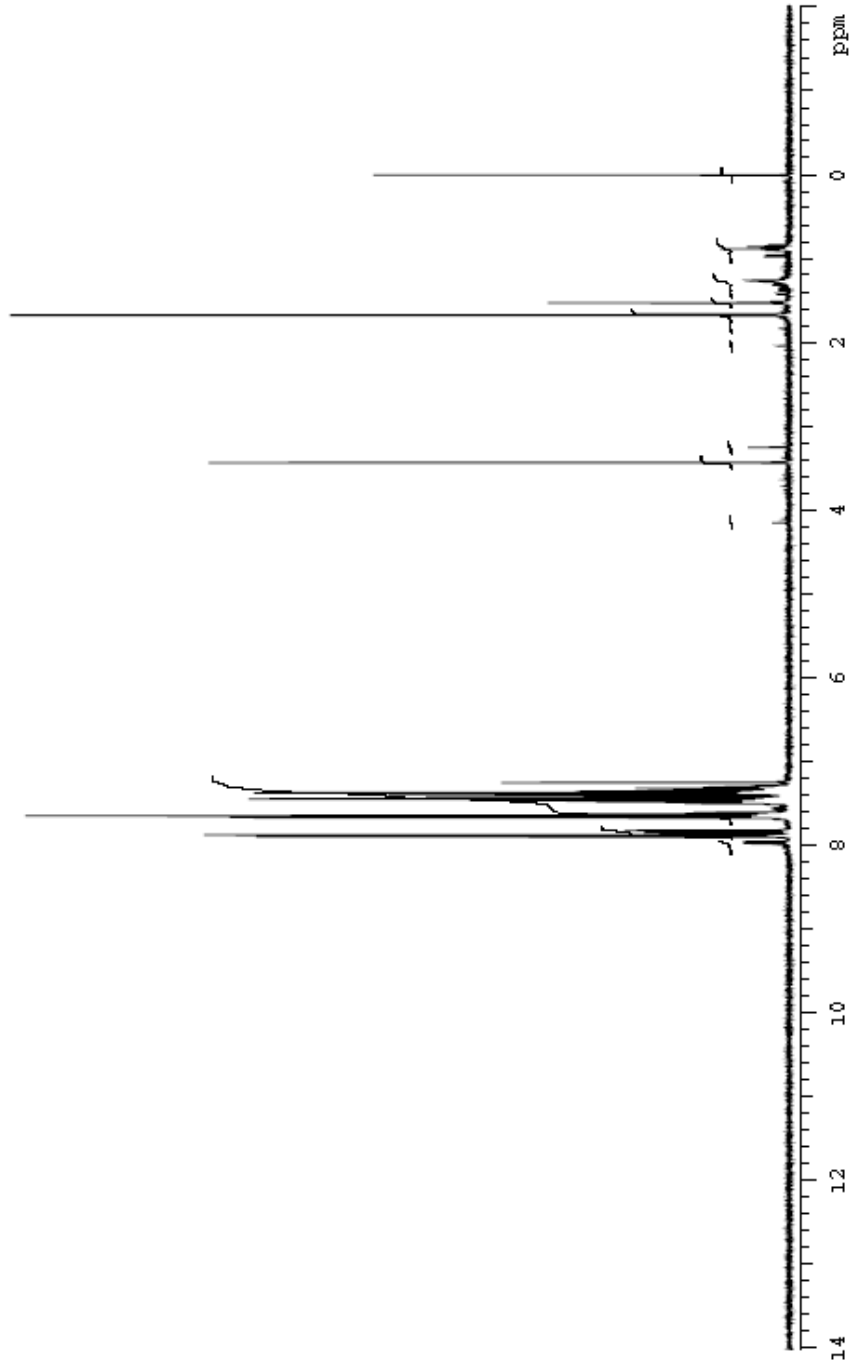
Plotname: PROTON_01_plot01

Datafile: A:\home\LU\wmm\p\o\data\wldon\KL-H-F4-B-4-20161103_01\PROTO_K_013.D

Roll date: 2016-11-03

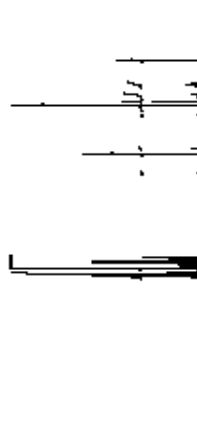
K1-R4-B6

Sample Name	K1-R4-B6	Pulse sequence	PROTON	Temperature	23	Study owner	weldon
Date collected	2016-11-08	Solvent	ddis	Spectrometer	agilent MM R-mmrc400	Operator	weldon



KL-H-F4-B6

Sample Name: KL-H-F4-B6 Pulse sequence: PROTON Study owner: veldon
 Date collected: 2016-11-08 Solvent: ddh2o Spectrometer: spect Operator: veldon



SAMPLE

date: Mo v 2016
 solent: ddh2o
 file: /home/llw/wwmrv/c/da/velon/kl-h-f4-b6-20161108_01/PROTON_01.f2
 0

PREP/URATION

zalmode: n
 wet: n
 SPECIAL
 temp: 23.0
 gain: 40
 spn: 0
 pres: 0.002
 p150: 11.100
 s15: 10.000

ACQUISITION

zlw: 6410.3
 sl: 2.668
 rp: 32782
 tb: 4000
 bs: 32
 d1: 1.000
 nl: 8
 cl: 8

FLAGB

ll: n
 ln: n
 dp: .
 fs: nn

TRANSMITTER

in: H1
 freq: 399.757
 for: 399.7
 tpr: 59
 pw: 6.660

PROCBIND

tn: not used
 DISPLAY
 sp: -208.2
 rf: 6408.8
 rp: 308.8
 ip: -66.7
 lp: 0

DECOUPLER

dn: C13
 dcr: 0
 dm: nnn
 decoupl: vwd_hc 65mm
 dpr: 34
 dmt: 28412

PILOT

wc: 284
 sc: 8
 us: 182
 in: 22
 s: calc ph

Plotname: PROTON_01_plot01

05b file /home/llw/wwmrv/c/da/velon/kl-h-f4-b6-20161108_01/PROTON_01.f2

Rollback 2016-11-08

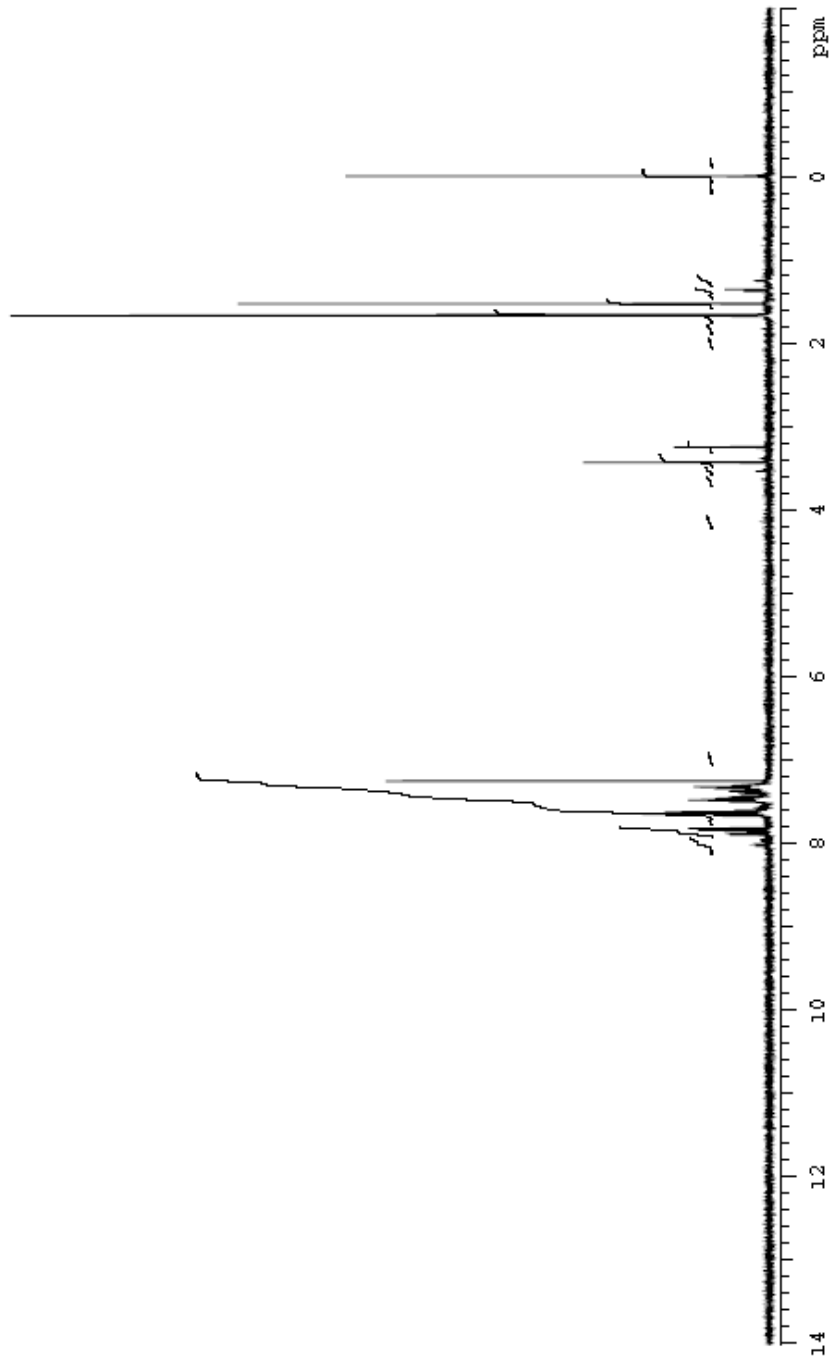
K1-R-4-B-8

Sample Name K1-R-4-B-8
Date Collected 2016-11-02

Pulse sequence PR130M
Solvent ddh₂O

Temperature 23
Spectrometer Agilent NMR spect400

Study owner wjldn
Operator wjldn



Path: /home/luu/numsp/20161102_01/PRO TO M_01.W

Roll date 2016-11-03

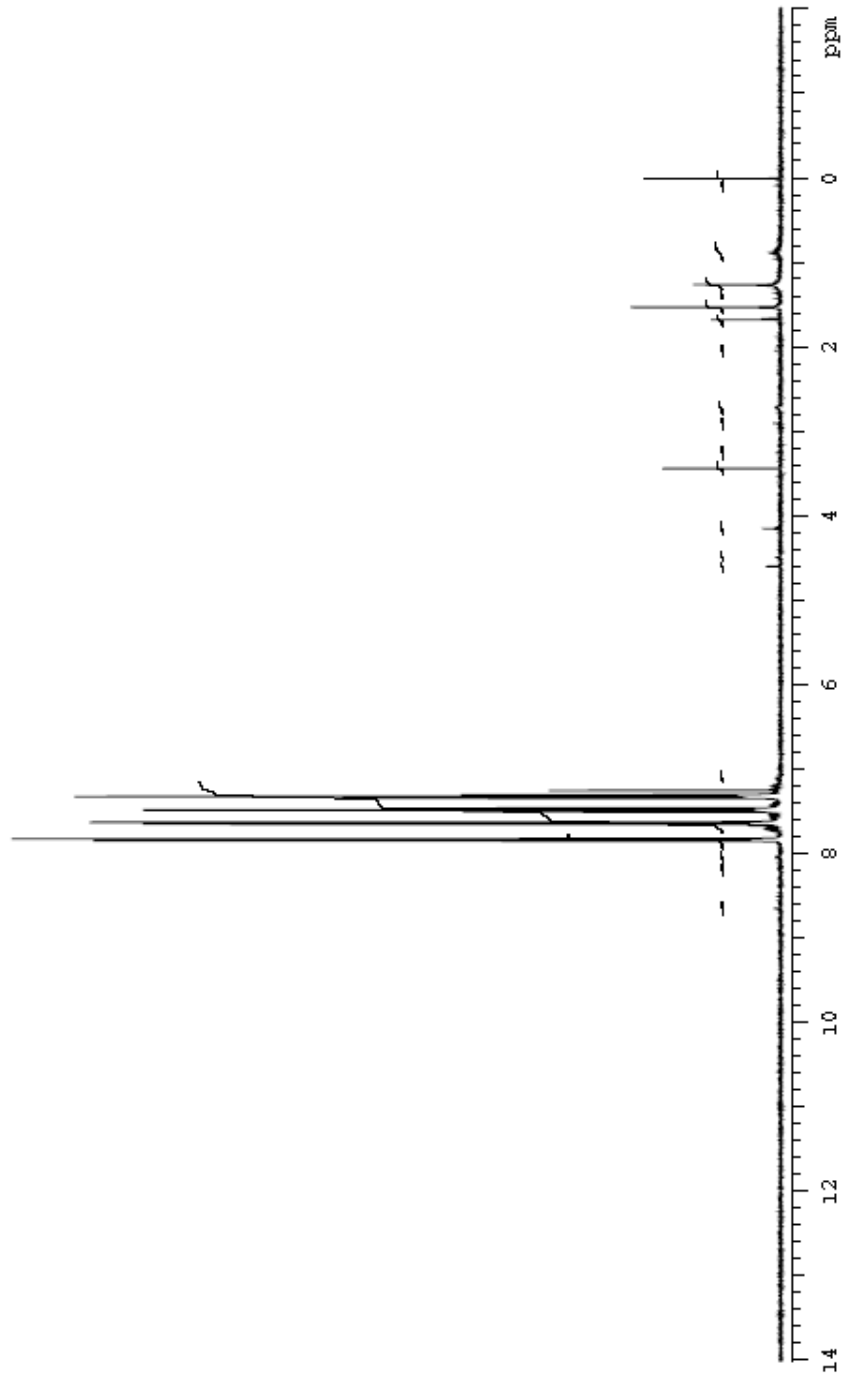
KL-R-F1-C3

Sample Name: KL-R-F1-C3
Date collected: 2016-11-03

Pulse sequence: PROTON
Solvent: ddh₂O

Temperature: 28
Spectrometer: agilent NMR-ann r340

Study owner: waldon
Operator: waldon

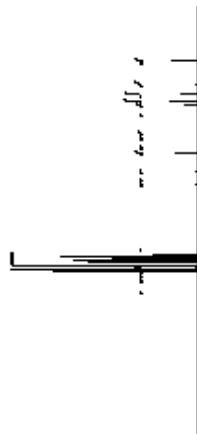


Path: /home/luu/annmr/spectra/kl-r-f1-c3_20161103_01/PROTON_01.fid

File date: 2016-11-03

KL-H-F1-C3

Sample Name: KL-H-F1-C3 Pulse sequence: PROTON Temperature: 23 Study owner: waldon
 Date collected: 2016-11-08 Solvent: ddh2o Specifier: 301011-M-R-umr0800 Operator: waldon



SAMPLE

date: No v 3 20 16
 solvent: ddh2o
 file: Home\1 LU\umr0800\2016-11-08\KL-H-F1-C3-20161108_01\PROTON_01_1 d

ACQUISITION

sw: 6410.3
 sh: 2.668
 rp: 32782
 sb: 4000
 bs: 32
 d1: 1.000
 ni: 3
 cl: 3

TRANSMITTER

h1: H1
 freq: 380.767
 lot: 388.7
 tour: 6R
 pow: 5.660

DECOUPLER

dn: C13
 dox: 0
 dm: n nn
 decouple: WALT_HCN6mm
 dpuw: 34
 dmy: 26412

PREPARATION

solmode: n
 wet: n
 SPECIAL

temp: 23.0
 gsm: 33
 sbr: 0
 hsl: 0.003
 mu50: 11.100
 dfo: 10.000

FLAGS

ll: n
 ln: n
 dp: ?
 hc: nn

PROCEDURE

Th: not used

DISPLAY

sp: 308.2
 wp: 6488.8
 rl: 308.8
 rp: 0
 lp: -46.7
 ip: 0

PLOT

wc: 234
 sc: 8
 us: 183
 Th: 18
 df: 0.00 ph

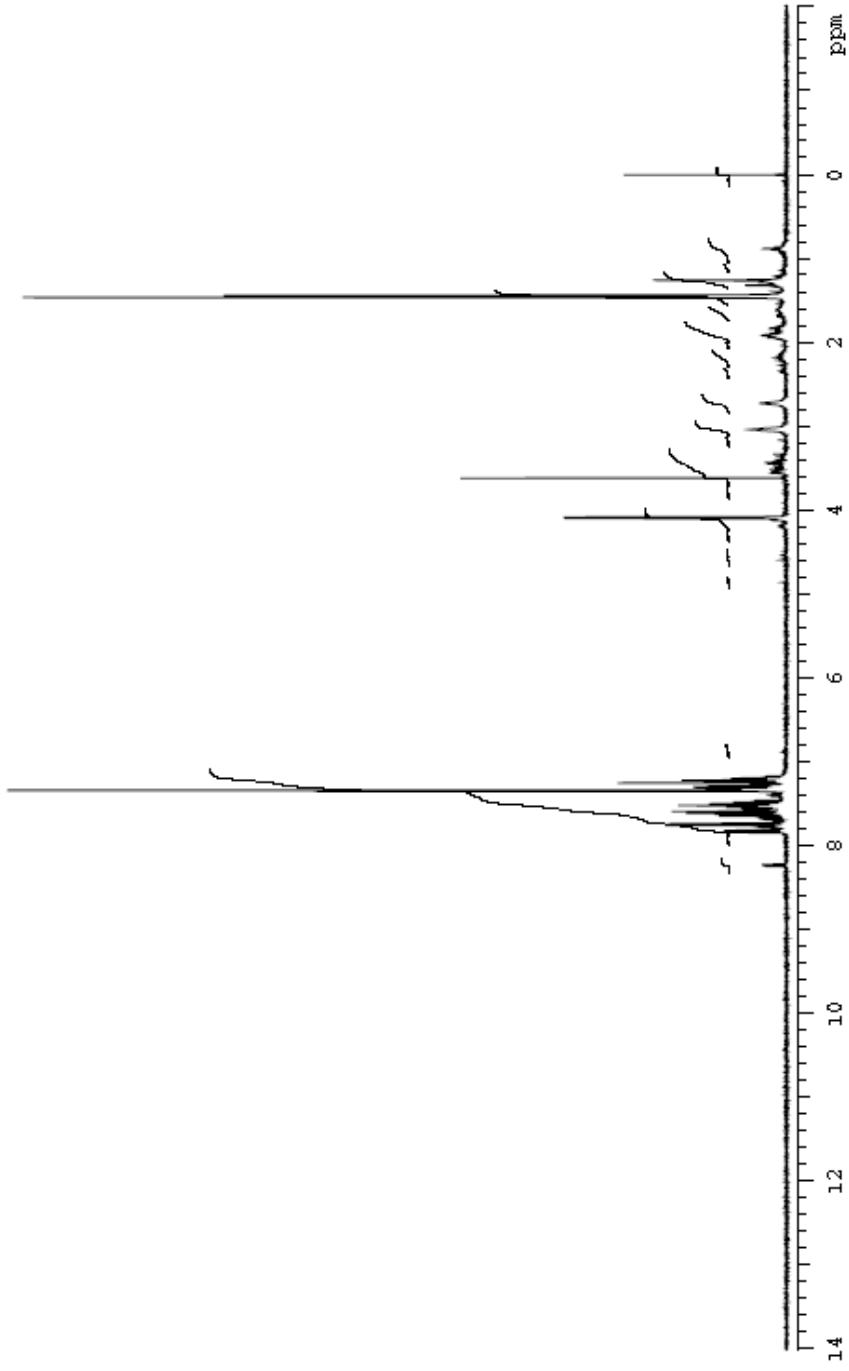
Plotname: PROTON_01_Plot01

Data file: Home\1 LU\umr0800\2016-11-08\KL-H-F1-C3-20161108_01\PROTON_01_1 d

Plot date: 2016-11-08

KL-H-F1-C4

Sample Name	KL-H-F1-C4	Pulse sequence	PROTON	Temperature	25	Study owner	veldon
Date collected	2016-11-03	Solvent	ddis	SpecName Et	Agilent-MMR-vmr000	Operator	veldon

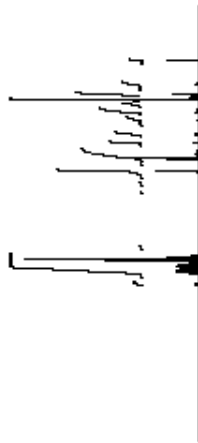


Path: /home/luu/Administrator/KL-H-F1-C4_20161103_01VP.R0 TO M_01.d

File date: 2016-11-03

KI-RF1C4

Sample Name: KI-RF1C4-4 Pulse sequence: PROTON Temperature: 23 Study owner: waldon
 Date collected: 2016-11-06 Solvent: ddh2o Specimen file: agilent-MMR-nmr000 Operator: waldon



```

SAMPLE
date      No v 32016
solvent   ddh2o
file      Name/LU/Name/CP
          data/waldon/KI-RF1C4-
          20161106_1/PROTON_01.1
          0

ACQUISITION
sw      6410.2
ai      2.668
rg      32782
rb      4000
bs      32
d1      1.000
rl      8
cl      8

PREPURATION
solmode  n
solvent  n
SPECIAL

temp     23.0
gain     32
spin     0
hs1      0.003
pulsed   11.100
sfs      10.000
FLASHB

ll      n
ln      n
dl      2
pc      nn

PROCESSING
Th      natu end
DISPLAY
sp      -308.2
up      8408.8
rf      308.8
rp      0
ip      -48.2
lp      0
PLOT
uc      284
sc      8
us      181
ln      8
si      0
af      0
ac      ph

TRANSMITTER
ln      H1
freq    388.767
bf      388.7
bw      68
pw      6.660
DECOUPLER
din     C13
dof     0
dm      nnn
decoupl W40_HC N6mm
dpor    34
dmy1    29412
  
```

Plotname: PROTON_01_plot01

data file home/LU/Name/CP/data/waldon/KI-RF1C4-4_20161106_1/PROTON_01.1.0

Rollback 2016-11-03

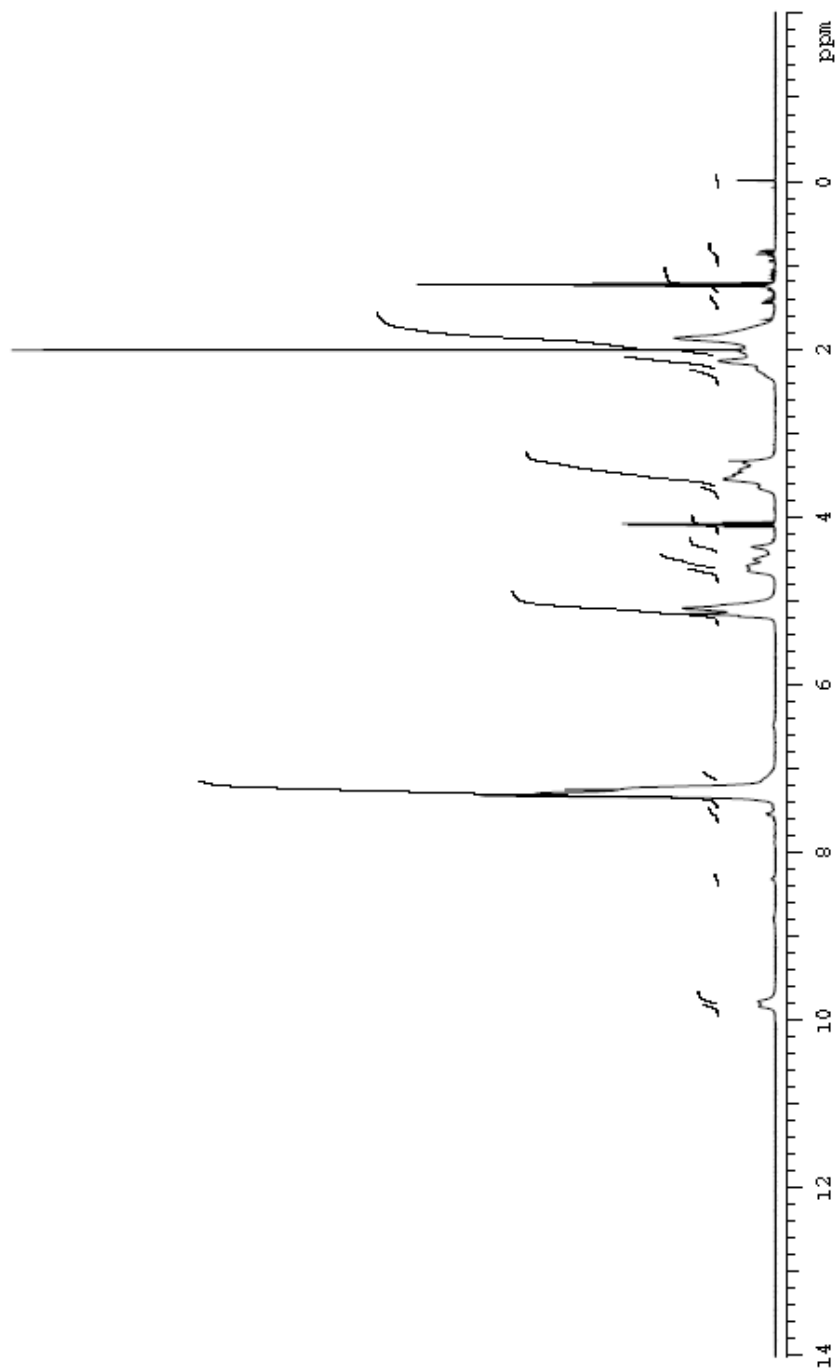
KL-H-F1-C6

Sample Name: KL-H-F1-C6
Date Collected: 2016-11-08

Pulse sequence: PROTON
Solvent: ddh₂O

Temperature: 25
Spectrometer: Agilent MM R-nm rdd00

Study owner: yaldon
Operator: yaldon

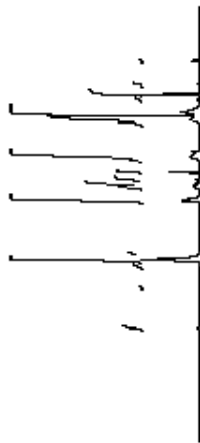


Path: /home/lui/analysis/database/kl-h-f1-c-6_2016-11-08_DIVPROTON_01.fid

File Date: 2016-11-08

KL-R-F1-C6

Sample Name: KL-R-F1-C6
 Date Collected: 2016-11-08
 Pulse Sequence: PROTON
 Solvent: ddh2o
 Temperature: 28
 Spectrometer: spect101r
 Study Owner: waldon
 Operator: waldon



SAMPLE		PREPARATION	
date	Mo v 8 20 16	solvent	n
solvent	ddh2o	wt	n
file	fname\1\wmm\rv\c\	SPECIAL	
	data\waldon\KL-R-F1-C6-	temp	28.0
	20161108_01\PROTON_D1.f	gain	24
		spn	0
		ref	0.003
		probd	11.100
		bits	10.000
		FLAGB	
		ll	n
		ln	n
		dp	:
		hc	nn
TRANSMITTER		PROCESSING	
fn	H1	fn	not used
freq	399.757	display	
kv	399.7	sp	-208.2
bw	68	wp	6408.8
pw	6.660	rf	208.8
		rp	0
		ra	-88.0
		lp	0
DECOUPLER		PLOT	
dn	C18	vc	234
dm	nm	sc	2
decoupl	WAlt_MC16mm	us	182
dpwr	34	fn	44
dm1	28412	pl	dic.ph

Plotname: PROTON_01_plot01

Path: /home/lu/wmm/ps/bast/kl-r-f1-c-6_20161108_01\PROTON_D1.f

Filedate: 2016-11-08

K1-H-82-H_2

Sample Name: K1-H-82-H_2

Pulse sequence: PR10N

Temperature: 28

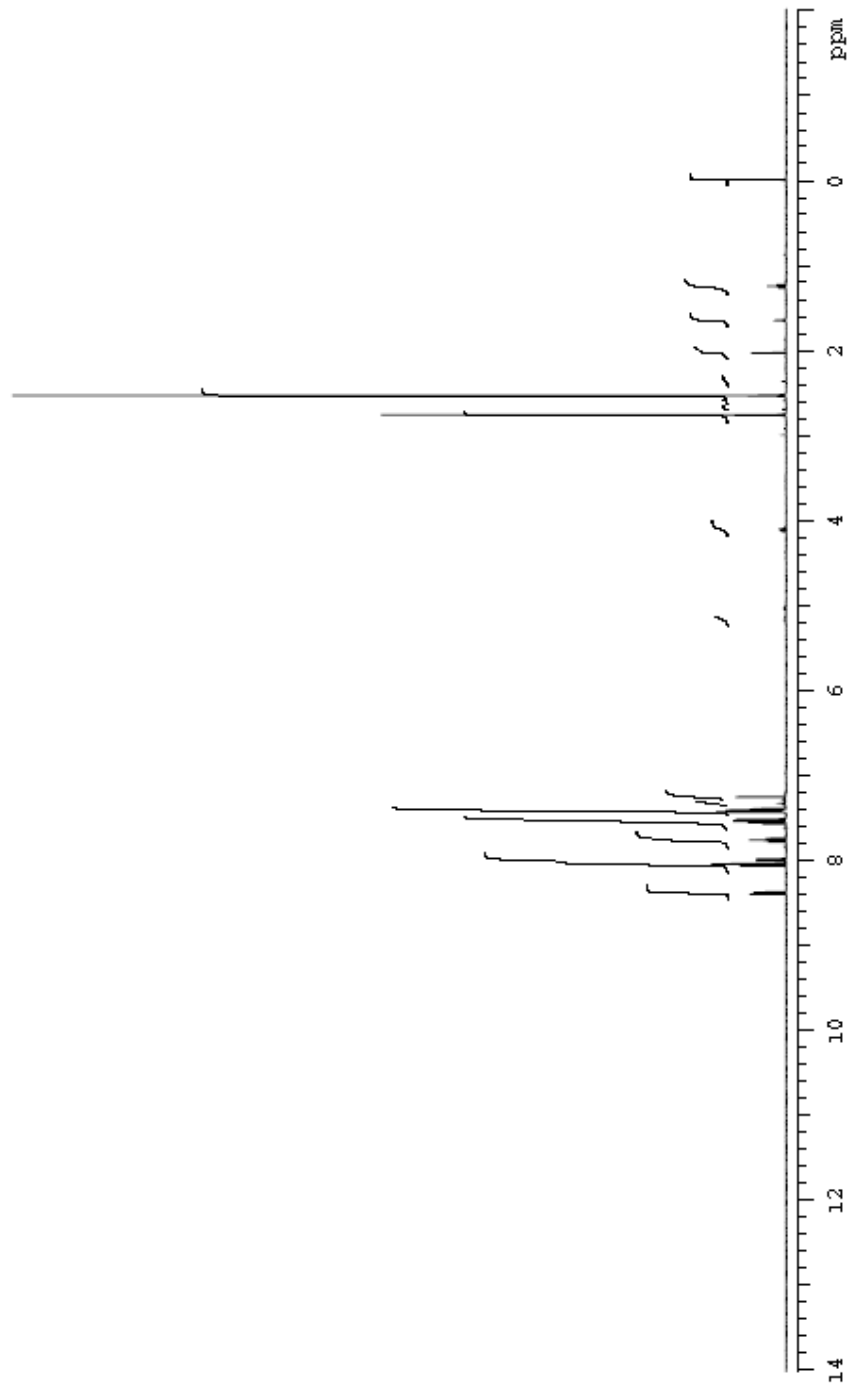
Study owner: vjidan

Date collected: 2016-11-08

Solvent: ddh2o

Spectrometer: agilent mmr-innova400

Operator: vjidan



Path: /home/luu/innisystem/network/K1-H-82-H_2_20161107_01/PROTO_N_01.fid

File date: 2016-11-17

KL-H-E2-H_2

Sample Name: KL-H-E2-H_2 Temperature: 28 Study Owner: weldon
 Date Collected: 2016-11-08 Spectrometer: Agilent MM-R-VMM-RS00 Operator: weldon



SAMPLE

```

date          20161108
solvent       MeOH
adddis       ad015
file          Home\LU\wmm\rv\
             data\weldon\KL-H-E2-H_2
             20161108_01\PROTO.M_01.s
             d
  
```

ACQUISITION

```

sqr          6410.2
rt           2.568
t0           237.82
bs          4000
d1          1.000
ni           8
ci           8
  
```

TRANSMITTER

```

in           H1
freq        388.757
tor         388.7
tpr         68
pwr         6.560
  
```

DECOUPLER

```

dn          C18
dof         0
dm          nnn
decouple    V40_HC Minn
dprw       34
dm1        28412
  
```

PREPURATION

```

salmode     n
wet         n
BPEXIAL
temp        28.0
d3in        42
d3rn        0
p000        0.002
p005        11.100
p010        10.000
  
```

FLAG

```

ii          n
in          n
op          y
hs         nn
  
```

PROCESING

```

in          not used
  
```

DB PLAY

```

sp          -308.2
wp          8408.8
rl          808.8
rb          0
rp          -62.8
lp          0
  
```

PLOT

```

wc          284
sc          8
uz          18
in          44
  
```

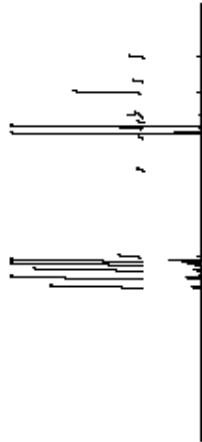
Filename: PROTON_01_Plot01

Datafile: Home\LU\wmm\rv\data\weldon\KL-H-E2-H_2_20161108_01\PROTO.M_01.s

Revised: 2015-11-17

K1-H-E2-H_3

Sample Name: K1-H-E2-H_3
 Date collected: 2016-11-9
 Pulse sequence: PROTON
 Solution: 00003
 Temperature: 23
 Spectrometer: agilent MM-Rnm r400
 Study owner: vwidan
 Operator: vwidan



SAMPLE

date: Mo 17 2016
 solution: 00003
 file: /home/llw/numris/col
 data:/vidan/K1-H-E2-H_3_
 20161117_01PROTON_01.f
 0

NAME: K1-H-E2-H_3
 solvent: n
 weight: n
 SPECIAL

ACQUISITION

sw: 6410.2
 ai: 2.668
 f0: 32782
 qb: 4000
 bs: 32
 d1: 1.000
 ni: 2
 ci: 2

temp: 23.0
 gain: 38
 spm: 0
 test: 0.003
 pres0: 11.100
 pres1: 10.000
 FLAG0
 FLAG1
 FLAG2
 FLAG3
 FLAG4
 FLAG5
 FLAG6
 FLAG7
 FLAG8
 FLAG9
 FLAG10
 FLAG11
 FLAG12
 FLAG13
 FLAG14
 FLAG15
 FLAG16
 FLAG17
 FLAG18
 FLAG19
 FLAG20
 FLAG21
 FLAG22
 FLAG23
 FLAG24
 FLAG25
 FLAG26
 FLAG27
 FLAG28
 FLAG29
 FLAG30
 FLAG31
 FLAG32
 FLAG33
 FLAG34
 FLAG35
 FLAG36
 FLAG37
 FLAG38
 FLAG39
 FLAG40
 FLAG41
 FLAG42
 FLAG43
 FLAG44
 FLAG45
 FLAG46
 FLAG47
 FLAG48
 FLAG49
 FLAG50
 FLAG51
 FLAG52
 FLAG53
 FLAG54
 FLAG55
 FLAG56
 FLAG57
 FLAG58
 FLAG59
 FLAG60
 FLAG61
 FLAG62
 FLAG63
 FLAG64
 FLAG65
 FLAG66
 FLAG67
 FLAG68
 FLAG69
 FLAG70
 FLAG71
 FLAG72
 FLAG73
 FLAG74
 FLAG75
 FLAG76
 FLAG77
 FLAG78
 FLAG79
 FLAG80
 FLAG81
 FLAG82
 FLAG83
 FLAG84
 FLAG85
 FLAG86
 FLAG87
 FLAG88
 FLAG89
 FLAG90
 FLAG91
 FLAG92
 FLAG93
 FLAG94
 FLAG95
 FLAG96
 FLAG97
 FLAG98
 FLAG99
 FLAG100

TRANSMITTER

h1: R1
 freq: 388.767
 lot: 388.7
 lbr: 68
 pw: 5.660

PROC: 000
 sh: not used
 DISPLAY

DECOUPLER

ch: C12
 det: 0
 dm: nnn
 deconv: WAG_HC 65mm
 dprw: 34
 dmt: 28412

sp: 208.2
 up: 8408.8
 r1: 208.8
 r2: 0
 r3: -67.8
 r4: 0
 r5: 0
 r6: 0
 r7: 0
 r8: 0
 r9: 0
 r10: 0
 r11: 0
 r12: 0
 r13: 0
 r14: 0
 r15: 0
 r16: 0
 r17: 0
 r18: 0
 r19: 0
 r20: 0
 r21: 0
 r22: 0
 r23: 0
 r24: 0
 r25: 0
 r26: 0
 r27: 0
 r28: 0
 r29: 0
 r30: 0
 r31: 0
 r32: 0
 r33: 0
 r34: 0
 r35: 0
 r36: 0
 r37: 0
 r38: 0
 r39: 0
 r40: 0
 r41: 0
 r42: 0
 r43: 0
 r44: 0
 r45: 0
 r46: 0
 r47: 0
 r48: 0
 r49: 0
 r50: 0
 r51: 0
 r52: 0
 r53: 0
 r54: 0
 r55: 0
 r56: 0
 r57: 0
 r58: 0
 r59: 0
 r60: 0
 r61: 0
 r62: 0
 r63: 0
 r64: 0
 r65: 0
 r66: 0
 r67: 0
 r68: 0
 r69: 0
 r70: 0
 r71: 0
 r72: 0
 r73: 0
 r74: 0
 r75: 0
 r76: 0
 r77: 0
 r78: 0
 r79: 0
 r80: 0
 r81: 0
 r82: 0
 r83: 0
 r84: 0
 r85: 0
 r86: 0
 r87: 0
 r88: 0
 r89: 0
 r90: 0
 r91: 0
 r92: 0
 r93: 0
 r94: 0
 r95: 0
 r96: 0
 r97: 0
 r98: 0
 r99: 0
 r100: 0

Filename: PROTON_01_Plot01

Path: /home/llw/numris/systems/vidan/K1-H-E2-H_3_20161117_01PROTON_01.fid

Rollback: 2015-11-17

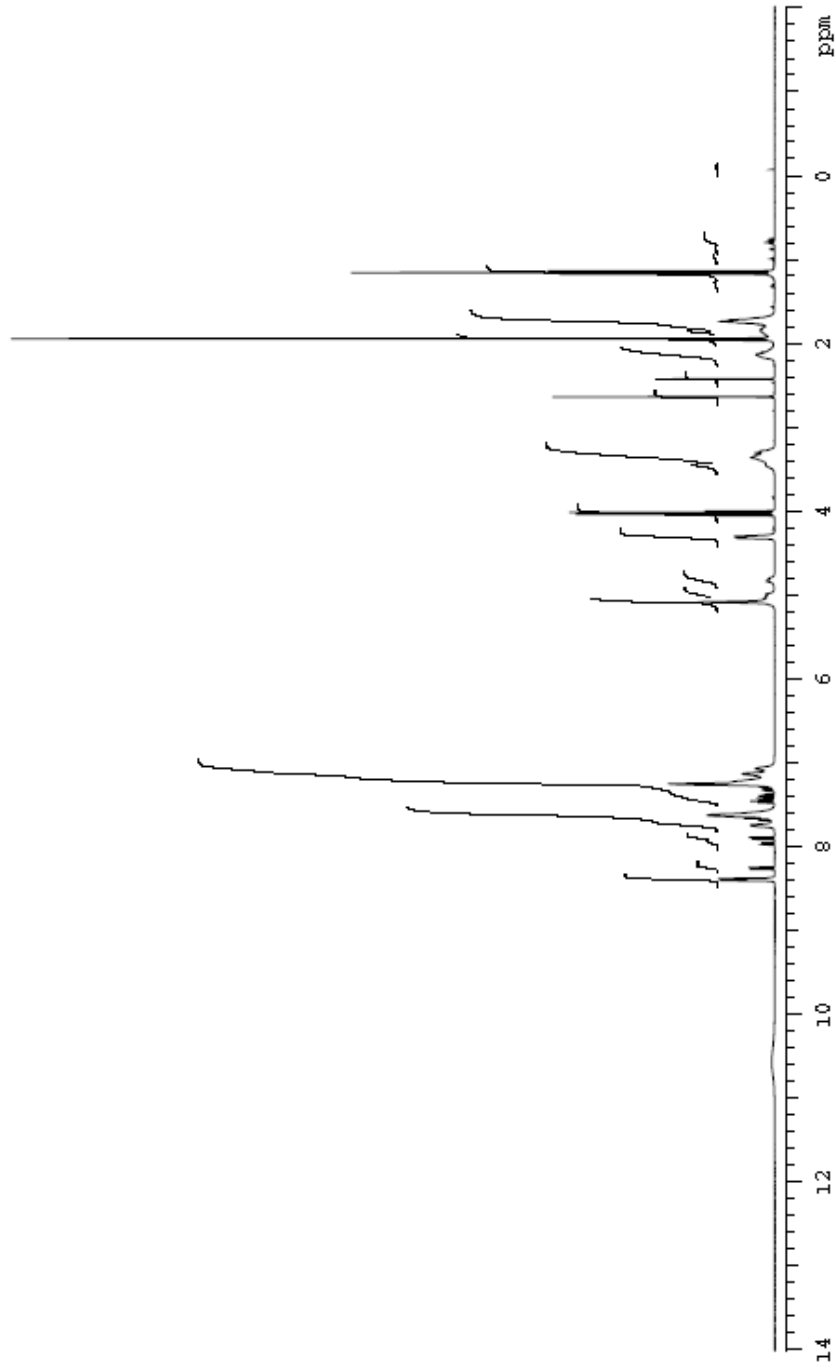
K1-H-82-H_5

Sample Name: K1-H-82-H_5
Date collected: 2016-11-07

Pulse sequence: PROTON
Solvent: ddh₂O

Temperature: 23
Spectrometer: agilentnmrmmrdd00

Study owner: veldon
Operator: veldon



Data file: /home/llw/analysis/data/veldon/K1-H-82-H_5_20161107_01VP/PROTON_01.fid

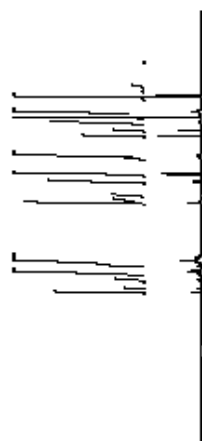
File date: 2016-11-17

KL-H-EE-H_5

Sample Name: KL-H-EE-H_5
 Date Collected: 2016-11-17
 Study Owner: J. Vidan
 Operator: J. Vidan

Run Sequence: PROTON
 Solvent: ddh2o

Temperature: 25
 Spectrometer: Agilent 1100-MS-MSD



PREPARATION

date: Nov 17 2016
 solvent: ddh2o
 file: Name\1100\emr\c\ddh2o\vidan\KL-H-EE-H_5
 20161117_01\PROTON_01.d

ACQUISITION

sw: 6410.3
 sl: 2.668
 rp: 32782
 sb: 4000
 bs: 32
 d1: 1.000
 nl: 3
 cl: 3

PREPARATION

zathode: n
 wet: n
 SPECIAL

temp: 25.0
 gain: 18
 spn: 0
 hpl: 0.003
 pused: 11.100
 slvs: 10.000

FLAG

ll: n
 ln: n
 dp: v
 hc: nn

PROBING

th: not used

DISPLAY

sp: -208.2
 up: 8409.8
 nl: 308.8
 rp: 0
 lp: -67.7
 ip: 0

PLOT

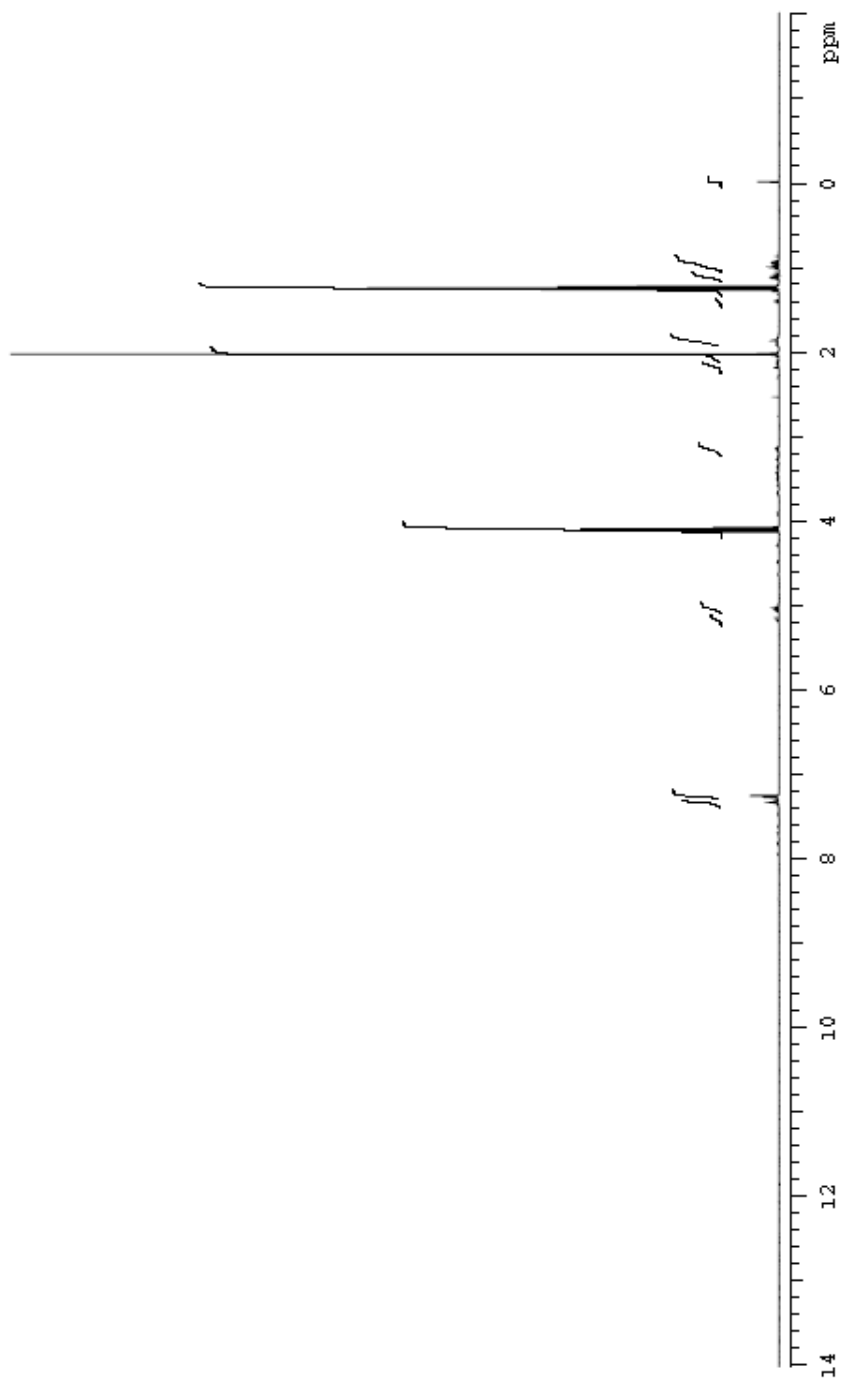
WC: 284
 SC: 77
 us: 44
 th: 44
 sl: 44

Filename: PROTON_01_plot01

Datefile: Home\1100\emr\c\ddh2o\vidan\KL-H-EE-H_5_20161117_01\PROTON_01.d

K1-H-02-H_B

Sample Name: **K1-H-02-H_B** Pulse sequence: **PROTON** Temperature: **25** Study owner: **veldan**
Date collected: **2016-11-17** Solvent: **dmso** Spectrometer: **Agilent MM RNM 600D** Operator: **veldan**



KL-H-ES-H_B

Sample Name: **KL-H-ES-H_B** Pulse sequence: **PROTON** Study owner: **aidan**
 Date collected: **2016-11-9** Solvent: **ddo3** Spectrometer: **agilent MM R-nmr060** Operator: **aidan**



SAMPLE

date: **Mo 17 2016**
 solvent: **ddo3**
 file: **home/LU/aimms/2016/11/09/kl-h-ES-H_B**
 data: **home/LU/aimms/2016/11/09/kl-h-ES-H_B**
 20161117_01PROTON_01.f1

PREPARATION

solmode: **n**
 wet: **n**
SPECIAL
 temp: **33.0**
 dsh: **38**
 spm: **0**
 hel: **0.003**
 p150: **11.100**
 d35: **10.000**
FLAGB
 ll: **n**
 ln: **n**
 dl: **2**
 hl: **nn**

ACQUISITION

sw: **6410.3**
 z1: **2.668**
 rp: **327.83**
 r: **4000**
 bs: **32**
 d1: **1.000**
 rl: **3**
 cl: **3**

TRANSMITTER

h1: **H1**
 str: **387.57**
 kor: **389.7**
 lpu: **58**
 pw: **6.660**

PROCEBING

th: **not used**
DISPLAY
 sp: **308.2**
 wp: **6408.8**
 rl: **308.8**
 rp: **0**
 mp: **-81.7**
 lp: **0**
PLOT
 wc: **234**
 sc: **3**
 us: **21**
 th: **44**
 ad: **ph**

DECOUPLER

d1n: **C13**
 d1r: **0**
 d1m: **nm**
 decouple: **W40_HCNMmm**
 d1pu: **34**
 d1m1: **26412**

Plotname: **PROTON_01_Plot01**

063116 home/LU/aimms/2016/11/09/kl-h-ES-H_B_20161117_01PROTON_01.f1

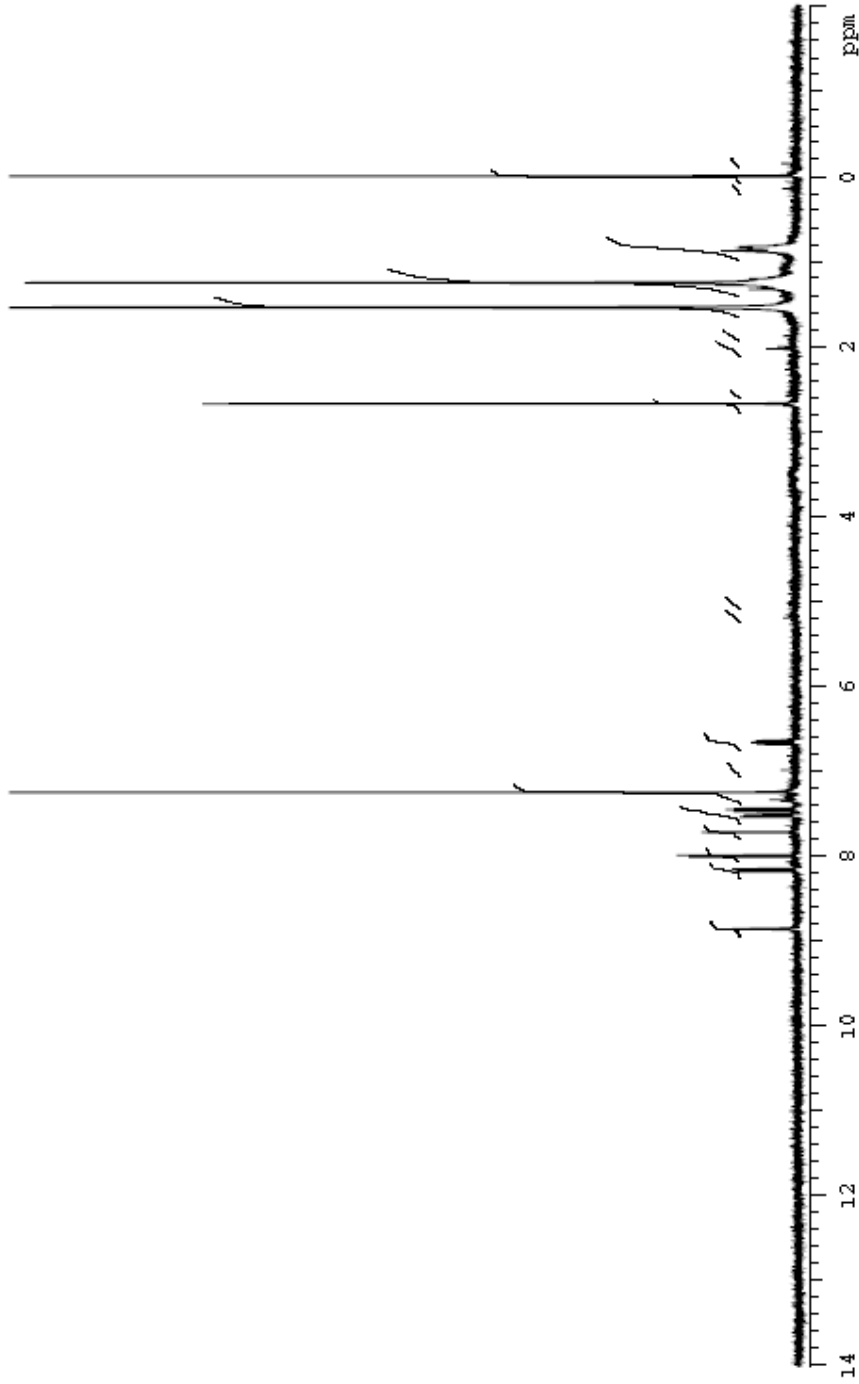
K1-R-DWJ33-84

Sample Name: K1-R-DWJ33-84
Date collected: 2018-01-08

Pulse sequence: PROTON
Solvent: ddh2o

Temperature: 26
Spectrometer: agilent MM R-ann rcd00

Study owner: weldon
Operator: weldon

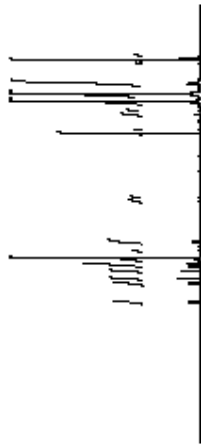


Path: /home/lui/administrator/kl-r-000_53-54_20180108_011P/ROTTO_K_D1.1d

File date: 20180108

KL-H-DW_88-84

Sample Name: KL-H-DW_88-84 Purity sequence: PROTON Study owner: weldon
 Date collected: 2018-01-08 Solvent: ddh2o Spectrometer: agilent MM R-mm r400 Operator: weldon



SAMPLE

date: Jan 8 2018 scanmode: n
 solvent: ddh2o wet: n
 file: Name: \L1\mmr\c\ SPECIAL
 data: weldon\KL-H-DW_88-84_20180108_01\PROTON_01_10

ACQUISITION

zpw: 6410.2
 zl: 2.568
 rf: 32782
 to: 4000
 bs: 32
 d1: 1.000
 d1: 2
 c1: 2

TRANSMITTER

in: H1
 freq: 399.767
 lot: 399.7
 lpar: 69
 pw: 6.660

DECOUPLER

dn: C18
 dcr: 0
 dm: nnn
 decouple: VWD_RC 16mm
 dpr: 34
 dmy: 28412

PREPARATION

temp: 25.0
 gain: 64
 spin: 0
 lock: 0.002
 pwr50: 11.100
 shwa: 10.000

FLAGS

ll: n
 ln: n
 dp: 2
 fs: nnn

PROCESSING

in: nstu
 out: ead

DISPLAY

z0: -308.2
 w0: 8408.8
 r1: 308.8
 rf: 0
 ip: -58.2
 lp: 0

PILOT

WC: 284
 zc: 2
 us: 362
 in: 14
 sh: adc ph

Plotname: PROTON_01_Plot_01

datafile: \home\l1\mmr\sys\data\weldon\KL-H-DW_88-84_20180108_01\PROTON_01_10

File date: 2018-01-08

APPENDIX C

VITA

Kenneth Laboy was born in Washington, DC on September 22, 1979. In 1998 Ken Graduated from Springbrook High School. He chose to enter the United States Navy and Served as a US Navy SEAL at SEAL Team 2. While in the SEAL Teams he deployed OCONUS to various regions. In 2004 He left the military in pursuit of a college degree. However, he was unable to complete this venture due to being involuntarily recalled to active duty once again in 2006. Here he became a plank owner of SEAL Team 18 and was deployed OCONUS to various combat zones.

In 2011, he officially discharged honorably from the US Navy and enrolled at La Sierra University in Riverside, CA. While at La Sierra, he worked as a Laboratory Technician under Dr. Marvin Payne and also worked as a Teacher's Assistant for the department of Physics under Dr. Ivan E. Rouse. He eventually earned his degree in Biochemistry (Bachelor of Science) and applied to a laboratory position under Dr. Michael Malerick working in the field of organometallics, where he worked on the total synthesis of chemotherapeutic pharmacophores based off Platinum derivatives using Molybdenum as the base cofactor for the pharmacophore. He was eventually granted admission into Loma Linda University School of Medicine Basic Sciences program. Here he was given the opportunity to work under Dr. David Weldon as a Graduate student in his laboratory transitioning into the field of Medicinal Chemistry.